



department
Mobility and
Public Works

Scientific support regarding hydrodynamics and sand transport in the coastal zone

MODELLING TOOLS AND METHODOLOGIES



00_072

WL Rapporten

Scientific support regarding hydrodynamics and sand transport in the coastal zone

Modelling tools and methodologies

Zimmermann, N.; Wang, L.; Mathys, M.; Trouw, K.; De Maerschack, B.; Delgado, R.;
Roelvink, J.A.; Monbaliu, J.; Bolle, A.; Toro, F.; Verwaest, T.; Mostaert, F.

July 2015

WL2015R00_072_19

This publication must be cited as follows:

Zimmermann, N.; Wang, L.; Mathys, M.; Trouw, K.; De Maerschack, B.; Delgado, R.; Roelvink, J.A.; Monbaliu, J.; Bolle, A.; Toro, F.; Verwaest, T.; Mostaert, F. (2015). Scientific support regarding hydrodynamics and sand transport in the coastal zone: Modelling tools and methodologies. Version 3_0. WL Rapporten, 00_072. Flanders Hydraulics Research & IMDC: Antwerp, Belgium.

I/RA/11355/12.051/NZI. IMDC, Antwerp, Belgium



Waterbouwkundig Laboratorium

Flanders Hydraulics Research

Berchemlei 115
B-2140 Antwerp
Tel. +32 (0)3 224 60 35
Fax +32 (0)3 224 60 36
E-mail: waterbouwkundiglabo@vlaanderen.be
www.watlab.be



International Marine and Dredging Consultants

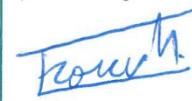
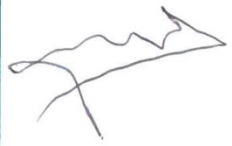
Coveliersstraat 15
B-2600 Antwerp
Tel. +32 (0)3 270 92 95
Tel. +32 (0)3 235 67 11
E-mail: info@imdc.be
www.imdc.be

Nothing from this publication may be duplicated and/or published by means of print, photocopy, microfilm or otherwise, without the written consent of the publisher.

Document identification

Title:	Scientific support regarding hydrodynamics and sand transport in the coastal zone: Modelling tools and methodologies		
Customer:	Coastal Division, FHR	Ref.:	WL2015R00_072_19
Keywords (3-5):	Longshore currents, cross-shore currents, Belgian Coast, numerical modelling		
Text (p.):	125	Appendices (p.):	12
Confidentiality:	<input type="checkbox"/> Yes	Exceptions:	<input type="checkbox"/> Customer
			<input type="checkbox"/> Internal
			<input type="checkbox"/> Flemish government
		Released as from:	
	<input checked="" type="checkbox"/> No	<input checked="" type="checkbox"/> Available online	

Approval

Author Nicolas Zimmermann (IMDC)  Koen Trouw (Fides Engineering) 	Reviser Toon Verwaest 	Project Leader Bart de Maerschack 	Research & Consulting Manager Toon Verwaest 	Division Head Mostaert, F. 
--	--	---	--	--

Revisions

Nr.	Date	Definition	Author(s)
1.0	01/06/2012	Concept version	Nicolas Zimmermann
1.1	31/07/2012	Substantive revision	J.A. Roelvink, Annelies Bolle, Jaak Monbaliu
1.2	01/08/2012	Substantive revision	Toon Verwaest
2.0	05/02/2013	Final version of Phase 1 (layout)	Nicolas Zimmermann
2.1	15/05/2015	Update to include lessons learnt of Phase 2	Nicolas Zimmermann, Koen Trouw
3.1	15/07/2015	Substaive Revision	Bart De Maerschack
4.0	17/07/2015	Final version	Nicolas Zimmermann

Abstract

This report gathers the experience gained in morphological modelling within the project "Sand dynamics in the Belgian coastal zone" carried out at Flanders Hydraulics. It aims to provide a single guideline document to help making decisions or understanding model results when setting up a morphological model. It reviews data and models available, draws attention to some focus points during the model setup and calibration, presents various input reduction techniques necessary for morphological modelling, special characteristics of inlet and embayment modelling, cross-shore profile applications, and various methods to implement structures in the model. Individual conclusions are summarized at the end of each chapter and in a more practical form at the end of the report.

Contents

List of tables.....	IV
List of figures	V
1 Introduction.....	1
1.1 The assignment.....	1
1.2 Aim of the study	1
1.3 Overview of the study.....	1
1.4 Structure of the report	2
2 Data and models available	3
2.1 Overview	3
2.2 Data sources	3
2.3 Models available	3
2.3.1 Overview	3
2.3.2 Zuno model (Netherlands)	3
2.3.3 Optos model (BMM / MUMM, Belgium)	5
2.3.4 Summary of model characteristics	7
3 Model setup.....	8
3.1 Overview	8
3.2 Data collection and analysis.....	8
3.3 Model choice	9
3.3.1 Model type.....	9
3.3.2 Longshore transport.....	9
3.3.3 Cross-shore transport	9
3.4 Boundary conditions.....	13
3.4.1 Resolution, nesting and domain decomposition	13
3.4.2 Flow boundary conditions	14
3.4.3 Sediment transport boundary conditions	16
3.4.4 Wave boundary conditions.....	17
3.4.5 Light model setup.....	17
3.5 Conclusion	18
4 Model calibration	19
4.1 Overview	19
4.2 Calibration procedure.....	19
4.3 Viscosity and roughness	20
4.4 Accuracy	21
4.4.1 Measurement accuracy.....	21
4.4.2 Modelling accuracy	21
4.4.3 Uncertainty due to natural variability.....	22
4.5 Harmonic analysis of the tide	23
4.6 Residual sediment transport	30
4.7 Conclusion	34
5 Input reduction.....	35
5.1 Overview	35
5.2 General remarks	35
5.3 Tide reduction	37
5.4 Wind reduction	45

5.5	Wave reduction	52
5.5.1	OPTI.....	52
5.5.2	Climate table and transport formula.....	58
5.5.3	One dimensional model for longshore transport.....	59
5.5.4	Profile model for cross-shore transport.....	59
5.5.5	Hydrological year	60
5.6	Morphology modelling.....	60
5.6.1	Methods	60
5.6.2	Parameters and current limitations	67
5.6.3	Scaling up the time horizon.....	68
5.7	Conclusion	70
6	Modelling inlets and embayments	72
6.1	Overview	72
6.2	Tools for inlet stability.....	72
6.2.1	Inlet theory	72
6.2.2	Escoffier diagram	74
6.2.3	Tidal prism relationship.....	77
6.2.4	Stability criterion for longshore transport.....	78
6.2.5	Modelling.....	78
6.3	Tools for embayments and tidal flats	80
6.3.1	Bay beaches	80
6.3.2	Experience from modelling the Baai van Heist	82
6.3.3	Suspended transport formulations in 2D models	82
6.4	Conclusion	86
7	Modelling cross-shore profile development.....	87
7.1	Overview	87
7.2	Short term (1 day) : storm response.....	87
7.3	Medium term (1 year) : erosion and recovery cycles	88
7.4	Long term (>10 years) : sea-level rise and climate change	97
7.5	Very long term : geological profile development and stratigraphy	102
7.6	Conclusion	103
8	Modelling structures	105
8.1	Overview	105
8.2	Structure types	105
8.2.1	Overview	105
8.2.2	Thin dams	105
8.2.3	Dry points.....	106
8.2.4	Levees.....	106
8.2.5	Groynes.....	106
8.2.6	CDW.....	107
8.2.7	Variable bed roughness	107
8.2.8	Non-erodible layers.....	108
8.3	Modelling structures in Delft3D and in XBeach.....	108
8.3.1	Modelling tests	108
8.3.2	Structure comparison.....	108
8.3.3	Model comparison.....	110

8.4	Conclusion	111
9	Summary of proposed methodologies.....	112
	References	121
	Annex A – Residual sediment transport calculation	1
	Derivation	1
	Discussion.....	2
	Example	4
	Annex B – Mormerge installation.....	8
	Annex C – Script for time-varying morfac simulation in XBeach	10

List of tables

Table 1-1 : Overview of reports	1
Table 2-1 : Overview of some models available at the Belgian coast.	7
Table 3-1: Relative importance of processes for onshore transport, offshore transport and bar behaviour, as compiled from literature.	10
Table 3-2: Implementation of processes in a 2DH model in Delft3D and XBeach from the point of view of sediment transport, and their importance for bar behaviour	12
Table 4-1 : Proposed best accuracy of model results compared to measurements. Relative accuracy for 1m waves, 1m/s current, 4m tide.....	21
Table 4-2 : Estimated variability stemming from random sampling and averaging over 30min in instationary model results, for 1m waves, 45° approach angle, 1m/s current, 4m tide.....	23
Table 4-3 : Six basic astronomical tidal frequencies, their physical cause and approximate period.	24
Table 4-4 : Doodson numbers and relative amplitude in the equilibrium tide of the main diurnal and semidiurnal tidal constituents.	25
Table 5-1 : Full wind climate reduction, with wind direction equal to wave direction and wind speed calculated for each wave class.....	49
Table 5-2 : Modelled wave height and direction per wave class compared to the measured value at Westhinder, for a single linear regression for the wind speed (including all wave directions).....	50
Table 5-3 : Modelled wave height and direction per wave class compared to the measured value at Westhinder, for multiple linear regressions for the wind speed (one per wave direction).....	51
Table 6-1 : Stability of an inlet according to Bruun (1978). P : tidal prism, M : gross longshore transport	78
Table 7-1 : WTI calibration settings with the Groundhog Day release of XBeach.....	87

List of figures

Figure 2-1 : Extent of the fine Zuno model.	4
Figure 2-2 : Extent of the LTV model (green) nested in the coarse Zuno model. Figure from Dujardin et al.(2010a).	5
Figure 2-3 : Extent of the Zeebrugge model (blue) nested in the Kustzuid v4 model (green, left), and in the LTV model (green, right). Figure from Dujardin et al.(2010b).....	5
Figure 2-4 : Extent of the Optos BCS model (rectangular area). Figure from Dujardin et al.(2010a).....	6
Figure 3-1 : Example of mother grid (blue) and daughter grid (green) with domain decomposition.....	13
Figure 3-2 : Example of mother grid (blue) and daughter grid (green) with nesting.	14
Figure 3-3 : Adjustment length of suspended sand transport. Figure from Van Rijn (1993), see reference for description.	16
Figure 4-1 : XBeach base simulation 1 (full line) and 2 (same settings ; dashed line) on a cross-shore profile, showing the variability of model results.	23
Figure 4-2 : Example of tidal energy spectrum of the y- velocity component, as obtained with a Fast Fourier Transformation (FFT) on 2 months of model results with a sampling interval of 10min.	26
Figure 4-3 : Example of harmonic analysis results obtained with the T_TIDE toolbox.....	27
Figure 4-4 : Amplitude of tidal velocity components along major and minor axis.....	28
Figure 4-5 : Phase of tidal velocity components along major and minor axis, up to the 6 th diurnal band,	29
Figure 4-6 : Example of main contributions to residual sediment transport in Blankenberge (Belgium) due to interaction between tidal components	32
Figure 4-7 : Example of residual current computed over a one month period for the mother model in Simona (blue), the daughter model in Delft3D (green) and the measurements (red) at several data stations.	33
Figure 5-1 : Patterns of sedimentation and erosion in Willapa Bay, USA, from 1998 to 2003.	36
Figure 5-2 : Map of relative error in residual sediment transport magnitude caused by the combined simplification of all forcing processes in Willapa Bay.....	37
Figure 5-3 : Gross alongshore sediment transport in 14 times the 8 th tide (upper left), in the full neap-spring cycle (upper right), reduction error once scaled for the average transport ratio between the two (lower left) and tidal cycle (lower right). Solid discharges (no porosity), model results in Delft3D.	39
Figure 5-4 : Net alongshore sediment transport in 14 times the 8 th tide (upper left), in the full neap-spring cycle (upper right), reduction error once scaled for the average transport ratio between the two (lower left) and tidal cycle (lower right). Solid discharges (no porosity), model results in Delft3D.	40
Figure 5-5 : Comparison of net alongshore sediment transport (upper left), gross alongshore transport (upper right) and initial erosion-sedimentation (lower left) between 14 times the 8 th tide (x axis) and the full neap-spring cycle (y axis). Tidal elevation in lower right figure. Solid discharges (no porosity), model results in Delft3D.	41
Figure 5-6 : Gross alongshore sediment transport in 14 times the 9 th tide (upper left), in the full neap-spring cycle (upper right), reduction error once scaled for the average transport ratio between the two (lower left) and tidal cycle (lower right). Solid discharges (no porosity), model results in Delft3D.	42
Figure 5-7 : Net alongshore sediment transport in 14 times the 9 th tide (upper left), in the full neap-spring cycle (upper right), reduction error once scaled for the average transport ratio between the two (lower left) and tidal cycle (lower right). Solid discharges (no porosity), model results in Delft3D.	43

Figure 5-8 : Comparison of net alongshore sediment transport (upper left), gross alongshore transport (upper right) and initial erosion-sedimentation (lower left) between 14 times the 9 th tide (x axis) and the full neap-spring cycle (y axis). Tidal elevation in lower right figure. Solid discharges (no porosity), model results in Delft3D.....	44
Figure 5-9 : Correlation between measured wind direction and wave direction from 1994 to 2005, with the significant wave height in meters on the colour axis.....	46
Figure 5-10 : Correlation between measured wind speed at MOW0 Wandelaar and wave height at Westhinder, with the wave direction on the color axis.....	47
Figure 5-11 : Correlation between measured wind speed at MOW0 Wandelaar and wave height at Westhinder for sector WSW only, with the wave direction on the color axis.....	48
Figure 5-12 : Correlation between measured wind speed at MOW0 Wandelaar and wave height at Westhinder for sector NNE only, with the wave direction on the color axis.....	48
Figure 5-13 : Schematic view of the OPTI procedure for climate reduction.....	53
Figure 5-14 : Evolution of the weights of each wave condition (x axis) during the exclusion loop (y axis), for three OPTI procedures on the same input data, showing that it results in three different reduced wave climates.....	53
Figure 5-15 : Statistics of the reduced wave climate at each step of the exclusion loop (x axis), for three OPTI procedures on the same input data, showing that the error increases towards the end.....	54
Figure 5-16 : Gross alongshore sediment transport integrated over two tides with the full yearly wave climate (upper left), the reduced wave climate (upper right), reduction error as a percentage (lower left) and correlation graph (lower right). Solid discharges (no porosity), model results in Delft3D.....	55
Figure 5-17 : Net alongshore sediment transport integrated over two tides with the full yearly wave climate (upper left), the reduced wave climate (upper right), reduction error.....	56
Figure 5-18 : Erosion-sedimentation integrated over two tides with the full yearly wave climate (upper left), the reduced wave climate (upper right), reduction error as a percentage (lower left) and correlation graph (lower right). Model results in Delft3D (no initial smoothing of bathymetry).....	57
Figure 5-19 : Example of longshore transport contributions per wave class (direction on x-axis, height on y-axis) for several coastline orientations combined, with four different transport formulae. Case study at the Carrara coastline, Italy. Figure from Walstra (2011).....	59
Figure 5-20 : Example of simplification of wave time series. Figure from Walstra (2011).....	60
Figure 5-21 : Erosion-sedimentation pattern after one year of morphological changes in the Belgian coastal zone, showing a noise of ± 5 -10cm even after bathymetry smoothing.....	61
Figure 5-22 : Schematisation of the MorMerge process for morphological modelling with a reduced wave climate. Figure from Lesser (2009).....	62
Figure 5-23: Observed (upper) and modelled (lower) sedimentation/erosion from Nieuwpoort to the Zwin inlet (in cm/year averaged over 10 years).....	63
Figure 5-24 : Long-term sedimentation rates in Blankenberge estimated from measurements. Figure from Teurlincx <i>et al.</i> (2009).....	64
Figure 5-25 : Erosion-sedimentation pattern in Blankenberge after one year, computed in XBeach. Reference results.....	64
Figure 5-26 : Example of sedimentation pattern obtained with unsuitable time series of forcing parameters (storms coinciding with low water and clustered at simulation end).....	65
Figure 5-27 : Example of sedimentation pattern obtained with unsuitable time series of forcing parameters (small update interval). Erosion-sedimentation pattern after a year (left), cumulative sedimentation volumes (right).....	66
Figure 5-28 : Reduced wave climate corresponding to Figure 5-26 (left) and Figure 5-27 (right).....	66

Figure 5-29 : Critical morfac according to the criterion of Ranasinghe et al. (2011) on a simplified coast (surf zone at bottom) under a calm wave climate	68
Figure 6-1 : Typical configuration of a tidal inlet (Google Images, 2013; from the U.S. Department of Transportation website).	73
Figure 6-2 : Example of a coastal inlet and a tidal basin North of Cape Hatteras in the USA, with flood delta, ebb delta and channel system visible.....	73
Figure 6-3 : Schematic Escoffier diagram, from Van de Kreeke (1992). Cross-sectional inlet area on x axis, current velocity though inlet on y axis.....	75
Figure 6-4 : Example of the effect of a river discharge on the hydraulic condition (Stive and Lam, 2012)....	75
Figure 6-5 : Example of the effect of longshore transport on the sedimentary condition (Stive and Lam, 2012).....	76
Figure 6-6 : Example of an Escoffier diagram with river discharge : an inlet with strong river discharge always remains open. From Stive and Lam (2012).	77
Figure 6-7 : Scale cascade of the Coastal Tract concept (Cowell et al., 2003).....	79
Figure 6-8 : Example of parabolic shape model applied on a satellite image (from Hsu et al., 2010).....	81
Figure 6-9 : Example of application and limitations of the parabolic shape model on bay beaches in Mexico.	82
Figure 6-10 : Shape factor function as a function of the adimensional parameter $wsvh$	84
Figure 6-11 : Computed relaxation time scale as a function of grain size (hence fall velocity) in Delft3D (Galappatti formulation), in XBeach (constant shape factor) and in the simple expression derived from the Rouse-like equilibrium concentration profile. Sandy sediments in the Baai van Heist are comprised between 100 and 200 μm	85
Figure 7-1 : Eroded volume along the Belgian coast during the Sinterklaas storm, compared to measurements.....	88
Figure 7-2 : Steep profile after one year without groundwater.....	89
Figure 7-3 : Steep profile after one year with groundwater.....	90
Figure 7-4 : Steep profile with multiple sediment fractions horizontally distributed after a year, showing fines on the beach.....	91
Figure 7-5 : Steep profile with multiple sediment fractions uniformly distributed after a year, showing a net mass loss.....	91
Figure 7-6 : Influence of morfac on the evolution of the cross-shore profile of Bredene after 1 year.....	92
Figure 7-7 : Comparison of profile development (full line) and cross-shore transport (dashed line) using the WTI and default settings with morfac 3 on the Bredene profile (cross-shore transport is positive if onshore directed).....	93
Figure 7-8 : Comparison of profile development (full line) and cross-shore transport (dashed line) using the WTI and default settings with morfac 3 on the Knokke profile (cross-shore transport is positive if onshore directed).....	93
Figure 7-9 : Comparison of profile development (full line) and cross-hore transport (dashed line) using the WTI and default settings with morfac 3 on the straight profile with $d_{50}=0.3\text{mm}$ (cross-shore transport is positive if onshore directed).....	94
Figure 7-10 : Influence of grain size on the development of the Knokke profile in the first year	95
Figure 7-11 : Influence of grain size on the development of the Knokke profile after 3 year.....	95
Figure 7-12 : Long term evolution of the Bredene profile, showing the model spin-up time of about a year.	96
Figure 7-13 : Time evolution of the Bredene profile during 1 year	96

Figure 7-14 Evolution of the shoreface nourishment during the third year : profile (full lines) and cross-shore transport (dashed lines).....	97
Figure 7-15 : Steep profile with groundwater and multiple sediment fractions horizontally distributed, as in Figure 7-4 but after 10 years.	99
Figure 7-16 : Steep profile as in Figure 7-15 but with morfac 10 instead of 30.	99
Figure 7-17 : Coastline movement in simulations without and with sea level rise of 1 cm/year	100
Figure 7-18 : Relative coastline movement with sea level of 1 cm/year compared to a reference simulation without sea level rise, showing a stable to accretive trend hidden behind short-term noise.	100
Figure 7-19 : Bar migration at Noordwijk modelled with Unibest TC (Walstra et al., 2012).....	101
Figure 7-20 : Bar growth or decay (left) and bar migration (right) in Noordwijk as a function of water depth and wave direction (Walstra et al., 2012).	102
Figure 7-21 : Barrier island formation with the geological model Barsim (source : CSDMS website)	102
Figure 7-22 : Inverse simulation of coastal stratigraphy with the Barsim model (Storms et al., 2013)	103
Figure 8-1 : Schematisation of thin dams blocking the flow in V (left) and U direction (right, thick lines) compared to the locations of water level points (crosses), depth points (intersections between full lines) and velocity points (dashes). Figure from THV IMDC-Soresma (2010).	105
Figure 8-2 : Schematisation of a dry point (grey) compared to the locations of water level points (crosses), depth points (dots) and velocity points (dashes). Figure from THV IMDC-Soresma (2010).....	106
Figure 8-3 : Hydro- and morphodynamic equilibrium of the open channel case, showing the perfect agreement with the analytical solution (“no weir” legend). Model results in Delft3D.	109
Figure 8-4 : Comparison of the morphodynamic equilibria of the open channel case with 3m weir as a structure and as a hard layer, showing the good agreement between methods and the effect of increasing the weir crest height. Model results in Delft3D.	110
Figure 8-5: Delft3D (left) and XBeach results (right) of a simplified model of the port of Blankenberge, with its entrance channel and a submerged sloping groyne on each side.....	111

1 Introduction

1.1 The assignment

In the frame of the project “Scientific support for hydrodynamics and sand dynamics in the coastal zone” executed by IMDC for Flanders Hydraulics Research (specification WL/09/23), tools are being developed in order to help answering morphology-related questions for Flanders Hydraulics Research itself and the relevant governmental services. The present “lessons learnt” report is one of these tools.

1.2 Aim of the study

The objective of the present report is to provide a single reference document containing the lessons learnt during the project, about long term sand morphology modelling in the surf zone. It is based on the entire work carried out during the project, and draws examples from several cases investigated during this project, each having its specific report. Conclusions presented are valid for the Belgian coast, but are expected to remain applicable in most situations.

1.3 Overview of the study

Table 1-1 lists the reports written in the frame of this project.

Table 1-1 : Overview of reports

Reference WL / IMDC	Title
Literature review	
WL2010R744_30_2 / I/RA/11355/10.144/MIM	Literature review of physical processes
WL2011R744_30_3 / I/RA/11355/10.156/NZI	Literature review of models
WL2011R744_30_4 / I/RA/11355/10.157/JDW	Literature review of data
Blankenberge case	
WL2011R744_30_7 / I/RA/11355/11.055/NZI	Simplified Blankenberge case : Comparison of Delft3D and XBeach results
WL2012R744_30_18	Update of the sediment budget for the nearshore of Blankenberge-Zeebrugge
WL2012R744_30_17 / I/RA/11355/12.098/NZI/	Calibration of the Oostende-Knokke hydrodynamic and sediment transport model (OKNO)
WL2012A744_30_12 / I/RA/11355/12.048/NZI	Effect of a beach nourishment on the sedimentation of the entrance channel of the port of Blankenberge : Application of a simplified model for the Blankenberge area
WL2012R744_30_11 / I/RA/11355/12.049/lwa/NZI	Longshore modelling : realistic Blankenberge case
WL2013R00_063 / I/RA/11355/13.221/NZI	Toegankelijkheid haven Blankenberge: Optimalisatie van de haveningang
WL2013R13_105 / I/RA/11355/13.222/LWA/NZI	Energy atolls along the Belgian coast: Effects on currents, coastal morphology and coastal protection

Knokke case	
WL2013R12_107_1 / I/RA/11355/13.219/NZI	Inschatting van de morfologische impact van strandsuppleties te Knokke op het Zwin en de Baai van Heist
WL2015R12_107_2 / I/RA/11355/15.143/NZI/	Literature review coastal zone Zeebrugge - Zwin
WL2015R12_107_3 / I/RA/11355/14.175/LWA/NZI	Long term morphological model of the Belgian shelf: Calibration
WL2015R12_107_5 / I/RA/11355/15.145/NZI/	Advies suppletie Knokke – Effect op de morfologie van het Zwin en van de Baai van Heist: XBeach - modellering
Cross-shore modelling	
WL2015R00_072_13 / I/RA/11355/12.050/MIM/NZI	Evaluation of XBeach for long term cross-shore modelling
WL2015R12_107_6 / I/RA/11355/15.144/NZI/	Inventarisatie randvoorwaarden en morfologische impact Sinterklaasstorm (6 december 2013)
WL2015R12_107_4 / I/RA/11355/15.134/THL	Hindcast of the morphological impact of the 5-6 December 2013 storm using XBeach
Lessons learnt	
WL2015R00_072_19 / I/RA/11355/12.051/NZI/	Modelling tools and methodologies

1.4 Structure of the report

The report addresses the following main topics :

- Identification of data and models available (chapter 2)
- Lessons learnt about the model setup (chapter 3)
- Lessons learnt about the model calibration (chapter 4)
- Lessons learnt about the input reduction (chapter 5)
- Lessons learnt about modelling inlets and embayments (chapter 6)
- Lessons learnt about modelling cross-shore profile development (chapter 7)
- Lessons learnt about modelling structures (chapter 8)
- A summary of proposed modelling methodologies (chapter 9)
- Some specific tools presented in annex

2 Data and models available

2.1 Overview

This chapter presents a short general overview of data available at Flanders Hydraulics at the Belgian coast and of overall hydrodynamic North Sea models.

2.2 Data sources

De Winter et al.(2010) gives an overview of available data for coastal morphodynamic models. It concludes that following data are available :

- Long term water level, wave height and wind velocity recordings at various stations off- and onshore (up to 1970-2015 depending on parameter and dataset)
- Bathymetrical data of the Belgian Continental Shelf, measured over a few decades (measuring frequency depending on location, between 5 and 10 years)
- Yearly measurements of the beach and foreshore topography and bathymetry. These data are available digitally since 1997 and on paper for the period 1963 – 1996
- Analysis of changes in volume of the beach and foreshore
- At a few locations short term (months) recordings of current velocities

Also some short time (tide – week) specific measuring campaigns are available at beaches, recording velocities, sediment concentrations and a couple other parameters. Generally, these campaigns are under difficult circumstances and with complex measuring techniques. This can affect the quality of the data (e.g. for sand concentration measurements, strong vertical gradients make it necessary to record continuously the exact height above the bottom, which is not evident in the dynamic surf zone).

Zimmermann et al.(2012b) discusses some data quality issues with some velocity data from the measurement network Meetnet Vlaamse Banken (MVB).

Trouw et al.(2010) gives an overview of coastal processes related to sand dynamics and of some relevant research projects executed along the Belgian coast.

2.3 Models available

2.3.1 Overview

Three institutions are currently known to have models which can deliver offshore hydrodynamic boundary conditions (water levels, velocities) :

- Rijkswaterstaat : the ZUNO models (Simona, Delft3D code)
- MUMM : the mu-models, further developed into the Optos models (Coherens code)
- KULeuven : used as basis for the models from MUMM, not operational anymore

2.3.2 Zuno model (Netherlands)

The Zuno model covers the Southern half of the North Sea continental shelf and part of the English channel West of the Dover Strait. This model has been developed in the Netherlands to investigate issues on the Dutch coast. It is hence not necessarily calibrated perfectly for the Belgian coast. However since the Belgian coast is quite close to the Dutch coast compared to the model extent, the calibration should also be acceptable here. Boundary conditions are generated by nesting into a Belgian continental shelf model (CSM). The following tidal components have been imposed through the water level at the boundaries of the CSM : M2, S2, N2, K2, O1, K1, Q1, P1, NU2, L2, SA. This implies that all higher harmonics are generated inside the model domain of the CSM and Zuno model. Surges are modelled by including a HIRLAM wind field.

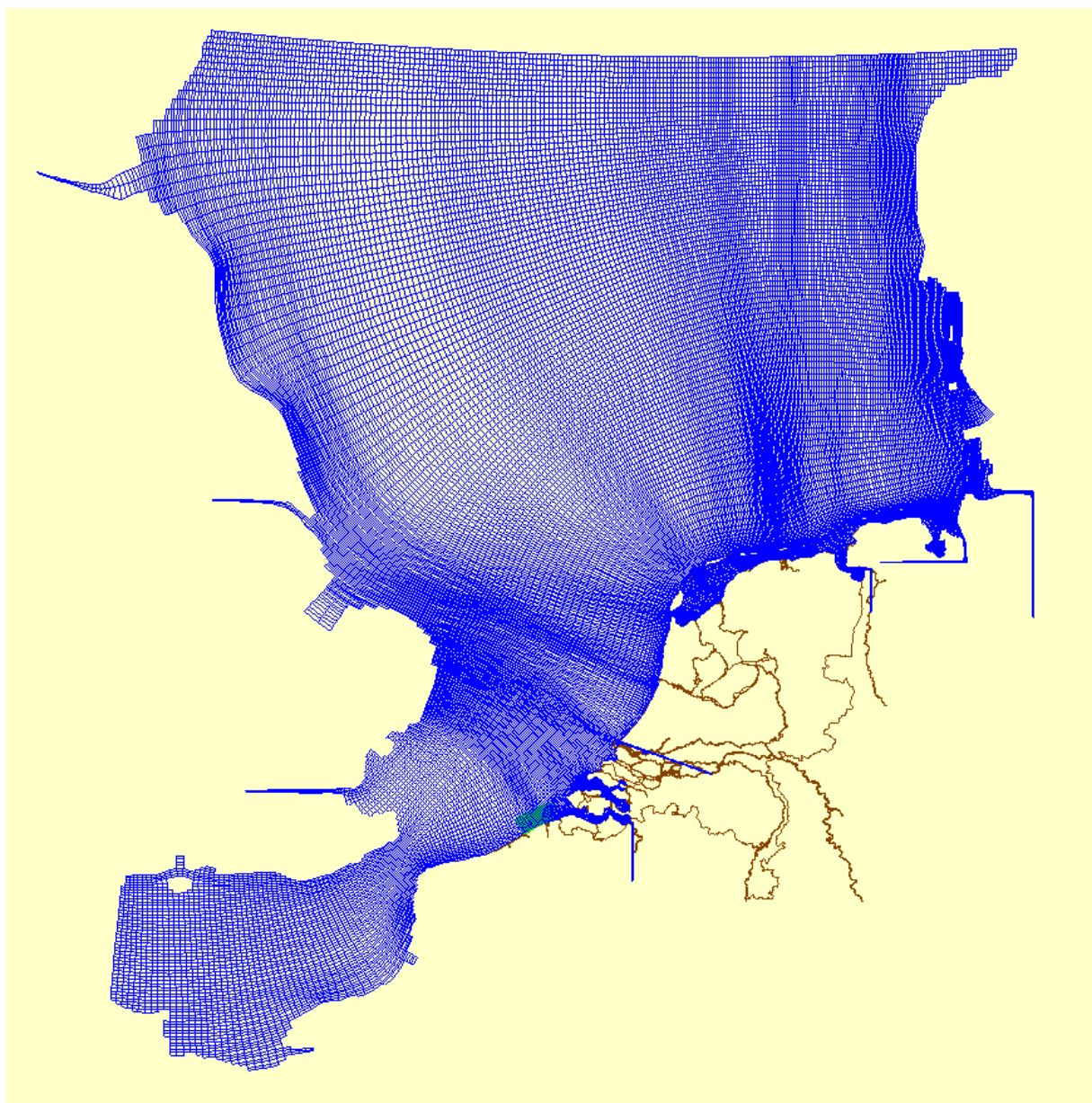


Figure 2-1 : Extent of the fine Zuno model.

Several versions of the Zuno model exist, both in the Netherlands and at Flanders Hydraulics. Flanders Hydraulics currently has a refined version of the model. However even the refined version is still relatively coarse near the Belgian coast (1.5 to 2km resolution nearshore, around 5km resolution in the coarse Zuno version), and probably too coarse to capture the circulation pattern in the mouth of the Westerschelde river. It hence ideally requires an intermediate model before realistic offshore boundary conditions can be generated near the Belgian coast.

The Zuno model has an additional limitation (Leyssen et al, 2012). The nesting into the CSM is done in the Netherlands with the script ModNST, which contains an error. This error is however compensated during the calibration via the roughness. Flanders Hydraulics on the other hand uses the Nesting (nesting) script, which is good but the error then comes from the suboptimal roughness. As a result the water levels at the Belgian coast obtained with the Nesting script are 10 to 20 cm lower than with ModNST and the M2 phase error increases from 5 to 10° (i.e. from 10 to 20min).

The Zuno model generates boundary conditions for several more detailed models developed at Flanders Hydraulics, such as the NEVLA and the LTV models in Simona (Western Scheldt and Belgian coast, 3D hydrodynamic ; Figure 2-2) the latter used in turn for the Zeebrugge model in Delft3D (Zeebrugge port, 3D hydrodynamic ; Figure 2-3). Figure 2-3 also shows the standalone model Kustzuid v4 which can also provide boundary conditions for the Zeebrugge model.

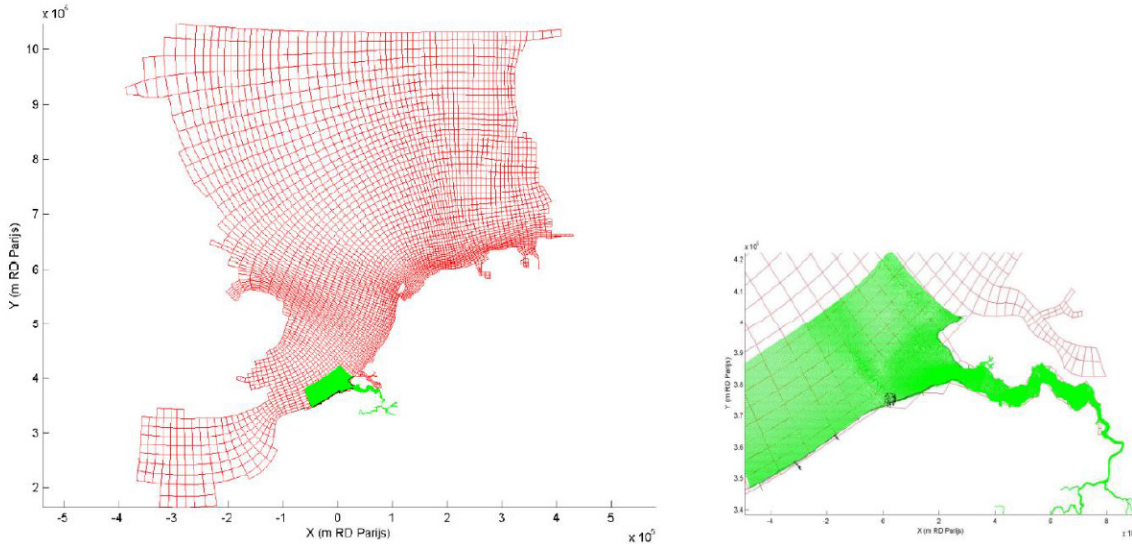


Figure 2-2 : Extent of the LTV model (green) nested in the coarse Zuno model.
Figure from Dujardin et al.(2010a).

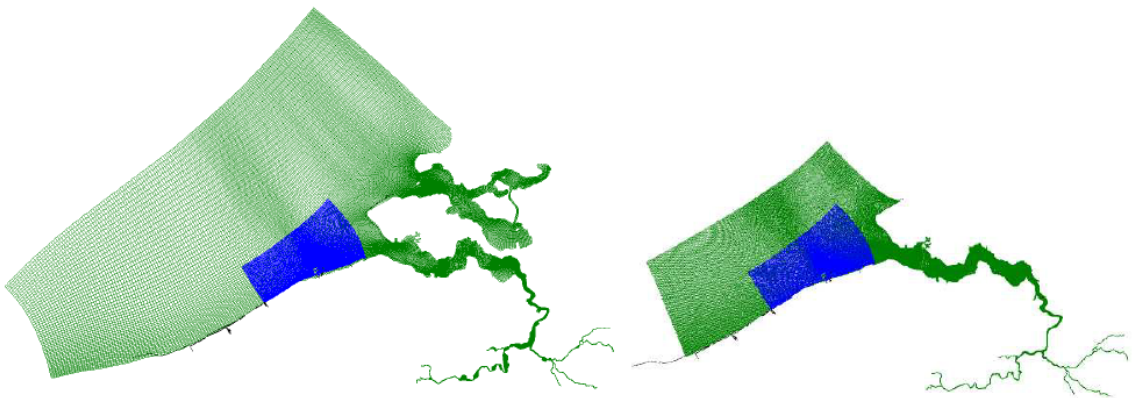


Figure 2-3 : Extent of the Zeebrugge model (blue) nested in the Kustzuid v4 model (green, left), and in the LTV model (green, right). Figure from Dujardin et al.(2010b).

2.3.3 Optos model (BMM / MUMM, Belgium)

The Optos set of models has been developed between 1990 and 1998 during the development of the hydrodynamic model Coherens v1. It consists of three models : OPTOS CSM for the entire European continental shelf, OPTOS NOS for the Southern North Sea (comparable to Zuno), and OPTOS BCS for the Belgian coast.

The largest of the three models, OPTOS CSM, is driven by astronomical boundary conditions for the water level. The most detailed of the three models, OPTOS BCS, is still large enough to provide boundary conditions for any detailed model along the Belgian coast (Figure 2-4). OPTOS CSM and OPTOS NOS are 2D while OPTOS BCS is 3D with 20 layers over the vertical and a horizontal resolution of around 800m.

An alternative version exists, OPTOS BCS-fine, which resolution is increased to 270m, but with only 10 layers over the vertical and with an Eastern boundary stopping at Vlissingen. In both versions the Scheldt river is only partly included.

The OPTOS model train has been extensively validated with over 400 velocity profiles (Fettweis et al., 2003).

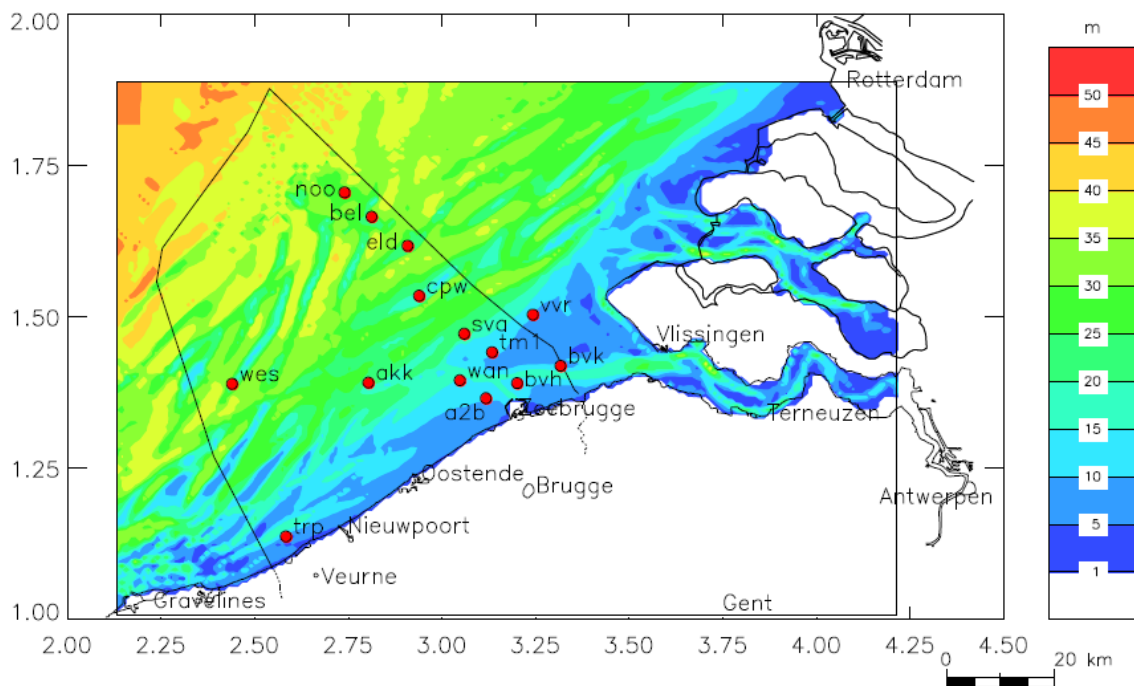


Figure 2-4 : Extent of the Optos BCS model (rectangular area).
Figure from Dujardin et al.(2010a).

2.3.4 Summary of model characteristics

Table 2-1 summarizes some main characteristics of numerical models available for the Belgian coast.

Table 2-1 : Overview of some models available at the Belgian coast.

Model	Extent	Resolution	Type	Boundary conditions
Zuno (Netherlands)	North Sea and English Channel	Several versions, 1.5 to 5km near Belgian coast	Several versions, 2D and 3D	From larger continental shelf model
Optos CSM (BMM/MUMM, Belgium)	European continental shelf	?	2D	Water levels with 4 diurnal and 4 semidiurnal tidal components
Optos NOS (BMM/MUMM)	North Sea and English Channel	Same as CSM	2D	From OPTOS CSM
Optos BCS (BMM/MUMM)	Northern France to Rotterdam, part of Scheldt	Coarse : 800m Fine : 270m	Coarse : 3D, 20 layers Fine : 3D, 10 layers	From OPTOS NOS
Kustzuid v4 (Flanders Hydraulics)	Northern France to Scharendijke (NL), Western and Eastern Scheldt included	800m near Belgian coast	2D, no salinity	Water levels with tidal components
LTV, NEVLA (Flanders Hydraulics)	Belgian coast and Western Scheldt	270m near Belgian coast	3D, 6 layers, salinity, wind	From Zuno (with wind)
Zeebrugge (Flanders Hydraulics)	Oostende to Cadzand	100-200m	3D, 6 layers, no salinity	From LTV

3 Model setup

3.1 Overview

This chapter discusses the choice and initial setup of a coastal model, with a particular focus on longshore transport, cross-shore transport and boundary conditions.

3.2 Data collection and analysis

Most applied modelling studies begin with the collection of data about the system considered. Data collection may encompass hydro-meteorological conditions, historical charts, literature, earlier projects, basically any kind of measured data and previous thinking effort about the same issue.

We would like to emphasize the benefits of spending sufficient time on data analysis. Causes of a particular behavior that the model will have to reproduce can often be deduced from available information. Data can often yield orders of magnitude of the importance of particular processes and help making decisions about model schematizations and assumptions. This preliminary data analysis is particularly important for morphological computations because brute force simulations are often not an option (Lesser, 2009). It should help to identify the spatial and temporal scales : data reduction will be affected by whether changes are due to long-term average processes or one-off events.

A model is in its essence nothing more than a set of complex calculations, based on numerous assumptions behind each model formulation. It does not seem to make much sense to carry out complex calculations without understanding what is going on. In that sense, some quick and 'simple' calculations can sometimes save a lot of time, for instance by reducing the number of sensitivity tests that will be carried out with the complex model and subsequently analyzed.

These simple calculations can be done with :

- experience,
- rules of thumb,
- or spreadsheets for instance.

Spreadsheets can be used to assess the variability of a given process computed with different formulations.

On the other hand a model can be used to :

- assess and verify hypotheses about system behavior,
- refine estimates,
- combine processes which cannot be done easily with simple calculations,
- and in some cases to verify that no important process has been forgotten.

A major advantage is that model output is visual thus far more informative. Measured data, simple calculations and complex modelling all belong together at each stage of the thinking process.

With regards to data collection, a clear distinction should be made between using a model for practical purposes or to investigate, say, the validity of formulations (research). The former generally only requires data about large scale effects (e.g morphological changes) while the latter requires very detailed information (e.g concentration profiles). Models used for forecasting often need to be fed continuously with data in order to correct the model by data assimilation.

3.3 Model choice

3.3.1 Model type

The model type should be chosen according to :

- Which processes are dominant based on the data analysis,
- Which processes could be dominant but cannot be verified with the current data,
- Which model type correctly models these processes (and is convenient).

By correctly modelling processes, we essentially mean whether the processes are present or not in the model, rather than which formulation has been used to model them. Differences in results between different formulations for a given process can be accounted for in the calibration. A model known to have good default values for its settings, if available, may be a good start.

In the framework of this project two models have been compared for nearshore application : the morphodynamic model Delft3D with a stationary wave module and the morphodynamic model XBeach with an instationary wave module. The reader is referred to Zimmermann et al.(2012a) and to Wang et al.(2012) for the model comparison focusing on longshore transport, and to Trouw et al.(2012) for cross-shore transport. Main findings are included in the next paragraphs.

3.3.2 Longshore transport

The theory behind longshore current generation is well-established and is based on the radiation stress of waves (Longuet-Higgins, 1970a,b). Waves approaching the coast with an angle refract and break. When breaking, waves transfer momentum to the water column, generating wave set-up (cross-shore component of radiation stress gradient) and a longshore current in the surf zone (longshore component of radiation stress gradient). This current is in equilibrium when the shear component of the wave force gradient is balanced out by the current-induced bottom shear stress. The current is maximum around the breaking depth, where wave breaking is the strongest, for an approach angle of around 45° at the breaker line.

The cross-shore profile of longshore current is hence a function on a first order of wave energy and approach angle, on a second order of wave breaking (roller), bottom friction and turbulent mixing (viscosity). All processes are accounted for in both Delft3D and XBeach, except for the roller model which is too simplistic and little convenient in Delft3D (Trouw et al, 2012). To allow the longshore current to propagate through the lateral boundaries, Neumann boundary conditions can be applied for the flow in Delft3D (see paragraph 3.4.2). If the velocity is imposed, it will take some distance for the longshore current (and transport) to develop (~km). To prevent local recirculations at the boundaries due to wave set-up, the keyword #CstBnd# can be used in Delft3D. XBeach does not display such issues because it already incorporates Neumann boundaries.

Results of longshore current are reasonably comparable between the two models, differences stem from different formulations for wave dissipation by bottom friction, instationarity of XBeach and sometimes numerical errors (Zimmermann et al, 2012a).

3.3.3 Cross-shore transport

The importance of cross-shore processes in cross-shore profile and bar growth modelling, and their implementation in XBeach and Delft3D, are reviewed in detail in Trouw et al.(2012). The main conclusions are presented below.

Physics

The relative importance of each process determines whether the sediment is transported onshore or offshore. It depends on the hydrodynamic conditions, which explains the seasonal variability of cross-shore profiles, which generally tend to be mild in the summer and steep in the winter.

Advances in bar growth modelling also pinpoint how easily a system can shift its morphological configuration (Walstra et al, 2011). This illustrates the delicate balance of large quantities.

Nevertheless, some processes appear more important than others. Table 3-1 judges the importance of each process for onshore transport, offshore transport and bar behaviour, as compiled from literature.

Less important processes are in red (minus), moderately important ones in yellow (equal) and the most important ones in green (plus). Some processes can contribute to both on- and offshore transport, some become particularly important for bar modeling.

Table 3-1: Relative importance of processes for onshore transport, offshore transport and bar behaviour, as compiled from literature.

Process	Onshore transport	Offshore transport	Bar behaviour
Stokes' drift	-		-
Return flow		++	++
Streaming	-		-
Wave asymmetry	+		+
Wave skewness	++		++
In- and Exfiltration	--	--*	--
Gravity		=	+
Turbulence	=	=	+
Wind stress	- ?	- ?	-
Fall velocity	-- ?	- ?	--
Bed forms	-	-	=
Long waves	-	++**	++
Wave roller			+
3D effects			- to ++

* except liquefaction

** indirectly via dune erosion (avalanching)

Modelling

For modelling purpose cross-shore transport can be reduced to a minimum number of dominant processes:

- Table 3-1 and attempts found in literature to model bar growth suggest that the dominant processes for onshore and offshore transport are respectively wave non-linearity (skewness in the shoaling zone, asymmetry in the surf zone) and the return flow (combined to turbulent mixing).
- Dune erosion by long waves and avalanching is critical to supply the underwater profile with sediment during storm and to create a bar. This in turn may require a robust drying and wetting scheme.
- The growth and migration of a bar is probably the most sensitive point since it requires sediment transport to converge on or around the top of the bar, directed onshore from the sea and offshore from the beach. The location of this convergence point in return strongly depends on the wave roller and on the concentration profile via turbulence, and possibly via bed forms and 3D effects. The wave direction has been shown to be of critical importance for the growth or decay of the bar (Figure 7-20 ; Walstra et al., 2012).

Based on these conclusions about physics, Table 3-2 summarizes which processes can be modelled with a 2DH model in Delft3D and XBeach. The following conclusions can be drawn :

- Delft3D is not suitable to model bar behaviour with a 2D model, primarily because dune erosion by long waves and offshore sediment transport by the return flow are not included. A 3D model has been shown to perform better (Brière and Walstra, 2006) but still misses dune erosion. XBeach on the other hand includes all main processes necessary to model bar behaviour, with the exception of the effect of vertical mixing by wave breaking turbulence on the relative importance of onshore-directed transport by wave non-linearity and offshore-directed transport by the return flow.
- In Delft3D, due to the way bed load and suspended transport have been implemented, wave-related transport in 2DH is always onshore and the only possible offshore-directed components are bed slope effects or suspended sediment diffusion. The return flow requires a 3D model. Since the bed slope effect scales on the bed load transport, if the wave-related scaling factors are set to zero, it is also zero. The diffusion component on the other hand is one to two orders of magnitude lower than the advection component, which explains why its effect is not visible (Zimmermann et al, 2012a).
- In addition, in Delft3D the default values for wave-related bed load and suspended load factors are too high and lead to an unrealistic steepening of the coastal profile. Values of 0 to 0.1 instead of 1 are suggested.
- The popular alternative approach of Bailard (1981) implemented in Delft3D in the transport formulae of Bijker (1971) may allow to get a tuneable balance between onshore transport by wave asymmetry and offshore transport by bed slope effects, however without return flow the physics of the model are still likely flawed.

Morphological simulations can also be sped up with a morphological acceleration factor, or morfac. The applicability domain of such a factor is however still debated. A morfac induces an amplitude and phase error in the propagation of a bed form (Ranasinghe et al, in prep). Although this error is generally an order of magnitude smaller than errors induced by the numerical scheme, it may be more critical to model bar growth and migration, because the exact location of the convergence of sediment transport is so important. It is hence advised to begin modelling without morfac whenever possible.

Table 3-2: Implementation of processes in a 2DH model in Delft3D and XBeach from the point of view of sediment transport, and their importance for bar behaviour (see also Table 3-1).

Process	Delft3D	XBeach	Bar behaviour
Stokes' drift	No	No	-
Return flow	No (hydrodynamics only)	Yes	++
Streaming	Yes (in bed load)	No	-
Wave asymmetry	No	Yes (in suspended load)	+
Wave skewness	Yes (in bed load)	Yes (in suspended load)	++
In- and Exfiltration	No	No (hydrodynamics only)	--
Gravity	Yes (correction of bed load transport)	Yes (correction of equil. concentration)	+
Turbulence	No	No	+
Wind stress	No*	No*	-
Fall velocity	No**	No**	--
Bed forms	Yes (predictor)	Limited (initial conditions only)	=
Long waves	No	Yes	++
Wave roller	Limited (not convenient)	Yes	+
3D effects	Limited (longshore current and wind only)	Yes	- to ++

* A wind field can be added but a 3D model would be required to model the cross-shore recirculation ; longshore flow forcing possible depending on flow boundary conditions used

** No intrawave lag effects, only underloading / overloading of suspended sediment

3.4 Boundary conditions

3.4.1 Resolution, nesting and domain decomposition

The grid resolution obviously has to be chosen such that the features or the area of interest are sufficiently well defined. This implies for instance a minimum of, say, 5 cells across a navigation channel, and ideally 10 cells across the surf zone (which width in turn depends on the bed slope and the applied wave height) or more if bars are present and are expected to migrate during the simulation.

Realistic boundary conditions are generally generated by a larger model by means of nesting or domain decomposition (DD). Satellite or time series measurements can be used at the boundaries of the largest model (typically a model of the Belgian continental shelf). Only nesting has been tried in this project, short remarks on DD are added below based on experience in other projects. The large grid will be called mother model and the small grid daughter model.

With domain decomposition, the daughter grid is basically a local refinement of the mother grid. Once the DD boundaries have been defined, both models act as one and only one simulation is required. The model setup is therefore easy. Disadvantages include a uniform time step in both mother and daughter model, a less flexible grid design, and in Delft3D some unexpected convergence issues if the time step is too large, possibly due to an explicit numerical scheme in the treatment of the DD boundaries.

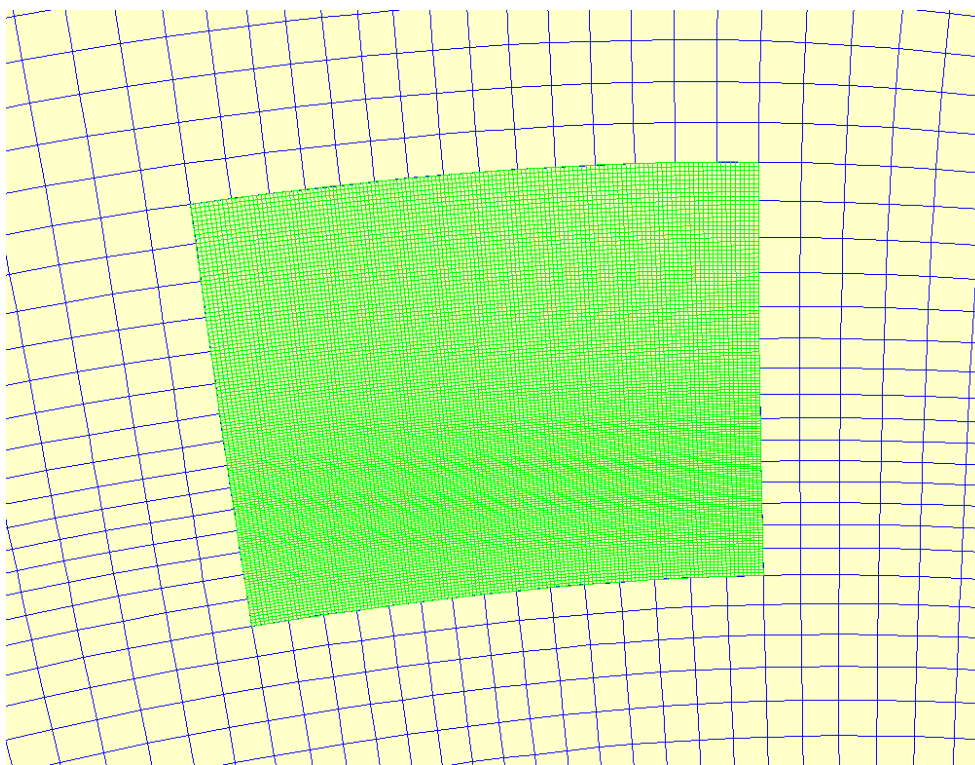


Figure 3-1 : Example of mother grid (blue) and daughter grid (green) with domain decomposition.

Nesting allows for a flexible grid design since the mother and the daughter grid are independent. However in Delft3D a nested run requires more steps than a DD model because the boundary conditions of the daughter model have to be generated. Another limitation particular to this model is that the nesting scripts of Delft3D do not allow the use of Neumann and Riemann boundaries (see paragraph 3.4.2). Both limitations can be circumvented with scripts, like the Nesting Tool developed for Simona and Delft3D models at Flanders Hydraulics. Nesting may save computation time if only the settings of the daughter model need to be varied and the boundary conditions only need to be generated once.

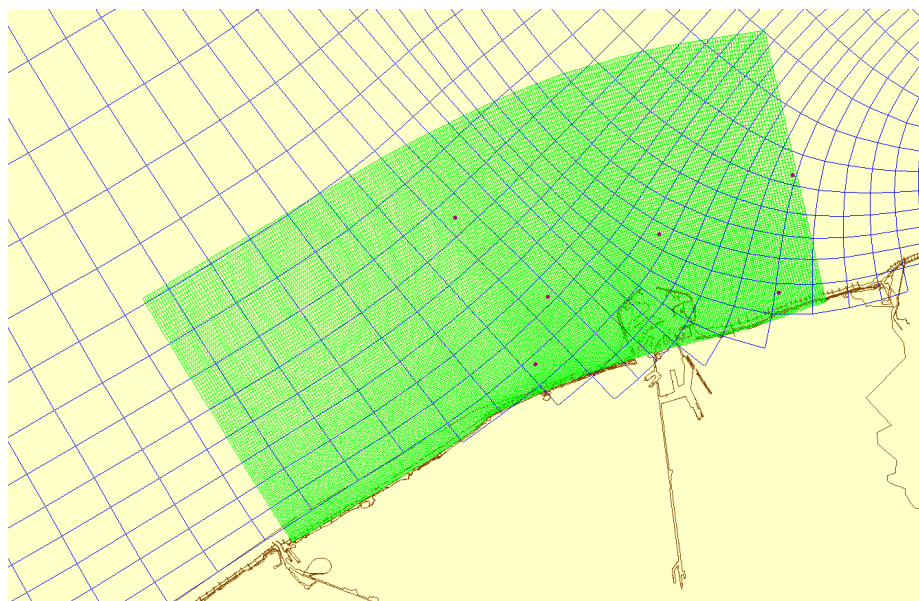


Figure 3-2 : Example of mother grid (blue) and daughter grid (green) with nesting.

XBeach does not have tools to do nesting or domain decomposition. However its boundary conditions can of course be generated by another model (for instance Delft3D) and applied manually.

3.4.2 Flow boundary conditions

The following boundary conditions are typically used depending on the situation (Delft3D example) :

- **Water level (W):** Water level and velocity are directly linked via the conservation of mass and momentum equations. When imposing the water level, deviation from measurements are likely to be higher for velocity.
- **Current (C):** Water level and velocity are directly linked via the conservation of mass and momentum equations. When imposing the velocity, deviation from measurements are likely to be higher for water level. Velocity vectors in Delft3D are always applied perpendicular to the boundary.
- **Riemann (R):** A Riemann boundary imposes a combination of water level and velocity. Its purpose is to impose a free propagation of the tidal wave rather than to impose its shape.
- **Neumann (N):** A Neumann boundary imposes the water level gradient. It is particularly useful when wind-driven current or longshore current has to be able to pass through the boundary. Control over the velocity is indirect via the water level slope and very sensitive to for instance jumps in the bathymetry. Segment-wise Neumann boundaries may create unphysical effects in the velocity field at the transition between segments, it is therefore suggested to either apply a single segment or a different time series at each grid cell along the entire boundary.
- **Flux (Q) :** A discharge combines the water level and the velocity without imposing any of them directly. It should have advantages similar to Neumann boundaries. It is often used to model rivers to make sure the correct amount of fresh water enters the domain.

XBeach has little choice for boundary conditions because it focuses on local surf zone applications. Neumann boundaries or walls are the standard options for lateral boundaries.

To keep some control over the model results, it is advised to include at least partly some water level and some velocity component in the choice of the boundary conditions, with an emphasis on the velocity component. Generally speaking, a small error in water level is often compensated by a large error in velocity. Although it has not been tested here, we suspect that a model with only water level boundaries may have large errors in the modelled velocity, because other model settings such as roughness and viscosity will never be perfect. The Delft3D manual does in fact advise against this option because the model would not be well-posed (Deltares, 2010a). It is more likely that the model is mathematically well-

posed but that the velocity is then purely dependent on the applied roughness. Conversely, a model with only current boundaries may display large errors in water level. In shallow water like on the Belgian coast, tidal propagation is very sensitive to roughness, which should ideally be the same in both mother and daughter grid before calibration.

For sediment transport and morphology modelling, it is more important to focus on the velocity because sediment transport is a power function of velocity. The water level on the other hand can influence wave energy dissipation, in particular in shallow water.

Tidal time series can also be specified as astronomical frequencies with a certain amplitude and phase obtained from a harmonic analysis. This is very practical if a particular tidal component needs to be scaled during calibration.

In Delft3D, current and water level boundaries can be specified with a reflection coefficient, which purpose it is to damp out unphysical oscillations during model spin up. The reflection coefficient aims to make these boundary types behave like a Riemann boundary. However if the model length is large enough (say 100km in this project), the period of the unphysical oscillations approaches that of tidal motion, and a reflection coefficient may lead to the undesired absorption of part of the tidal wave energy. In that case the reflection coefficient is best removed and replaced by a longer simulation time to account for spin up (say +1 day for tide), or by the use of a restart file.

The spin up time does not only depend on the tidal propagation. Simulations with salinity may require a spin up time of up to several months in estuaries, where mixing of salt and fresh water is slow. A restart file then becomes particularly handy.

3.4.3 Sediment transport boundary conditions

For sand transport, it is common to apply an equilibrium concentration condition at the boundaries because sand reacts fast to changes in current conditions (pick up and settling). Sometimes this assumption is not valid, like in zones of strong velocity gradient.

For mud transport it is important to obtain realistic boundary conditions, because the slow adaptation to changes in current conditions often results in sediment under- or overloading in the water column. The concentration in the water column can be quite different from the equilibrium concentration.

Van Rijn (1993) describes a criterion for sediment under- and overloading, and the adaptation length scale, to decide whether nested transport boundary conditions are required.

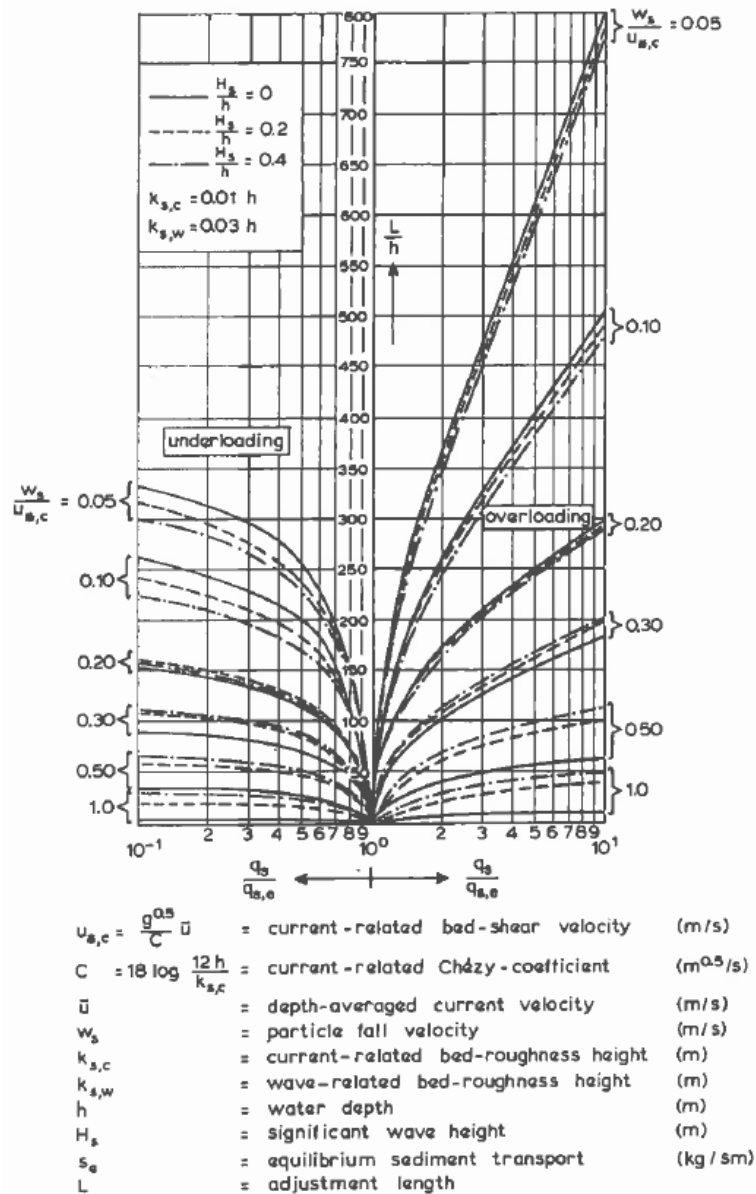


Figure 3-3 : Adjustment length of suspended sand transport.
 Figure from Van Rijn (1993), see reference for description.

With both types of boundaries, generally mass is not conserved within the model domain because it depends on the local current.

3.4.4 Wave boundary conditions

An existing wave model has been used in this project, so little attention has been focused on wave boundary conditions and calibration. Wave energy loss issues are however worth mentioning.

Waves leaving the model domain have by definition to be generated within the model domain. This seems obvious but it is important to realize that due to directional spreading, there will always be a part of the imposed spectrum which will go out of the model. This energy loss often explains differences between applied and observed / modelled wave height. It also results in triangular-shaped zones near the boundaries in which the wave height and direction are suboptimal. Wave conditions always need to be applied on all boundaries.

Dissipation processes other than breaking have the same effect. In shallow water like on the Belgian coast, wave energy loss by bottom friction (and to less extent by white-capping) quickly becomes important over a distance of several kilometers. In reality if the waves are locally generated (wind sea), the wind compensates at least partly this energy loss.

The only physically correct way to compensate these effects is to include wind and wave growth by wind in the model. A simple wind-wave correlation yielded in this project very reasonable conditions to compensate energy loss effects. If wind is excluded on purpose, it is advised to turn off wave dissipation by bottom friction and by white-capping. In earlier XBeach versions¹, a model which does not contain wave growth by wind, wave dissipation by bottom friction was turned off by default, possibly because it was then mainly used as a standalone model.

3.4.5 Light model setup

An alternative 'light' model setup can be used if the tidal current is known to propagate alongshore, with little ellipticity. Open boundaries of the type Neumann-Water level-Neumann (NWN) can be used to impose the alongshore tidal velocity with the water level slope.

In practice it means that a measured water level signal is imposed at the offshore water level boundary and that the phase lag and slope of the propagating tide between the two lateral boundaries are computed with the celerity of a shallow water wave (Deltares, 2010a). This option has been tested with a sinusoidal tide, is easy to implement and works well. However for tidal residual sediment transport it is critical that the real shape of the tide is imposed by using all main tidal constituents.

¹ possibly than the Easter 2012 version, to be verified

3.5 Conclusion

We advise the following concerning the model setup :

- It is important to spend sufficient time on data collection and analysis, including existing literature. Initial assumptions on the system behaviour will partly determine the model setup (time scale, spatial scale, model reduction). Input reduction, if needed, will also depend on it.
- The model type should obviously be chosen depending on the processes which should be reproduced. Delft3D is suitable for complex continental shelf models and can model reasonably well longshore transport, but it fails to model the coastline evolution and in 2D mode the cross-shore profile evolution due to missing processes (return flow, avalanching). XBeach may model well the cross-shore profile and the moving interface, but is limited in its extent due to limited boundary conditions, long computation time due to its explicit numerical scheme, and a couple of missing processes (wave growth by wind, triad wave-wave interaction). Instationary models like XBeach become important when important thresholds are present, like to model wave run-up, overtopping and inundation.
- Longshore transport is based on relatively simple physics (radiation stress), but is very sensitive to what happens in the surf zone (roughness, wave breaking). To allow the longshore current to propagate through the lateral boundaries, Neumann boundary conditions can be applied in Delft3D. This is the default option of XBeach. To prevent local recirculations at the boundaries due to wave set-up, the keyword #CstBnd# should be used in Delft3D. XBeach does not display such issues due to a different implementation.
- Cross-shore transport on the other hand is more complex. Literature generally agrees that some processes are more important than others. The balance between onshore transport by wave non-linearity (skewness in the shoaling zone, asymmetry in the surf zone) and offshore transport by the return flow (combined to turbulent mixing) determines how the profile evolves. Dune erosion by long waves and avalanching is critical to supply the underwater profile with sediment during storm and to create a bar.
- Bar growth and migration are highly sensitive to the location of the convergence point, which in return strongly depends on the wave roller and on the concentration profile via turbulence, and possibly via bed forms and 3D effects.
- Domain decomposition has the advantage of easy model setup but requires an equal time step in mother and daughter grid, which can affect computation time. Nesting allows a flexible grid design but requires extra scripts to automate the process (in Delft3D ; manual work in XBeach). The grid resolution should define sufficient well the features and areas of interest. We suggest for instance a minimum of 5 cells across a channel, and ideally 10 cells across the surf zone (width depends on bed slope and wave height).
- Concerning flow boundary conditions, it is advised to apply both a water level and a velocity component along at least a boundary section, because if one of the two is missing there will be little control on it. It is advised to focus more on velocity than on the water level, because it is more sensitive to a small error in water level than the other way round. Also, the velocity accuracy is more important for sediment transport computation. Neumann boundaries can be applied to let model-generated currents pass through, but since it is only based on the water level slope, the velocity is very sensitive to for instance jumps in the bathymetry near the waterline.
- For wave boundary conditions, especially in shallow waters like on the Belgian coast, wave dissipation is important and has to be compensated by wind growth. If wind is excluded on purpose, it is advised to turn off or reduce strongly wave dissipation by bottom friction and by white-capping. In earlier XBeach versions, a model which does not contain wave growth by wind, wave dissipation by bottom friction was turned off by default, possibly because it was then mainly used as a standalone model.
- For sediment boundary conditions, the concentration is generally in equilibrium with the flow for sand, but not for mud, for which nesting is required. The under- and overloading criterion of Van Rijn can be used to assess whether an equilibrium is present or not.
- It may be possible to set up a computationally light model which is still realistic with Neumann boundary conditions if the tidal current is known to propagate alongshore and if realistic water level time series are applied.

4 Model calibration

4.1 Overview

This chapter discusses the calibration procedure of flow and sediment transport, as well as the accuracy that can be expected from the model.

4.2 Calibration procedure

The confidence in model results obviously depends on the methodology and results of the calibration procedure.

Reproducing exactly a measured time series is very nice, but it is equally important that the calibration covers the entire model domain rather than a single point, and a large spectrum of different conditions. In fact some parameters, especially for sediment transport, can be so variable in the model domain and so sensitive to change that it is easy to compensate an error by another error. Multiple points improve the applicability of the model and help to identify the cause of deviation from measurements.

The objective of the calibration procedure is to prove that model results can be trusted. Three sub-steps have been identified :

- Verification : Verify that the nested model produces results which are equally or more realistic than the coarser model it is nested in. No data is needed for this step, these are the mathematics.
- Calibration : Compare the model results against data and modify realistically some boundary conditions or settings until a good agreement with the data has been reached. These are the physics.
- Validation : Compare the results of the calibrated model against a new set of data to verify its predictive capability.

During the verification, several sets of boundary types can be tested and results of the daughter model compared to those of the mother model. Results will invariably differ between the two because settings are never exactly the same : roughness and viscosity values for instance can be different, the bathymetry resolution is higher and includes new details. In addition, each boundary type has its own constraints which impact the calculated physics. Imposing the velocity for instance prevents wind and wave-driven residual currents to pass freely through the boundary (paragraph 3.4.2).

If both models do not agree well, it will make the calibration more difficult because usually the mother model used to generate the boundary conditions has already been calibrated itself. The mathematical cause of the deviation should be addressed, and this may sometimes imply to change some settings related to physics like the roughness and the viscosity. Paragraph 4.4 presents some examples of accuracies which can be expected from model results.

During the calibration, some settings related to physics will be varied until a good agreement with data is reached. We will argue here that the verification and calibration are closely linked together, because if settings need to be changed in one of the two phases, it will affect the second. There seems to be no way to avoid the iterative process. We therefore advise to address the two phases at once, that is :

- As a starting point, to match settings of the mother and daughter model as closely as possible (equivalent roughness and viscosity taking into account the change in resolution).
- In a second step, to compare the results of the mother model, the daughter model and the measurements all together, despite the fact that data is not needed for the verification. It can also help to identify when deviations between the mother and the daughter models have a physical origin.

Finally the validation is an independent step which attempts to make a forecast with the calibrated model.

The quality of the calibration procedure depends on the quantity and quality of available data. Comparison of results can be visual (time series) and refined with a harmonic analysis (flow) or a residual transport calculation (sediment transport). It is important to get the ellipticity of the tide right.

4.3 Viscosity and roughness

Two parameters will be discussed more in detail.

The viscosity is a numerical artifice introduced by modellers to simulate the transfer of momentum to adjacent grid cells by subgrid turbulence, which by definition cannot be resolved since it would become too computationally intensive. A full computation is the purpose of direct numerical simulation (DNS), which is used to study turbulence for instance. The viscosity is therefore a measure of the subgrid turbulence intensity in each grid cell.

It is usually not known, but the coarser the grid, the more important the fraction of unresolved turbulence and the higher the viscosity can be chosen. A reasonable viscosity estimate can be derived from a subgrid scale model (SGS), such as the Smagorinsky model, which relates the viscosity coefficient ν to the local grid resolution (CFD-Online, 2011 ; cell size Δ , velocity U , constant C_s) :

$$\nu = (C_s \Delta)^2 \frac{\partial U}{\partial x} = (0.2 * 10\text{m})^2 \frac{1\text{m/s}}{100\text{m}} = 0.04 \text{m}^2/\text{s}$$

SGS models might be particularly well-suited for grids with a strong spatial variation of the resolution. Typical, probably upper-limit values of viscosity may then be, say, $10\text{m}^2/\text{s}$ for a cell size of 1km , $1\text{m}^2/\text{s}$ for a cell size of 100m and $0.1\text{m}^2/\text{s}$ for a cell size of 10m .

A couple of techniques try to improve the modelling of turbulence intensity, in the most simple case with SGS models, in the best case with a full turbulence energy balance, such as in a wave roller model. Unfortunately such models also introduce new calibration parameters and most of the time too little data is available for calibration (numerous horizontal and vertical velocity profiles needed). It is therefore advised to keep it as simple as possible. The same philosophy applies to the diffusivity of scalars used in the transport of tracers and sediment.

The roughness is surprisingly similar to the viscosity. It is a measure of the energy dissipation due to subgrid variation in water depth, for all sizes of bed forms from the individual grains (skin friction) to the largest unresolved dunes (form drag). Theoretically it also includes, via the roughness length, a third contribution due to sediment transport, in which the high sediment concentration layer near-bed can to some extent be interpreted as a change in roughness height. Here again, generally very little is known about in situ roughness, so it is advised to keep it as simple as possible.

It is common practice to use the roughness as main calibration parameter for the hydrodynamics. There is nothing wrong with that, as long as it is based on physical considerations. It could be argued for instance that the area is known to have some dunes (increased roughness), or that the bed is muddy which means very flat (decreased roughness). A bed roughness predictor may help to quantify orders of magnitude of a realistic roughness.

Great care should be taken however on the impact of such a calibration in morphological models. The roughness directly impacts the bottom shear stress, which determines sediment transport. The roughness has a particularly strong impact in the surf zone because it is so shallow. Longshore current velocities up to 50% higher have been modelled when taking a lower Manning roughness which only slightly improved the calibration offshore. As a consequence, transport values in the surf zone were three times higher than measured. This was first dismissed as normal since confidence in transport formulae is low, which shows how easily it can be overlooked.

A space-varying roughness value has another negative side effect. It creates unphysical discontinuities in sediment transport, which result in local erosion and sedimentation hiding the natural evolution in the rest of the model domain. It is therefore strongly advised to not touch the roughness during the calibration of a morphological model if an alternative exists. Such an alternative could be the modification of the boundary conditions themselves rather than parameters within the model domain.

4.4 Accuracy

4.4.1 Measurement accuracy

For results interpretation, the uncertainty of various measurement techniques has been described in De Winter et al.(2011).

4.4.2 Modelling accuracy

The accuracy of model results is judged based on comparison with data. There is quite a lot of research going on about the quantification of modelling uncertainty. This would be a topic for a separate project, instead some general ideas are presented about which accuracies can be expected and where they stem from.

Table 4-1 proposes some commonly accepted (best) accuracies for various parameters with some justification below. Estimates are rather optimistic and some uncertainties like for the current velocity are much higher in the surf zone. Estimates are rather intended to be a guideline than reference targets.

Some measurements often have an accuracy which is lower than that of the model, especially in the surf zone where measuring is difficult. Note also that measurements and model results can only be compared properly when averaged with the same time parameters (sampling frequency and averaging period) and over the same spatial extent (part of the water column for ADCPs). The measured turbulence for instance depends directly on the sampling frequency and the averaging period.

Table 4-1 : Proposed best accuracy of model results compared to measurements.
Relative accuracy for 1m waves, 1m/s current, 4m tide.

Parameter	Good absolute accuracy at point in time	Good relative accuracy at point in time
Water level	±20cm	±5%
Velocity magnitude	±0.1m/s	±10%
Velocity direction	±10°	NA
Wave height	±20cm (low waves)	±5% (general)
Wave direction	±10°	NA
Sediment transport	uncertain	factor 2 to 10

Uncertainties resulting from model reduction can for example be understood as follows :

- Water level : Aside from the tide, the water level may fluctuate due to wind, wave and barometric set-up. The atmospheric pressure generally varies between 990 and 1030 hPa, with an average at 1013hPa. A variation of pressure by +1hPa decreases the water level by -1cm, hence a water level variation of ±20cm can be expected under normal circumstances if the pressure field is not modelled. The nearshore wave setup at the coastline can also be estimated easily from linear wave theory as $5/16 \cdot \gamma \cdot H$ (Holthuysen, 2010), where γ is the breaker parameter and H the wave height. The nearshore wave setup can reach up to a meter during large storms.
- Velocity : Along the Belgian coast an increase in alongshore wind speed by +1m/s results in a residual velocity increase of +1-2cm/s (Baeye, 2012). For 10m/s wind speed, the residual velocity would be in the order of 0.1-0.2m/s. Alternatively, in shallow water a variation of the bed level of say 25cm for a depth of 5m corresponds to a variation of the velocity by 5% due to mass conservation.

- **Velocity direction** : The velocity direction may be influenced by the vertical current structure, for instance in the surf zone by the combination of return flow and longshore current. The wind can also easily account for deviations. For a wind-generated residual current of 0.1m/s perpendicular to the tidal current of 0.5m/s, a deviation $\arctan\left(\frac{U_{wind}}{U_{tide}}\right)$ of around 10° can be expected.
- **Wave height** : Differences can arise depending on how the significant wave height is defined ($1/3^{\text{rd}}$ zero-crossing wave height $H_{1/3}$, spectral wave height H_{m0} , in the past visual wave height H_{vis}). Both model and instrument also use cut-off frequencies: waves above or below a certain frequency cannot be measured or are chosen not to be modelled. This is often the case for very short waves, which can under mild conditions account for a substantial fraction of the spectral energy, as well as for long waves in the surf and swash zone. Turbulence can also increase the wave height by up to 30% in very unstable conditions compared to the mean wind used in a stationary model (Cavaleri et al., 2007).
- **Wave direction** : For a realistic wind sea spectrum, possibly with a swell component, the definition of the wave direction is difficult to say the least. The wave direction depends on the weighting used (mean, median, peak direction, etc). The uncertainty may be estimated as a fraction of the directional spreading (30° spreading near Belgian coast), or due to wave-current interaction. With a wave with a phase velocity of 10m/s and a perpendicular current (gradient) of 1m/s, a deviation $\arctan\left(\frac{U_{current}}{U_{wave}}\right)$ of around 10° can be expected.
- **Sediment transport** : This parameter is generally out of control without calibration since it depends on the transport formula used, which may still yield strongly varying results (Zimmermann et al, 2012a). In addition, if sediment transport is a function of velocity at the power 3.4 (Soulsby-Van Rijn formula), an uncertainty in velocity of 15% implies an uncertainty in sediment transport of 60%. Note that this is still well within the generally accepted uncertainty in sediment transport formulae, of a factor 2 to 10 depending on the formula used.
- **Morphology** : The error on the sediment transport does not always impact the morphology, which in nature often converges towards a static or dynamic equilibrium. It will then depend on which processes determine the morphological equilibrium. The shape of a river delta for instance may depend on the balance between sediment transport from the river and longshore transport from waves. Channel sedimentation on the other hand is likely only dependent on sediment transport via the time scale at which the system evolves when it is out of equilibrium.

There is a simple way which may in some cases improve the accuracy of modelled water levels and velocities. The measurement period to be simulated can be chosen by performing a harmonic analysis on the data and deriving the residual time series (so excluding harmonic components). A period can then be selected where these residual time series are the most negligible. The uncertainty associated with the meteorological input will then be lower.

The uncertainty of a final calibrated model is typically estimated by doing a sensitivity analysis. Key parameters are varied between a lower and an upper bound which should be realistic values derived from the uncertainty of the input parameters.

4.4.3 Uncertainty due to natural variability

Uncertainties can also be understood as resulting from natural variability. In the instationary model XBeach, model output of waves and currents has to be averaged over a certain period to yield meaningful results. This period should be long enough to contain enough short and long waves, but short enough to not be influenced by the varying tidal water level.

A test has been done in Zimmermann et al.(2012a) to quantify the uncertainty due to natural variability. A base model has been run twice with the exact same model settings to assess the variability of instationary model results. The only difference between the two simulations is the random time series of long waves applied at the boundary. Figure 4-1 shows an example of the variation of results with an instationary model, two different random time series generated from the same wave parameters, and an averaging period of 30min for the output. Table 4-2 shows the resulting estimated variability. Results suggest that in any case it is not possible to do better than the model accuracy of Table 4-1, simply because measurement data also results from averaging over a given period (typically 20min for waves).

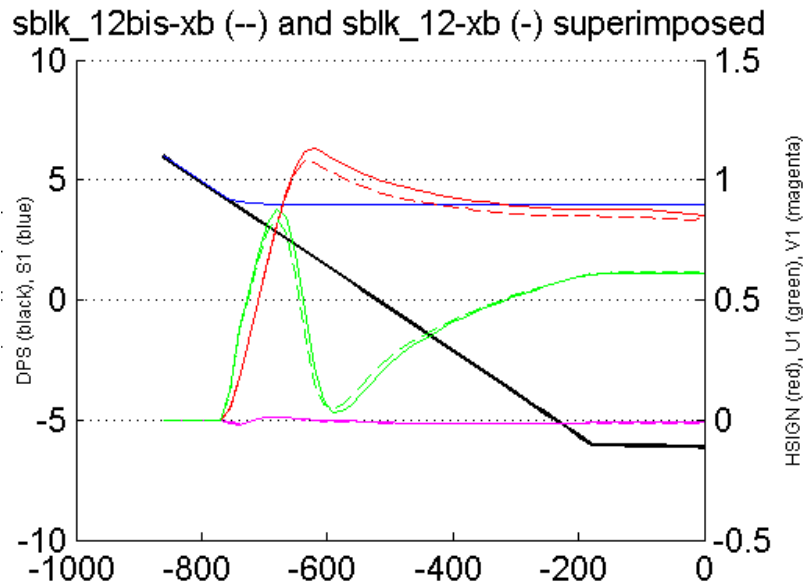


Figure 4-1 : XBeach base simulation 1 (full line) and 2 (same settings ; dashed line) on a cross-shore profile, showing the variability of model results.

Table 4-2 : Estimated variability stemming from random sampling and averaging over 30min in instationary model results, for 1m waves, 45° approach angle, 1m/s current, 4m tide.

Parameter	Estimated absolute variation	Estimated relative variation
Wave height H	±5 cm	±5%
Wave direction θ	±4 °	±10%
Longshore current	±0.05-0.1 m/s	±5-10%
Cross-shore current	±0.01-0.02 m/s	±10-15%
Total longshore transport	±0.5*10 ⁻⁴ m ³ /s/m	±20%
Total cross-shore transport	±1*10 ⁻⁵ m ³ /s/m	±20%

4.5 Harmonic analysis of the tide

An harmonic analysis consists in the decomposition of a signal, here from the tide, in the frequency space. It assumes, similar to a wave spectrum, that the tidal wave is the superposition of several sinusoidal functions of different frequencies. Contrary to the more complex case with waves, this spectrum is not directional and the basic astronomical frequencies driving the tide are known.

Any frequency in the tidal spectrum is the combination of at most six basic astronomical frequencies (Doodson, 1921 ; Pugh, 1987) as described in Table 4-3. Contributions of other stars are negligible. Any other frequency arises from the interaction of these six basic frequencies and is called an overtide. The weights of the basic frequencies in a given tidal component are integers called the Doodson numbers.

Table 4-3 : Six basic astronomical tidal frequencies, their physical cause and approximate period.

Name	Frequency	Period	Physical cause
ω_1	14.5 °/h	24h50min	Rotation of the Earth around its axis*
ω_2	0.55 °/h	27 days	Rotation of the Moon around the Earth
ω_3	0.041 °/h	365 days	Rotation of the Earth around the Sun
ω_4	0.0046 °/h	8.9 years	Precession of the Moon's perigee
ω_5	-0.0022 °/h	18.6 years	Precession of the Moon's plane of orbit
ω_6	$1.96 \cdot 10^{-6}$ °/h	21 000 years	Precession of the perihelion

* more precisely the advance of the Moon's longitude, which includes a correction for the displacement of the Moon and the Sun during a day

In literature tidal components are mostly denoted with a letter followed by a number indicating the diurnal band to which it belongs (2 for twice a day, 7 for seven times a day...). The component M2 for instance is the most important semi-diurnal component, the tide twice per day as we know it in Belgium. Table 4-4 gives an example of the Doodson numbers of some common semi-diurnal and diurnal components.

Table 4-4 : Doodson numbers and relative amplitude in the equilibrium tide of the main diurnal and semidiurnal tidal constituents. Table from Hoitink et al.(2003). i_a to i_f correspond to the basic frequencies ω_1 to ω_6 .

	i_a	i_b	i_c	i_d	i_e	i_f	H ($M_2 = 1$)
$2Q_1$	1	-3	0	2	0	0	0.011
σ	1	-3	2	0	0	0	0.013
Q_1	1	-2	0	1	0	0	0.079
ρ	1	-2	2	1	0	0	0.015
O_1	1	-1	0	0	0	0	0.415
M_1	1	0	0	-1	0	0	0.012
M_1	1	0	0	0	0	0	0.007
M_1	1	0	0	-1	0	0	0.033
Ψ_1	1	0	2	-1	0	0	0.006
π_1	1	1	-3	0	0	1	0.011
P_1	1	1	-2	0	0	0	0.193
S_1	1	1	-1	0	0	0	-
K_1	1	1	0	0	0	0	0.399
K_1	1	1	0	0	0	0	0.185
λ	1	1	1	0	0	-1	0.005
φ	1	1	2	0	0	0	0.008
θ	1	2	-2	1	0	0	0.006
J_1	1	2	0	-1	0	0	0.033
OO_1	1	3	0	0	0	0	0.018
$2N_2$	2	-2	0	2	0	0	0.025
μ_2	2	-2	2	0	0	0	0.031
N_2	2	-1	0	1	0	0	0.192
ν_2	2	-1	2	-1	0	0	0.036
M_2	2	0	0	0	0	0	1.000
λ_2	2	1	-2	2	0	0	0.007
L_2	2	1	0	-1	0	0	0.028
L_2	2	1	0	1	0	0	0.007
T_2	2	2	-3	0	0	1	0.027
S_2	2	2	-2	0	0	0	0.465
R_2	2	2	-1	0	0	-1	0.004
K_2	2	2	0	0	0	0	0.087
K_2	2	2	0	0	0	0	0.040

An harmonic analysis can be done in two ways : with a mathematically correct direct or fast Fourier transformation (DFT, FFT) or with a more practical least square equation (LSE). In both cases it is possible to get the signal back by a reverse process, and the frequencies which can be resolved in a time series both have a lower and an upper bound :

- The Rayleigh criterion states that the lowest frequency which can be detected (ω_{min}) is limited by the duration of the time series. The largest wave period which can be resolved (T_{max}) is at most the duration of the time series (T_{obs}) :

$$T_{max} < T_{obs} \quad or \quad \omega_{min} = \Delta\omega > \frac{2\pi}{T_{obs}}$$

In practice an observation duration of 1 month is generally sufficient : with $\Delta\omega = 0.5$ °/hour only few important components are not resolved and their contribution is aggregated into the nearest frequency. Common components close to each other are for instance (K1,P1), (N2,NU2) and (S2,K2).

- The Nyquist criterion states that the highest frequency which can be detected (ω_{max}) is limited by the data acquisition frequency. The smallest wave period (T_{min}) has to be at least twice the measurement time step (Δt_{obs}) in order to resolve at least half a wave length :

$$T_{min} > 2\Delta t_{obs} \quad or \quad \omega_{max} < \frac{\pi}{\Delta t_{obs}}$$

In practice a data sampling interval of at least 1 hour is generally sufficient : with $\omega_{max} = 1/2$ hours, components up to the 12th diurnal band are resolved. Higher frequencies are however possible in some complex river and estuarine situations. In most of the cases no energy is found back at the 12th diurnal band.

A harmonic analysis can be done on any signal. In particular since there is a strong relation between water level and current velocity, it can be done on the x and y components of the current velocity (interpretation may be easier if it is split between major and minor axis of the current ellipse). Results of a harmonic analysis also contain any constant or periodic local effect, such as a tidal eddy, residual currents like longshore, river or wind-induced current and possibly weather effects like surges. Irregular local effects can sometimes be filtered out.

The FFT method is simply a time-saving recursive use of the DFT and can be done with Matlab for instance. A FFT decomposes the tidal signal on the entire frequency spectrum as defined above. The frequency interval is defined by the Rayleigh criterion. Figure 4-2 shows an example of a tidal energy spectrum obtained with a FFT, showing clearly the presence of the bulk of the energy around the M2 component and the presence of overtides, in particular at the even diurnal bands. A spectrum obtained from measurements typically shows more noise, in particular for low frequencies since the inaccuracy is highest for few resolved periods.

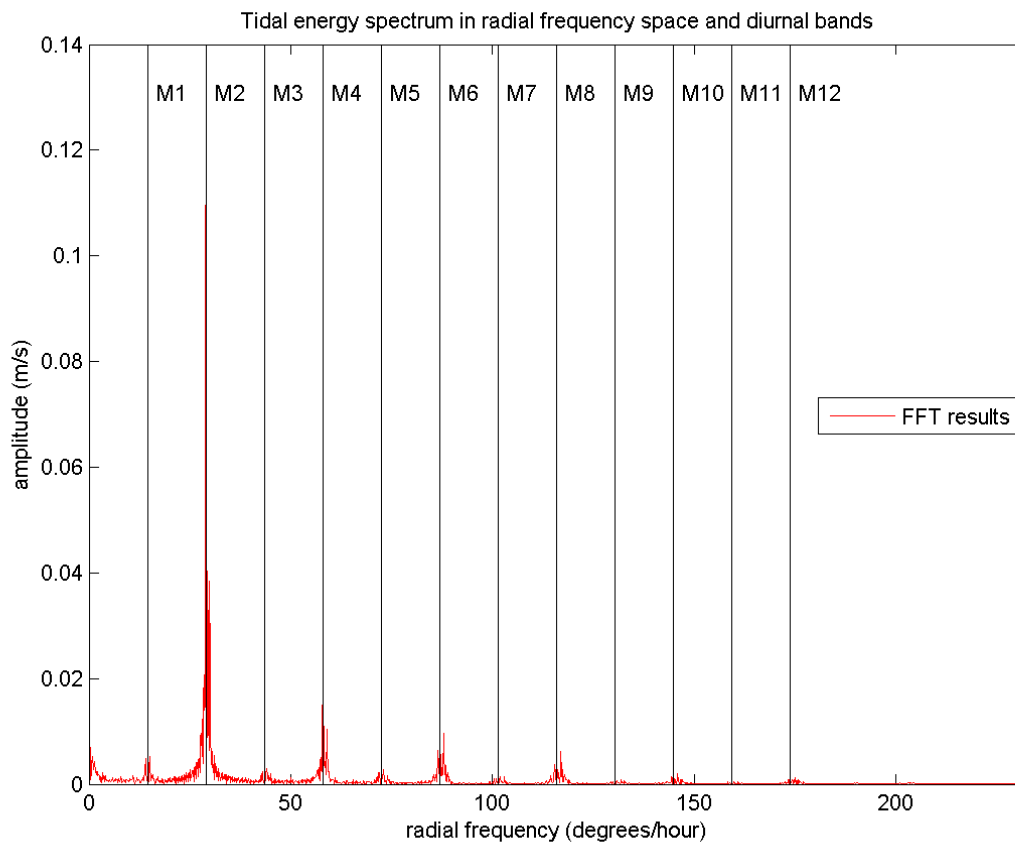


Figure 4-2 : Example of tidal energy spectrum of the y- velocity component, as obtained with a Fast Fourier Transformation (FFT) on 2 months of model results with a sampling interval of 10min. Vertical lines indicate the diurnal energy bands M1 to M12.

The FFT allows to see at a glance where the energy is located in the tidal spectrum. The FFT has however some major drawbacks : to get amplitudes it is still necessary to integrate the spectrum around a particular component. For this reason the more practical LSE method is generally used because the base frequencies are known.

The LSE method determines the amplitudes and phases of a tidal signal for a given set of components by least square minimization, and can be done with the T_TIDE toolbox for Matlab for instance (Pawlowicz, 2002). T_TIDE can determine a complete set of components based on the Rayleigh criterion, filtering out components too close to each other to be distinguished. Otherwise the most important components have to be known beforehand to be sure not to forget some. The amplitudes and phases are more meaningful and comparable than with the FFT method. T_TIDE also allows to filter out irregular background signals and to

get an uncertainty estimate. The mean current is not calculated but it is present in the residual signal which can be derived by subtracting the recomposed time series from the original signal (Figure 4-3).

Figure 4-4 and Figure 4-5 give an example of a harmonic analysis with T_TIDE for components determined by T_TIDE itself. Results are very similar if the components are provided to T_TIDE, but there might be some slight differences for components of negligible amplitude and the most energetic components are not always the most well-known ones (4th and 6th diurnal bands here). For these reasons it is advised to let T_TIDE determine the necessary components.

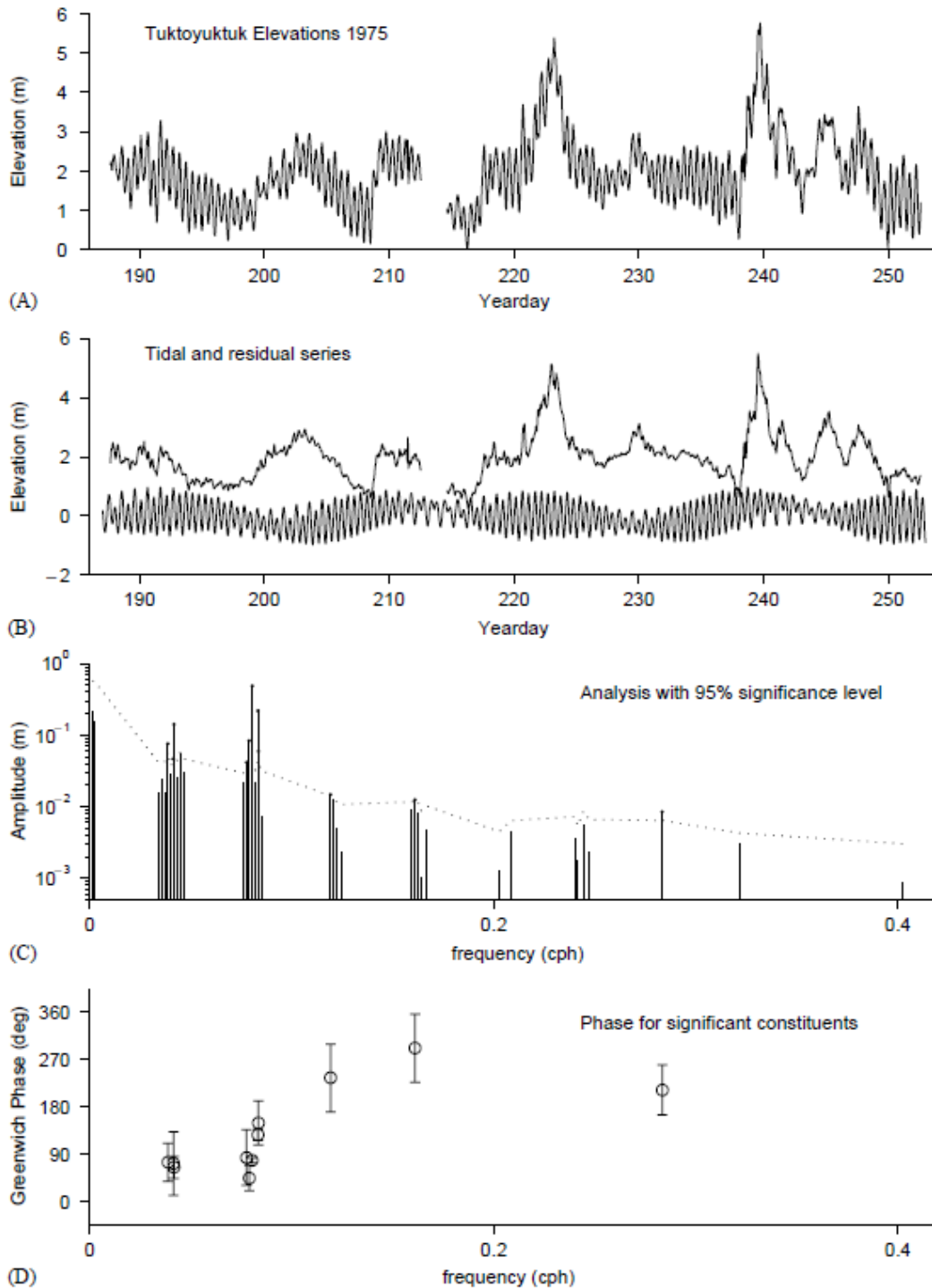


Figure 4-3 : Example of harmonic analysis results obtained with the T_TIDE toolbox : (top) original signal, (A) decomposed into tidal and residual signals, (B) constituents in frequency space and (C) phases in frequency space. Figure from Pawlowicz (2002).

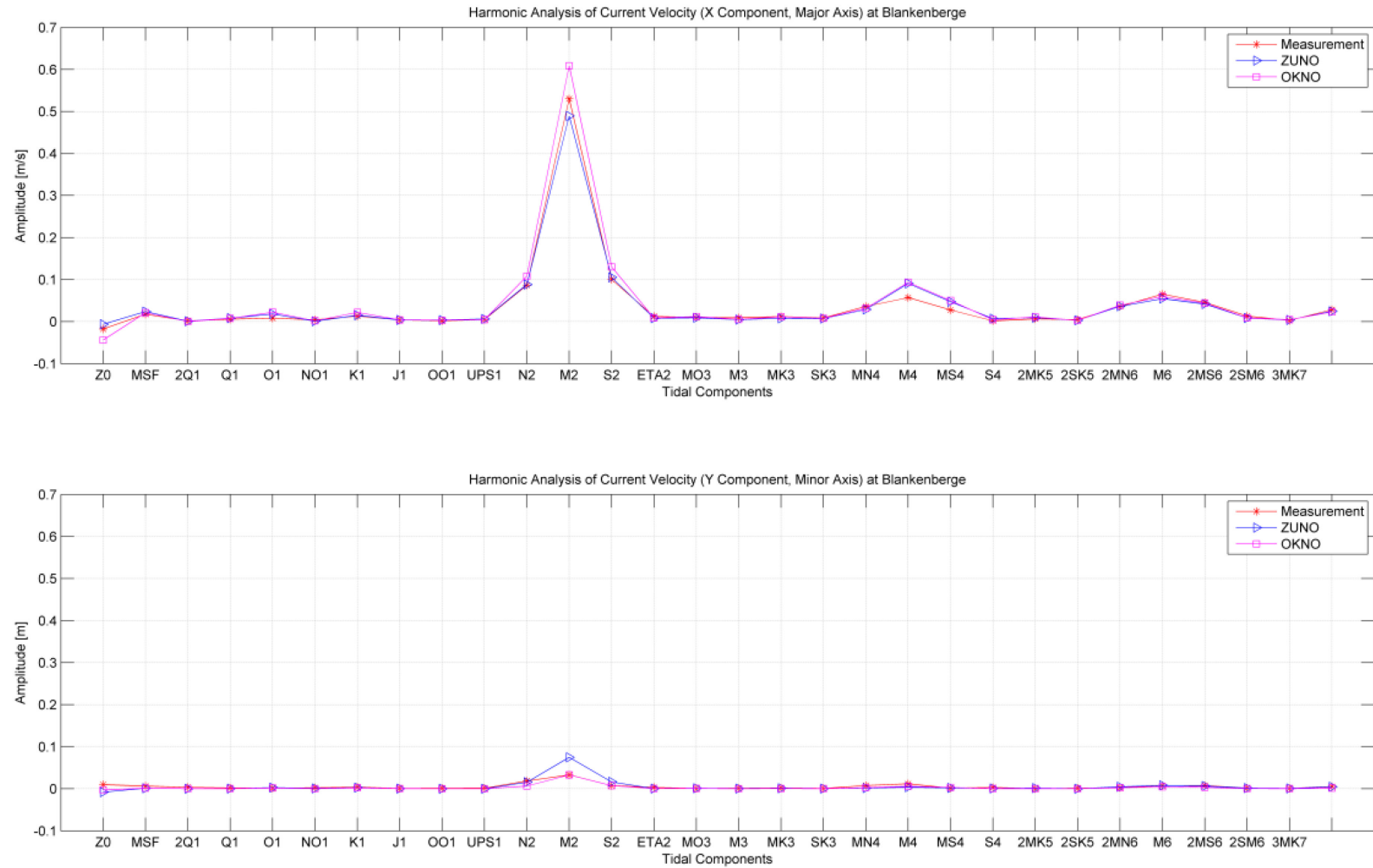


Figure 4-4 : Amplitude of tidal velocity components along major and minor axis , up to the 6th diurnal band, at Blankenberge tripod for measured data (red), Zuno model results in Simona (blue) and OKNO model results in Delft3D (magenta). Components determined by T_TIDE.

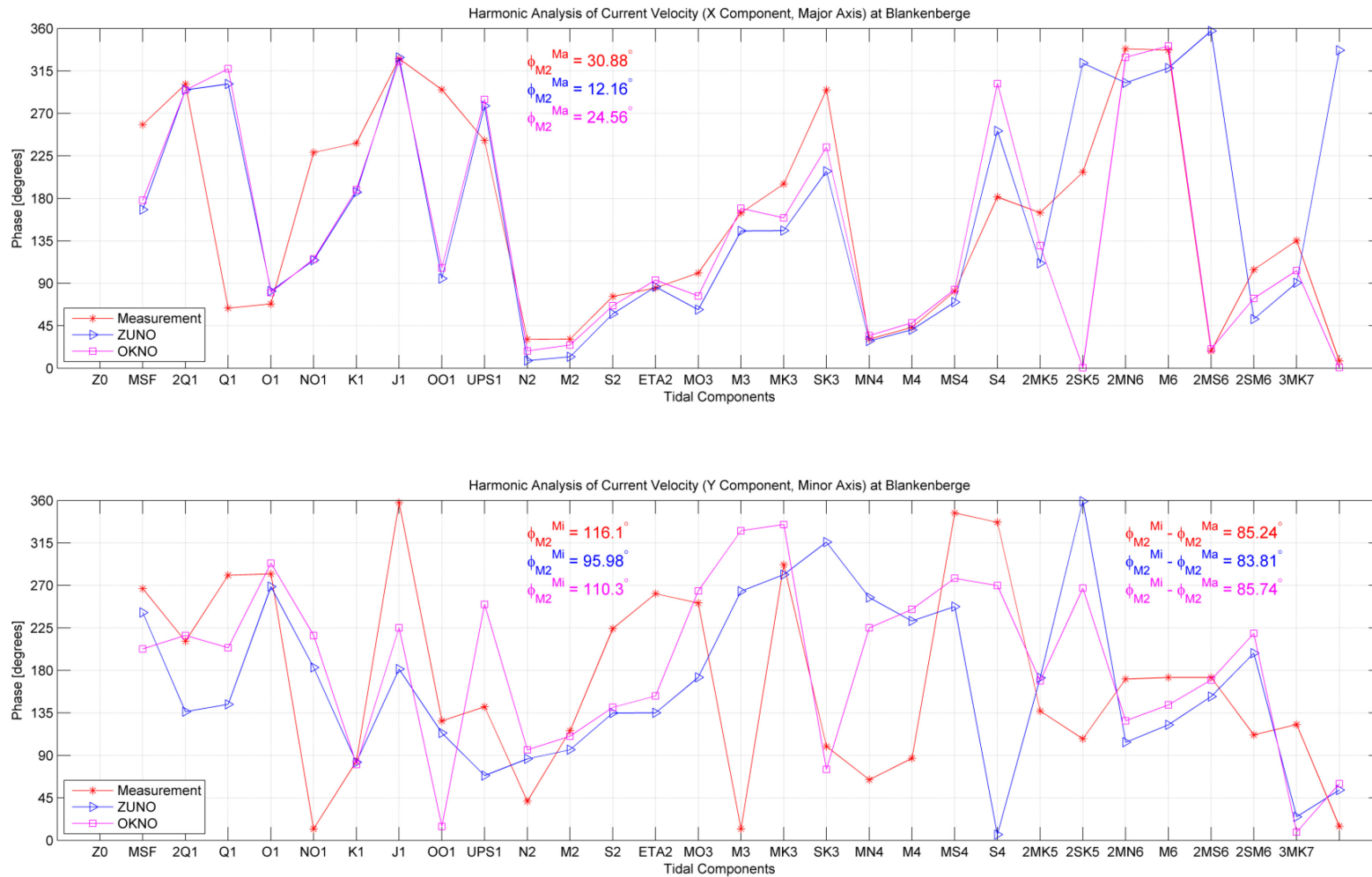


Figure 4-5 : Phase of tidal velocity components along major and minor axis, up to the 6th diurnal band, at Blankenberge tripod for measured data (red), Zuno model results in Simona (blue) and OKNO model results in Delft3D (magenta). Components determined by T_TIDE. Note the lack of phase agreement for components of negligible amplitude.

The results of the LSE harmonic analysis are independent of the components selected, except when components are too close to each other and cannot be resolved, and sometimes when the amplitude of a component is very small, hence more of an error than an important component.

Except some particular application (Roelvink and Reniers, 2011), the FFT method is not very useful for morphodynamic modelling. It should be more useful for other types of signals for which energetic frequencies are not known a priori, like a wave spectrum. It could also be used to identify energy at levels higher than the 12th diurnal band, but this would always be considered as noise in morphodynamic modelling.

4.6 Residual sediment transport

When calibrating a model for sediment transport, the difficulty lies in the fact that net transport data is generally not available. It is easier to measure the sediment concentration and the current velocity independently than a sediment flux. This may work well for river situations, but it becomes difficult in a tidal environment, since the net transport results from the difference between two large quantities. In that case the shape of the tide becomes particularly important.

Several studies have attempted to measure how well a model reproduces the net sediment transport by using an harmonic analysis. The idea is that if sediment transport can be approximated by a certain power of the current velocity, it is possible to identify which tidal components contribute to the net sediment transport, and to focus the calibration on those particular components.

Van de Kreeke and Robaczewska (1993) suggest, based on a study of the Ems-Dollard estuary in Germany, that the long-term residual transport is mainly a function of the residual current Z0 and the interaction of the M2 tide with its even overtides only (M4, M6, etc). Other important components such as S2 result in periodic net transport at the beat frequency of (here) S2 and M2. Hoitink et al.(2003) show however that due to the decomposition of any tidal component on six basic frequencies, some components other than direct overtides of M2 may also interact with a beat frequency of zero, as for instance (K1,O1,M2).

Van de Kreeke and Robaczewska (1993) assume that M2 is the dominant component and that all other components are an order of magnitude lower. They compute the residual transport q as a simple time-averaged power function of the velocity u, itself a function of velocity amplitudes A_k and phases α_k of each component k :

$$\begin{aligned} \langle q \rangle &= f \langle u^3 \rangle \\ \langle u^3 \rangle_{\infty} &= \lim_{T \rightarrow \infty} \left(\frac{1}{T} \int_0^T u(t)^3 dt \right) \\ \langle u^3 \rangle_{\infty} &= \frac{3}{2} A_{Z0} A_{M2}^2 + \frac{3}{4} A_{M2}^2 A_{M4} \cos(2\alpha_{M2} - \alpha_{M4}) + \frac{3}{2} A_{M2} A_{M4} A_{M6} \cos(\alpha_{M6} - \alpha_{M4} - \alpha_{M2}) + \text{smaller terms} \end{aligned}$$

Note that although the emphasis in the paper is on the contribution of the even overtides M4 and M6, the main contribution in the example used in the paper comes from the residual current, due to tidal residual eddies in the estuary.

Hoitink et al.(2003) add diurnal components K1 and O1. They assume that K1, O1 and M2 are the most important components, followed by the other components, but do not consider the residual current :

$$\langle u^3 \rangle_{\infty} = \frac{3}{2} A_{K1} A_{O1} A_{M2} \cos(\alpha_{K1} + \alpha_{O1} - \alpha_{M2}) + \frac{3}{4} A_{M2}^2 A_{M4} \cos(2\alpha_{M2} - \alpha_{M4}) + \text{smaller terms}$$

The (M2, M4, M6) term is also present but is included in the smaller terms in their result. Different, more complex results are obtained in both papers if the sediment transport is assumed to be a power 5 of the velocity instead of 3.

We will argue here that these formulae should not be applied directly. A more generic approach is developed in Annex A to estimate all possible residual transport contributions for any set of tidal components.

Both studies are very site-specific since they assume a particular set of tidal components. It can be noted for instance that Hoitink et al.(2003) do not assume any residual current and hence miss an important term for transport. In addition the relative importance of each term (both presented and neglected) is determined by the relative amplitude of each component, which by definition is site-specific, and applying directly the results of these studies to a random location would possibly be wrong.

In fact all transport terms mentioned above are found back in the generic approach proposed, as well as additional terms which are not all negligible. The first main difference is the contribution of the tidal residual current, which interacts with all other components. Although other components are individually small, the contribution of their sum is not always small. Additionally Figure 4-6 shows an example for the Belgian coast in which some new contributions are presented. It is however possible that in many cases the residual current and the M4 component will yield the highest contributions to residual sediment transport. Note also that overtides creating net residual transport are often not applied at the boundary but fully generated inside the model domain.

The great variability surrounding these estimates also has to be acknowledged. Figure 4-7 shows how greatly the residual current can vary between the mother model providing the boundary conditions and the nested daughter model. It is therefore very important to calibrate the model only against a large number of spatially spread data points.

Finally it is advised to look at the gross and net transport together. It is possible that large errors in net transport are overshadowed by smaller errors in gross transport.

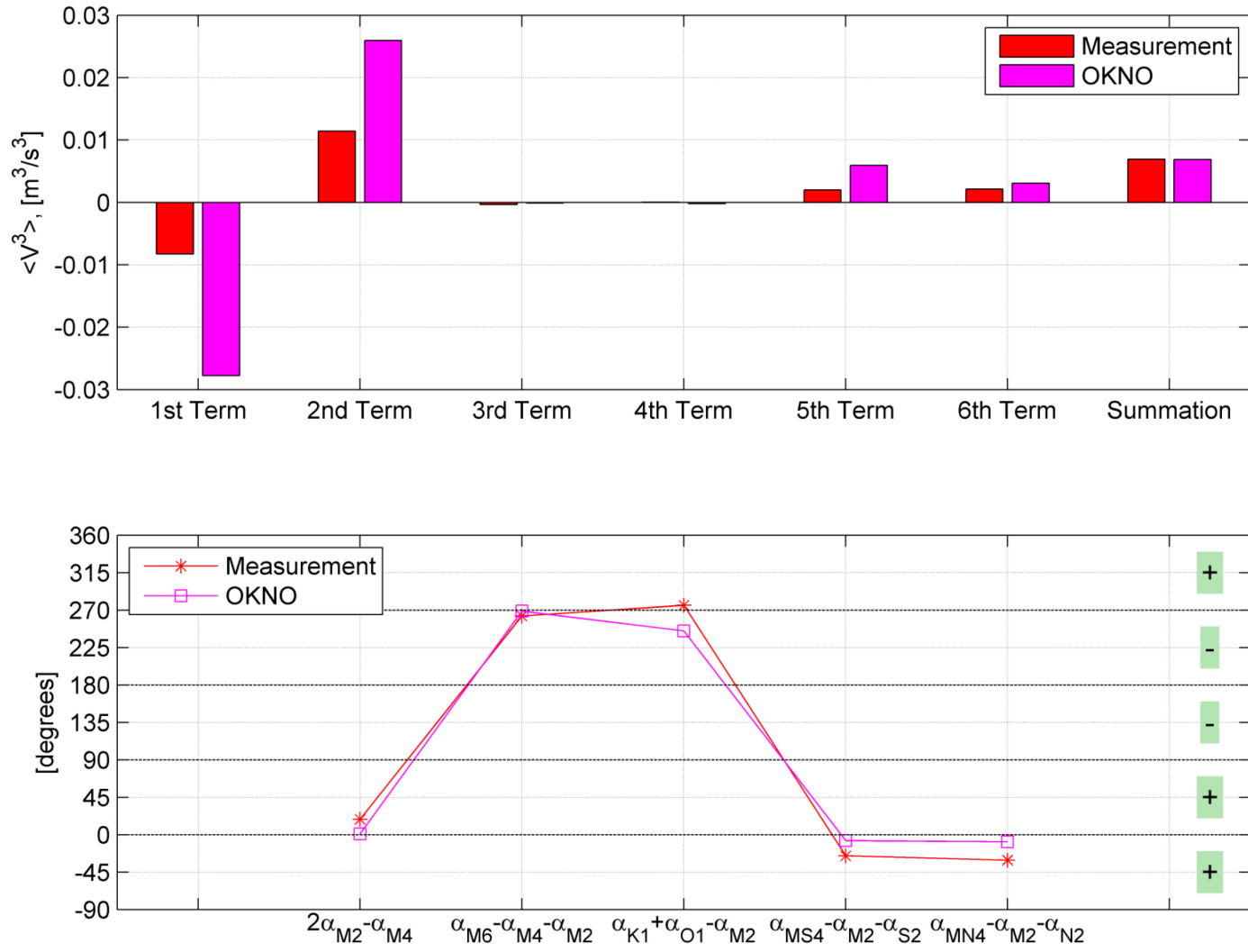


Figure 4-6 : Example of main contributions to residual sediment transport in Blankenberge (Belgium) due to interaction between tidal components : first term (Z0, all, all), second term (M2, M2, M4), third term (M2, M4, M6), fourth term (K1, O1, M2), fifth term (M2, S2, MS4), sixth term (M2, N2, MN4). OKNO model in Delft3D.

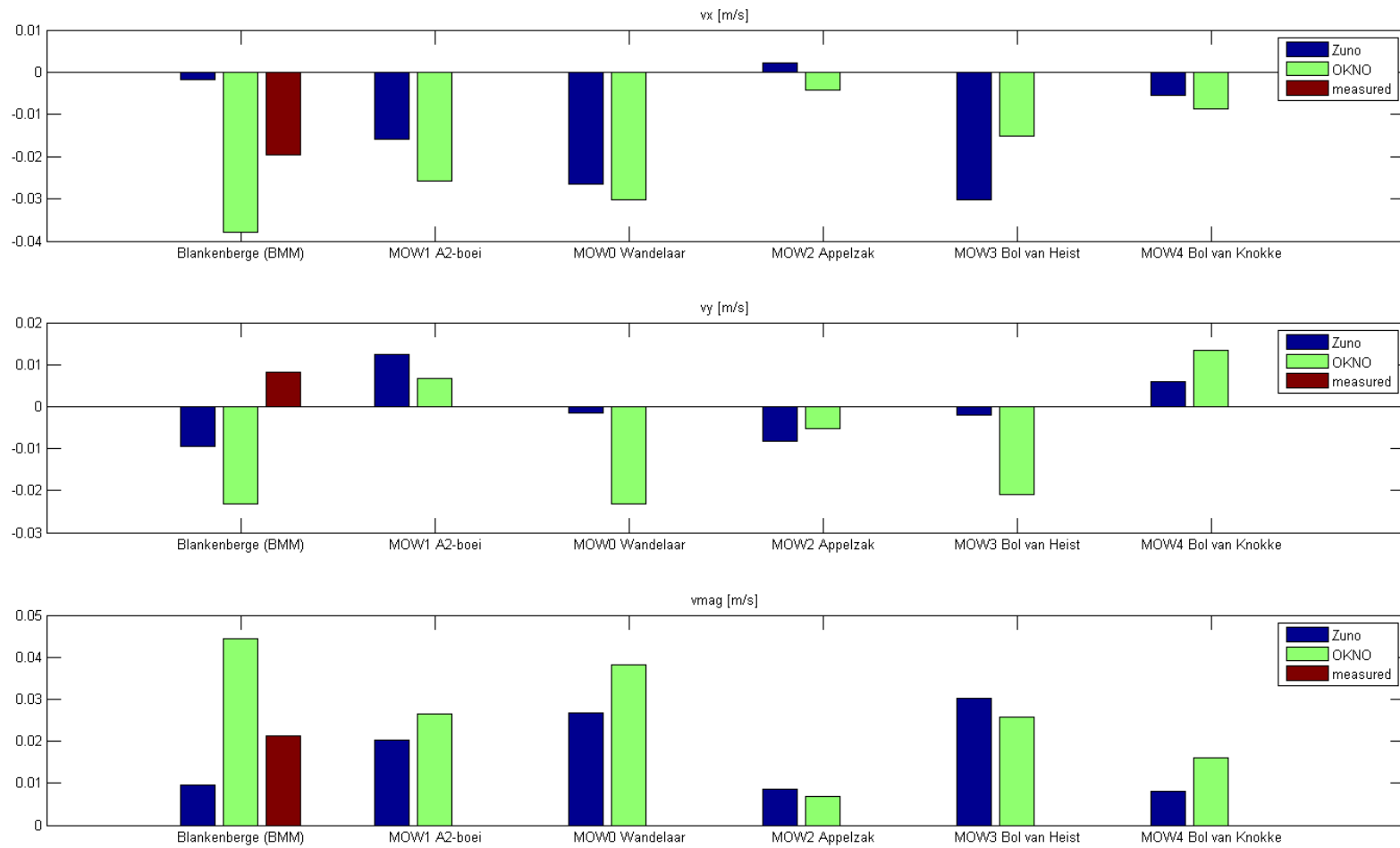


Figure 4-7 : Example of residual current computed over a one month period for the mother model in Simona (blue), the daughter model in Delft3D (green) and the measurements (red) at several data stations.

4.7 Conclusion

We advise the following concerning the model calibration :

- The calibration should address both mathematical and physical errors at the same time. It is advised to always compare results of the mother model, the daughter model and measurement data at the same time.
- The viscosity and especially the roughness are commonly used as calibration parameters for respectively eddies and flow velocities. Both are artifices to model respectively the subgrid turbulence and the subgrid variation in water depth. They can hence both be dependent on the grid resolution. Due to frequent lack of data, it is advised to keep them as simple as possible. Advanced models like subgrid scale models, a turbulence balance equation or roughness predictors may be used without extra calibration to provide estimates of realistic values of these parameters.
- A change in roughness directly affects sediment transport via the bottom shear stress, in particular in the surf zone (transport by up to a factor three observed). Discontinuities in the roughness field also create unrealistic erosion-sedimentation patterns at the transition. This implies that the best calibration for hydrodynamics may be the worst for sediment transport and morphology. Default roughness values have been shown in this project to yield transport estimates in excellent agreement with data. In case calibration is needed, the boundary conditions could be modified directly instead of the roughness.
- Commonly accepted accuracies can be derived from missing physical processes, like the time series of residual water level (setup) and velocities (wind). The natural variability or instationary model results also provide upper bounds for reasonable accuracies. Some measurements often have an accuracy which is lower than that of the model, especially in the surf zone where measuring is difficult. For these reasons, it is advised to not overcalibrate the model, spatially spread data is more important.
- Comparison for the calibration can be done with time series, a harmonic analysis or an estimate of the residual sediment transport based on tidal components. The least square equation (LSE) method is the most useful method for tidal harmonic analysis. The use of a fast Fourier transformation (FFT) is limited and more relevant for the analysis of signals for which frequencies are not known a priori (waves).
- Known formulae to compute the residual sediment transport based on tidal components are those of Van de Kreeke and Robaczewska (1993) and Hoitink et al.(2003). These are very instructive papers, however it is advised not to apply these formulae directly as they are both incomplete and site-specific. Net transport contributions are case-specific, but main net contributions are likely to include in most cases the M2, M4 components and especially the (even small) residual current. A general method is presented in annex.

5 Input reduction

5.1 Overview

This chapter discusses specificities of morphological modelling and input reduction methods for the tide, the wind and wave climates.

5.2 General remarks

Ideally time series of all input parameters are needed to obtain the most realistic results (wind, wave, tide, discharge, low-frequency fluctuations, source-sinks), but this generally results in unrealistically large computation time for long-term morphology simulations. There are several ways to reduce the computation time :

- Morphological acceleration : It is possible to accelerate the morphology based on the different time scales of hydrodynamics and morphology (De Vriend et al, 1993). There are several ways to decouple the two (Lesser, 2009), Delft3D and XBeach for instance use a morphological acceleration factor (morfac) to multiply all bed level changes with this factor.
- Input reduction : Input reduction aims to reduce the full time series to a manageable set of conditions. The reduced set can then be combined to morphological acceleration to shorten computation time.
- Model reduction : Model reduction consists in reducing the accuracy of the model with the eye on computation time. This could be to remove secondary processes, decrease the grid resolution, increase the time step, choose a 2D instead of a 3D model, or reduce the number of sediment fractions.
- Computer power : Obviously a faster computer is better. In addition parallel computing can significantly decrease computation time, but is not always possible (no MPI with morphology in Delft3D v4.0).

Lesser (2009) and Walstra (2011) discuss extensively input reduction, including several methods which are not presented here. Lesser (2009) shows that input can be reduced with very little loss of accuracy (Figure 5-2), but that the quality of the input reduction depends on a good understanding of spatial and temporal scales of the system, hence on a good initial data analysis. The morfac is not well understood yet but it has been shown to work well in several studies (Roelvink, 2006 ; Van der Wegen and Roelvink, 2008). Ranasinghe et al.(in prep.) show that the morfac induces a phase and an amplitude error on bed form propagation under steady current, but that these errors are an order of magnitude lower than errors due to the numerical implementation. To our knowledge the accuracy of the morfac in more complex cases with oscillating tide and waves has not been investigated thoroughly yet.

The main limiting factor according to Lesser (2009) are processes which are still not well understood. He notes in particular that morphology is very sensitive to the bed roughness formulation and that some bed slope processes might be missing in Delft3D. In general, uncalibrated morphological models do not perform well yet. It is however very helpful to understand the qualitative system behaviour.

In fact, Lesser (2009) attempts to measure modelling errors with the Brier Skill Score (BSS ; Sutherland, 2004). A calibrated morphological model is run with realistic time series as a brute force simulation, and also run for all reduction methods separately, for a simulation accelerated with the morfac, and for all reduction methods and morfac combined (minimum computation time). The BSS of the brute force simulation compared to measurements is negative, which means that a no-change simulation would have in average performed better than the current model (Figure 5-1). The BSS of the model with both individual and full input reduction compared to the brute force simulation was, on the other hand, always good to excellent (Figure 5-2). The main contribution to the error were the wind and wave reductions, and a correlated wind-wave reduction reduced that error.

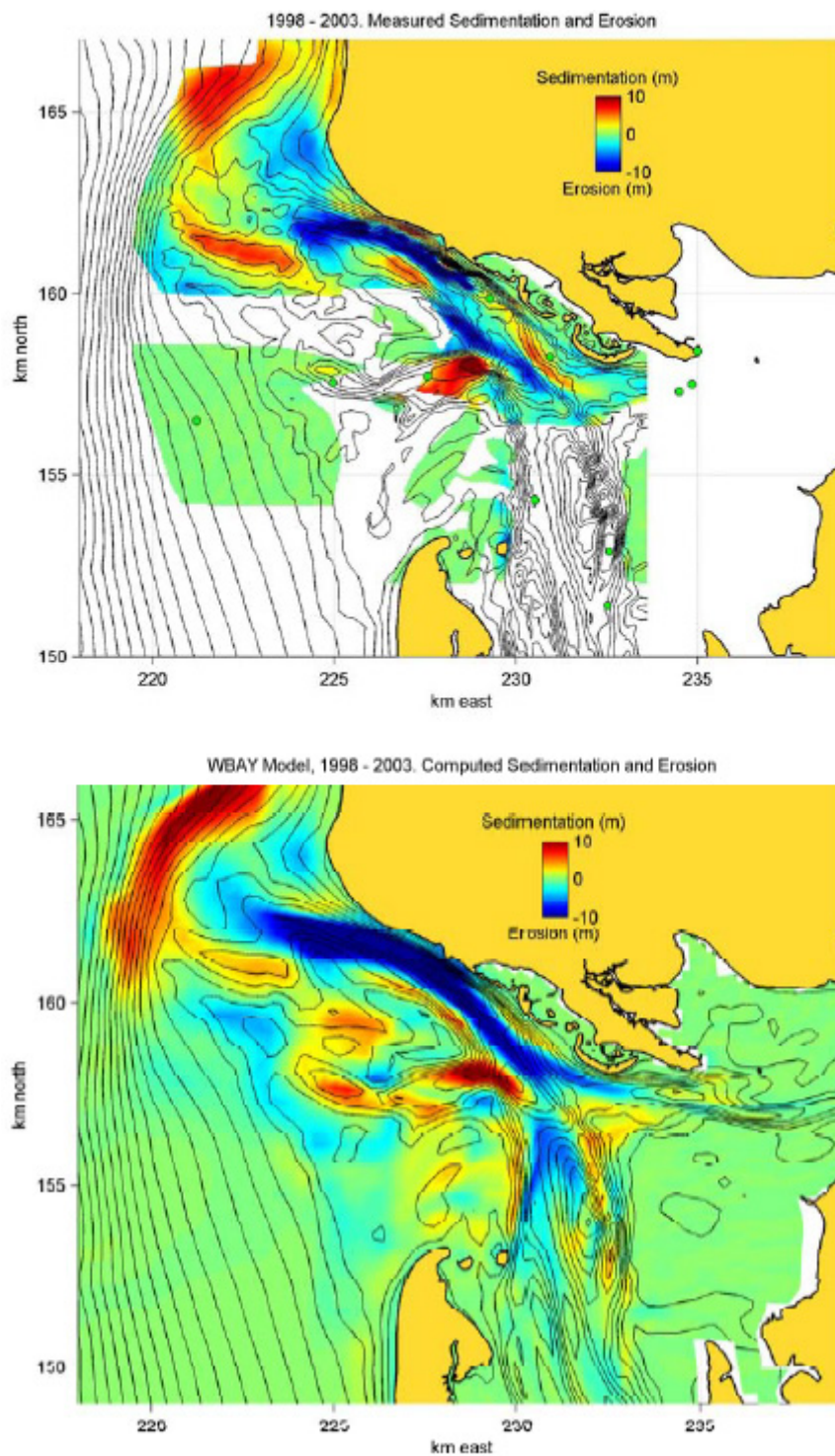


Figure 5-1 : Patterns of sedimentation and erosion in Willapa Bay, USA, from 1998 to 2003. Measured(upper panel) and computed by benchmark simulation (lower panel). Figure from Lesser (2009).

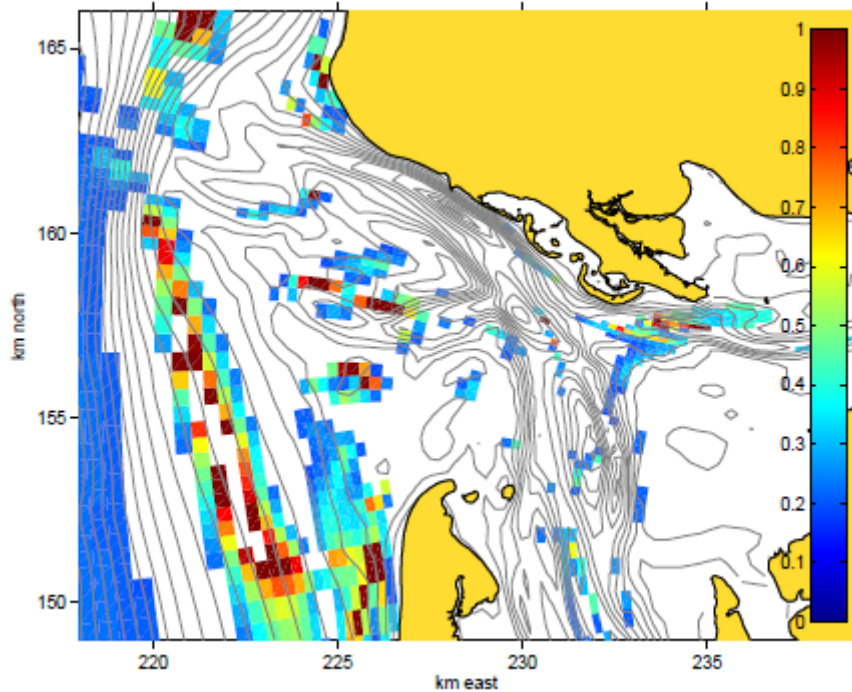


Figure 5-2 : Map of relative error in residual sediment transport magnitude caused by the combined simplification of all forcing processes in Willapa Bay. Errors lower than 20% are shown in white.
Figure from Lesser (2009).

This example already highlights one of the difficulties of input reduction: the quality of the reduction can only be verified if a full time series is also run as ground truth. This is time-consuming, especially if the purpose is to use input reduction routinely for example in engineering projects. Besides if this ground truth exists, then the reduction may not be needed anymore. An alternative 'truth' can be selected to save time. The choice of the reduction target is highlighted many times in the reduction methods tested in this project (Wang et al, 2012) and presented below.

5.3 Tide reduction

For long term morphodynamic simulation, the full tide climate needs to be reduced. A full (also representative) neap-spring tidal cycle can be reduced to a single representative tide. In that way it is possible to use a morphological acceleration factor (morfac) to simulate longer time scales by multiplying bed changes by this morfac at each time step. This would be troublesome if applied with a neap-spring tidal cycle due to history effects : with a morfac of 100 it would be equivalent to simulating first 100 neap tides and then 100 spring tides, instead of 200 representative tides.

There are several ways to derive a representative tide. All methods, such as those presented by Latteux (1995), have in common that a tide is selected which reproduces best chosen targets. A commonly used target may be to reproduce the net residual transport over a neap-spring tidal cycle. If gross transport is also important, additional targets for transport in specific directions may also be used.

Below a possible reduction method is detailed and illustrated :

- The model is first run over a full neap-spring tidal cycle and the net residual sediment transport is computed from the entire time series (target).
- The net transport is then also computed independently for each tidal cycle of the time series used, and compared to the target. This can be done for each grid cell or through cross-sections for instance.
- The tide which compares best is then selected as the representative tide and made cyclic.

For illustration, several figures are shown below for two tides which could potentially be selected as representative tides. Figure 5-3 to Figure 5-5 show the 8th tide of the neap-spring tidal cycle, which has the best slope on the correlation graph but a consistent error in spatial agreement in the zone of interest (bad correlation, good slope). Figure 5-6 to Figure 5-8 show the 9th tide of the neap-spring tidal cycle, for which transport needs to be scaled but spatial agreement is much better once scaled (good correlation, bad slope).

Final scaling can be done in several ways :

- Transport can be scaled directly via a transport coefficient in the model. However once adding the waves it will scale the full transport due to the current and waves instead of only scaling the tidal contribution. This option can hence only be used if the current contribution is dominant, or if the waves have been added beforehand in the tidal reduction.
- Transport can be scaled via the morphological factor. Transport values are then left wrong but bed updates are corrected. Like the transport coefficient however the contribution from waves will be scaled down.
- Transport can be scaled via the boundary conditions. Sediment transport is assumed to be a power of the velocity (equal to that in the model used), and the velocity is scaled to yield the correct transport values. Water levels are scaled equally assuming a linear relation between water level and velocity. This method yields correct transport values, but currents and water levels are wrong. Waves can be superimposed to the current with this method.

To make the tide cyclic, the representative tide is repeated, provided there is no strong discontinuity in velocity between consecutive cycles. Roelvink and Reniers (2011) use an inverse Fast Fourier Transformation (FFT) to make it cyclic without discontinuity. We think however that it adds an unnecessary reduction step, because a harmonic analysis over a period of 24 hours only may have a high uncertainty in the result and the quality of the transport reduction would need to be checked again. This has not been verified here.

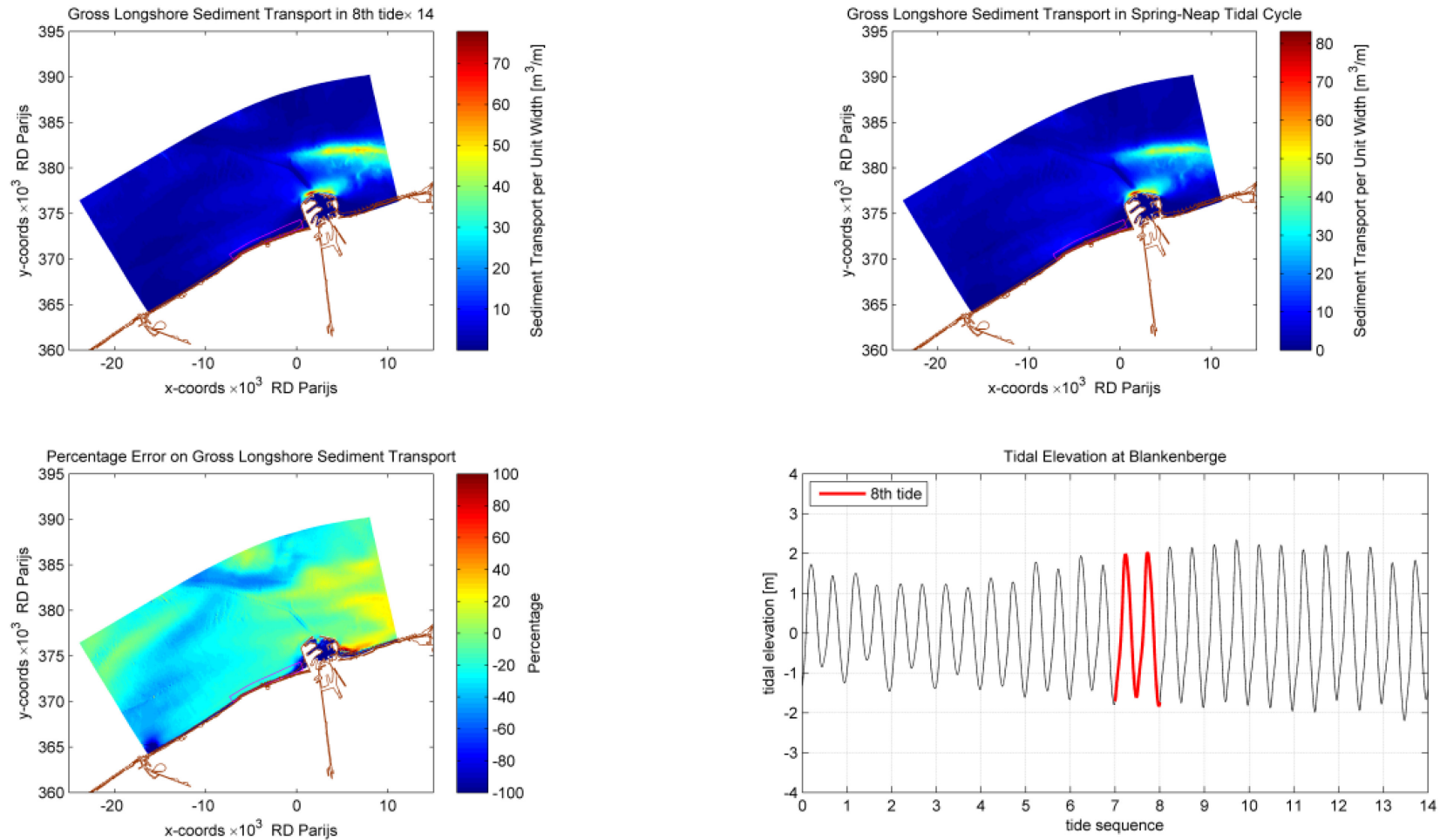


Figure 5-3 : Gross alongshore sediment transport in 14 times the 8th tide (upper left), in the full neap-spring cycle (upper right), reduction error once scaled for the average transport ratio between the two (lower left) and tidal cycle (lower right). Solid discharges (no porosity), model results in Delft3D.

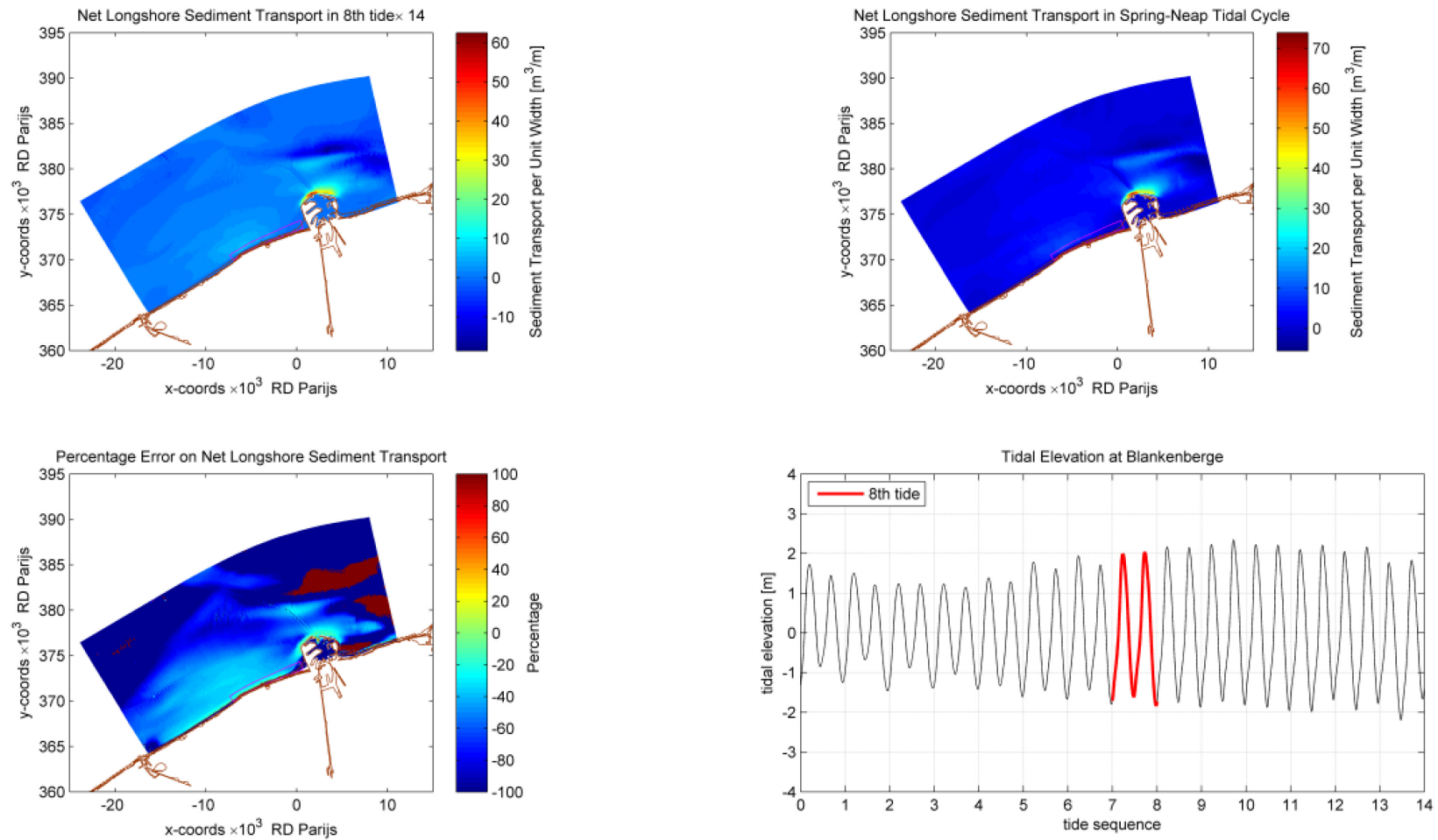


Figure 5-4 : Net alongshore sediment transport in 14 times the 8th tide (upper left), in the full neap-spring cycle (upper right), reduction error once scaled for the average transport ratio between the two (lower left) and tidal cycle (lower right). Solid discharges (no porosity), model results in Delft3D.

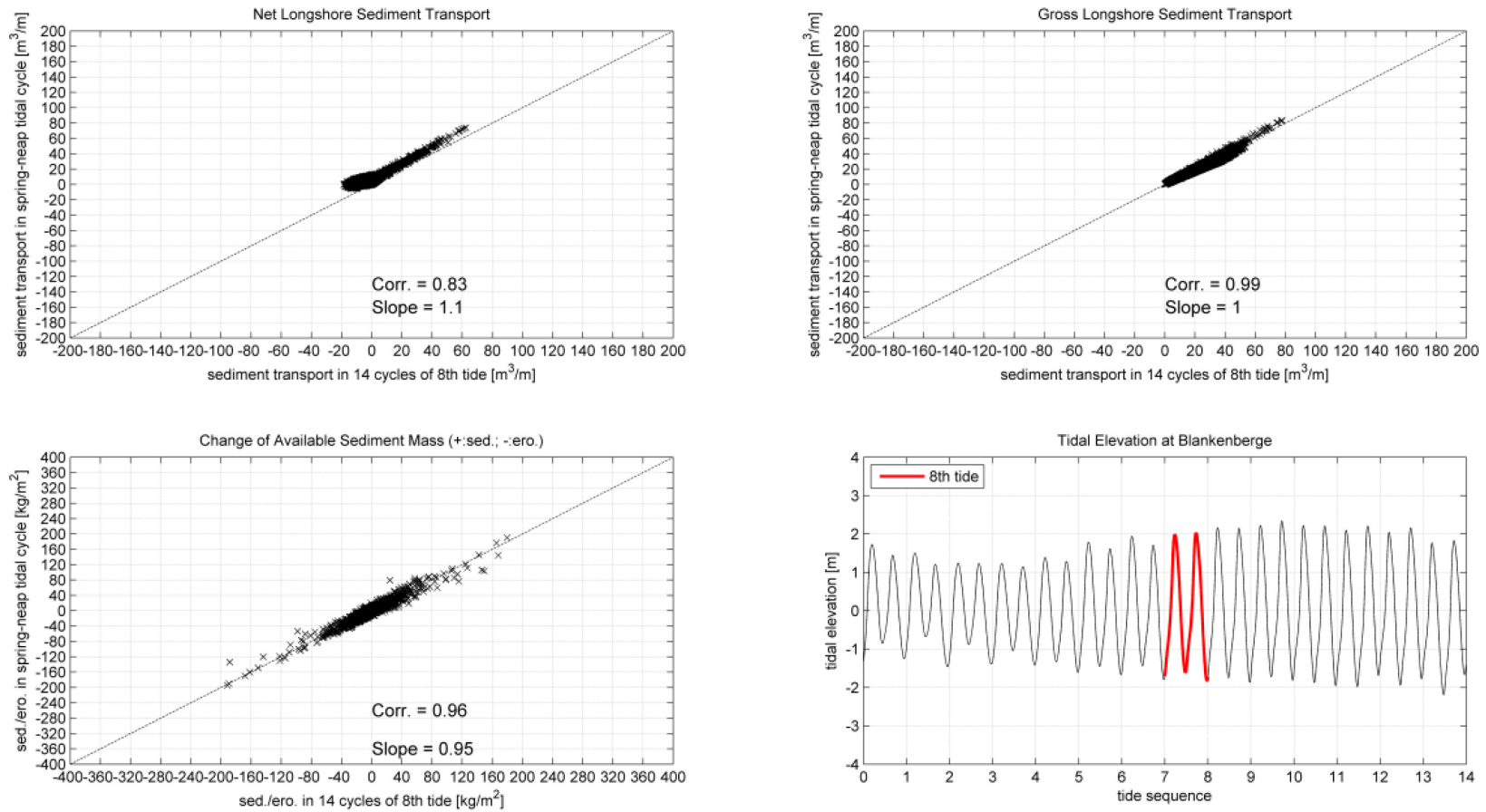


Figure 5-5 : Comparison of net alongshore sediment transport (upper left), gross alongshore transport (upper right) and initial erosion-sedimentation (lower left) between 14 times the 8th tide (x axis) and the full neap-spring cycle (y axis). Tidal elevation in lower right figure. Solid discharges (no porosity), model results in Delft3D.

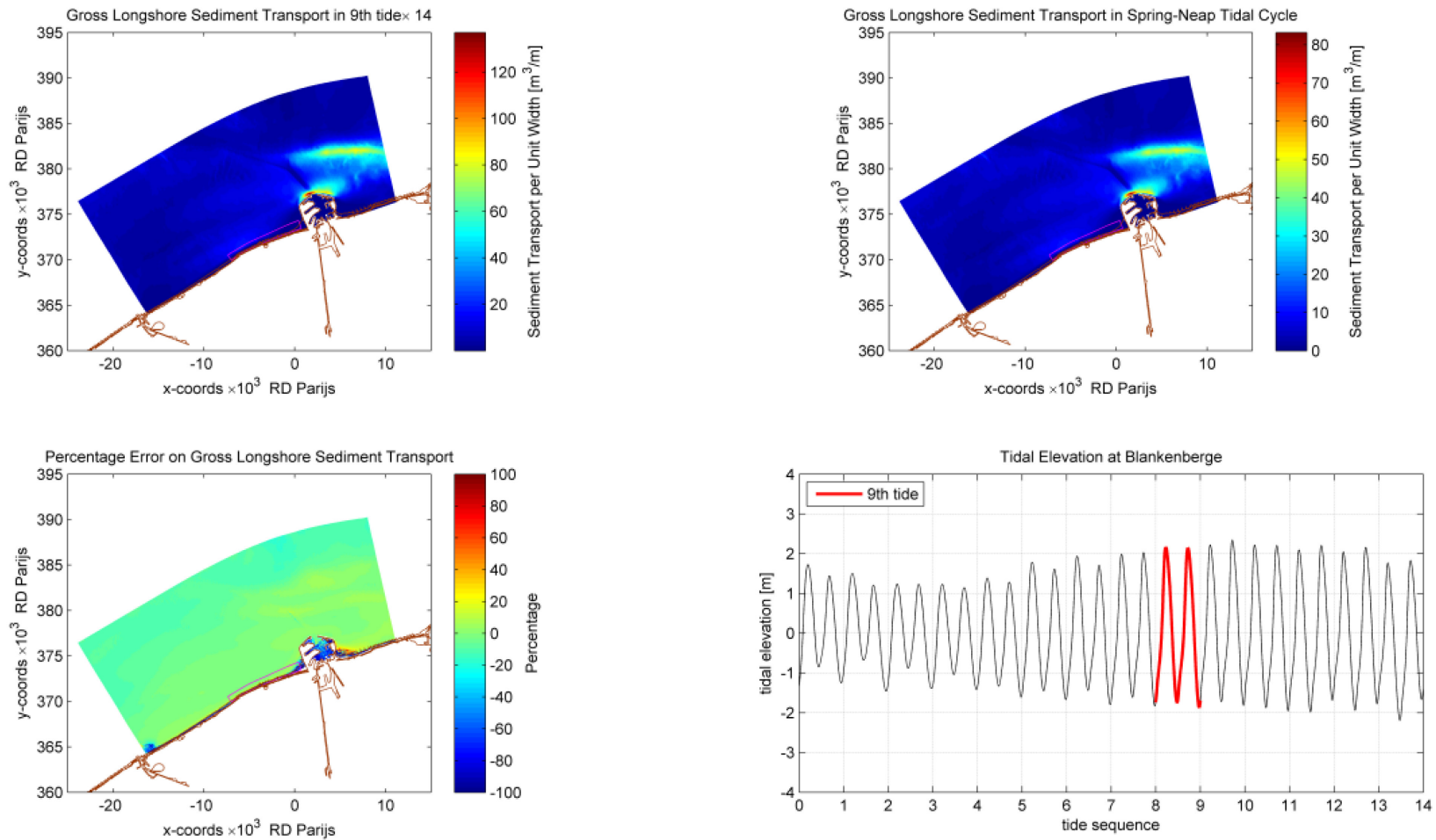


Figure 5-6 : Gross alongshore sediment transport in 14 times the 9th tide (upper left), in the full neap-spring cycle (upper right), reduction error once scaled for the average transport ratio between the two (lower left) and tidal cycle (lower right). Solid discharges (no porosity), model results in Delft3D.

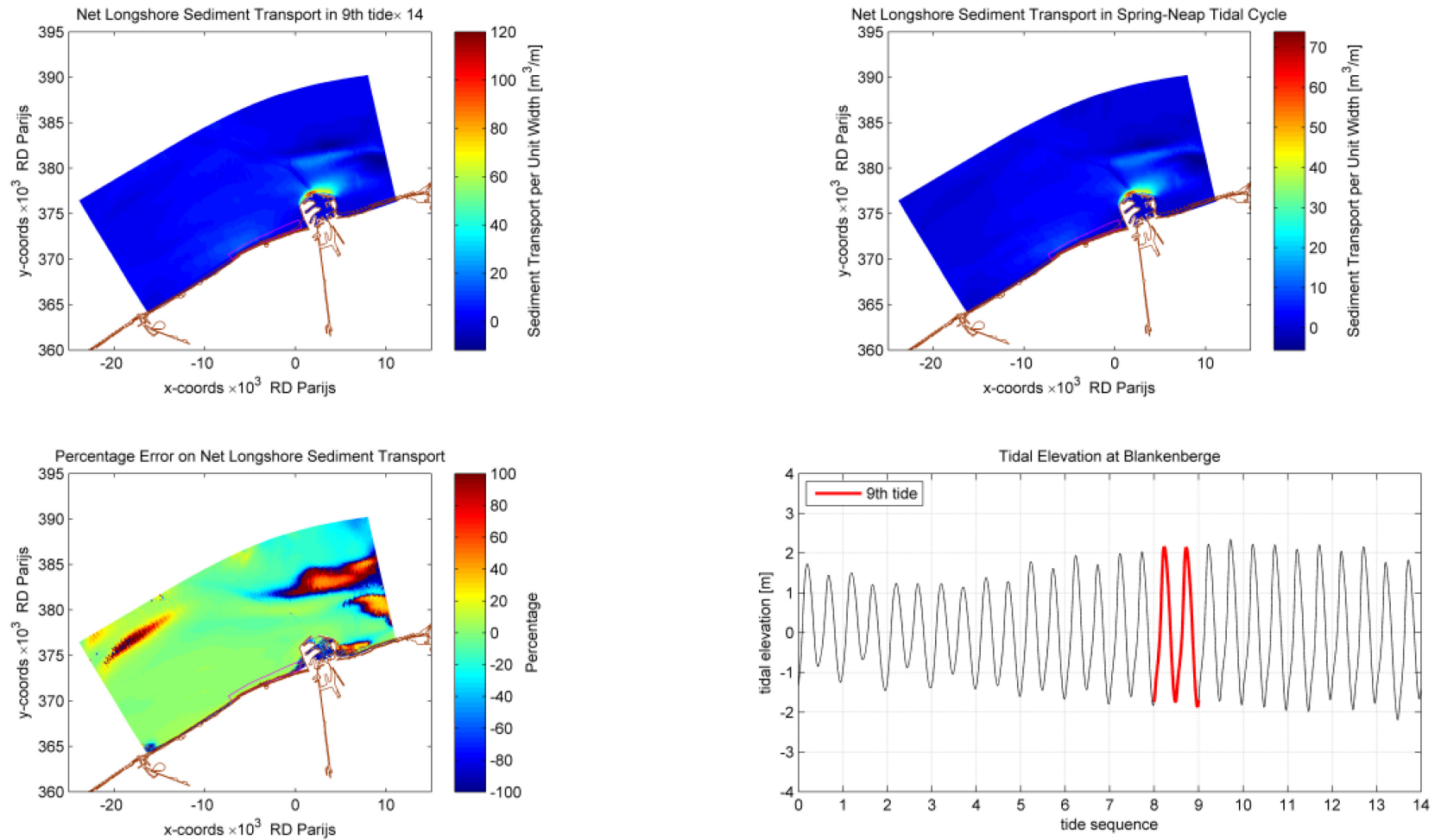


Figure 5-7 : Net alongshore sediment transport in 14 times the 9th tide (upper left), in the full neap-spring cycle (upper right), reduction error once scaled for the average transport ratio between the two (lower left) and tidal cycle (lower right). Solid discharges (no porosity), model results in Delft3D.

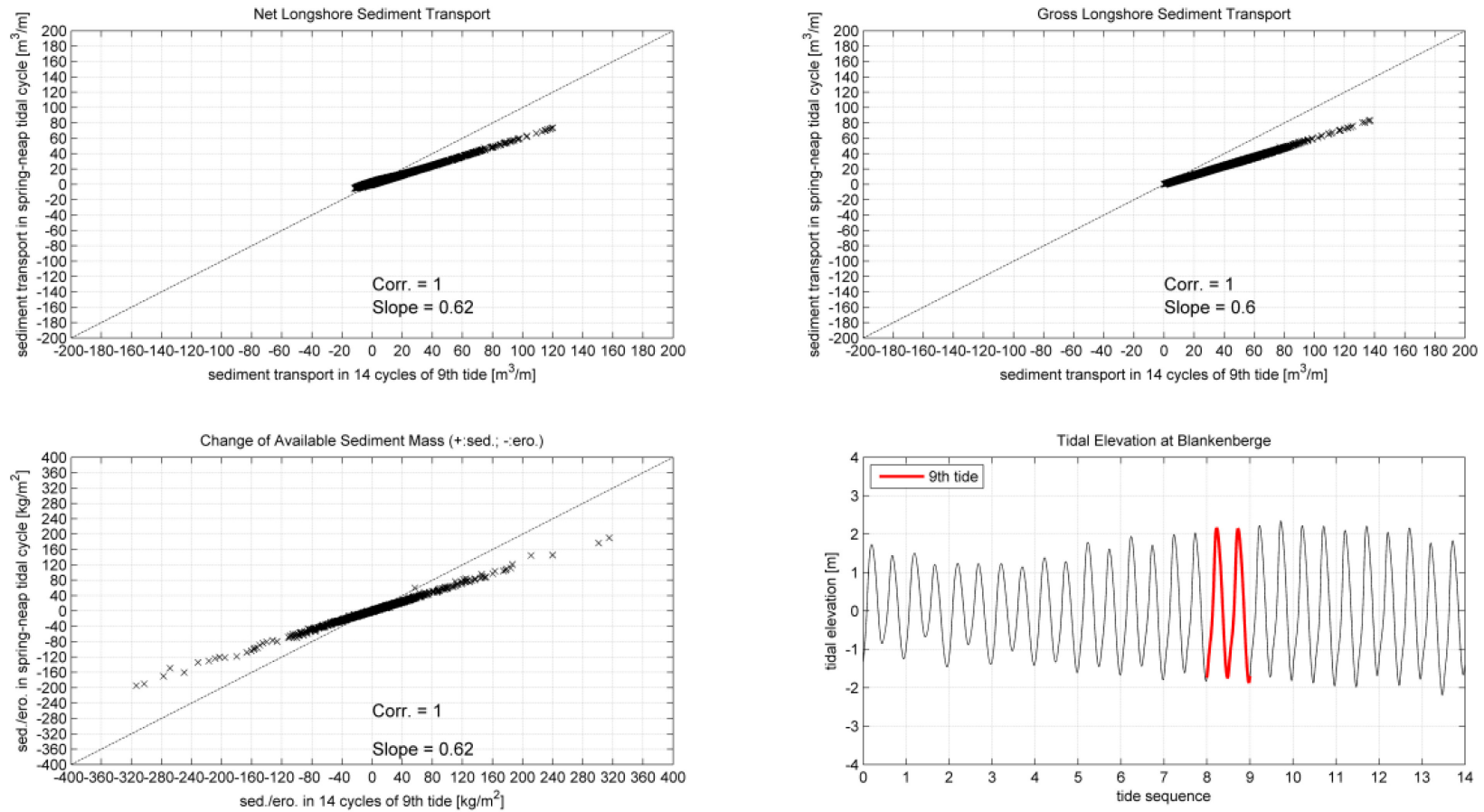


Figure 5-8 : Comparison of net alongshore sediment transport (upper left), gross alongshore transport (upper right) and initial erosion-sedimentation (lower left) between 14 times the 9th tide (x axis) and the full neap-spring cycle (y axis). Tidal elevation in lower right figure. Solid discharges (no porosity), model results in Delft3D.

Several remarks can be made regarding this approach :

- Latteux (1995) as well as experience within this project show that it is very important to verify visually the spatial agreement between results with the representative tide and the full neap-spring cycle.
- Latteux (1995) also indicates that in cases with complex bathymetries there may not always be a single representative tide which will match the full cycle. It is then possible to divide the tidal climate into classes and to select a reduced set of representative tides. Or it is also possible to select a representative tide which just agrees in the area of interest.
- Finally both Latteux (1995) and Winter (2005) show that in some particular cases natural variation is needed to simulate the full dynamics and that it is then better to apply the full natural time series (sometimes even spring-neap cycle not sufficient). Lesser (2009) argues that a more careful reduction is needed, but that it will still work. Flexibility is required.
- Note also that when working with velocity vectors, the ellipticity is more important than the magnitude. The same analysis can then be done by splitting the comparison into x and y components, or into major and minor axis components of the tidal ellipse.
- Like for the mathematical estimate of sediment transport based on tidal components, it is advised to verify the agreement for both gross and net transport.

Roelvink and Reniers (2011) propose an alternative method where the tide is constructed from dominant tidal constituents based on the residual sediment transport analysis (paragraph 4.6). The net transport contribution of the interaction between the diurnal constituents K1, O1 and the semidiurnal M2 is replaced by a fictitious component C1.

5.4 Wind reduction

The difficulty of the wind reduction is that it is at least partly correlated to the wave climate, and wind influences the residual current. The wind reduction should reflect this correlation :

- The wind direction drives on a first order the wave and residual flow direction. If the correlation in direction is strong enough, this gives a good physical basis to choose the wind direction equal to the wave direction (Figure 5-9).
- The wind speed is physically well correlated to the wave height, except for swell. However in this project a single correlation for all directions has been found too simplistic, because it underestimates sometimes greatly low wave heights for wind coming from land (Figure 5-10). For a given wave height, directions with a short fetch require a stronger wind speed than directions with a longer fetch (swell). Lesser (2009) also finds the wind reduction to be an important source of error. It is therefore advised to select one wind class per wave class (direction, height).
- If enough data is available, it is possible to average all wind conditions for a given wave class. A linear regression can also be made for all wave heights of a given wave direction. The second method has the preference since little data is available for high wave events, which are the most important for sediment transport.
- Although not encountered here, there might be swell-dominated cases for which wind and wave climates are not correlated. It is then possible to choose the wind independently, for instance such that it reproduces the mean annual surface shear stress vector, which is representative of the residual flow.

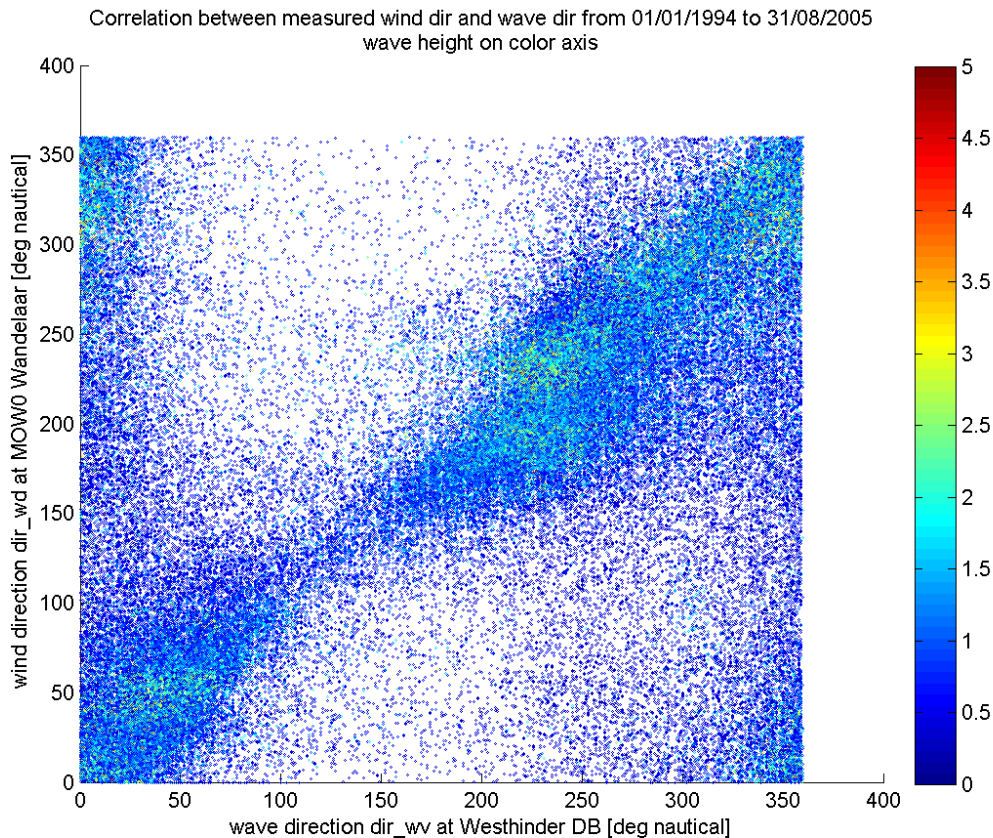


Figure 5-9 : Correlation between measured wind direction and wave direction from 1994 to 2005, with the significant wave height in meters on the colour axis.

Figure 5-10 shows an example of correlation between the wind speed and the significant wave height at the Belgian coast, with the wave direction on the colour axis. The black line delimits the significant wave height of a fully developed sea as a function of the wind speed, according to the formula of Sverdrup-Munk-Bretschneider (SMB). The SMB criterion states that wave growth stops when the wave phase velocity is equal to the wind speed. This figure shows that :

- The highest wind speeds come from the South-West (wind climate).
- For a given wind speed, the highest waves come from the North-West (long fetch, sea), and the lower waves from the South-West (short fetch, land).
- Swell comes mainly from the North (longest fetch).

This illustrates why a single wind speed for all wave directions of a given wave height is insufficient. With a single linear regression, modelled low wave heights are underestimated by up to 50% and modelled wave directions deviate up to 20° because outgoing wave energy is not compensated enough by wave growth by wind inside the model ().

Figure 5-11 and Figure 5-12 show the same kind of linear regression for the wave sectors WSW and NNE. The linear regressions of each wave direction sector result in the wind speed.

Table 5-1 (with a correction factor of 0.94 here to bring it to 10m above MSL). Multiple linear regressions for the wind reduction improve the wave modelling (Table 5-3). However in this example an error still remains, of up to -25% on modelled wave heights and up to $\pm 14^\circ$ deviation on modelled wave directions for small waves coming from land. This is possibly due to the simplified wave boundary conditions, which are constant all along the boundaries of the model domain, or to the stationary character of wave simulations. Turbulence around a mean wind speed is known to increase the maximum wave height the wind can generate (Cavaleri et al., 2007). This effect is possibly more visible for small waves like here.

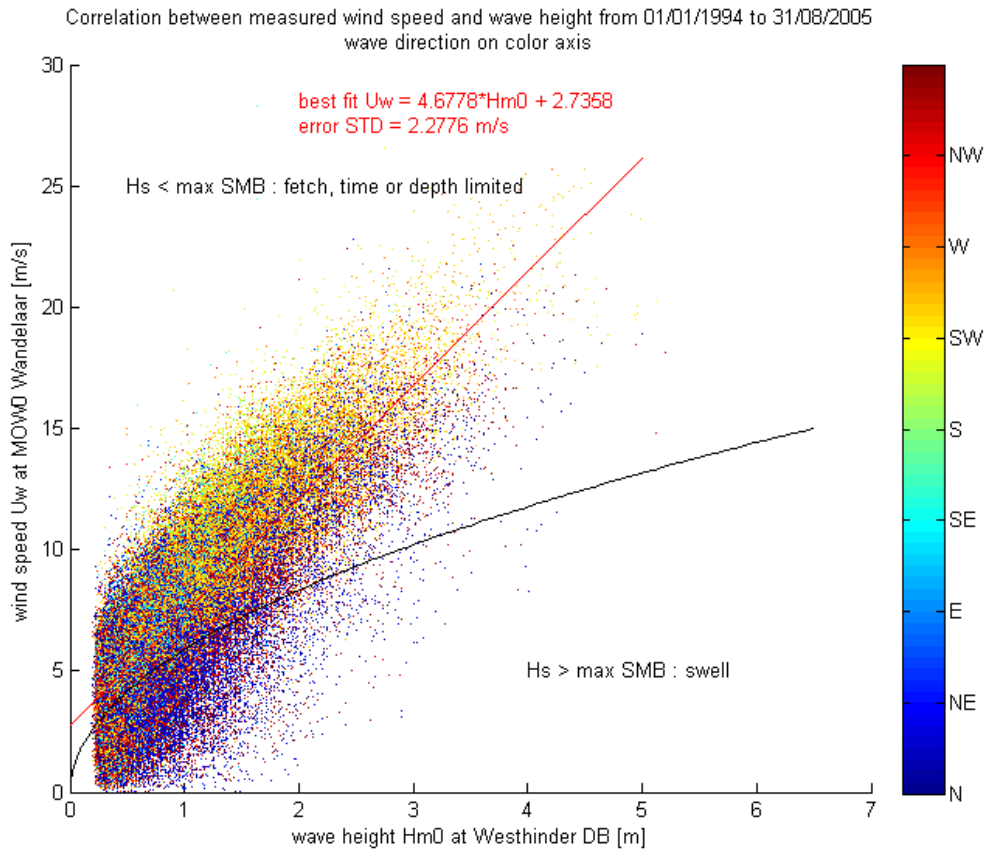


Figure 5-10 : Correlation between measured wind speed at MOW0 Wandelaar and wave height at Westhinder, with the wave direction on the color axis. The black line delimits the significant wave height of a fully developed sea as a function of the wind speed according to the formula of Sverdrup-Munk-Bretschneider (SMB).

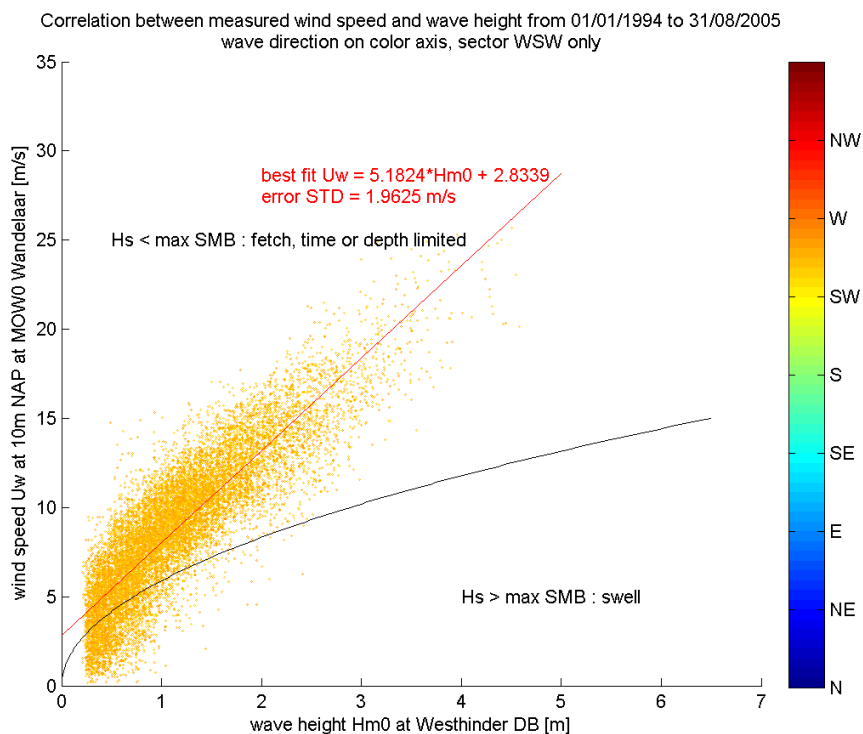


Figure 5-11 : Correlation between measured wind speed at MOW0 Wandelaar and wave height at Westhinder for sector WSW only, with the wave direction on the color axis. Fully developed sea according to Sverdrup-Munk-Bretschneider formula (SMB, black).

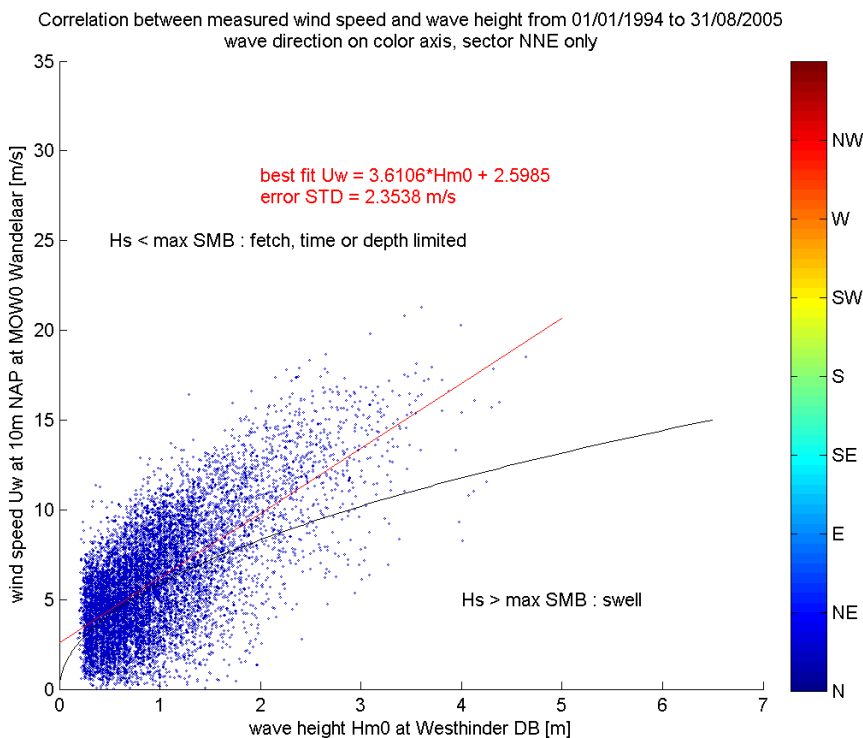


Figure 5-12 : Correlation between measured wind speed at MOW0 Wandelaar and wave height at Westhinder for sector NNE only, with the wave direction on the color axis. Fully developed sea according to Sverdrup-Munk-Bretschneider formula (SMB, black).

Table 5-1 : Full wind climate reduction, with wind direction equal to wave direction and wind speed calculated for each wave class. Wave directions in blue come from the land side. The color scale represents the wind speed.

wind speed at 10m above MSL per wave class [m/s]																
'Hs/dir'	'N'	'NNE'	'NE'	'ENE'	'E'	'ESE'	'SE'	'SSE'	'S'	'SSW'	'SW'	'WSW'	'W'	'WNW'	'NW'	'NNW'
'0.25'	3,40	3,50	3,85	4,04	3,88	3,83	3,85	3,93	4,35	4,67	4,79	4,13	3,76	3,67	3,56	3,48
'0.75'	5,26	5,31	5,93	6,27	6,48	6,51	6,69	6,98	7,27	7,32	7,19	6,72	6,35	6,12	5,83	5,56
'1.25'	7,13	7,11	8,01	8,49	9,08	9,20	9,53	10,03	10,18	9,97	9,58	9,31	8,95	8,58	8,10	7,63
'1.75'	8,99	8,92	10,09	10,72	11,68	11,88	12,38	13,09	13,10	12,62	11,98	11,90	11,55	11,04	10,37	9,71
'2.25'	10,86	10,72	12,17	12,94	14,28	14,56	15,22	16,14	16,02	15,27	14,38	14,49	14,15	13,50	12,65	11,78
'2.75'	12,72	12,53	14,26	15,17	16,87	17,25	18,06	19,19	18,93	17,92	16,77	17,09	16,74	15,96	14,92	13,86
'3.25'	14,59	14,33	16,34	17,40	19,47	19,93	20,91	22,24	21,85	20,57	19,17	19,68	19,34	18,41	17,19	15,93
'3.75'	16,45	16,14	18,42	19,62	22,07	22,62	23,75	25,29	24,76	23,22	21,57	22,27	21,94	20,87	19,46	18,01
'4.25'	18,32	17,94	20,50	21,85	24,67	25,30	26,59	28,34	27,68	25,87	23,96	24,86	24,54	23,33	21,73	20,08
'4.75'	20,18	19,75	22,58	24,08	27,26	27,98	29,44	31,40	30,59	28,52	26,36	27,45	27,13	25,79	24,01	22,15

Table 5-2 : Modelled wave height and direction per wave class compared to the measured value at Westhinder, for a single linear regression for the wind speed (including all wave directions). Model results in Delft3D (SWAN for waves). The color scale is a measure of error (red is a large error).

		Ratio between modelled wave height at Westhinder and applied wave height at boundaries															
dir [° naut]	N	NNE	NE	ENE	E	ESE	SE	SSE	S	SSW	SW	WSW	W	WNW	NW	NNW	
Hs [m]	0	22,5	45	67,5	90	112,5	135	157,5	180	202,5	225	247,5	270	292,5	315	337,5	
0,75	1,01	0,98	0,92	0,82	0,70	0,59	0,51	0,50	0,58	0,68	0,79	0,88	0,96	1,00	1,01	1,01	
1,25	1,02	0,99	0,93	0,85	0,76	0,69	0,63	0,60	0,66	0,74	0,83	0,90	0,97	1,01	1,02	1,02	
1,75	1,03	1,01	0,98	0,93	0,86	0,81	0,74	0,71	0,77	0,87	0,94	0,98	1,00	1,03	1,04	1,04	
2,25	1,05	1,04	1,02	1,00	0,95				0,83	0,96	1,03	1,04	1,05	1,05	1,06	1,05	
2,75	1,05	1,04	1,05	1,04	1,00					1,01	1,05	1,08	1,07	1,06	1,05	1,05	
3,25	1,06	1,06								1,02	1,07	1,09	1,09	1,07	1,06	1,06	
3,75	1,06	1,06									1,05	1,06		1,07	1,05	1,05	
4,25	1,06	1,07									1,05	1,06					
		Difference between modelled wave direction at Westhinder and applied wave direction at boundaries															
dir [° naut]	N	NNE	NE	ENE	E	ESE	SE	SSE	S	SSW	SW	WSW	W	WNW	NW	NNW	
Hs [m]	0	22,5	45	67,5	90	112,5	135	157,5	180	202,5	225	247,5	270	292,5	315	337,5	
0,75	0	-3	-9	-16	-21	-19	-8	4	18	19	15	10	4	1	0	0	
1,25	0	-2	-7	-12	-16	-16	-10	3	15	15	11	8	4	1	0	0	
1,75	0	-1	-4	-8	-12	-15	-12	2	14	12	6	3	2	0	0	0	
2,25	1	1	-1	-4	-10				15	11	4	-1	-1	-1	0	0	
2,75	1	2	1	-2	-8					10	2	-2	-3	-2	0	0	
3,25	2	3								9	2	-3	-4	-2	0	1	
3,75	3	4									2	-3		-3	0	1	
4,25	4	5									2	-3					

Table 5-3 : Modelled wave height and direction per wave class compared to the measured value at Westhinder, for multiple linear regressions for the wind speed (one per wave direction). Model results in Delft3D (SWAN for waves). The color scale is a measure of error (red is a large error).

Ratio between modelled wave height at Westhinder and applied wave height at boundaries																
dir [° naut	N	NNE	NE	ENE	E	ESE	SE	SSE	S	SSW	SW	WSW	W	WNW	NW	NNW
Hs [m]	0	22,5	45	67,5	90	112,5	135	157,5	180	202,5	225	247,5	270	292,5	315	337,5
0,75	1,01	0,98	0,94	0,88	0,82	0,75	0,72	0,75	0,85	0,93	0,98	0,98	1,00	1,02	1,02	1,02
1,25	1,01	0,97	0,92	0,86	0,84	0,80	0,78	0,82	0,89	0,95	0,97	0,97	0,98	1,01	1,02	1,02
1,75	1,02	0,98	0,93	0,89	0,90	0,87	0,85	0,88	0,95	1,00	1,00	1,02	1,01	1,02	1,03	1,02
2,25	1,03	0,99	0,96	0,92	0,95				0,96	1,04	1,03	1,05	1,04	1,04	1,05	1,04
2,75	1,02	0,99	0,96	0,93	0,97					1,04	1,03	1,06	1,05	1,04	1,04	1,04
3,25	1,03	1,00								1,03	1,02	1,07	1,07	1,05	1,05	1,04
3,75	1,03	1,00									1,01	1,04		1,04	1,04	1,03
4,25	1,03	1,00									0,99	1,04				
Difference between modelled wave direction at Westhinder and applied wave direction at boundaries																
dir [° naut	N	NNE	NE	ENE	E	ESE	SE	SSE	S	SSW	SW	WSW	W	WNW	NW	NNW
Hs [m]	0	22,5	45	67,5	90	112,5	135	157,5	180	202,5	225	247,5	270	292,5	315	337,5
0,75	0	-3	-7	-11	-14	-14	-8	3	12	13	7	4	2	0	0	0
1,25	0	-3	-8	-12	-13	-14	-10	2	13	12	6	4	3	1	0	0
1,75	0	-3	-7	-10	-11	-14	-13	1	14	11	5	1	1	1	0	0
2,25	0	-3	-6	-8	-10				15	10	4	-1	-2	0	0	0
2,75	1	-2	-4	-7	-9					9	3	-2	-2	0	0	0
3,25	1	-1								9	3	-2	-3	-1	0	1
3,75	2	0									3	-2		-1	0	1
4,25	3	1									3	-2				

5.5 Wave reduction

There are several ways to reduce the wave climate, however the principle beyond is always the same. It is currently too time-consuming for long-term and even shorter term morphological modelling to include the entire wave climate in the computation. Like the tide, the wave climate is therefore limited to a reduced set of wave conditions, which should be such that a user-defined target is reproduced as closely as possible. This target can be anything, like for instance the erosion-sedimentation, the gross or net sediment transport, in magnitude or vector, at a local point, through a cross-section or integrated over an area. Multiple targets can also be defined. Reduction techniques then only differ in the targets and methodologies employed.

5.5.1 OPTI

OPTI is an automated optimization tool developed by Deltares to reduce the number of wave conditions to be used in morphological simulations (Mol, 2007).

Its principle is best understood by comparison to a manual approach. In the other reduction methods discussed, the selection of the reduced set of wave conditions usually occurs based on expert judgment. Wave conditions are for instance clustered into classes and from each class one wave condition is chosen to represent the entire class. Several users would then probably end up with different reduced wave climates. None of the users is likely to have selected the (mathematically) optimal reduced climate because of the large number of possible choices.

OPTI proposes a more optimal reduced climate by testing automatically a large number of reduced climates and selecting the best one. OPTI follows the steps below (Figure 5-13) :

- First, wave conditions with a negligible probability of occurrence and with a negligible contribution to sediment transport can be removed manually, to decrease the total number of wave conditions.
- Short separate morphological simulations are then run outside OPTI for each remaining wave condition. From this the initial effect of each wave condition can be assessed. This is the time-consuming part of the OPTI procedure.
- Input files have to be prepared to provide the necessary information to OPTI : wave conditions, probability of occurrence, resulting morphological change have to be specified.
- OPTI then determines an overall averaged morphological change due to all wave conditions, by weighting the result of each wave condition with its frequency of occurrence from the wave climate table, and summing them up. This is the target.
- OPTI then enters an exclusion loop in which at each step one wave condition is removed, until none remains. At each step of the loop, the weights of the wave conditions are varied randomly between zero and twice the previously assigned weights. The new overall morphological change is compared to the target and statistics are computed.
- At each step of the exclusion loop, a second iteration loop is present. The random variation of the weights is repeated a selected (large) number of times, typically 100 to 1000 times, and the set of weights with the best agreement with the target will be selected (RMSE). The higher the number of iterations, the more optimal the resulting set of weights, but the longer the computation time.
- At the end of each step of the exclusion loop, the condition contributing the least to the overall morphological change with the optimal set of random weights is removed (standard deviation).
- At each time step the following parameters are written to output files : the optimal set of random weights, statistics of its difference with the target, and the overall morphological change with the optimal set of random weights. It is then possible to determine how many wave conditions are needed in the reduced wave climate based on the evolution of the statistics during the exclusion loop.

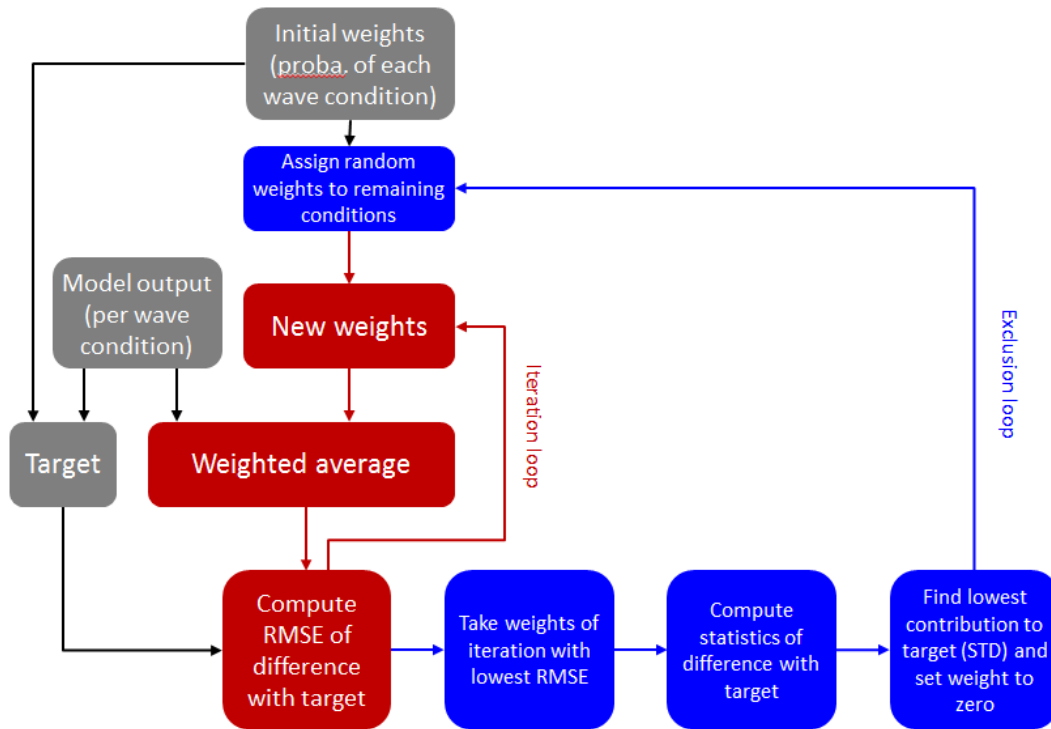


Figure 5-13 : Schematic view of the OPTI procedure for climate reduction.

Figure 5-14 and Figure 5-15 show post-processed output of an OPTI procedure. Inputs and outputs of the scripts are detailed with the scripts and are not described in this report.

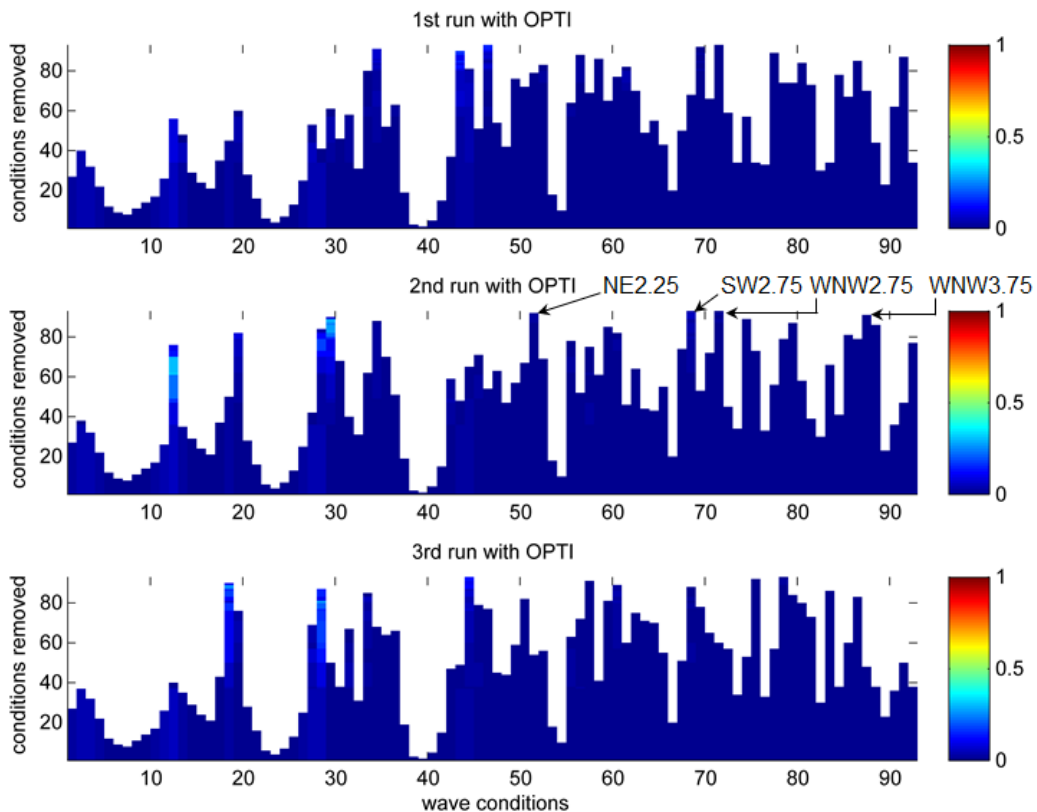


Figure 5-14 : Evolution of the weights of each wave condition (x axis) during the exclusion loop (y axis), for three OPTI procedures on the same input data, showing that it results in three different reduced wave climates.

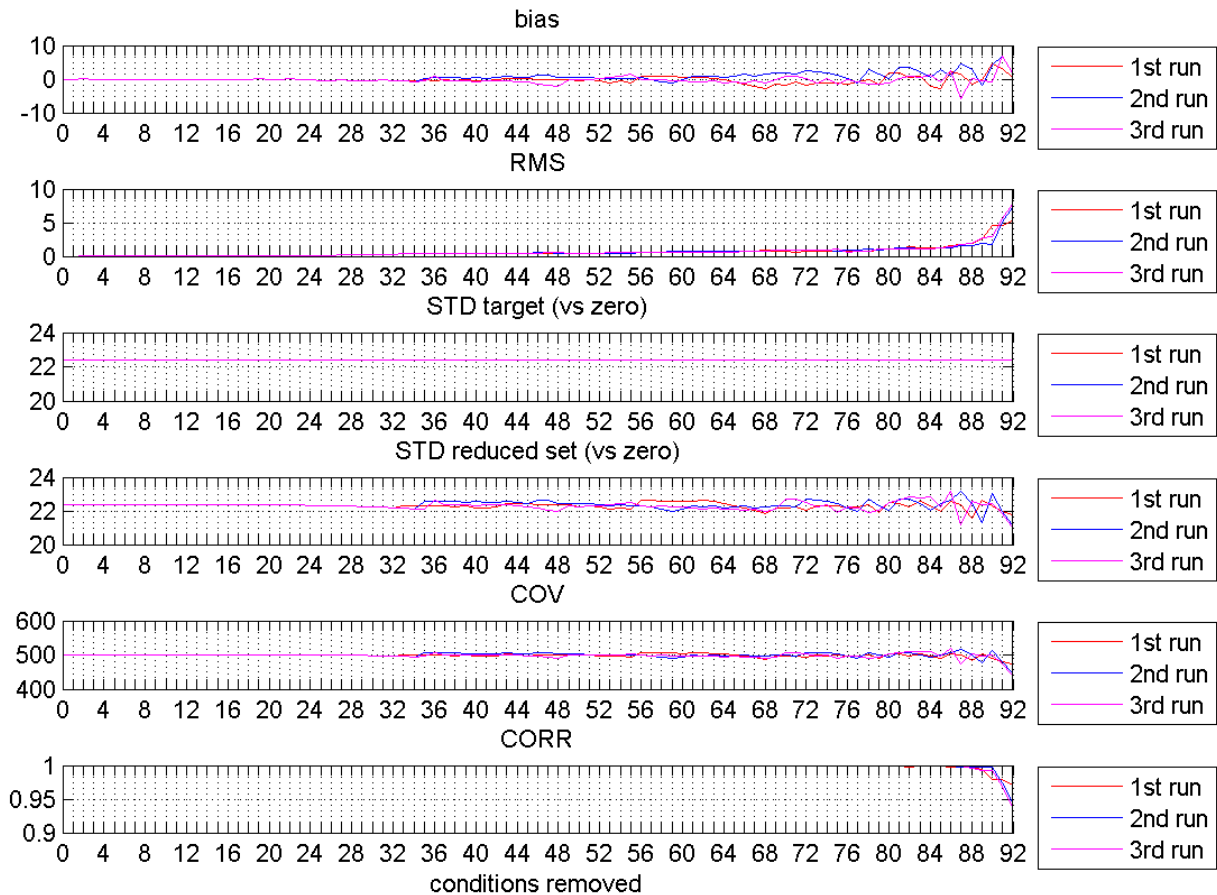


Figure 5-15 : Statistics of the reduced wave climate at each step of the exclusion loop (x axis), for three OPTI procedures on the same input data, showing that the error increases towards the end. The target in this example is the net alongshore transport in $m^3/year/m$.

With the reduced wave climate, it is possible to compute the gross transport (Figure 5-16), net transport (Figure 5-17) and initial erosion-sedimentation pattern of the yearly wave climate (Figure 5-18). The spatial quality of the wave reduction can be verified in the same way as the tide reduction. Here it is important to verify both the reduction offshore and in the surf zone, where transport values are much higher.

The erosion-sedimentation maps mainly show that an initial smoothing of the bathymetry occurs during this simulation period of two tidal cycles, which overshadows other bed changes (Figure 5-18). It does not affect the quality of the wave reduction, and it is expected to play a less important role for long-term simulations of the morphology with the reduced climate. If needed, this effect can be reduced by smoothing the input bathymetry before running the model.

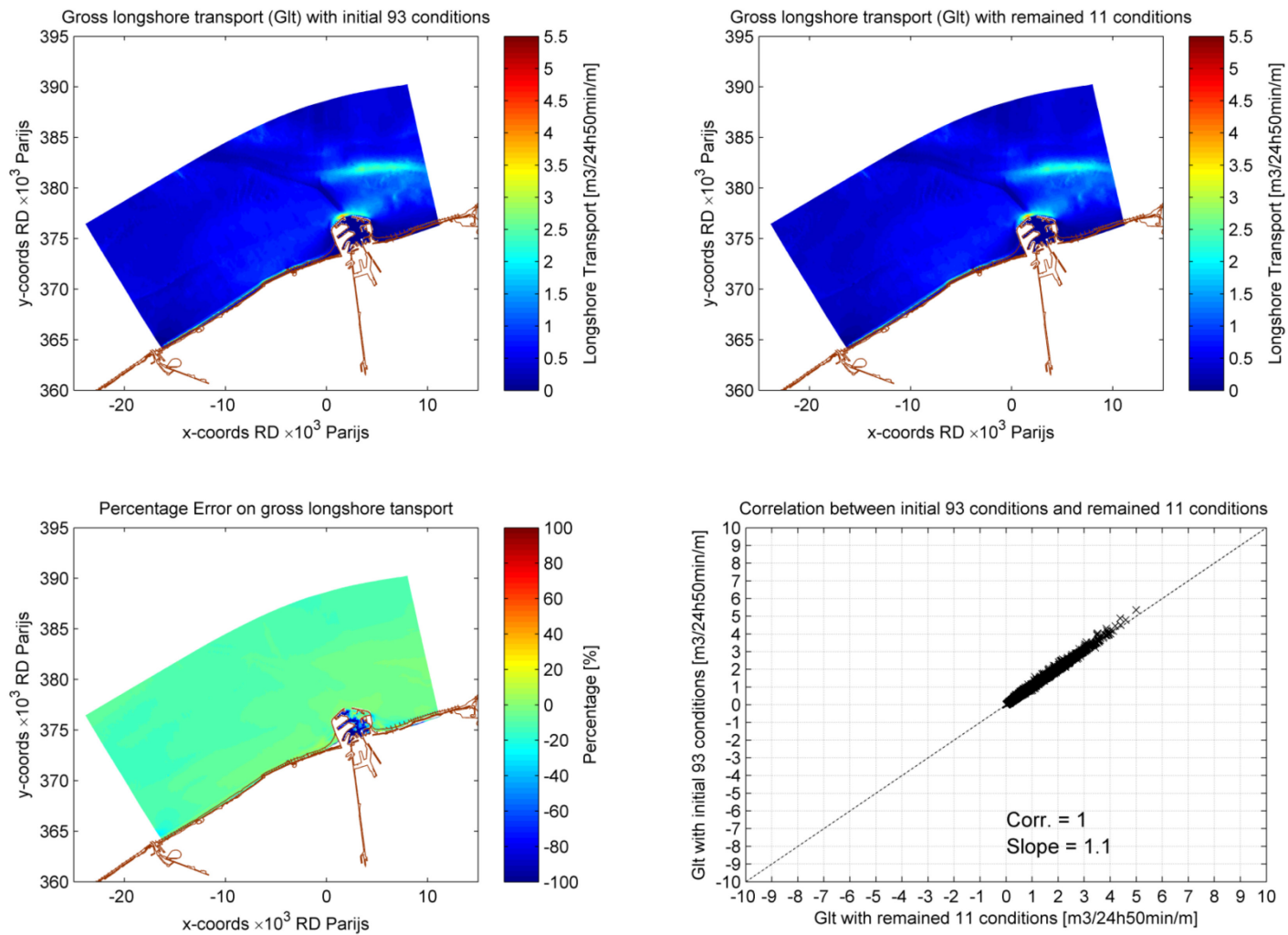


Figure 5-16 : Gross alongshore sediment transport integrated over two tides with the full yearly wave climate (upper left), the reduced wave climate (upper right), reduction error as a percentage (lower left) and correlation graph (lower right). Solid discharges (no porosity), model results in Delft3D.

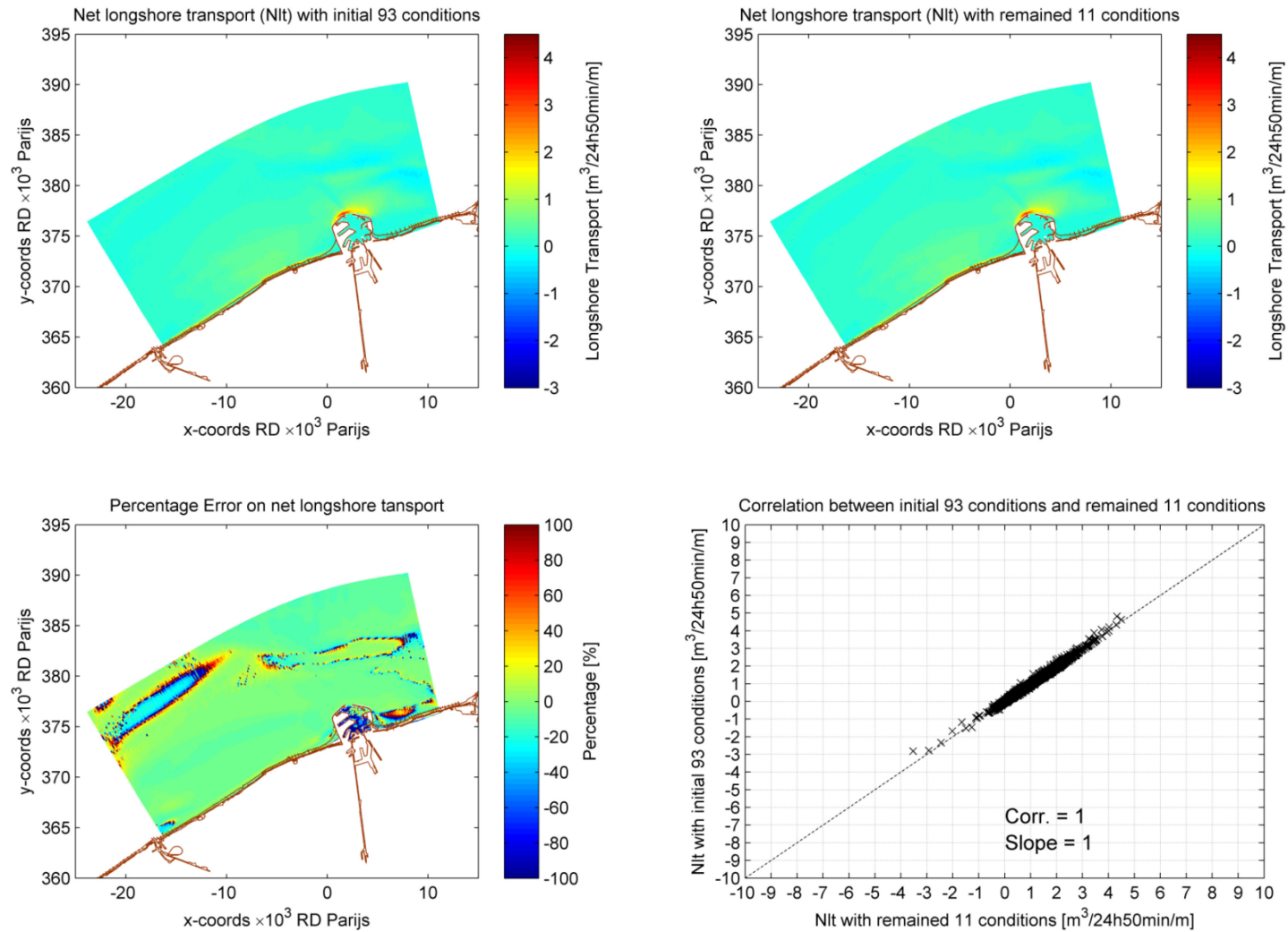


Figure 5-17 : Net alongshore sediment transport integrated over two tides with the full yearly wave climate (upper left), the reduced wave climate (upper right), reduction error as a percentage (lower left) and correlation graph (lower right). Solid discharges (no porosity), model results in Delft3D.

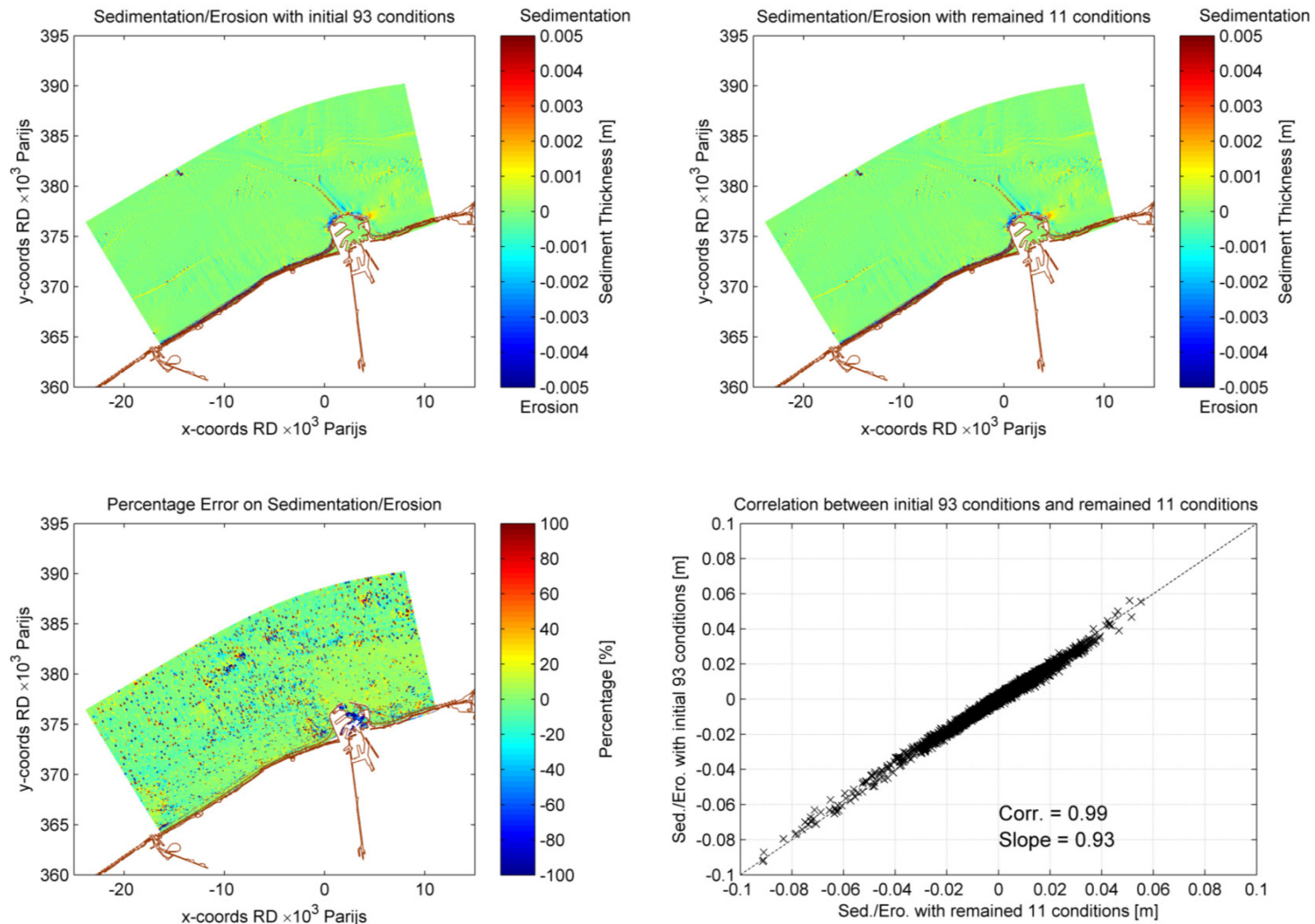


Figure 5-18 : Erosion-sedimentation integrated over two tides with the full yearly wave climate (upper left), the reduced wave climate (upper right), reduction error as a percentage (lower left) and correlation graph (lower right). Model results in Delft3D (no initial smoothing of bathymetry).

Several additional remarks should be made with regards to the use of OPTI :

- The target used in the base version of OPTI is the cumulative erosion-sedimentation in each grid cell, but it can be modified to use any single or multiple targets, as long as all these targets are comparable (normalize if necessary, for instance when using multiple variables as targets). It can hence also be used for other reduction procedures, such as the tide if one tide is not sufficient.
- The target used by OPTI is more trustable than targets derived with tools different than the model which will in the end be used to do the morphological computations. Walstra (2011) shows that if the target is the sediment transport magnitude from a theoretical transport formula, it is important to use the same transport formula in the reduction and in the morphodynamic simulations to prevent reduction errors.
- OPTI is a long procedure since all wave conditions have to be simulated first. However it may still save a lot of time because the full climate does not need to be computed for detailed nested models, and because the reduced climate can be used for many different scenarios. Also, it implies that later on the reduced climate is used together with a morphological acceleration factor, otherwise no time is gained.
- OPTI is not an excuse to present the reduced climate as being more objective than an expert judgment. In fact there are limitations to the distribution used to derive the random weights. Also, the results of OPTI may not always be more optimal than expert judgment (see below).
- It is important to understand how the random weights are chosen. Each optimal weight of the previous exclusion step is varied between 0 and 2 times its value. This implies that a weight which has fallen near zero will almost inevitably be discarded, no matter whether the initial contribution was high or low. Its loss will be compensated by an increase of other weights, but these may have initially be minor. If the OPTI procedure is run several times, it is likely that several reduced climates will emerge. In that sense it is nothing more than expert judgment, but with the physics hidden in the statistics.
- The original OPTI script obtained for this project has no truly random seed to begin the generation of random weights. As a consequence OPTI would always yield the same reduced climate when run several times for a given number of random iterations. This can easily be corrected and does indeed yield different reduced climates (Figure 5-14) and statistics (Figure 5-15). At the first steps of the exclusion loop (30 first here), the same conditions are removed in different runs because OPTI does not find a reduced climate which is closer to the target than simply removing the lowest contribution.
- The original OPTI script can also be adapted according to the suggestion of Lesser (2009), who shows that the RMSE can be reduced by assigning after each exclusion step the weight of the condition previously removed to the most closely correlated remaining condition. This has not been tested, but is an attractive solution because it includes more physics in the procedure.
- The selected reduced set of wave conditions should ideally include both small and large waves and all major wave directions to keep some physics. It is advised to select more than four wave conditions, even if four could be sufficient according to OPTI results.
- The result of the OPTI procedure should always be compared to the target to verify the spatial agreement. It gives an idea of where the reduction is trustable and where it is less.

5.5.2 Climate table and transport formula

The target used in the wave reduction can alternatively be a transport formula. The expected longshore transport can for example be computed for each wave class (direction, height) of the climate probability table with the CERC formula. From that the expected gross and net transport can be computed, and a number of wave conditions selected to achieve those targets (at least one in each direction).

Such an approach has the advantage of being quick to apply compared to OPTI, but it has several pitfalls :

- In the case of the CERC formula, the climate table needs to be representative of the nearshore zone (breaker line). This is often more difficult to obtain than offshore data.
- To keep some control over the model input at the boundaries, there should be little wave transformation between the boundaries and the breaker line, in particular little refraction. If the condition selected in the climate table is applied directly at the boundary, waves may for instance refract towards the coast to represent a different wave class at the breaker line.

- The transport formula used for the reduction should be similar to the one used in the model, else the reduction may end up being suboptimal (Figure 5-19 ; Walstra, 2011).

Zimmermann et al.(2012b) details such a reduction procedure.

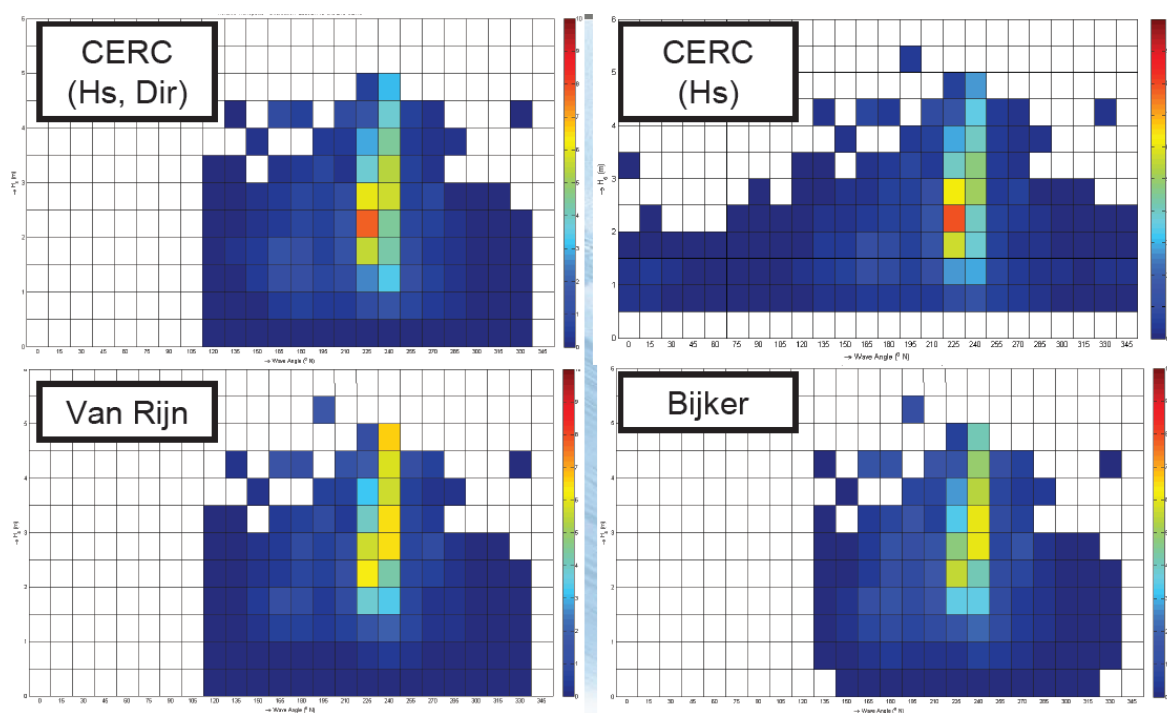


Figure 5-19 : Example of longshore transport contributions per wave class (direction on x-axis, height on y-axis) for several coastline orientations combined, with four different transport formulae. Case study at the Carrara coastline, Italy. Figure from Walstra (2011).

5.5.3 One dimensional model for longshore transport

A one-dimensional model may be another option to reduce the wave climate which should not require too much time. 1D models like Litdrift can compute quickly the cross-shore distribution of the longshore sediment transport for each wave condition. Conditions may then be selected and weighted to reproduce the full distribution of gross and net transport at one or more locations.

5.5.4 Profile model for cross-shore transport

It may seem desirable to extend this kind of wave climate reduction to cross-shore transport, in order to simulate very long time series of cross-shore profile development, with storms and recovery periods.

We think however that this is much more difficult than a reduction of longshore transport, because the cross-shore profile is very dynamic under storm conditions. It is likely that a given wave climate reduction will be applicable for a point in time only, as long as the morphology of the cross-shore profile does not change too much. Instead it may be possible to start from a full time series of wave conditions and to take average values over a chosen time interval, which could for instance reproduce the sediment concentration under waves and currents at the breaker line (Figure 5-20). The longer the time interval, the coarser the reduction but the higher the morfac which can be applied. This approach could be justified by a proof of concept over a shorter time period.

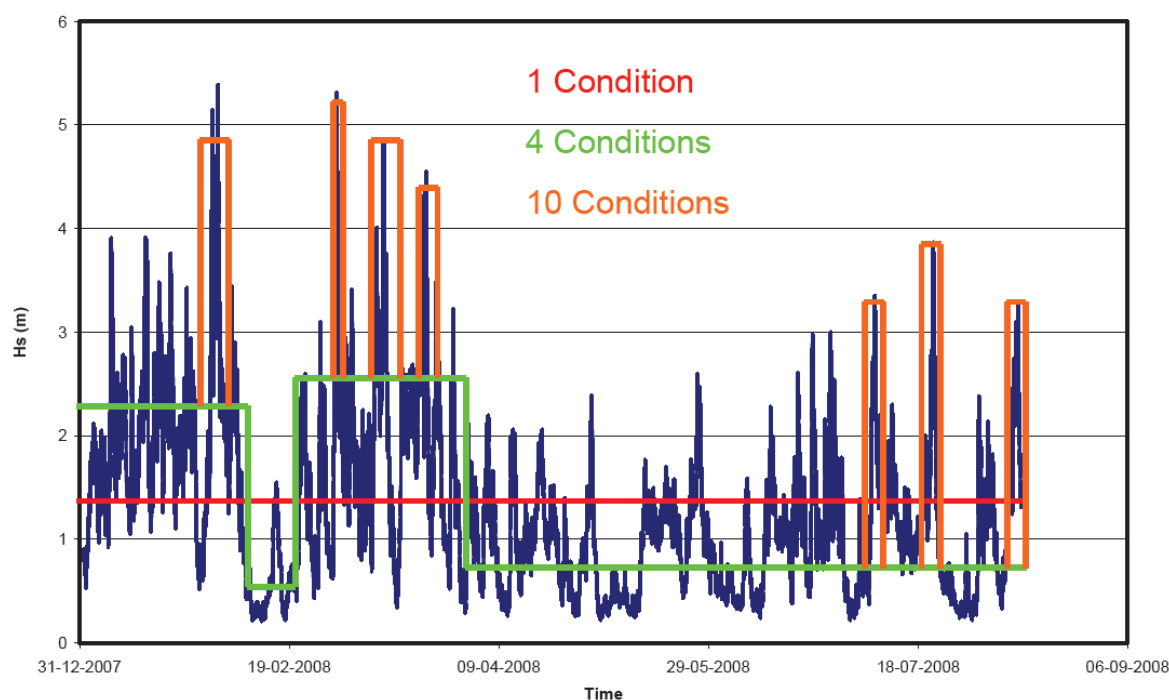


Figure 5-20 : Example of simplification of wave time series. Figure from Walstra (2011).

5.5.5 Hydrological year

Another project, not presented here due to confidentiality of the example, uses a method that will be called here the hydrological year method. The example project uses this method to study flow regimes. It is strongly based on expert judgement and could possibly be extended to morphological modelling.

First the full time series of all hydro-meteorological parameters are taken over many years. These time series are analysed and a physically and statistically representative hydrological year is taken. Within this year, several sub-periods are selected which are representative of different typical regimes of the system (say a period of weak NW winds, moderate waves, strong river discharge). The model is run and analysed for each typical regime.

Instead of separating the individual reductions for tide, wind and waves, this kind of method keeps at all time the full correlation between all hydro-meteorological parameters. The risk of making an important error in the reduction procedure decreases. This kind of approach is expected to be important in complex systems like estuaries, where it may not always be possible to test all the important combinations of various parameters like with wind-wave classes.

5.6 Morphology modelling

5.6.1 Methods

Generally speaking, continuity is very important for morphology. Space-varying input values such as a roughness field and probably a natural distribution of sediment fractions should not present discontinuities. The initial bathymetry should also be smoothed out before being used for morphology. Even then, natural² evolutions can often only be separated from noise resulting from input uncertainty (measurements) after several years of morphological changes (Figure 5-21).

² “natural” in the sense of modelled behaviour which is physically acceptable, by opposition to “noise” in the sense of initial adjustment of the model bathymetry (spin-up) due to an imperfect model setup compared to reality

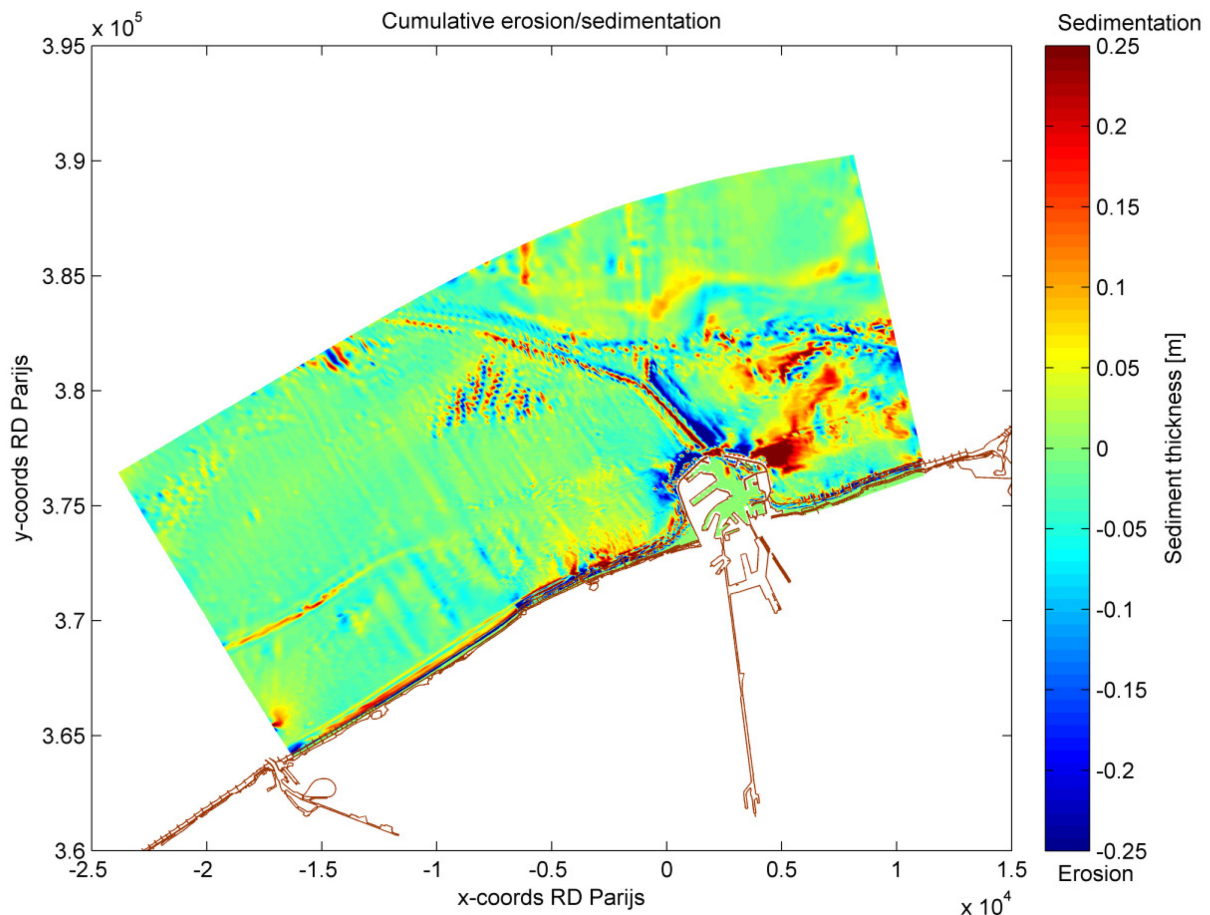


Figure 5-21 : Erosion-sedimentation pattern after one year of morphological changes in the Belgian coastal zone, showing a noise of $\pm 5\text{-}10\text{cm}$ even after bathymetry smoothing.

Once the wind, the wave climate and the tide have been reduced, the simplified conditions with their weights have to be recombined to model their long-term effect on the morphology with a morphological acceleration factor (morfac). Several methods exist :

- **MorMerge** : In the MorMerge system implemented in Delft3D, the effect on morphology of each wave condition of the reduced climate is computed at each time step and merged according to weights specified at the beginning (Figure 5-22). This method avoids history effects because it is like computing the mean effect of the full climate at each time step.
- **Time-varying morfac** : The different weights of each wave condition can be taken into account with a time-varying morphological acceleration factor (morfac) and a constant duration of each condition. Mild conditions which occur often can be accelerated more than storm conditions which occur rarely. Such a method requires special care during the setup of the time series of waves. A transition tide with morfac zero is needed between two successive conditions, and the morfac change should better happen at the turn of the tide, when the suspended sediment concentration is low, to avoid mass balance effects (Lesser, 2009). History effects may be present.
- **Constant morfac** : The different weights of each wave condition can be taken into account with a constant morfac and a different duration for each condition. In this method the morfac is however limited by the duration of the shortest condition, reduction of computation time may not always be sufficient. History effects may be present (which is in some cases desirable). This method has been successfully applied in XBeach and in Delft3D for the sedimentation of the port entrance in Blankenberge (Zimmermann et al., 2013a).

An exercise by Ali Dastgheib (Unesco-IHE, personal communication) shows that the MorMerge and time-varying morfac methods yield very comparable results. As explained above we think that this conclusion does not apply to the surf zone (cross-shore profile distortion).

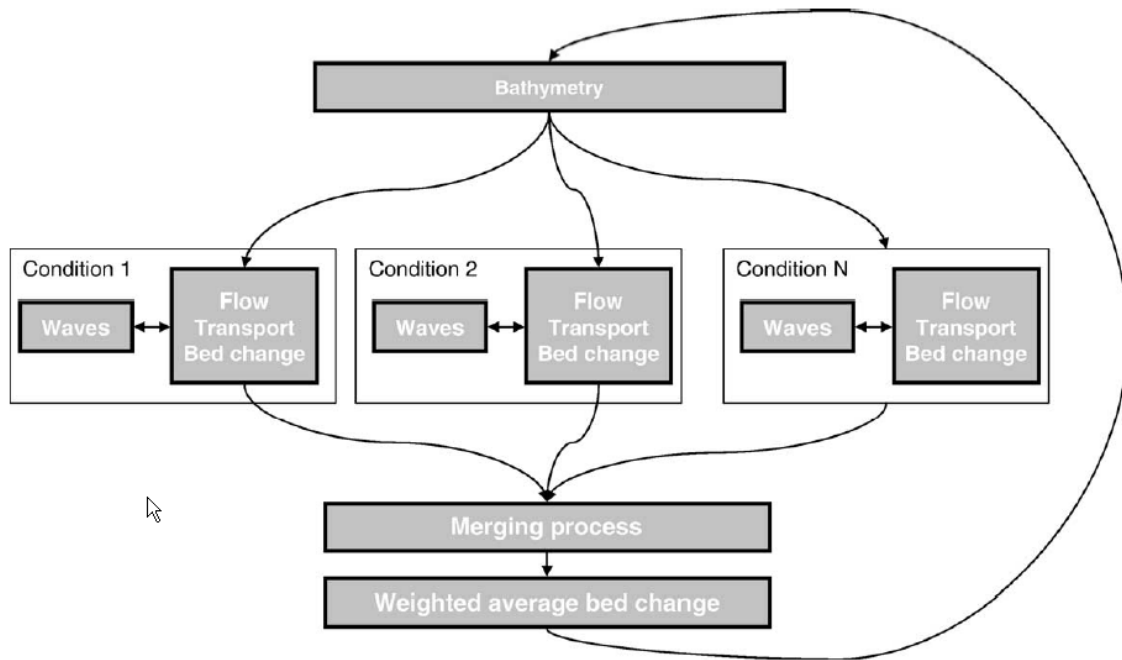


Figure 5-22 : Schematisation of the MorMerge process for morphological modelling with a reduced wave climate. Figure from Lesser (2009).

The maximum morfac which can be used depends very much on the application. It can typically be in the range 1-10 for storm erosion, 10-100 for the long term average evolution of the surf zone, for 100-1000 for the evolution of inlets and estuaries without waves. Dastgheib (2012) shows a very long term application for the Wadden Sea evolution in the Netherlands over 5000 years, with a simplified model setup.

Mormerge

This method has been applied to model the morphological evolution of the Belgian coast over 10 years (Wang et al., 2014 ; Figure 5-23). MorMerge is an undocumented tool of Delft3D, its installation and use are described in Annex B.

The Mormerge approach has the major advantage to generate smooth results because the yearly climate is applied at each time step. The stability associated with this smoothness allows to use a larger morfac and therefore to reach longer time scales with this method (paragraph 5.6.3).

Results show a good quantitative agreement on the transport rates in the surf zone. The major morphological changes expected are qualitatively reproduced by the model, where the system is strongly out of equilibrium (coastline orientation in Wenduine, sedimentation in approach channel of Zeebrugge, sedimentation West of Zeebrugge, erosion in Knokke, sedimentation in the Zwin inlet). The Baai van Heist is an exception, there 3D effects and multiple sediment fractions have been shown to play a role. On the other hand, at places with weak anthropogenic impact like on the shelf, the morphological evolution is poorly predicted. This is expected because the sea bed is in a weak dynamic equilibrium, it is constantly weakly adjusting to the natural forcing. The natural evolution is easily overshadowed by the effect of model inaccuracies such as spatially varying roughness and sediment characteristics, as well as human activities such as dredging, dumping and regular nourishments. A great deal of interpretation is therefore necessary to analyse long term modelling results.

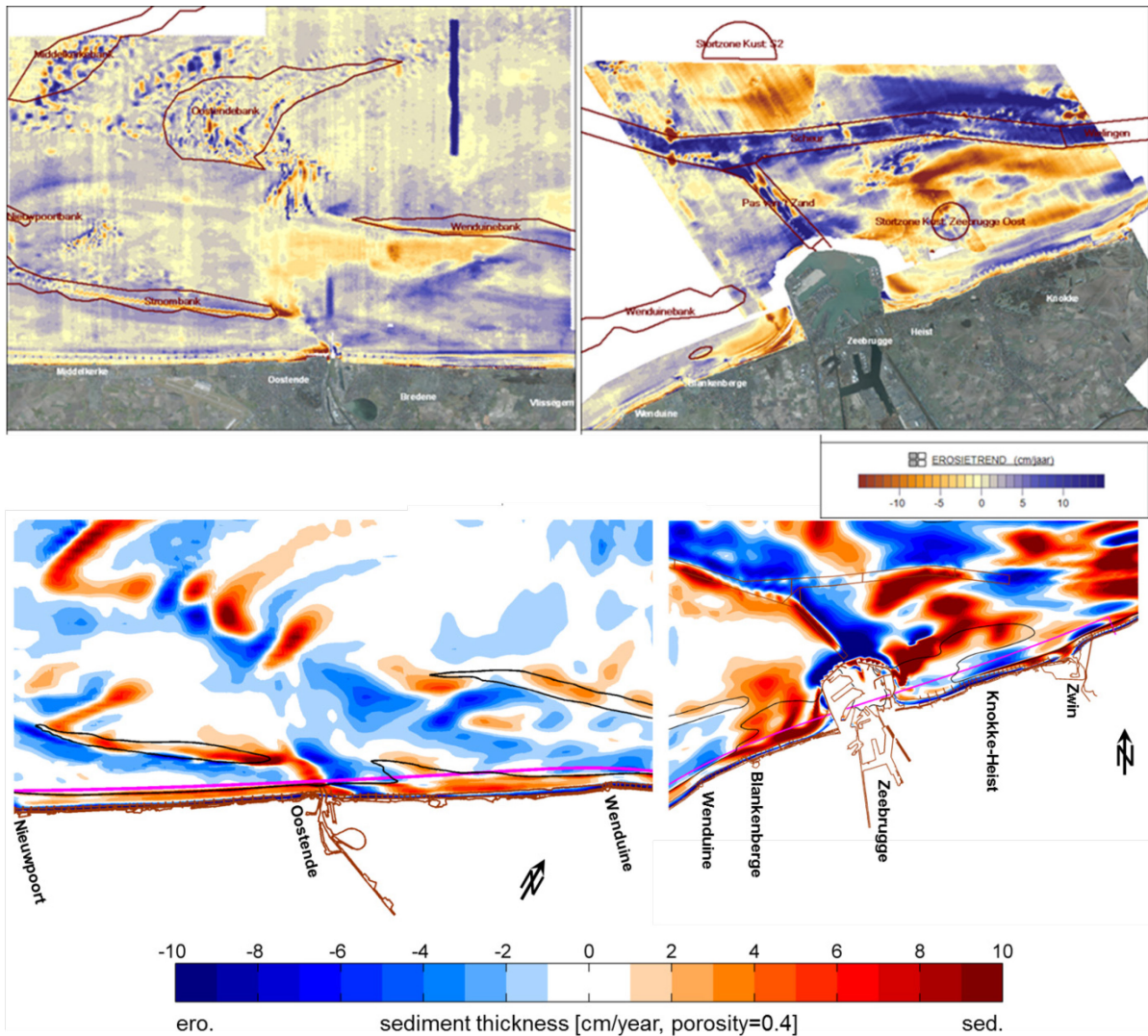


Figure 5-23: Observed (upper) and modelled (lower) sedimentation/erosion from Nieuwpoort to the Zwin inlet (in cm/year averaged over 10 years).

Time-varying morfac

This method has been tested in XBeach for the morphological evolution of the coast near Knokke (Lanckriet et al., 2015b). It allows to speed up the simulation more than the constant morfac approach, but it strongly distorts the cross-shore profile because wave conditions are sped up too much and not “mixed” (i.e. there is no calm period between two storms). Also in XBeach the difficult implementation complicates pre- and post-processing.

This, the slower code, and the lack of a MorMerge method in XBeach make it difficult to model periods longer than a few years in 2D. An example of a bash script to run a time-varying morfac simulation in XBeach is shown in Annex C.

Constant morfac

The constant morfac approach has the big advantage of being easy to implement and provides valuable information about individual storm events, however it also introduces undesired side effects due to the decoupling of hydro- and morphodynamic time scales : the equivalent of an entire storm is modelled with a constant water level, and wind generated currents do not have the time to be established. An example of long-term morphology computed with the constant morfac approach is presented in Wang et al. (2012 ; Figure 5-24, Figure 5-25).

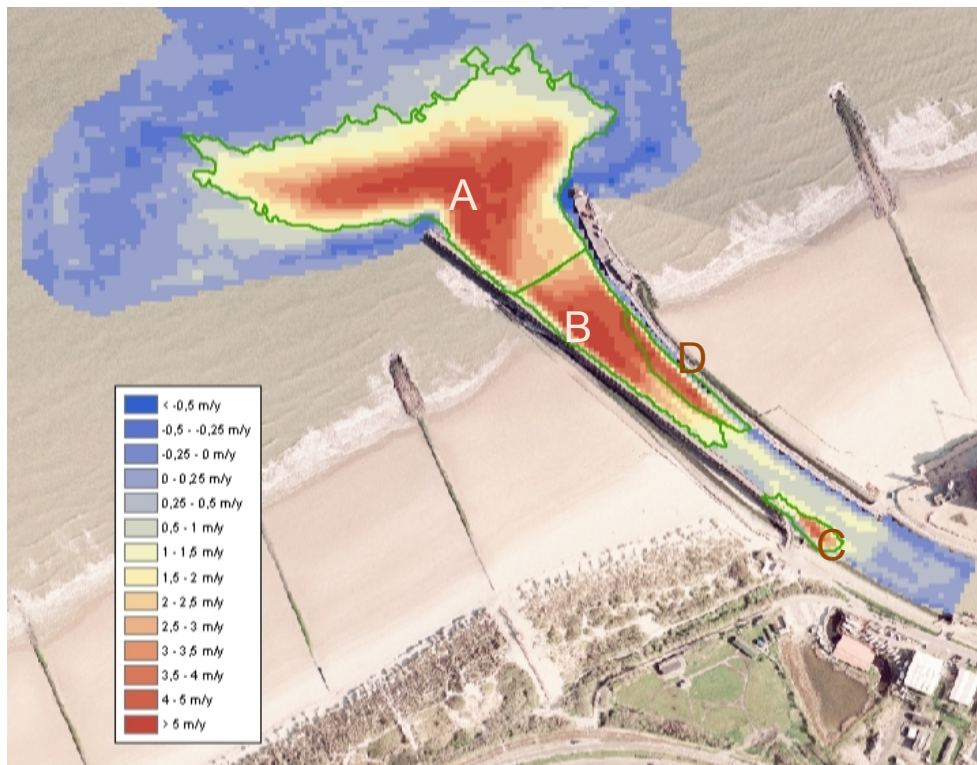


Figure 5-24 : Long-term sedimentation rates in Blankenberge estimated from measurements. Figure from Teurlinx *et al.* (2009).

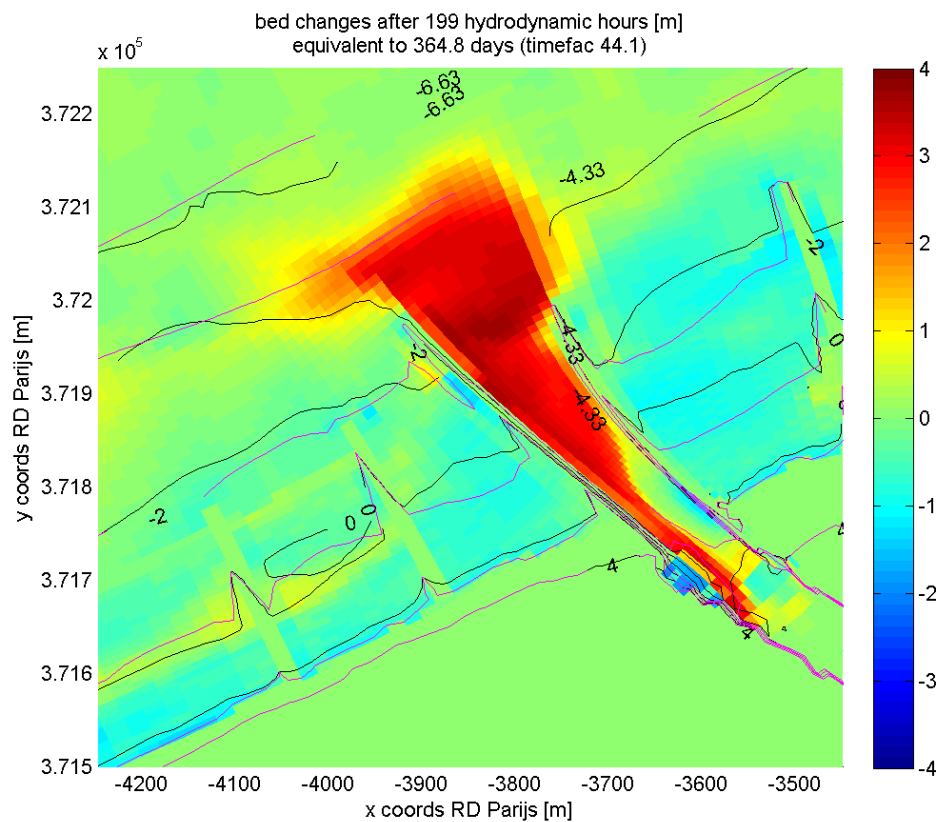


Figure 5-25 : Erosion-sedimentation pattern in Blankenberge after one year, computed in XBeach. Reference results. Differences with measurements are mostly due to side effects of the modeling methodology.

The difficulty of the constant morfac approach comes from the choice of the wave update interval. The choice of this duration is important for both Delft3D and XBeach :

- In Delft3D, stationary wave computations are carried out at a regular communication interval. The shorter this interval, the shorter individual wave conditions can last and the better the time series can be reproduced, however the longer the program will spend computing wave fields. A too large interval results in bed instability when combined to a large morfac. In that sense part of the time gained with a larger morfac is lost in additional wave computations. The long computation time of the wave field seems to always be the limiting factor. The standard communication interval is 20min, here it has been reduced to 10min.
- In XBeach, for each wave condition a time series of instationary waves is generated, after which this time series is repeated until the desired duration is reached. This time series should contain enough waves to generate representative results once averaged, it typically lasts for one hour and XBeach suggests a duration at least greater than 20min.
- In addition the duration of one wave condition determines how much time is available for the wind to establish the wind-driven current. This is very important because its time scale ranges from less than an hour in very shallow water such as in the surf zone, to more than a day in deeper water and/or for larger wind velocities. Roelvink and Reniers (2011) present simple equations to estimate this effect. Sudden changes in wind conditions also create unrealistic jumps in current velocities.

The modulation of water levels at an unrealistic morphological time scale can also lead to undesired side effects. If a given wave condition is applied during one hour with a morfac of 20, it is equivalent to simulating 20h of morphology. This means that the occurrence of a large wave height corresponds to almost a day of storm. In the meanwhile however the water level has almost not varied. If the sedimentation depends on the water level, such as in the entrance channel to the port of Blankenberge, the resulting sedimentation pattern will depend on the time series applied (Figure 5-26, Figure 5-28). This effect can be reduced by making each wave condition occur under different water levels (shorter duration), but then the previously mentioned side effects become important (Figure 5-27, Figure 5-28).

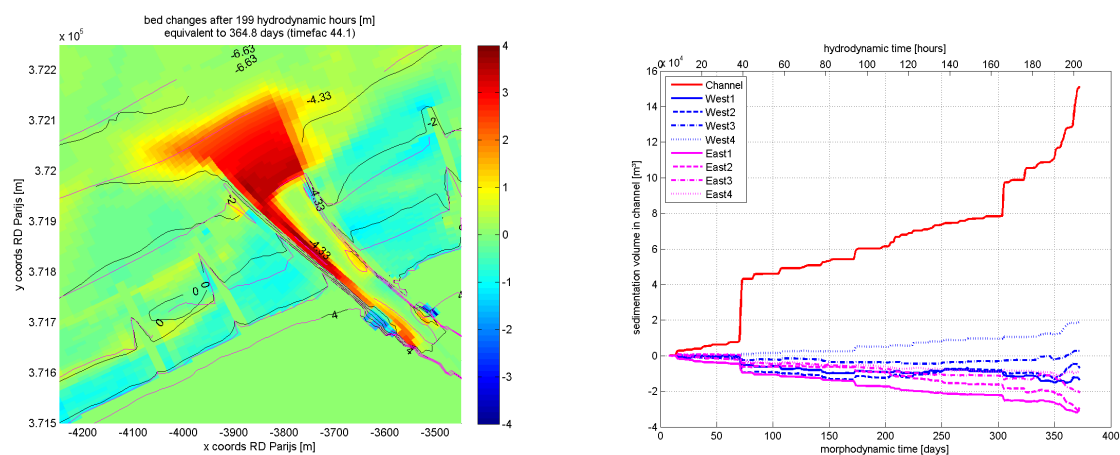


Figure 5-26 : Example of sedimentation pattern obtained with unsuitable time series of forcing parameters (storms coinciding with low water and clustered at simulation end). Erosion-sedimentation pattern after a year (left), cumulative sedimentation volumes (right).

Another issue which is specific to XBeach are the two different ways morphology can be accelerated :

- The default option morfacopt=1 shortens the hydrodynamic time series by the morphological acceleration factor (morfac). It means that for instance with a morfac of 10, every one hour only 6 min are computed, the bed change is multiplied by morfac and then the model skips the data until the next hour. This is very convenient to use directly real measured time series of a year while reducing the computation cost. But it is not compatible with advection, because water level variations are accelerated, hence velocities and sediment transport exaggerated. This issue is also visible in 1D long term profile modelling in the long wave fluxes (Zimmermann et al., 2015).

- The alternative option morfactopt=0 keeps the hydrodynamics as is, but multiply the bed change by morfac at each time step. This means that input reduction is necessary to reduce the computation cost. It comes with its own side effects described above.

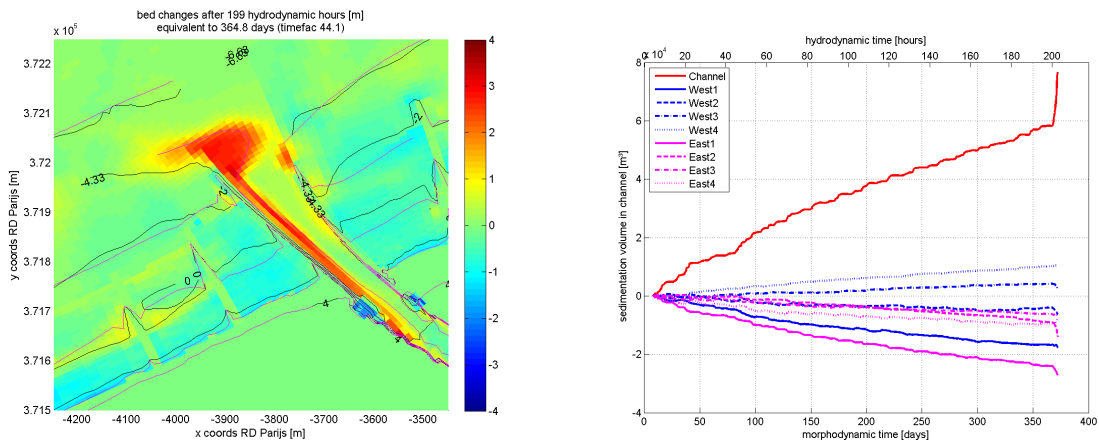


Figure 5-27 : Example of sedimentation pattern obtained with unsuitable time series of forcing parameters (small update interval). Erosion-sedimentation pattern after a year (left), cumulative sedimentation volumes (right).

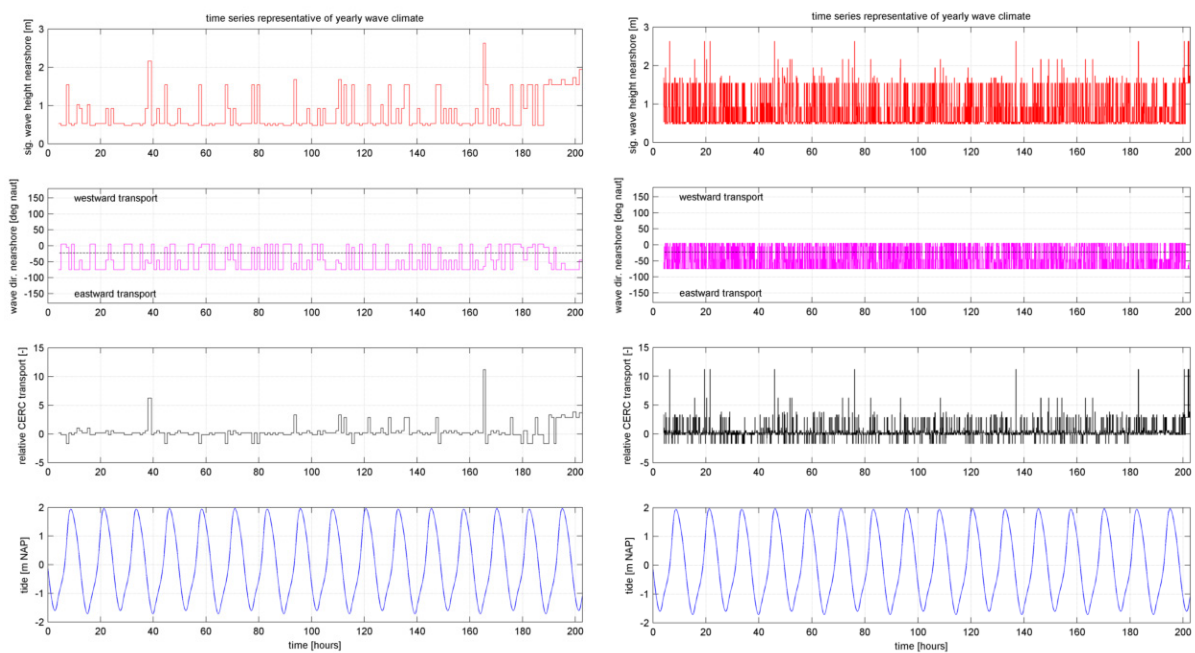


Figure 5-28 : Reduced wave climate corresponding to Figure 5-26 (left) and Figure 5-27 (right). From top to bottom: significant wave height, wave direction, relative longshore transport estimated with the CERC formula, and tide.

The decoupling of time scales is quite similar to that of physical models. Changing the morphological time scale affects other time and spatial scales. In physical models this is accepted and the time and spatial scales relevant for the study are reproduced closely by changing parameters such as the forcing, some densities or the vertical scale for instance. It is well-known that it is not possible to scale everything in physical models, errors are accepted in the reproduction of less relevant processes. A similar thinking could be adopted for morphological modeling. Important processes such as the wind could be scaled to still generate the correct results while accepting errors in secondary processes. Unfortunately it is often not easy : it is for instance possible to decrease the time scale of the wind by increasing the bed roughness or decreasing the depth, however this affects in turn the currents.

Finally the generation of suitable time series is not evident and requires some extra thoughts and some knowledge of statistics. Below some possible methods are presented.

Time series generator

Starting from a measured time series, it is possible to generate realistic looking time series for use in morphological models, for instance for probabilistic design. Instead of time-consuming input reduction, it would allow to simulate several possible shorter climates and to estimate the expected variability in results (like ensemble-averaging).

In literature, the generation of realistic time series is referred to as resampling. Below follow some stochastic methods :

- Markov chains determine the probability of the state at time t based on the known state of time $t-1$, $t-2$, et cetera based on the order of the Markov chain. Shannon (1948) illustrates this nicely by applying it to the English language. It can be used if several time series are needed, for instance for probabilistic design.
- Auto-regressive models are close to Markov chains in the sense that the prediction at time step t depends on the data at the previous steps. Instead of using probabilities however, the method works based on a linear regression.
- Block resampling consists in cutting the observed time series in blocks of random length and in rearranging these blocks.

Monbet et al. (2007) review stochastic models for wind and sea state time series, with amongst others resampling methods. They also discuss the issues of correlated variables and circular variables like the wind direction.

Scheffner et al. (1992) present an application of such a stochastic method to generate realistic time series of wave height, period and direction exhibiting the same statistical properties as the measured data. Aillot and Prevosto (2001) also present two methods to generate realistic time series of correlated wave height and direction.

Attention points lie in the difficulty to produce time series which also respect some statistical properties. The extreme value distribution of the resampled time series may for instance differ from the distribution of the original time series.

5.6.2 Parameters and current limitations

Lesser (2009) suggests that the current limitations of morphology modelling lie in the roughness formulations, the bed slope effects and the transport formulae. The error due to a good input reduction is much lower than that due to lack of knowledge in the formulations of physical processes. However one has to keep in mind that an input reduction is derived for one specific application and cannot be transferred to another application of the model. Typically all errors linked to the reduction are hidden in what is *not* in the reduction target. It has for instance been shown that a representative tide derived for a 2D model is not representative anymore for a 3D model (Wang et al., 2015), because the calibration of hydrodynamics is different. Davies and Thorne (2008) review recent advances in morphology modelling, including knowledge about bed roughness, turbulence and measurement techniques for bed forms.

Geometry (bathymetry and topography) may often determine the qualitative system behaviour to a large extent, even before any calibration. Van der Wegen and Roelvink (2010) reproduce closely the current bathymetry of the Western Scheldt river with simple model settings and an initially constant depth.

Sediment fractions strongly influence transport behaviour (Hassan, 2012, Trouw, 2013), because the fraction in suspension may be much finer than the average grain size and has a lower fall velocity. It also directly impacts the bathymetry through spatial segregation of grain sizes. Coarser fractions can fill in channels which are too deep when using a single grain size (Dastgheib, 2008). This can partly compensate unrealistic coefficients for bed slope effects.

The roughness is often one of the most sensitive calibration parameters for hydrodynamics and sediment transport. It remains however difficult to estimate in advance, because of several reasons :

- Data is often not available. Megaripples and dunes can be derived from multibeam echosounder data with geostatistical and spectral methods (Van Dijk et al, 2008), but the resolution is not sufficient yet for smaller ripples. Measurement techniques for smaller bed forms do exist, like the Acoustic Ripple Profiler (Davies and Thorne, 2008), but only cover a small area, and only one moment in time.
- The roughness coefficient used in models is generally not directly related to geometric characteristics of bed forms. Possible roughness coefficients are either constant (Darcy-Weisbach, Chezy), dependent on the depth (Manning power law, White-Colebrook log law) and/or sometimes related to a roughness length z_0 (White-Colebrook log law). This roughness length comprises a skin friction (flat bed grain size), a form drag (bed form geometry) and a sediment transport contribution (momentum transferred from flow to sand grains ; Soulsby, 1997), each with several formulations. It hence depends on local hydrodynamic conditions, including wave-current interaction, and like the viscosity on the grid resolution (subgrid bed forms). The finer the grid, the lower the form drag contribution will be.
- It is advised to keep roughness calculations simple, because the full approach is still partly based on very uncertain formulations for the roughness length and implicit relations are present. A roughness predictor can be considered to evaluate the expected spatial and temporal variability of the roughness field and to help determine calibration values (Villaret et al, 2012), but should not be considered as ground truth either. The roughness predictor of Van Rijn for instance does not predict a significantly lower roughness for a muddy sea bed, which strongly limits its applicability. As a consequence the predicted roughness does not vary spatially enough to give a clear added value compared to a constant value.

The roughness formulation influences the equilibrium morphology even in simple test cases (Lesser, 2009). It also controls strongly whether a negative or a positive feedback exists between the flow and the morphology, that is whether bed forms will develop or not (Ter Brake and Schuttelaars, 2011).

5.6.3 Scaling up the time horizon

The methods presented above allow to simulate long term morphology. However some specific issues arise in the surf zone because it is an order of magnitude more dynamic than on the continental shelf. This is why many morphological applications exclude the surf zone.

Ranasinghe et al. (2011) proposed a CFL criterion based on the bed form migration speed to determine the maximum morfac acceptable before impacting results ($CFL < 0.05$). Applying this criterion in the surf zone even under normal conditions (wave height 1m, approach angle 45 degrees) results in a critical morfac of about 5 to 10 in the surf zone compared to 300 on the shelf (Figure 5-29). Obviously a higher morfac has to be used to keep computation time realistic.

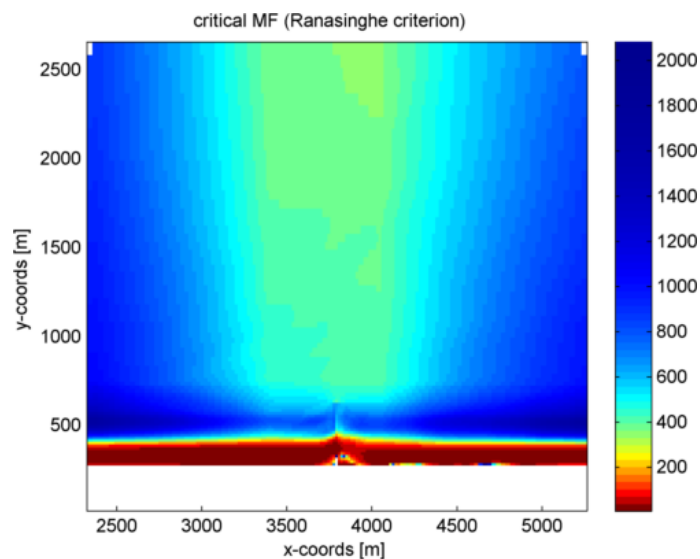


Figure 5-29 : Critical morfac according to the criterion of Ranasinghe et al. (2011) on a simplified coast (surf zone at bottom) under a calm wave climate (wave height 1m, approach angle 45 degrees).

Some practical tests have been executed to determine starting from which morfac results in the surf zone effectively become unrealistic from an engineering point of view. Two conclusions have been drawn from these tests :

- Firstly a much higher morfac than predicted by Ranasinghe et al. (2011) can be used in practice, albeit indeed with some slight influence on the results from morfac 10 on. Results were qualitatively still acceptable up to morfac 50 for normal conditions. Storm conditions are expected to be much more restrictive.
- Secondly the maximum morfac which can be used is directly related to the wave update interval used. When morphological changes near the waterline become too important, stability issues arise. In the tests, the critical wave update interval was about 2h with a morfac of 10, but only 1h with a morfac of 50. This has strong implications for the computation time, because we would ideally like a high morfac and a large wave update interval. Part of the time gained by using a higher morfac is lost decreasing the update interval. Wave computations are the most time-consuming part of the morphological simulation.

Stability issues can be avoided by allowing the coastline to erode (not the case with default settings in Delft3D), by avalanching in XBeach or with dry cell erosion in Delft3D. This reduces instabilities near the waterline and allows to apply a higher morfac.

Another problem related to the surf zone is the cross-shore profile conservation over long time horizons. On a time scale larger than a year the shape of the cross-shore profile is generally conserved : erosion in the winter is compensated by onshore transport during summer. Ideally, a long term morphological model should therefore also conserve the profile. In XBeach this requires extra calibration because the profile is free to evolve. In Delft3D offshore transport is not modelled in 2D, so onshore transport has to be turned off. This profile is not fully stable though because it flattens due to sediment diffusion over long time horizons. It can be tuned with limited onshore transport. Some research models avoid this issue by combining a 2D model for the shelf with a coastline model for the surf zone.

In Delft3D, the longest time horizons (>10 years) of a 2D morphological simulation including waves, the tide and the surf zone have been achieved with the following settings :

- Mormerge method
- Dry cell erosion
- Reduced climate with 4 wave conditions
- Wave update interval of 1h

With a 3D model, Mormerge has been replaced with the variable morfac approach to further reduce computation time. The time horizon is comparable to that reached in the Sand Motor study in the Netherlands (20 years, 2D model). 3D morphology computations are often unstable or yield unrealistic results, and should be avoided.

In the Zandmotor study in the Netherlands, the evolution of a large scale nourishment was predicted over 20 years with a comparable method : 4 wave conditions, no tide, the Mormerge method and a special module to include dune erosion and stabilize the cross-shore profile.

In XBeach, the slower computation due to the explicit numerical scheme, and the absence of the Mormerge method limit the time horizon for this kind of simulations to about a few years (Lanckriet et al., 2015b). The following settings were used :

- Constant morfac approach
- Morfac of about 30-40
- Reduced climate with 11 wave conditions
- Instationary long waves

Stationary wave computations and a variable morfac approach may reduce the computation time slightly, but did not yield an order of magnitude improvement (rather a factor 2). With a great deal of effort (or patience) a period up to 5 years can be modelled, but with side effects on the cross-shore profile evolution if the morfac is too high. It is worth noting that for a yet to be identified reason, the computation time in XBeach can strongly depend on the duration of instationary time series, it cannot deal with too large boundary datasets. In the 2D model of Knokke (Lanckriet et al., 2015b), a duration of 20 min instead of the default 60 min for keyword rt (duration of long waves record at the boundary) was found to reduce the computation time by a factor 5.

For both cases presented above (Delft3D and XBeach), the computation time is in the order of 5 days on the hardware available for the project.

If waves and the surf zone are omitted, time scales of centuries to millennia can be easily achieved in Delft3D with enough model simplifications (Dastgheib, 2013).

5.7 Conclusion

We advise the following concerning morphological modelling and input reduction :

- Input reduction is often necessary to reduce computation time. It has been shown to work very well and most importantly it should not be the limiting parameter of a study if executed correctly. However the reduction itself also takes time and errors can easily arise.
- The quality of the reduction depends to a large extent on a good understanding of the system. An automated statistical procedure like OPTI can help to find a better reduction but will never replace data analysis and expert judgement. Spatial scales, temporal scales and main driving processes should already be more or less identified before the reduction.
- All input reduction techniques reduce complex input according to a target. This target should be chosen very carefully, because the error will arise in what it does not include. It is in particular very important to keep existing correlations between parameters in the reduction, and to verify the quality of the reduction at each step, in particular its spatial agreement.
- A target can be a weighted combination of several parameters. For sediment transport for instance, it is advised to look at net transport, but also at gross transport and if available at erosion-sedimentation. The transport formula used for the reduction and in the final model should be the same.
- As shown earlier by Latteux (1995), a good spatial transport pattern may be preferable to good transport values, which can still be scaled later with various methods. The scaling method also generates errors and should be selected according to the desired property. In a situation in which waves and currents are equally important, it is possibly better to scale the flow boundary conditions.
- Generally speaking, continuity is very important for morphology. Space-varying input values such as a roughness field and probably a natural distribution of sediment fractions should not present discontinuities. The initial bathymetry should also be smoothed out before being used for morphology.
- Morphological modelling can then be done with the reduced set of conditions with a time-varying morfac or the MorMerge method. Both methods are said to perform equally well. History effects are lost with MorMerge, and transition periods are needed with a time-varying morfac to prevent mass balance issues. Alternatively, the constant morfac approach is the most easy to implement and provides valuable information about individual storm events, but it comes with its own side effects. Mormerge, together with some specific settings to avoid stability issues, is the most suitable method to reach longer time horizons.
- One of the main difficulties of the constant morfac approach comes from the choice of the wave update interval. It impacts the computation time, the stability when combined with a high morfac and the time available to establish wave- and especially wind-driven currents when decoupling the hydro- and morphological time scales. The modulation of water levels at an unrealistic morphological time scale can also lead to undesired side effects. Finally the generation of time series requires particular care, Markov chains could be used to generate realistic records.

- Current limitations of morphological modeling possibly lie in the roughness formulations, bed slope effects and transport formulae. However simple geometry often already determines a large part of the system behaviour, even before calibration. Sediment fractions can have important effects on the results.
- In Delft3D, time horizons of 10 years and more can be achieved by increasing the wave update interval, combined with dry cell erosion for model stability, a reduced number of wave conditions and the application of the Mormerge or the variable morfac approach.
- In XBeach, the instationary character and the lack of a Mormerge method restrict the time horizon to at most a few years with the constant morfac approach. The duration of the boundary time series (keyword rt) determines to a large extent the computation time of large models and should be kept low. Stationary wave computations and a variable morfac approach may yield an additional speed-up of a factor 2. The latter is not user-friendly, it is suggested to run one simulation per wave condition and sum up the results in the post-processing instead.

6 Modelling inlets and embayments

6.1 Overview

Coastal inlets and embayments are particular morphological elements for which specific research has been conducted and tools developed. On the Belgian coast, they concern the Zwin inlet and the Flemish Bays concept. Following potential questions from the Coastal Division regarding these topics, some literature was reviewed and some tools were investigated. This chapter presents the main conclusions.

6.2 Tools for inlet stability

6.2.1 Inlet theory

Coastal inlets and tidal basins have been the source of research for a long time because they are often important for navigation and spatial planning. The Coastal Inlet Research Program (CIRP) of the US Army Corps of Engineers for instance analyses the behaviour of inlets on the American coast and develops tools to evaluate the impact of human activities.

For a comprehensive review of the theory of coastal inlets and tidal basins, the reader is referred to Tung (2011) and associated references. Below a summary is given of some main concepts.

Figure 6-1 schematises the conceptual behaviour of a coastal inlet. Figure 6-2 gives an example of a real coastal inlet. An inlet is an opening between the sea and a water body behind a dune system or barrier islands. This opening is maintained by the current (tide, river) and closed by sediment fluxes (longshore transport). The relative importance of these processes determines the long term or temporary (in)stability of the inlet. The tidal current keeps the inlet gorge free of sediment, which settles on both sides to form a flood and an ebb tidal delta. In order to drain the basin behind, a channel system often develops. The dimensions of the inlet gorge, the deltas and the channel system depends on the tidal prism, the volume of water entering the basin during each tidal cycle. Long term sedimentation in the low energy tidal basin environment, combined with net sediment import from tidal asymmetry, can form tidal flats which can grow into salt marshes and control the tidal prism. Wind can also supply sediment into the inlet from the adjacent dune system. Coastal inlets are generally asymmetric due to longshore transport, the direction of tidal propagation in relation with the Coriolis force, and / or the basin geometry.

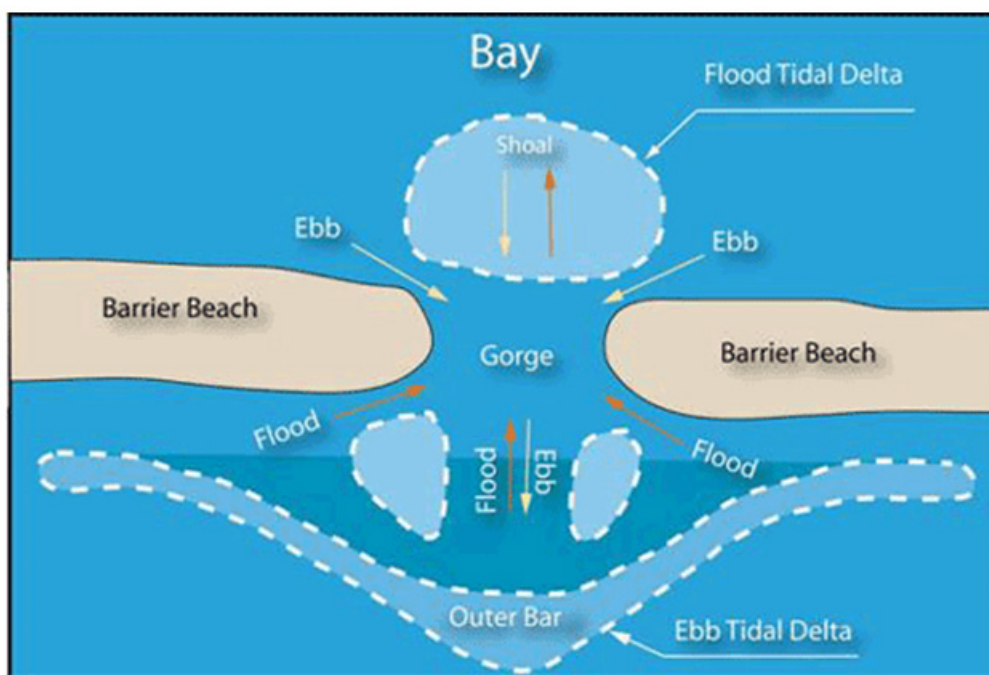


Figure 6-1 : Typical configuration of a tidal inlet (Google Images, 2013; from the U.S. Department of Transportation website).

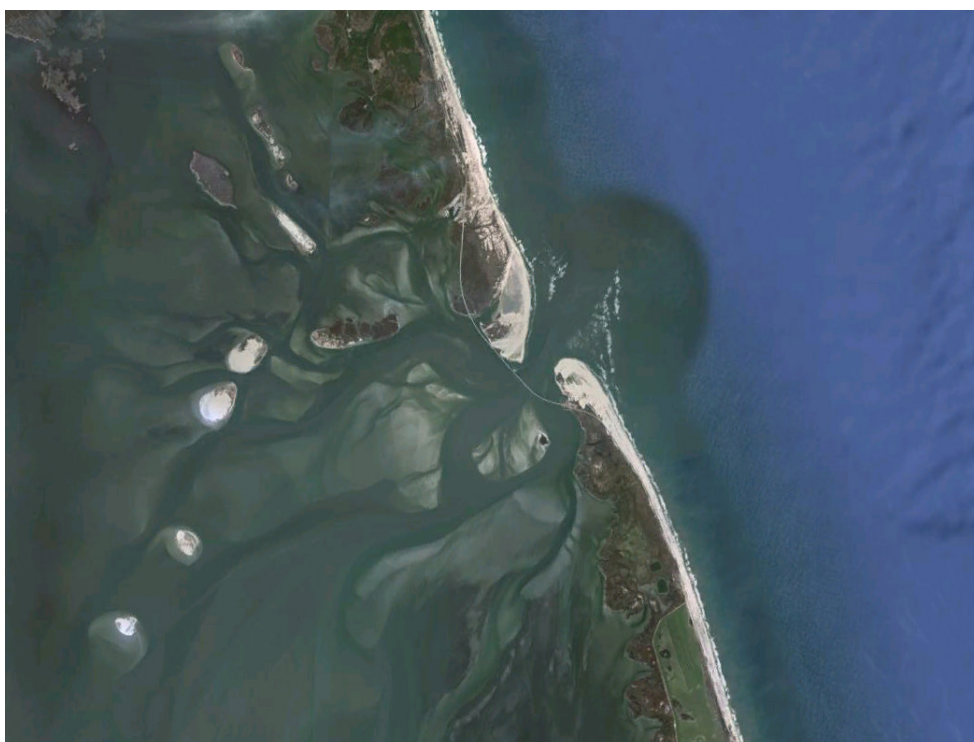


Figure 6-2 : Example of a coastal inlet and a tidal basin North of Cape Hatteras in the USA, with flood delta, ebb delta and channel system visible.

Coastal inlets are hence by definition highly dynamic systems : the exact situation of the system depends on the evolution of the tide, waves, discharge, water level and wind. The most dynamic morphology is found in and near the inlet entrance, where the strongest currents are present. The variability of the forcing parameters often leads to cyclical behaviours of the different elements, such as the cyclical migration of the

inlet entrance and of the ebb tidal delta, the meandering of the channels and the seasonal closure of the inlet. The ebb delta also acts as a natural bypass system for longshore transport.

These dynamics and the often limited morphological data make modelling such systems a challenging task. But some simple analyses can already yield interesting insight into the system behaviour :

- The identification of the relative importance of the forcing parameters and of their variability
- The historical evolution of the inlet (sometimes more than 100 years of evolution reported) compared to the human impacts (sediment, tidal prism) and the forcing parameters
- The analysis of the inlet stability in view of the variability of the forcing parameters.

The geometry also often determines qualitatively the morphology of the system.

The following paragraphs describe some methods to evaluate the stability of coastal inlets.

6.2.2 Escoffier diagram

The Escoffier diagram can be used to evaluate the stability of the inlet. Despite its limitations, this method is still used often because of its simplicity. Van de Kreeke (1992) explains the method more in detail and provides further references.

Escoffier considers an inlet as a channel which continuously fills in by longshore transport, and is kept open by the tidal current. When the tidal current is strong enough to remove the sediment, the inlet remains open and is considered stable. This principle is quantified with the Escoffier diagram such as in Figure 6-3. It consists of two parts :

- A hydraulic condition (closure curve) : To a given cross-sectional area corresponds a given current velocity. For large areas the tidal prism of the basin behind to be filled determines the velocity. The larger the area, the smaller the velocity. For small areas the bed roughness limits the water exchange. So the smaller the area, the smaller the velocity. These two conditions lead to the bell shape of the hydraulic condition. Closure curves depend on the inlet characteristics and are often computed numerically, or with one of the few analytical solutions (Walton, 2004).
- A sedimentary condition (equilibrium velocity) : In order to evacuate a given flux of incoming sediment, the velocity has to be larger than a critical value, the equilibrium velocity. By comparing the equilibrium velocity to the hydraulic condition, the evolution of the inlet from a given initial condition can be evaluated. When the real velocity is lower than the equilibrium velocity, the inlet fills in and when it is larger it expands. For the sedimentary condition, Escoffier observes that the peak velocity in inlets generally lies around 1 m/s, and that this must therefore be the equilibrium velocity. This velocity corresponds to the start of large transport fluxes for medium sand on the Shields diagram. Alternatively the equilibrium velocity can be computed with a transport formula such that it matches the total incoming longshore transport (inlet-directed transport ~ gross transport ; physically better, see example below).

When these two conditions are compared, they generally yield two equilibrium points : one unstable (point A1 on Figure 6-3) and one stable (point A2). Each cross-section larger than that of point A1 will eventually reach point A2, each smaller one will eventually close. This determines the stability of the inlet.

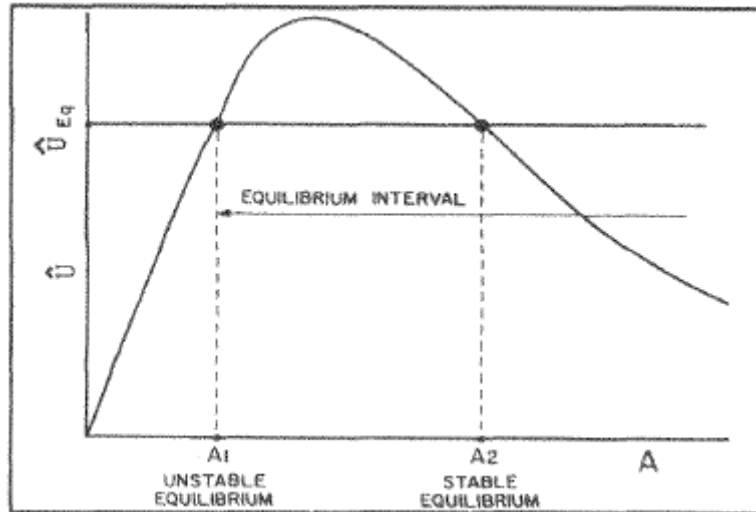


Figure 6-3 : Schematic Escoffier diagram, from Van de Kreeke (1992). Cross-sectional inlet area on x axis, current velocity though inlet on y axis.

The seasonal variability of the forcing parameters can easily be integrated into such a reasoning. Both conditions, and hence the stability, will fluctuate in time (Figure 6-4, Figure 6-5).

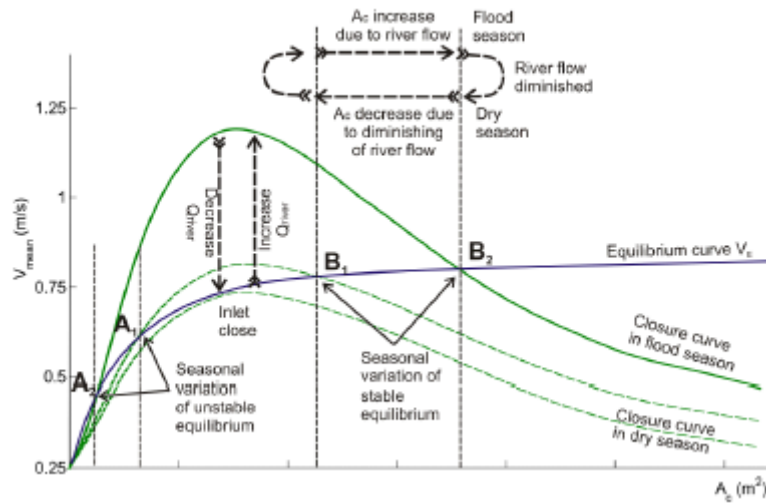


Figure 6-4 : Example of the effect of a river discharge on the hydraulic condition (Stive and Lam, 2012)

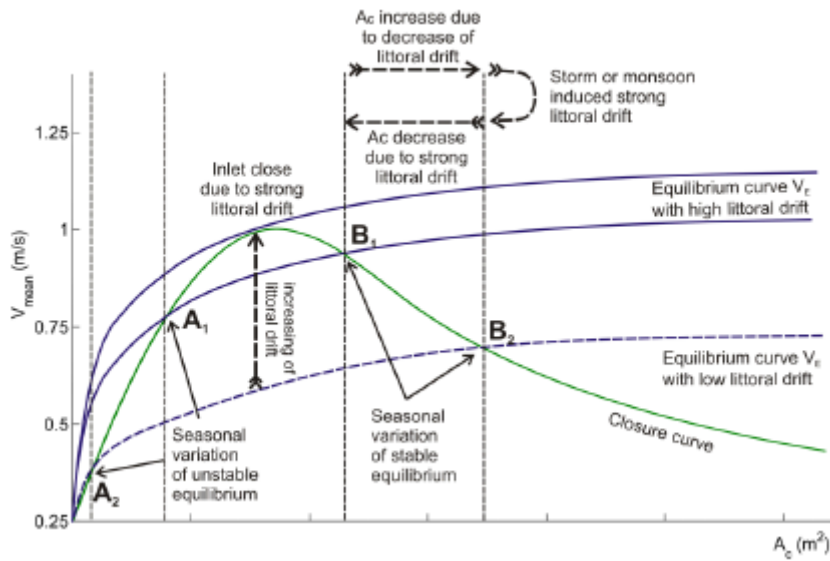


Figure 6-5 : Example of the effect of longshore transport on the sedimentary condition (Stive and Lam, 2012)

Finally an example is given of a sedimentary condition for this method. If sediment transport (S) is a simple power law of the velocity (U) and of the inlet width (W) :

$$S_{in} = S_{out}$$

$$S_{out} = mU_{eq}^n * W$$

then the velocity in the inlet gorge must be larger than the equilibrium velocity

$$U_{eq} = \left(\frac{S_{in}}{mW} \right)^{1/n}$$

to keep it free of the incoming longshore transport (S_{in}). This kind of equation can easily be extended, for instance to account for a critical velocity for sediment transport, to model the width as a function of depth (shape conservation) or to account for a realistic expression of the parameter m .

The limitations of the Escoffier diagram lie in the equations chosen and on the uncertainty surrounding the data (inlet characteristics). Analytical expressions make strong assumptions such as a linear shear stress or the absence of river discharge. Results are very sensitive to the exact shape of the closure curve, especially when the equilibrium velocity is close to the maximum of the closure curve.

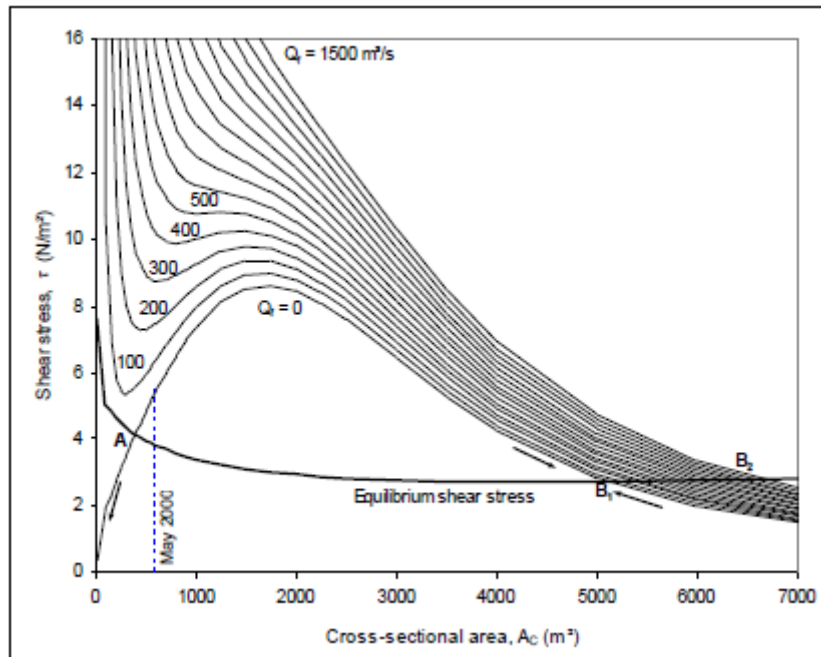


Figure 6-6 : Example of an Escoffier diagram with river discharge : an inlet with strong river discharge always remains open. From Stive and Lam (2012).

6.2.3 Tidal prism relationship

The tidal prism relationships are closely related to the Escoffier diagram, but are used to estimate the inlet cross-sectional area rather than its stability.

Several researchers have developed simple formulas based on empirical data to predict the minimal stable cross-sectional area of an inlet based on its tidal prism (Jarrett, 1976; O'Brien, 1966). The underlying idea is that the inlet gorge must be able to fill the tidal prism (P) within a (half) tidal cycle (T) (hydraulic condition). With an equilibrium velocity of 1 m/s (sedimentary condition), this yields a relation between cross-sectional area A and tidal prism P :

$$P = A * U * \frac{T}{2}$$

$$A = \frac{2}{UT} P = cP$$

Or if the equilibrium velocity is a function of the longshore transport (sedimentary condition) :

$$A = \frac{2}{T} \left(\frac{mW}{S_{in}} \right)^{1/n} P = cP$$

This explains why inlets with a strong longshore transport are relatively smaller (Kraus, 1998) and why naturally protected inlets are relatively larger. We further note that tidal prism relationships underestimate the minimal stable cross-sectional area for very small inlets (Byrne et al., 1980, cited in Stive et al., 2012) because in reality there is little to no longshore transport (large bypass offshore of the inlet gorge ; case of the Zwin inlet).

Empirical relations are more general than the previous equation and contain two coefficients c and d , which depend on the inlet type and typically lie around 10^{-4} for c and 1 for d :

$$A = cP^d$$

This kind of equation is useful for two reasons :

- The relation is by definition equal to the intersection between the hydraulic and the sedimentary condition of the Escoffier diagram, hence it gives a second way to find the location of the stable point A2 on Figure 6-3. By comparing the formula prediction with measured data, the stability can be evaluated.
- The relation can quantify the first order effect of human impacts like land reclamation : a smaller tidal prism requires a smaller cross-sectional area.

It is noted that more complex equations do not always have an improved prediction potential. Stive and Rakhorst (2008) shows that a simple linear relation performs just as well as the empirical equations of Jarrett and O'Brien. For this reason it is recommended to compute the cross-sectional area with coefficients c and d respectively equal to 10^{-4} and 1, and to apply an uncertainty of $\pm 30\%$. If results differ by an order of magnitude with the measured stability, the physically based formulas of Stive and Rakhorst (2008) and of Kraus (1998) can be used, or one's own relation be calibrated on known systems.

Similar equations exist for other elements of the system (flood and ebb delta, channel volume, tidal flats). These relations generically fall under the name "regime theory", which is also used for estuaries.

6.2.4 Stability criterion for longshore transport

Bruun et al. (1978) evaluates the stability of an inlet based on the ratio between gross longshore transport M along the adjacent beaches and tidal prism P (Table 6-1). Also this method can be interpreted seasonally.

Table 6-1 : Stability of an inlet according to Bruun (1978). P : tidal prism, M : gross longshore transport

Ratio	Stability
$150 < P/M$	Stability is good, little bar and good flushing
$100 < P/M < 150$	Stability is fair, offshore bar formation more pronounced
$50 < P/M < 100$	Stability is fair to poor, entrance bar rather large
$20 < P/M < 50$	Stability is poor, typical bar-bypassing
$P/M < 20$	Stability is poor, entrance unstable and may close

6.2.5 Modelling

Coastal inlets are systems developing on large spatial and temporal scales, while process-based models usually restrict to modeling on a time scale of days to a few years. To prevent heavy computations, a few conceptual models have been developed which schematize the system in a simple way and predict its evolution on the long term (decennia to centuries).

Conceptual models directly or indirectly use the Coastal Tract concept (Cowell et al., 2003). The Coastal Tract helps to separate system units, external boundary conditions and internal noise through a good understanding of the spatial and temporal scales of each unit or group of units. On a long time scale, the tide can for instance be considered as diffusive noise, in the same way that turbulence is a diffusive schematisation of the non-modelled variability of advection.

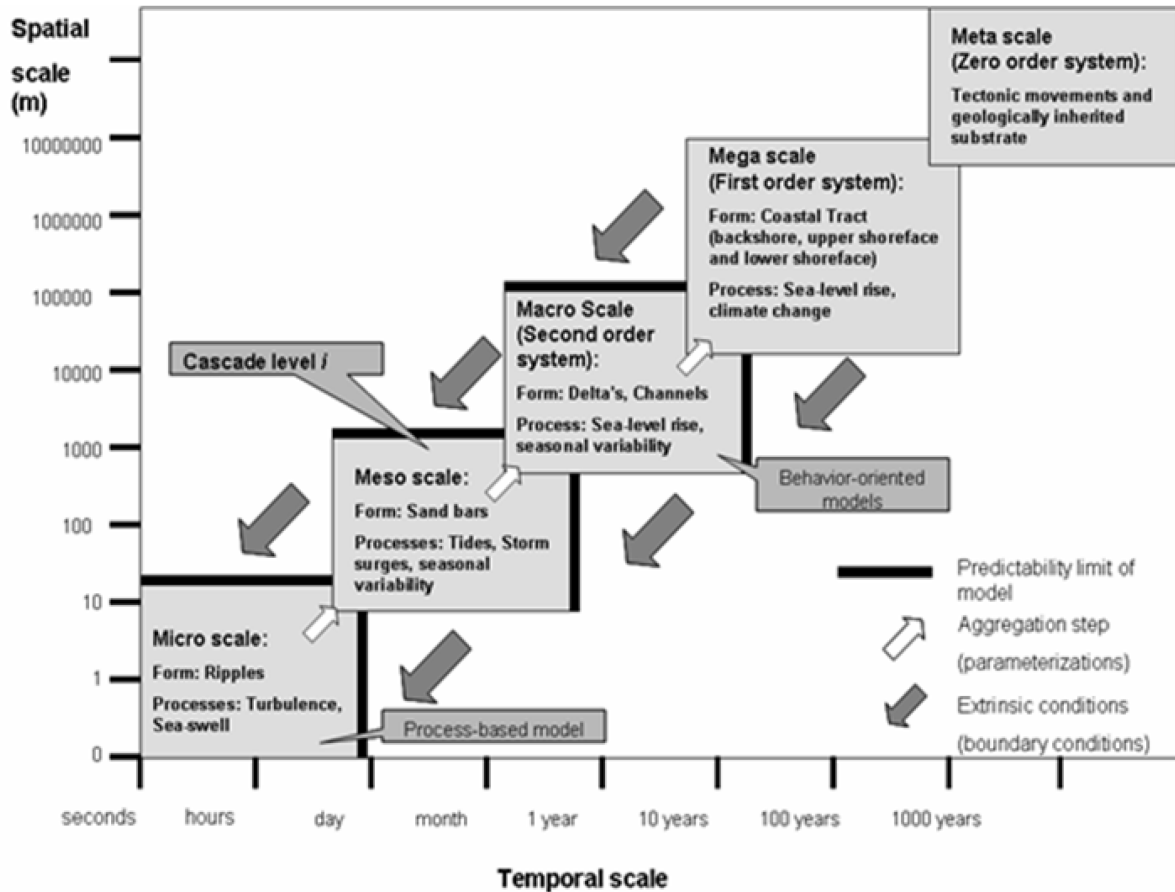


Figure 6-7 : Scale cascade of the Coastal Tract concept (Cowell et al., 2003)

The ASMITA model (Stive et al., 2003) is an application of the Coastal Tract on coastal inlets and tidal basins. The system is schematized by a limited number of large scale elements such as the inlet gorge, the ebb delta and the tidal basin. The important hypothesis is that each element has an equilibrium state under constant hydrodynamic conditions. The development of each element is determined by how far each element is from its equilibrium state (mass balance) and by the importance of diffusive fluxes between elements (advection-diffusion equation). Kragtwijk et al. (2004) presents the general version of the model. Analytical expressions for the equilibrium state and the time scales can be derived from a linearised version of the model. Because of the simplicity of the model, extensions to account for sea level rise and dredging are easy to integrate.

Despite its simplicity, ASMITA can model complex behaviours very fast and can evaluate the dynamic stability of the system. This has for instance been done for the Wadden Sea. The largest limitation is the uncertainty around the input parameters (equilibrium concentration, diffusion coefficients) : these require a lot of data about the historical development of the system and an intensive calibration. It is also necessary to understand the system well in advance to choose a good schematization. Finally, it does by definition not give any information about local changes such as the meandering of a channel.

The Inlet Reservoir Model (Kraus, 2000) is a comparable and elegant alternative to ASMITA : elements are fully determined by their equilibrium volume, the model is hence easy to apply. The transport flux from one element is determined by how far from equilibrium the element is (linear perturbation). Time scales result from transport fluxes compared to element volumes. The Inlet Reservoir Model is a linear perturbation model and is therefore in theory limited to small changes to stable inlets. It is used in the coastline evolution model GenCade of the US Army Corps of Engineers.

Because ASMITA relies on many input parameters (and therefore calibration parameters), it is recommended to first use the Inlet Reservoir Model in case a simple conceptual model on an element scale is needed.

6.3 Tools for embayments and tidal flats

Embayments and tidal flats are relevant to at least the two following topics on the Belgian coast : the equilibrium coastline position in some of the Flemish Bay scenarios ("Vlaamse Baaien 2100"), and the sedimentation in the Baai van Heist. Specific tools and aspects of morphological modelling are described below.

6.3.1 Bay beaches

Bay beaches are referred to by many different names in literature. They are curved beaches between two headlands. They are interesting for design of artificial beaches because their shape generally corresponds to a kind of equilibrium shape. A potential application on the Belgian coast could arise within the Flemish Bays project, for instance if a pocket beach is designed between the port of Zeebrugge and the extended port of Blankenberge. A review of the static bay beach concept is presented in Hsu et al. (2010).

The planform shape of a headland bay beach (HBB) can belong to one of three categories :

- Static equilibrium : The long term stability of the beach is independent of external sediment sources. Waves break perpendicular to the coast and there is little to no longshore transport along the entire beach length.
- Dynamic equilibrium : A sediment supply from an external source is needed to maintain the equilibrium (bypass at headland, river). If supply reduces, the shoreline may recede up to the static equilibrium profile.
- Unstable or natural reshaping : This corresponds to an accreting state in the lee of a usually human construction (jetty, groyne, breakwater), accompanied by updrift erosion. It may lead to a new static or dynamic equilibrium if the natural behaviour is unhindered.

Empirical equations of HBB have been derived to predict the static equilibrium shape :

- The logarithmic spiral model has first been introduced by Krumbain (1944) but it has no physical background and it does not match the straight downdrift section of the beach.
- The parabolic shape model of Hsu and Evans (1989) is more elegant. The shape is entirely defined by the diffraction point, the wave direction and a downdrift control point, and it yields information on the type of equilibrium depending on the coastline position compared to the static equilibrium. In practice it remains a very subjective method where the choice of the downdrift control point is critical to the fit.
- The hyperbolic-tangent shape model of Moreno and Kraus (1999) also fits better than a log spiral. The shape is defined by the headland point and the general orientation of the coastline. The method is recommended by Moreno (2003) for engineering use, but there is still little physical background. According to Hsu et al. (2010) it gives no information about beach stability. It is probably equally subjective as the parabolic shape model.

These simple shape equations are easily programmed into GIS tools. The Mepbay model for instance simply computes the shape and only requires a satellite image and knowledge of the wave direction for interpretation. The SMC model is more elaborate and first computes waves, currents and sediment transport for interpretation. Due to its ease of use, Mepbay has been applied on several beach development projects. It also works for salient and tombolos. Examples of uses are presented in the review of Hsu et al. (2010 ; Figure 6-8). It is generally applied to 300-400m bays, but not only.

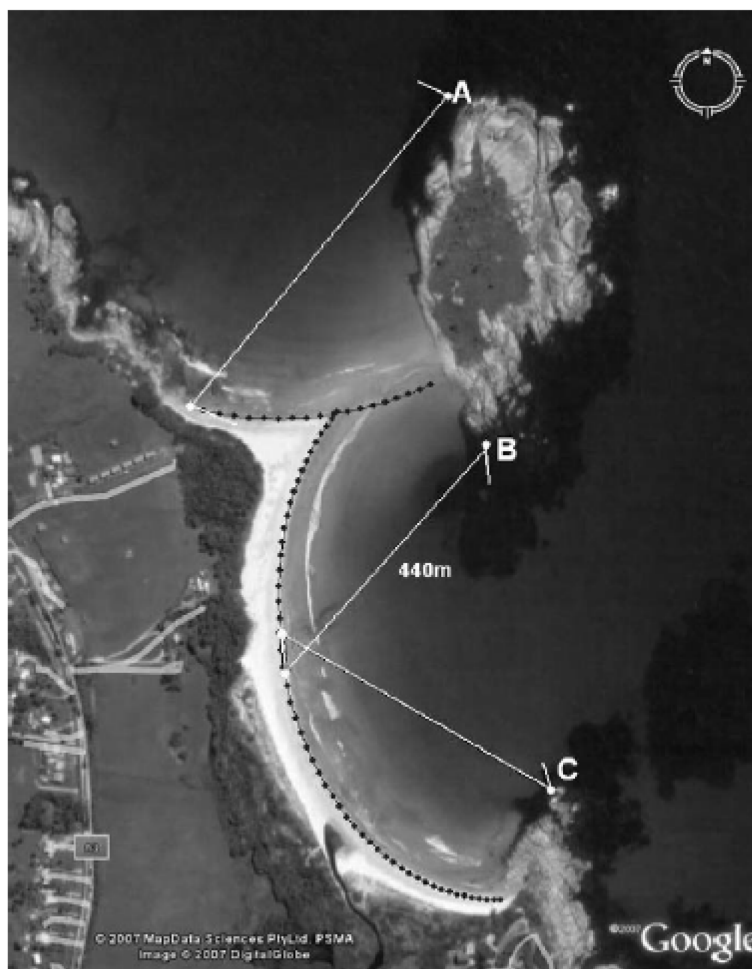


Figure 6-8 : Example of parabolic shape model applied on a satellite image (from Hsu et al., 2010).

For the interpretation, if the parabolic shape computed is landward of the coastline then the beach is in dynamic equilibrium, if it is on the coastline it is a static equilibrium and if it lies seaward of it then natural reshaping occurs.

Limitations to the applicability are tidal currents and obstacles to wave propagation, such as shoals leading to multiple diffraction points. The downdrift control point should be chosen where the beach is tangent to the wave direction. Practice has shown that the parabolic shape model has a reasonable predictive power, but that its application requires a good understanding of the system in advance, and of the method and its limitations (Figure 6-9). It can hence be considered as an “expert judgement” tool. It is useful because it is fast to apply, but it does not replace more advanced investigations like for instance numerical modelling.

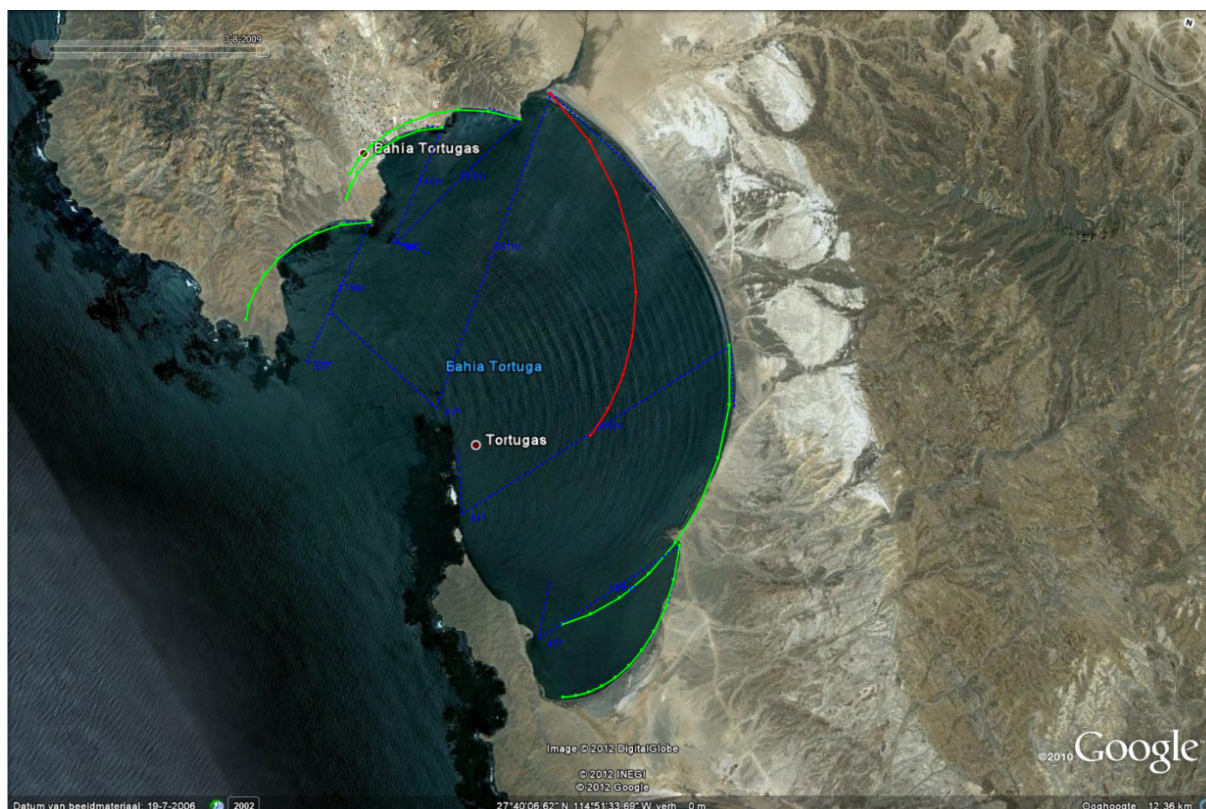


Figure 6-9 : Example of application and limitations of the parabolic shape model on bay beaches in Mexico. Good fit on green curves, bad fit on red curve, physically doubtful fit on southmost beach (incorrect wave direction).

6.3.2 Experience from modelling the Baai van Heist

Bay beaches can probably be modelled with a 2D long term morphology model. The Baai van Heist shares some common features with bay beaches, in the sense that the coastline shape is locally affected by its sheltered location. The modelling of the tidal flat in this bay is supposed to be closely linked to that of 2D coastline modelling.

Wang et al. (2015) presents numerical modelling work on the sedimentation in the Baai van Heist, East of Zeebrugge. The area experiences long term sedimentation of about 200 000 m³/year on the tidal flat, which the model cannot reproduce easily. Although the cause has not been clearly identified, investigations suggest that for this specific case, both 3D modelling and a spatially-varying grain size distribution are necessary to improve results. The reader is referred to the report for further details.

It is worth noting that this issue has been encountered as well in a project in the Netherlands. A 2D morphological model proved incapable of reproducing the observed sedimentation in the leeside of the port of IJmuiden (personal communication Dano Roelvink).

6.3.3 Suspended transport formulations in 2D models

The necessity to use 3D modelling for the sedimentation in the Baai van Heist may stem from the limitations of the suspended transport formulation used in 2D models. The basic concept is presented below (rough math only).

2D models such as Delft3D and XBeach assume that the suspended transport concentration c adjusts to the bed load equilibrium concentration c_{bed} at the bed with a relaxation time scale T . They hence model an exponential return to the equilibrium state from an initial underloading or overloading situation (Figure 3-3) with a source term in the advection-diffusion equation :

$$\frac{\partial \bar{c}}{\partial t} + u \frac{\partial \bar{c}}{\partial x} + v \frac{\partial^2 \bar{c}}{\partial x^2} = \frac{\bar{c}_{eq} - \bar{c}}{T}$$

in which for simplicity of the argument the spatial derivatives will now be omitted.

The main uncertainty lies in the equation used for the relaxation time scale T . A simple equation can be derived from the 2DH formulations for the advection-diffusion of mud and from a 1DV equilibrium concentration profile (such as the Rouse profile).

The most simple 2DH advection-diffusion equation for mud features a balance between the erosion rate E from the bed shear stress and the deposition rate D from the fall velocity (Partheniades-Krone formulation). It reads in depth-averaged form :

$$h \frac{\partial \bar{c}}{\partial t} = E - D$$

$$h \frac{\partial \bar{c}}{\partial t} = M(\tau - \tau_{cr}) - w_s \bar{c}$$

$$\boxed{h \frac{\partial \bar{c}}{\partial t} = w_s (\bar{c}_{eq} - \bar{c})}$$

with $\bar{c}_{eq} = \frac{M}{w_s} (\tau - \tau_{cr})$

When using similar source-sink terms for erosion-deposition in the 3D advection-diffusion equation, and integrating it vertically, the following very similar equation is obtained for 2DH advection-diffusion (personal communication George Schramkowski) :

$$\boxed{\frac{\partial \bar{c}}{\partial t} = \frac{w_s}{h} (c_{bed\ eq} - c_{bed})}$$

the difference being that the concentration is defined near the bed instead of depth-averaged. The near-bed equilibrium concentration can be related to the depth-averaged equilibrium concentration with the Rouse profile, and the instantaneous near-bed concentration is related to the instantaneous depth-averaged concentration with a perturbation analysis (yielding a comparable coefficient for small deviations).

The 1DV equilibrium concentration profile stems from a vertical balance between turbulent upward flux with diffusion coefficient ν and downward flux with settling velocity w_s :

$$w_s c_{eq} + \nu \frac{\partial c_{eq}}{\partial z} = 0$$

which can be integrated into :

$$c_{eq}(z) = c_{bed\ eq} e^{-\frac{w_s}{\nu}(z+h)}$$

yielding a depth-averaged equilibrium concentration in the water column :

$$\bar{c}_{eq} = \frac{\nu}{hw_s} \left(1 - e^{-\frac{w_s}{\nu}h} \right) c_{bed\ eq}$$

$$\boxed{\bar{c}_{eq} = \alpha c_{bed\ eq}}$$

The shape factor α is the ratio between suspended sediment concentration and near-bed concentration. It equals 0 if there is only bed load transport and 1 if there is fully mixed suspended load transport. It is a function of $x = \frac{w_s}{\nu} h$ (Figure 6-10) :

- For a low fall velocity (mud), a high diffusivity (turbulence) or a small depth (tidal flat), sediment stays in suspension (small x , large shape factor) ;
- For a high fall velocity (sand), a low diffusivity (low energy area) or a large depth (shelf), sediment stays near the bed (large x , small shape factor).

The exact expression of the shape factor depends on the assumptions made, in particular for the diffusivity profile. Combining the two equations (depth-integrated 3DH with source-sink from mud and 1DV equilibrium profile) yields an expression for the relaxation time scale :

$$T = \alpha \frac{h}{w_s}$$

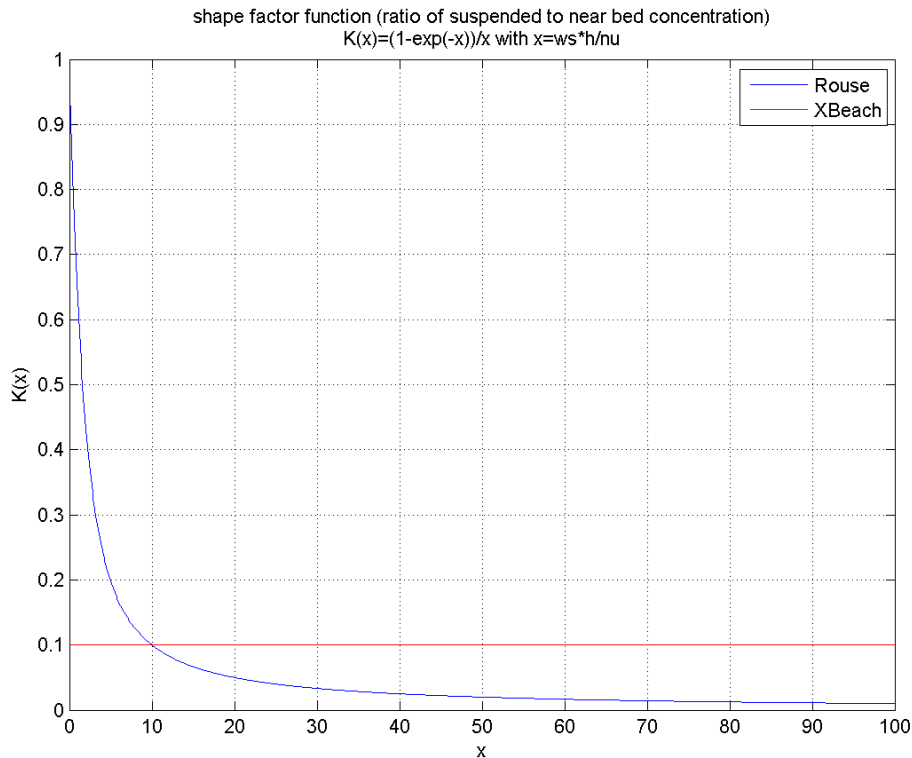


Figure 6-10 : Shape factor function as a function of the adimensional parameter $\frac{w_s}{\nu} h$

As an example the shape factor of the relaxation time scale is computed for four typical cases :

- Sandy shelf : $w_s = 0.02 \text{ m/s}$, $h = 10 \text{ m}$, $\nu = 0.01 \text{ m}^2/\text{s} \rightarrow \alpha = 0.05$
- Sandy flat : $w_s = 0.02 \text{ m/s}$, $h = 1 \text{ m}$, $\nu = 0.01 \text{ m}^2/\text{s} \rightarrow \alpha = 0.4$ (10x larger)
- Muddy shelf : $w_s = 0.002 \text{ m/s}$, $h = 10 \text{ m}$, $\nu = 0.01 \text{ m}^2/\text{s} \rightarrow \alpha = 0.4$ (10x larger)
- Muddy flat : $w_s = 0.002 \text{ m/s}$, $h = 1 \text{ m}$, $\nu = 0.01 \text{ m}^2/\text{s} \rightarrow \alpha = 0.9$ (20x larger)

The first value (sandy shelf) is close to the default value used in XBeach (constant shape factor of 0.1). The computation shows that for a constant diffusivity, the shape factor and hence the importance of suspended transport can easily vary by more than an order of magnitude. A 2D morphological model using a constant value of the shape factor therefore presents serious shortcomings to model suspended sediment transport, hence the evolution of tidal flats, accurately.

Delft3D on the other hand uses the Galappatti formulation for the relaxation time scale (Wang and De Vriend, 2004). This non-documented formulation (in the manual) is more rigorous : it is derived from the linear perturbation analysis of the full 3D advection-diffusion equation. Probably because of this more rigorous approach and of the assumption made for the diffusivity, the resulting expression of the relaxation time scale differs considerably from the simple expression presented above (u_* is the bed shear velocity) :

$$T_{D3D} = w_s \exp[(1.547 - 20.12u_*)w_s^3 + (326.832u_*^{2.2047} - 0.2)w_s^2 + (0.1385\log(u_*) - 6.4061)w_s + (0.547u_* + 2.1963)]$$

Figure 6-11 compares the relaxation time scale in Delft3D, in XBeach and as computed from the simple expression presented above in the case of a tidal flat (1m depth, diffusivity 0.01 m²/s) and with a formula for the fall velocity. It shows that the relaxation time scale of Delft3D is significantly larger. In this particular case the relaxation time scales of XBeach and of the simple expression are very comparable. When varying the parameters, the simple expression yields quite variable results depending on the diffusivity, but is generally found to predict a shorter time scale than XBeach. The time scale of XBeach is found to be comparable to that of Delft3D for a shape factor of 0.5 instead of 0.1.

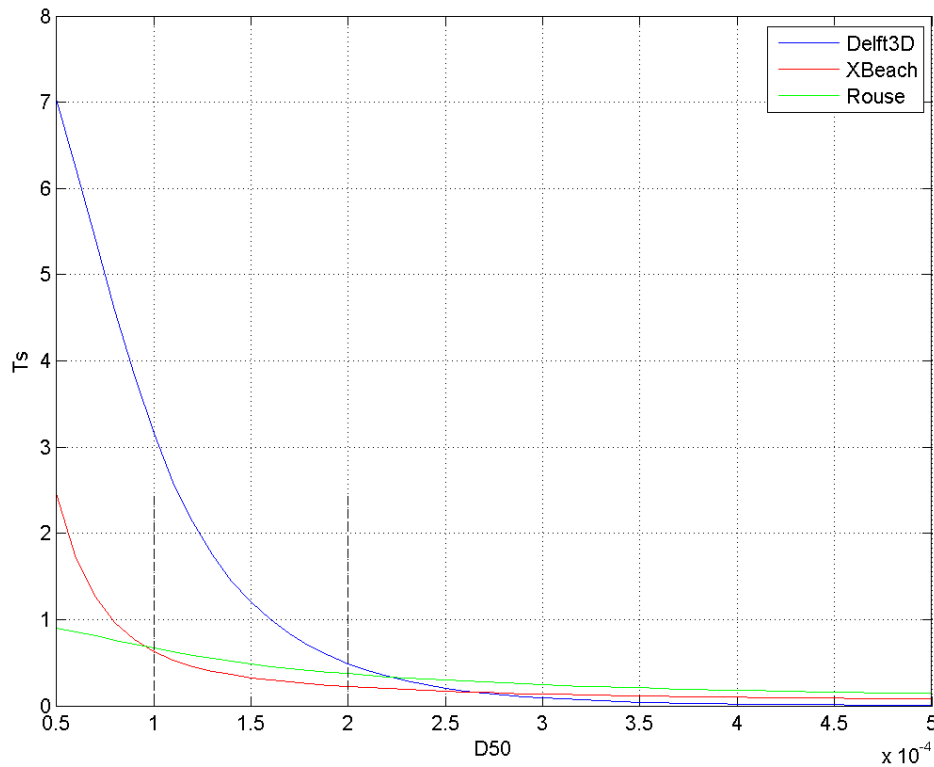


Figure 6-11 : Computed relaxation time scale as a function of grain size (hence fall velocity) in Delft3D (Galappatti formulation), in XBeach (constant shape factor) and in the simple expression derived from the Rouse-like equilibrium concentration profile. Sandy sediments in the Baai van Heist are comprised between 100 and 200 μm .

This implies that Delft3D is the most likely to transport suspended sediment further into the embayment and on the tidal flat. XBeach will not always be capable of modelling sedimentation in embayments and on tidal flats. The simple expression will not solve the problem since it predicts shorter time scales than both Delft3D and XBeach. Based on the exercise and on some additional non-reported tests, it is however not excluded that another expression may yield larger time scales more able to transport sediment further onto the flat.

Finally, the equations above also show the very close similarity between sand and mud models :

$$\frac{\partial \bar{c}}{\partial t} = \frac{E - w_s \bar{c}}{h} \quad \text{for mud } (\alpha \sim 1)$$

$$\frac{\partial \bar{c}}{\partial t} = \frac{\bar{c}_{eq} - \bar{c}}{T} = \frac{w_s}{\alpha h} (\bar{c}_{eq} - \bar{c}) \quad \text{for sand}$$

The main difference is that a mud model imposes the sediment flux at the bed (erosion rate E as a function of shear stress) while a sand model imposes the sediment concentration at the bed (equilibrium bed load concentration $c_{bed\ eq} = \frac{\bar{c}_{eq}}{\alpha}$). These two equations are equivalent if

$$E = \frac{w_s}{\alpha} \bar{c}_{eq} = w_s c_{bed\ eq}$$

Under a certain number of conditions (such as a constant shape factor, a similar dependency of the erosion term E and of the equilibrium bed load concentration $c_{bed\ eq}$ on the shear stress, adding the shape factor α to the mud equation...), a spatially varying erosion rate M (see definition of E) can hence be computed, for which a mud model would yield similar results to a sand model. The larger underlying issue would be to reconcile the many data measurements of sand concentration and mud erosion rate.

6.4 Conclusion

We advise the following concerning morphological modelling of inlets and bay beaches :

- Tidal inlets are subject to very complex behaviours because wind, waves, tide, surge and river discharge can all play an equally important role. For this reason, it is important to make important efforts in the (historical data) analysis of the system.
- Several tools can help in estimating temporal and spatial scales, as well as in evaluating the system stability and the impact of human activity :
 - Tidal prism relationships and the stability criterion of Bruun et al. (1978) are the most simple tools, and can help in evaluating the cross-sectional area and the stability of an inlet. It is recommended to compute the minimum stable cross-sectional area $A = cP^d$ with coefficients c and d respectively equal to 10^{-4} and 1, and to apply an uncertainty of $\pm 30\%$, rather than to use empirical formulas such as those of Jarrett and O'Brien. If results differ by an order of magnitude with the measured stability, the physically based formulas of Stive and Rakhorst (2008) and of Kraus (1998) can be used, or one's own relation be calibrated on known systems.
 - If simple modelling is desired, without setting up a complex 2D model, the Escoffier diagram and the Inlet Reservoir Model can be used. The first allows to evaluate the sensitivity of the inlet stability to the temporal variations in forcing. The second allows to quantify the long term evolution of the different inlet elements interacting with each other, and in response to human impacts, and is to be preferred over the ASMITA model which relies on many calibration parameters.
 - Process-based morphological modelling is possible but should not focus on reproducing exactly the observed behavior, except if it is robust and the cause well identified. Instead it should focus on qualitative behavior and relative impact (of processes or human impact). Simulations on a time scale of a storm to a year can be done with the methods described in the previous chapter, albeit with potentially complex input reduction. Simulations on a time scale of decennia to centuries (inlet evolution) can be done in most cases by assuming that the tide is the dominant forcing, thus neglecting waves.
- Bay beaches are interesting for design of artificial beaches because their shape generally corresponds to a kind of equilibrium shape. The state of this equilibrium (static equilibrium, dynamic equilibrium, natural reshaping) can be assessed with the Mepbay software based on the empirical equation for a parabolic beach profile. Care and expert judgement is however necessary for the interpretation of results.
- From a modelling perspective, bay beaches are related to longshore transport. A coastline model or a long term 2D model can therefore be used. However difficulties can be encountered with both methods. A coastline model is difficult to calibrate for strongly curved beaches. In a 2D model, the time horizon involved will often be a limiting factor.
- Tidal flats in embayments such as the Baai van Heist are difficult to model, in this particular case because the lack of data does not allow to clearly discard or validate some assumptions. 2D morphological model are based on a relaxation time scale for suspended sediment, which formulation may present serious shortcomings for tidal flats. The Galappatti formulation used in Delft3D is better than the constant time scale used in XBeach, but may still be insufficient. Other major limitations include the lack of data on the spatial variability of the grain size, of the bed roughness, and the vertical stratigraphy. A 3D morphological model may perform better but can easily present instabilities.

7 Modelling cross-shore profile development

7.1 Overview

The main processes driving cross-shore transport and their implementation in the morphological models Delft3D and XBeach have been discussed in paragraph 3.3.3. In this chapter applications at various time horizons are discussed :

- Short term (1 day) : storm response
- Medium term (1 year) : erosion and recovery cycles, evolution of a nourishment
- Long term (>10 years) : sea-level rise and climate change, of interest for the evolution of a nourishment and for long term coastal advance and retreat
- Very long term (geological time scale) : geological profile development and stratigraphy

All applications are carried out with XBeach. The specific details of the modelling exercises can be found back in their respective reports (Lanckriet et al., 2015, Zimmermann et al., 2015).

7.2 Short term (1 day) : storm response

The response of the coastal profile to a storm is well understood (in terms of governing processes) and easy to model (models validated against data). In the frame of the “Wettelijk Toetsinstrumentarium 2017” project in the Netherlands (WTI ; Deltares, 2015), aiming at defining the methods to test the coastal safety, a set of calibration parameters has been defined for the Groundhog Day 2014 release of XBeach focusing on dune erosion. Their optimal value has then been determined by an automatic optimisation procedure based on a large number of simulations compared to laboratory and field data of the Dutch coast (Table 7-1).

Table 7-1 : WTI calibration settings with the Groundhog Day release of XBeach

parameter	Default	WTI settings
fw	0.000	0.000
cf	0.003	0.001
gammax	2.000	2.364
beta	0.100	0.138
wetslp	0.300	0.260
alpha	1.000	1.262
facSk	0.100	0.375
facAs	0.100	0.123
gamma	0.550	0.541

These calibration settings, combined with a pseudo 2D approach to partially resolve edge waves (here 5 cells of 200m each in alongshore direction), have been shown to yield outstanding results in a hindcast of the Sinterklaas storm in Belgium (Lanckriet et al., 2015 ; Figure 7-1). This agreement is supposed to come from the close similarity between Belgian and Dutch beaches in terms of forcing, beach slope and sediment characteristics. These same settings still yield surprisingly good results for applications on the medium term (see paragraph 7.3), meaning that the calibration on storm events does not significantly impact the accretive events.

The parameters changed the most compared to their default value are the bed friction on the flow (cf) and the importance of onshore transport due to wave skewness (facSk, in the surf zone) and wave asymmetry (facAs, in the swash zone). This compares to the following experience within the Sand Dynamics project :

- The 2D models of Blankenberge and Knokke suggest that a higher value of the bed friction c_f (instead of lower) is needed to avoid overestimating longshore transport, but these were done with an earlier release of XBeach. XBeach is notorious for changing both the process formulations and the default values in different releases. We note however that a coefficient c_f of 0.001 as proposed, corresponds to a Chezy friction parameter of about 90. This is physically doubtful and suggests that the statistical procedure compensates errors by other errors (in other parameters / processes).
- The long term profile evolution presented in paragraph 7.4 confirms the necessity to increase onshore transport, albeit with wave asymmetry instead of skewness, but infirm the general applicability of the WTI settings : with the same settings and the Groundhog Day release, the studied profile (swell-dominated, coarse grain, steep slope) becomes unstable over a year contrary to a Belgian profile. Hydro-meteorological conditions different from North Sea conditions will probably also lead to different results.

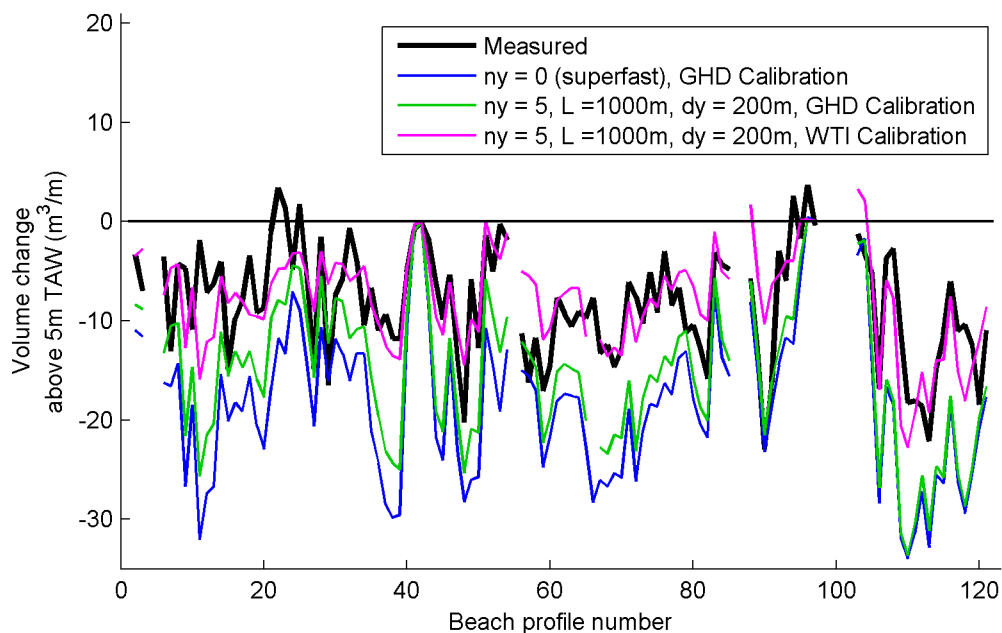


Figure 7-1 : Eroded volume along the Belgian coast during the Sinterklaas storm, compared to measurements.

7.3 Medium term (1 year) : erosion and recovery cycles

Beach recovery during calm weather is not well understood yet. Onshore transport is believed to be due to wave skewness and wave asymmetry, however it is difficult to quantify. From a hydrodynamic point of view both skewness and asymmetry can be quantified from wave theory. From a sedimentary point of view, the efficiency of this skewness and asymmetry strongly depend on the grain size via time lag effects (see also review of O'Donoghue and Van der A (2012)). Coarser grain sizes, moved onshore during the uprush but already settled when the less energetic downrush comes, will experience more onshore transport than finer grain sizes, which stay in suspension both during the uprush and the downrush. XBeach uses an elegant formulation to account for onshore and offshore transport. Onshore transport is calibrated with factors for the efficiency of wave skewness ($facSk$) and wave asymmetry ($facAs$).

A theoretical modelling exercise has been set up to evaluate the capability of XBeach in modelling medium term erosion and recovery cycles (Zimmermann et al., 2015). Two main profile types are considered :

- A steep beach profile in a swell-dominated environment, with very coarse sand on the beach ($600 \mu m$) and fines on the shelf³ ($< 100 \mu m$). This profile is chosen because it presents a calibration challenge for medium term modelling.

³ Data courtesy of IMDC, exercise not associated with the project the data stems from.

- A mild beach profile typical of the Belgian coast in a wind sea-dominated environment, with medium sand on the beach and on the shelf (200-300 μm). This profile is chosen to verify the applicability of the conclusions regarding the first profile to the Belgian coast.

The objective of this exercise is to answer the following questions :

- Can the profile be stable in medium (1 year) to long term applications (>10 years) ?
- Can XBeach be used to evaluate the medium to long term evolution of a nourishment ?
- Does XBeach handle multiple sediment fractions properly ?

The latter question is relevant for nourishments. Computations are done with the Easter 2012 release of XBeach. Long term morphology is computed by using a truly 1D model (so-called “superfast” model) and a morphological acceleration factor of 10 to 30, in combination with the measured time series of waves and $\text{morfacopt} = 1$ (only applicable without advection).

Theoretical profile

In general the exercise shows that the cross-shore profile can be calibrated to remain stable over a period of a year. In both cases the main calibration parameters are the factors for onshore transport. For the steep profile onshore transport alone is insufficient (Figure 7-2 ; $\text{facAs} = 0.4$ instead of 0.1), another process is necessary. The inclusion of groundwater – with permeability 10^{-2} m/s, at the upper limit of what is physically expected for very coarse well-sorted sand – strongly improves the results for this steep profile (Figure 7-3), but the question remains open whether it creates artificial damping of morphodynamic activity. The shallow profile is more stable and the onshore transport factors are sufficient for calibration.

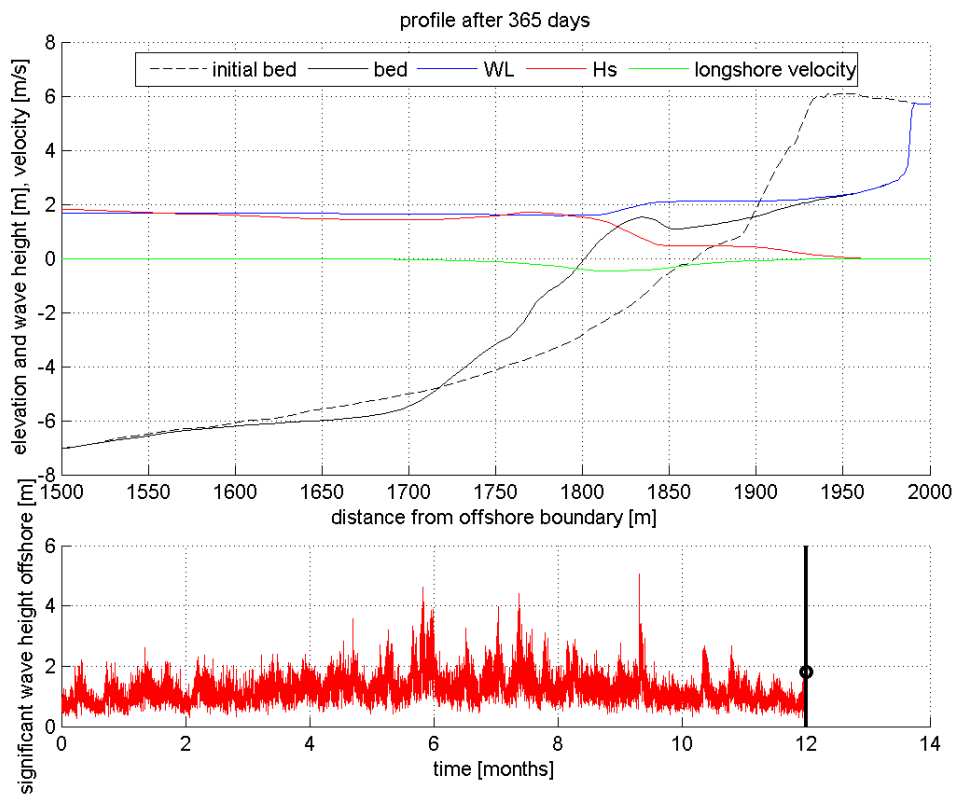


Figure 7-2 : Steep profile after one year without groundwater

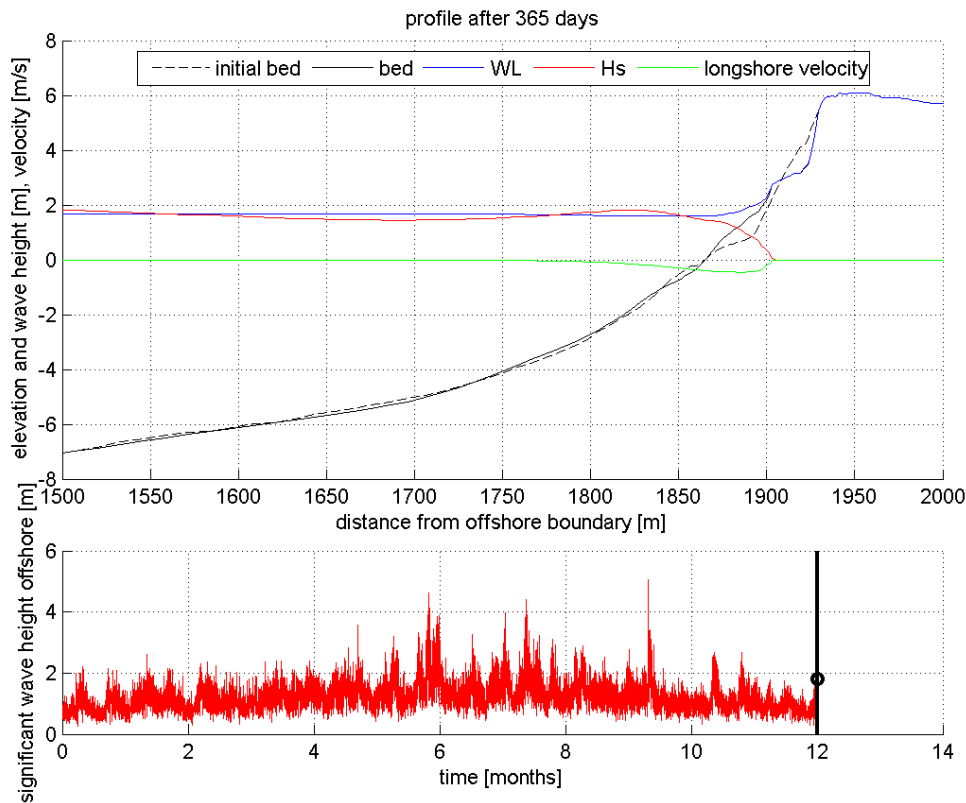


Figure 7-3 : Steep profile after one year with groundwater

The WTI settings have also been tested on both profiles with the Groundhog Day 2014 release of XBeach : they yield a particularly good calibration for the mild Belgian profile, but do not yield realistic results on the steep profile (Zimmermann et al., 2015). This is expected since these settings have been derived for the Dutch coast.

Finally a test with multiple sediment fractions for the steep profile shows two limitations of XBeach :

- Fines are unexpectedly found onshore (Figure 7-4) because the onshore transport factors are the same for all fractions, instead of accounting for time lag effects in reality (lower onshore transport for smaller grain sizes). The source code has been modified to assign one value of the onshore transport factors for each fraction in order to calibrate them separately. With facAs set to respectively 0, 0.1 and 0.4 for the 60 μm , 100 μm and 540 μm fractions instead of 0.4 for all fractions, fines do not end up on the beach. These values suppose that onshore transport is limited or non existent for sediment smaller than 100 μm , and becomes more important for coarser sand (O'Donoghue and Van der A, 2012).
- With a spatially uniform grain distribution of sediment fractions (1/3 each), mass is not conserved (Figure 7-5). This issue is related to the morfac chosen and is discussed further in the next paragraph. It is not related to sediment losses at the offshore boundary.

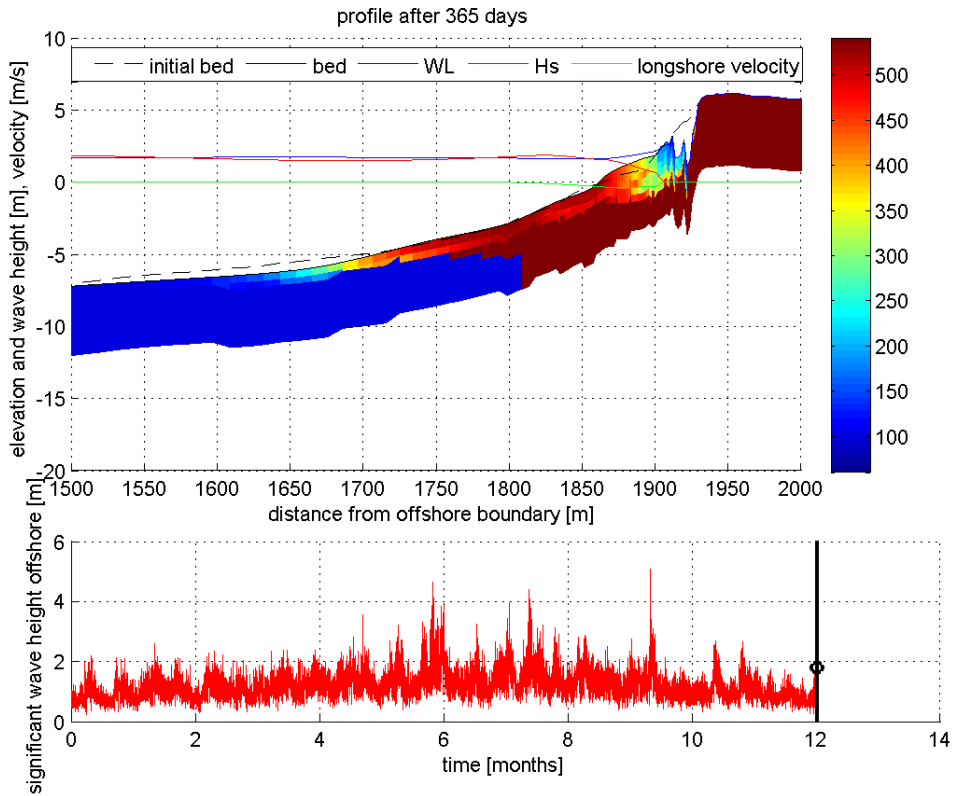


Figure 7-4 : Steep profile with multiple sediment fractions horizontally distributed after a year, showing fines on the beach

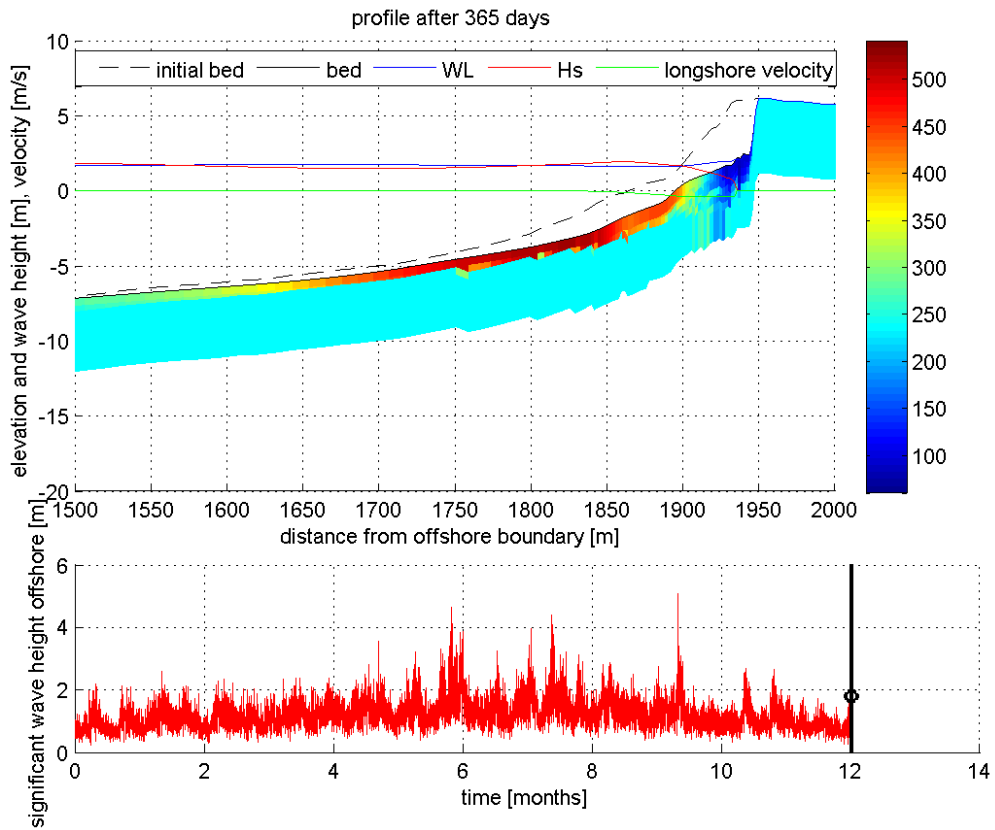


Figure 7-5 : Steep profile with multiple sediment fractions uniformly distributed after a year, showing a net mass loss

Process formulations and default values also change between versions, as a consequence the calibration values of the Easter 2012 release cannot be used in the Groundhog Day 2014 release.

Belgian Coast

For the Belgian coast, a measured time series of waves and water levels during 1 year was applied on 3 existing cross-shore profiles (Knokke, Bredene, Mariakerke ; Zimmermann et al. ; 2015). Since the shape of these profiles is in dynamic equilibrium, XBeach should reproduce this stability. Important parameters that are tested are the morfological acceleration parameter morfac, the WTI settings and the grain size.

Effect of morfac

Since a complete time series is used, and thus with each time a different tide, the only way morfac can be used is morfactopt=1. This option implies that calculations are done for a reduced period (factor morfac) and that the morphological result is multiplied with morfac.

This method has consequences for the hydrodynamics. If e.g. the water level increases by 0.5m over 1 hour and morfac 10 is used, this increase of water level occurs in the model in 6 minutes. Thus, the discharge of water at the offshore boundary is 10 times higher. This increase in cross-shore velocities causes also considerable cross-shore sediment transport over the profile.

The effect of morfac is illustrated for the Bredene-profile (Figure 7-6). It should be noted that for this profile, morfac 10 even causes a change of direction of cross-shore transport (offshore directed for morfac 10, onshore for morfac 1 and 3). For this reason, morfac 3 was selected as optimal choice.

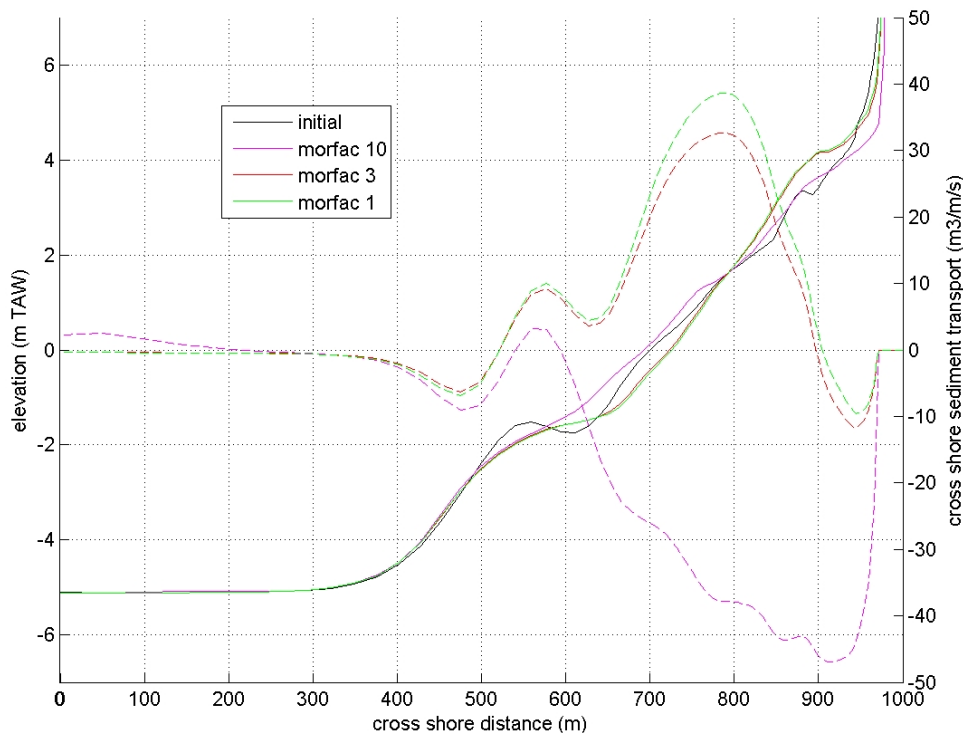


Figure 7-6 : Influence of morfac on the evolution of the cross-shore profile of Bredene after 1 year

Use of the WTI-settings

Using the morfac 3 simulations (Figure 7-7) shows that, for the Bredene profile, the WTI settings cause a net onshore directed sediment transport, while the default settings cause net offshore directed transport. The profile shape after a year suggests that the WTI settings yield physically better results than the default settings.

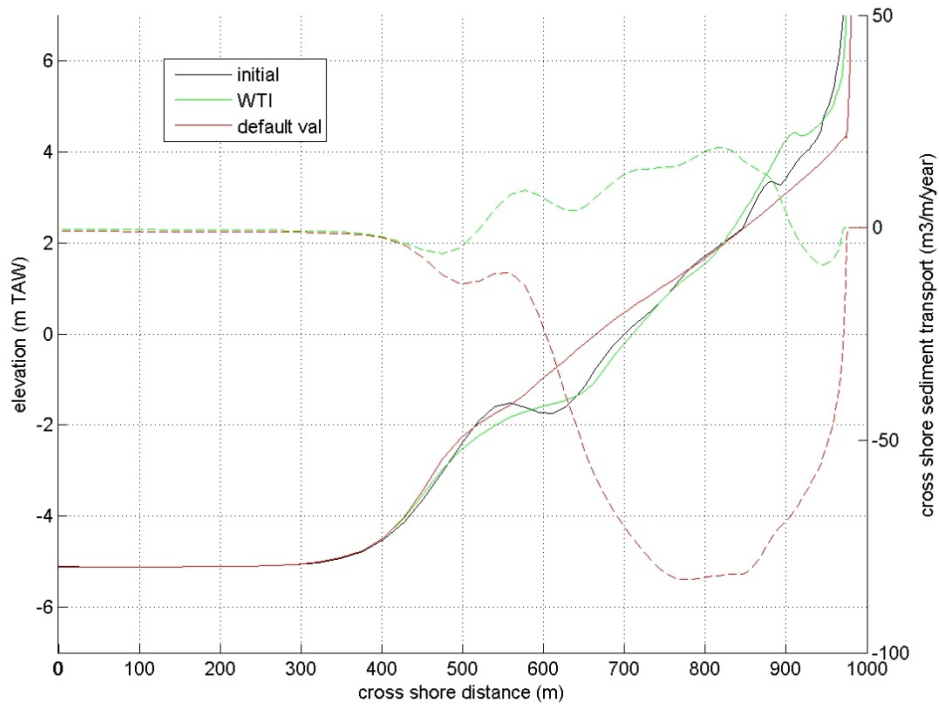


Figure 7-7 : Comparison of profile development (full line) and cross-shore transport (dashed line) using the WTI and default settings with morfac 3 on the Bredene profile (cross-shore transport is positive if onshore directed)

Also for a profile in Knokke-Heist, the use of the WTI settings gives a stable regeneration of the measured profile shape (Figure 7-8).

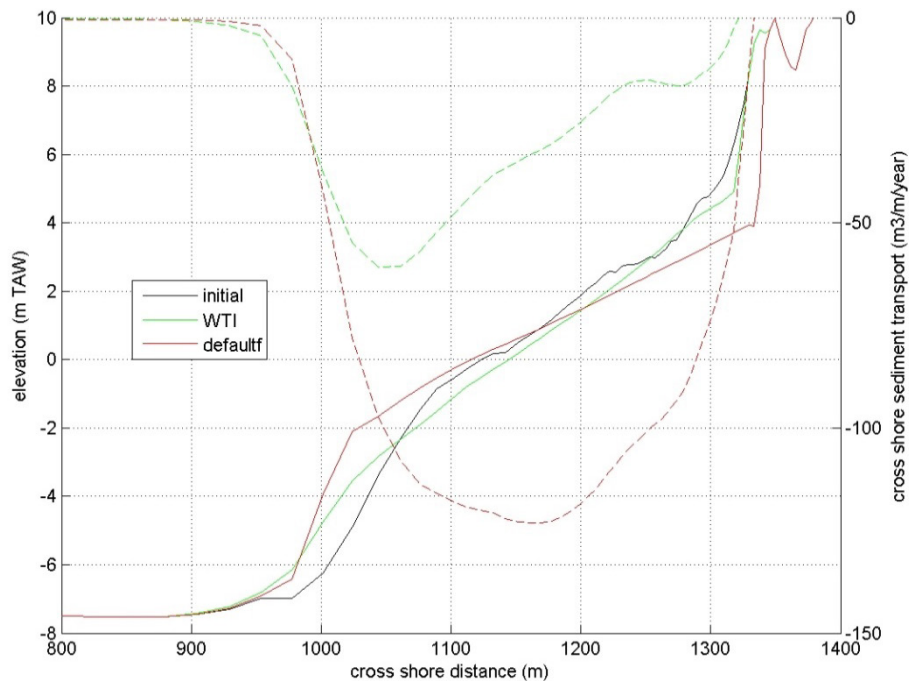


Figure 7-8 : Comparison of profile development (full line) and cross-shore transport (dashed line) using the WTI and default settings with morfac 3 on the Knokke profile (cross-shore transport is positive if onshore directed)

In Figure 7-9, the use of WTI settings is evaluated for the straight profile for the 0.3mm :

- a) is a simulation with the WTI parameters of XBeach,
- b) is a simulation with the default parameters of XBeach,
- in c) the default parameters are used, except for the parameters that cause onshore transport (facSk and facAs, for which the WTI settings are used
- in d) also the roughness coefficient is changed to the WTI setting (a decrease of roughness),
- and in e) also the wave parameters are changed to the WTI settings (e.g. limiting the wave height in the shallow zone).

The difference between run a) and run e) is the wet slope, which is only relevant for dune erosion. As can be seen, all parameters, except the wet slope, have an important influence on the cross-shore sediment transport. Figure 7-9 shows the result for the medium sand (300 μm). The results also show that parameters partly compensate each other in the total net cross-shore transport.

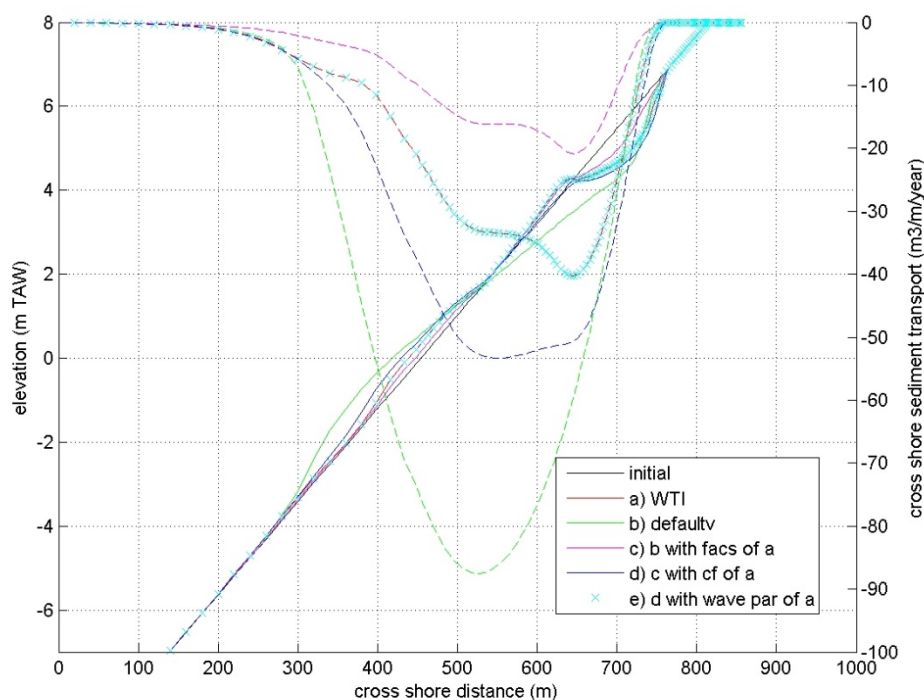


Figure 7-9 : Comparison of profile development (full line) and cross-hore transport (dashed line) using the WTI and default settings with morfac 3 on the straight profile with $d_{50}=0.3\text{mm}$ (cross-shore transport is positive if onshore directed)

Influence of grain size

The influence of the grain size is rather small. Figure 7-10 compares the results for the Knokke profile after 1 year for resp. 300, 200 and 100 μm . The difference between 300 μm and 100 μm is less than a factor 2.

After 3 years (Figure 7-11), the slope of the Knokke profile between LW (0.5m TAW) and HW (4.5m TAW) evolved from 1/34 to 1/36, with the same evolution for 200 μm and 300 μm sand. The only difference is that the 200 μm sand is eroded with 3m more than the 300 μm sand. This is at first sight in contradiction with the observation that the slope of beaches strongly depends on the grain size. Between -2m TAW and +5m TAW some more flattening of the profile for the fine sediment is visible. Probably, over a long time span, the difference will grow. However, due to the small cross-shore transport rates (less than 50 $\text{m}^3/\text{m}/\text{year}$), it takes a long time to change the slope of a profile from 1/35 to e.g. 1/50 (between -4m TAW and +5m TAW a volume of 600 m^3 is involved).

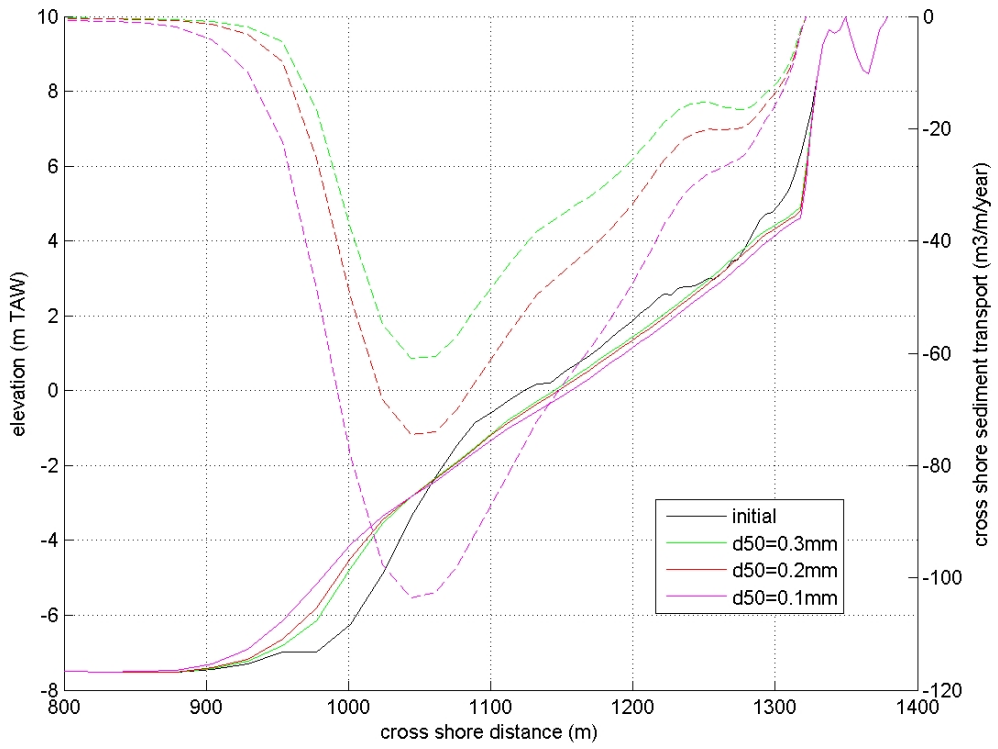


Figure 7-10 : Influence of grain size on the development of the Knokke profile in the first year

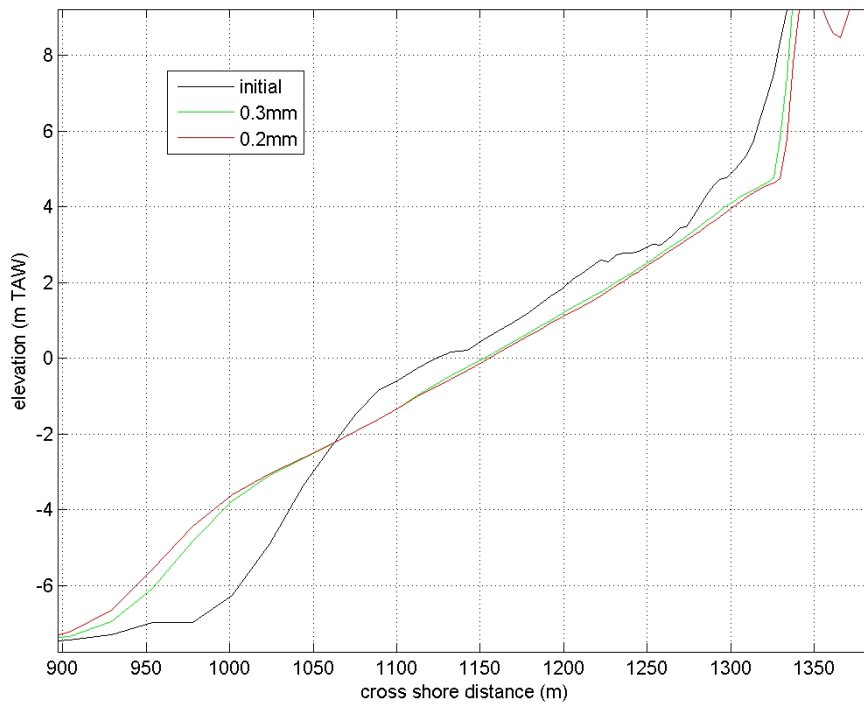


Figure 7-11 : Influence of grain size on the development of the Knokke profile after 3 year

Long term development

A simulation over a few years of the cross-shore profile at Bredene shows that the spin-up time of the model is about one year (200 μm , WTI settings ; Figure 7-13). After that the model can be considered to predict the long term profile development. It is observed that the equilibrium profile is somewhat steeper than the measured profile above the +2m TAW level. A berm can be observed near HW spring (4.5m TAW), this is not very clear from the measurements. However, Figure 7-13 shows that although the profile reaches an equilibrium, through the year some larger fluctuations can be observed. At some periods during the year, the profile is less steep and the berm near HW spring is less pronounced.

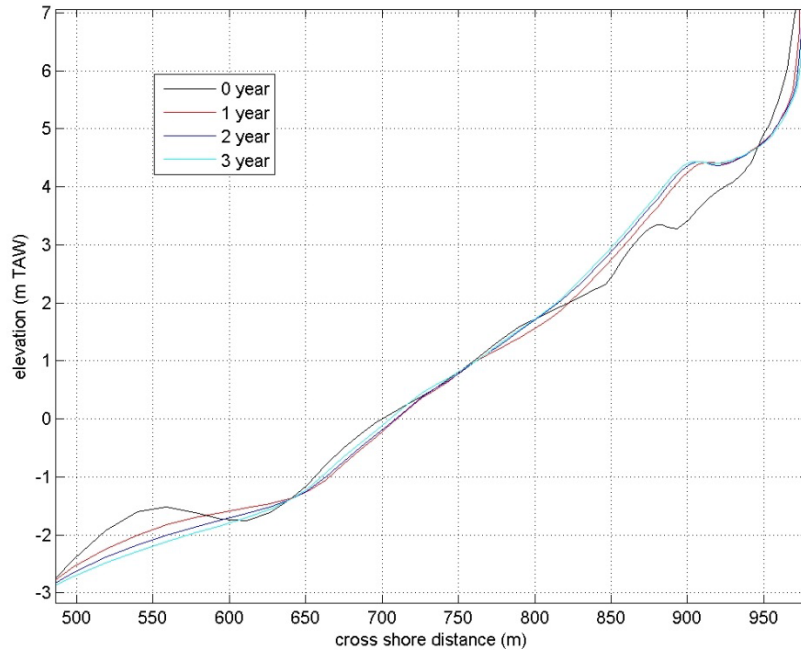


Figure 7-12 : Long term evolution of the Bredene profile, showing the model spin-up time of about a year

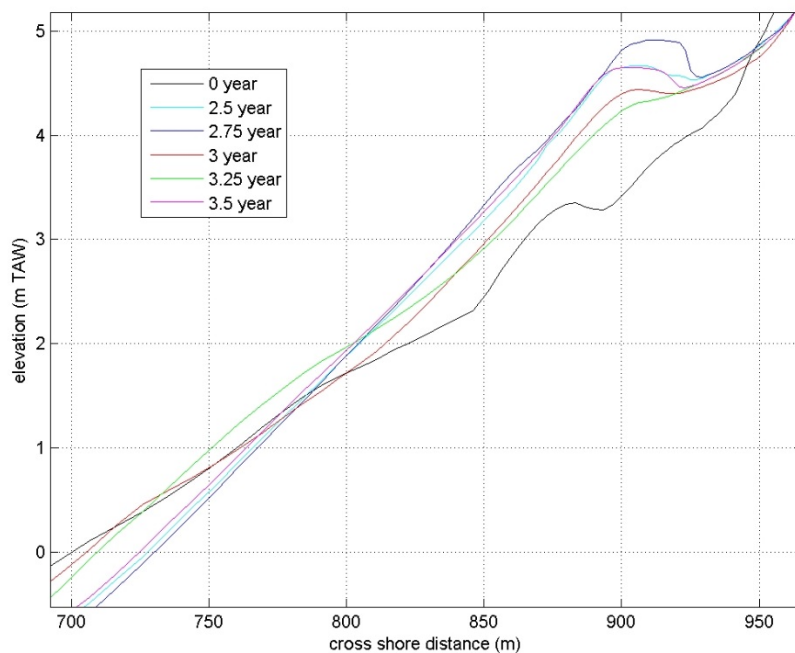


Figure 7-13 : Time evolution of the Bredene profile during 1 year

Shoreface nourishment

On the Bredene profile a fictive shoreface nourishment of $400 \text{ m}^3/\text{m}$ has been simulated (berm at -1m TAW). The modelled evolution after 3 years is shown in Figure 7-14. The results show that the nourished sand is slowly moving in the onshore direction, suggesting that XBeach is indeed capable of simulating the long term evolution of nourishments.

In the first year the foreshore nourishment has a negative effect of $-9 \text{ m}^3/\text{m}$ on the intertidal zone (between $+0.5\text{m}$ TAW and 4.5 m TAW), in the second year a positive effect of $4 \text{ m}^3/\text{m}$ (so 13 m^3 sand extra has moved onshore), in the third year $37 \text{ m}^3/\text{m}$ positive (33 m^3 extra) and in the last half year $50 \text{ m}^3/\text{m}$ positive ($26 \text{ m}^3/\text{m}/\text{year}$ extra). It should be noted that these values are rather limited compared to the extra $400 \text{ m}^3/\text{m}$ sand of the nourishment itself.

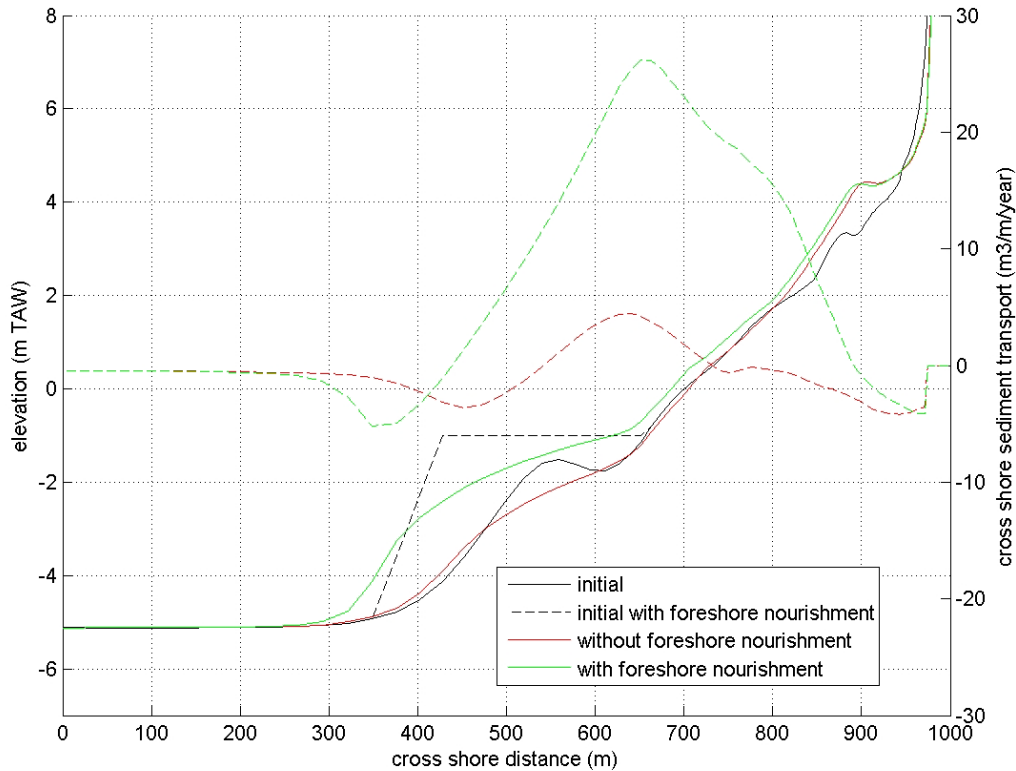


Figure 7-14 Evolution of the shoreface nourishment during the third year : profile (full lines) and cross-shore transport (dashed lines).

7.4 Long term (>10 years) : sea-level rise and climate change

The effect of sea level rise on coastal retreat is currently not modelled. It is usually estimated based on long term trends and on the Bruun rule. The Bruun rule relates the coastal retreat to sea level rise by assuming conservation of the profile shape and of mass up to the closure depth. There is however considerable debate about the applicability of this rule. As an example the physical background of the steep profile used in the previous paragraph is discussed.

The steep profile is thought to continuously loose sediment due to a variety of reasons, one of which being that fines present in and eroded from the coast deposit on the shelf and never come back. This small grain size combined to long swell waves imply a closure depth much larger than commonly computed from empirical formulas (30m instead of 8m), therefore large accommodation space for coastal retreat due to sea level rise (SLR).

The need for a modelling tool to assess the effect of sea level rise on coastal retreat therefore exists, but the capabilities are not there yet. Since the modelled cross-shore profile can be kept stable over a year, the exercise of the previous paragraph has been extended to a time horizon of 10 years to evaluate the capabilities and limitations of XBeach for such a task.

The objective of this exercise is to answer the following additional question :

- Can XBeach be used to estimate long term sediment losses and the relative impact of sea-level rise ?

Figure 7-15 shows that scaling up the time horizon to 10 years exacerbates the mass balance issue which was previously only visible with the uniform distribution of the sediment fractions (Figure 7-5). Further investigation shows that the mass balance is not closed in XBeach, and that small errors get compounded by the morfac, probably at each change in wave condition. A smaller morfac yields smaller mass losses and more fines on the beach (Figure 7-16)⁴. The issue is not solved with the more recent Groundhog Day 2014 release of XBeach.

The same simulation can nevertheless be run with sea level rise, and the results analysed to quantify its relative impact. Figure 7-17 shows the coastline movement in two simulations without and with sea level rise, corresponding to the profile shown in Figure 7-15. The continuous retreat is due to the mass balance issue. At first sight sea level rise does not seem to have an impact. This is confirmed by Figure 7-18, showing the relative coastline movement between the two simulations, hence the relative impact of sea level rise. The long term trend is hidden behind short term noise, but is stable to slightly accretive. The model does not predict erosion from sea level rise, but a profile shape change leading to a slight accretion (erosion of shelf, accretion of surf zone). This diagnostic is confirmed by additional non-reported tests eliminating possible sources of errors (such as a test without multiple fraction to remove the unrealistic mass loss of the fines).

⁴ The height of the berm formed by the fines is surprisingly good, giving some credence to the calibration with groundwater.

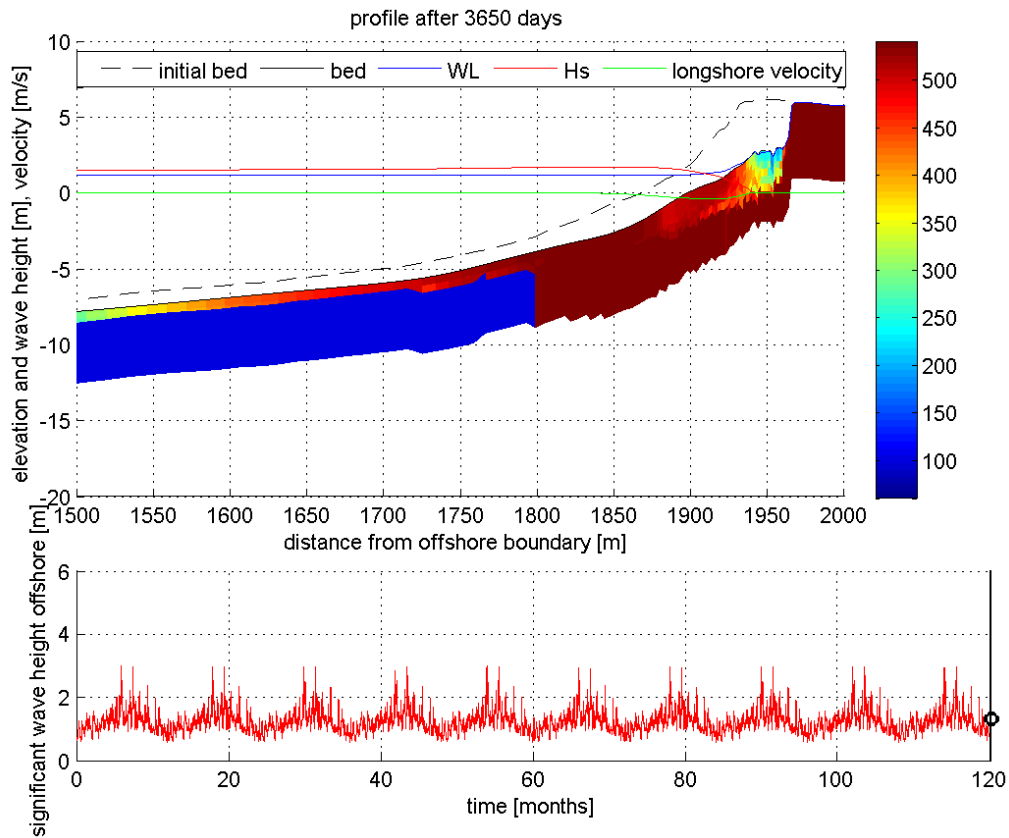


Figure 7-15 : Steep profile with groundwater and multiple sediment fractions horizontally distributed, as in Figure 7-4 but after 10 years.

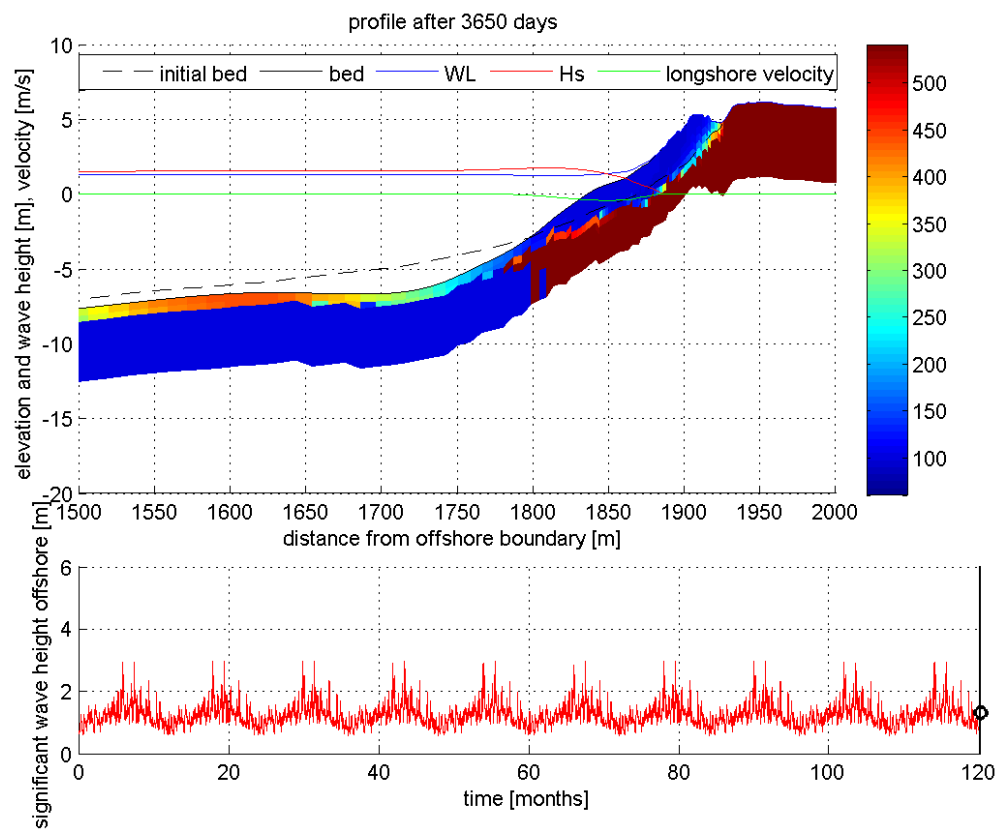


Figure 7-16 : Steep profile as in Figure 7-15 but with morfac 10 instead of 30.

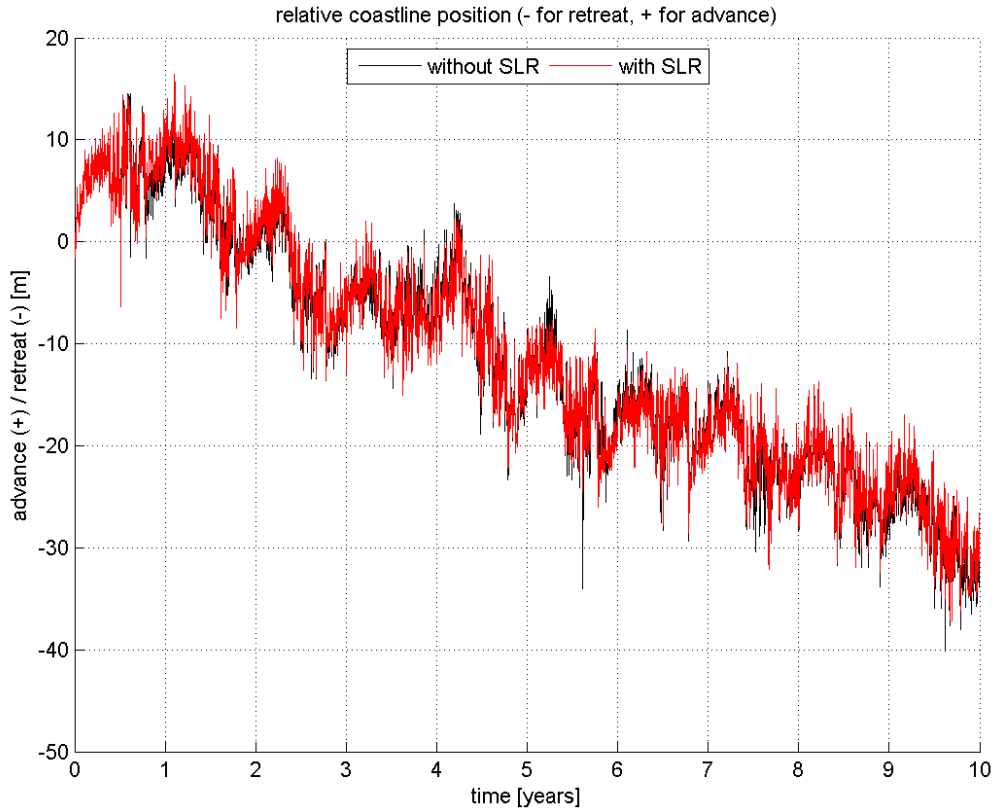


Figure 7-17 : Coastline movement in simulations without and with sea level rise of 1 cm/year

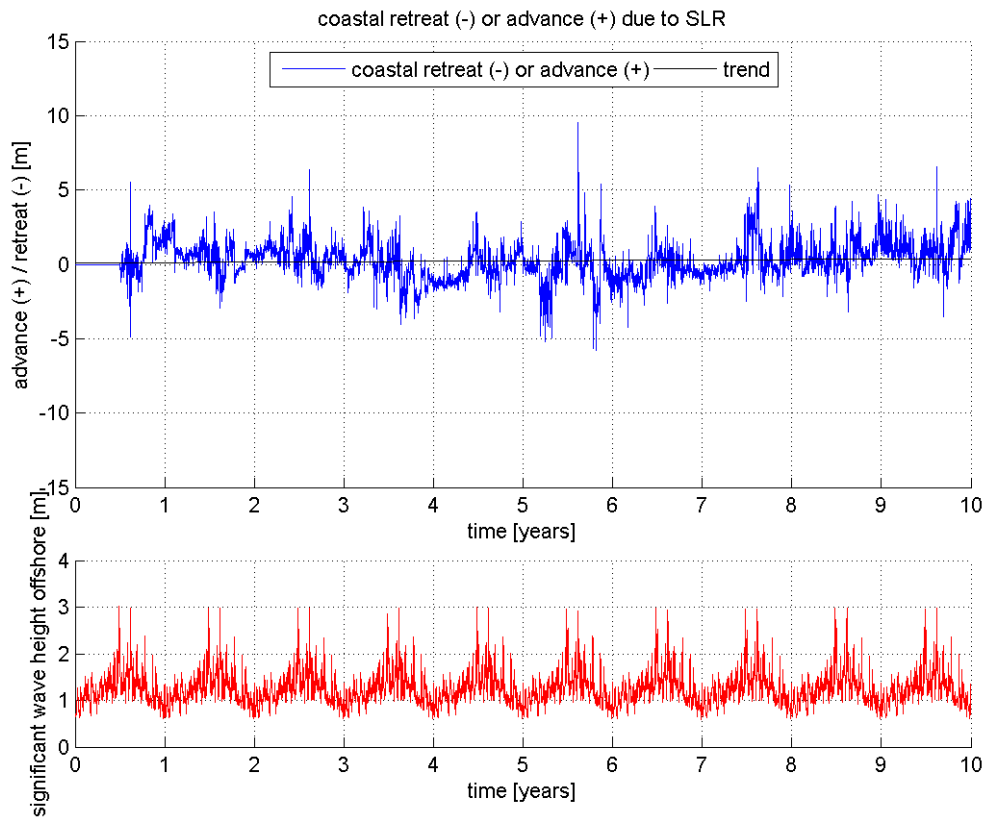


Figure 7-18 : Relative coastline movement with sea level of 1 cm/year compared to a reference simulation without sea level rise, showing a stable to accretive trend hidden behind short-term noise. The wave time series is identical in the two simulations.

To conclude, XBeach is not able yet to model coastal erosion due to sea-level rise, but not far either. This exercise is to our knowledge the first attempt to model cross-shore development at such a long time scale. Some additional research is needed to address the remaining issues :

- Concerning the excessive fines on the beach, the code has been modified to include a calibration parameter for onshore transport for each fraction. It proves to be a handy workaround to prevent unrealistic behaviour.
- Concerning the mass balance issue, the Groundhog Day release of XBeach contains improvements described in the thesis of De Vet (2014). A test shows however that it does not solve the problem.
- Concerning the lack of coastal retreat, further investigations are needed to identify possible missing processes and whether this is physically possible.
- Some methodologies may need to be developed to compensate for the lack of data on grain sizes and stratigraphy of the shelf. An initialisation run for the bed composition seems a promising method.

Coastal retreat is probably difficult to model because it is a slight and progressive natural change. By contrast other long term applications are probably easier. The exercise suggests that XBeach is capable of modelling the long term evolution of beach and shoreface nourishments, which are a large departure from the equilibrium profile. Long term bar migration has also been modelled successfully in Unibest TC (Walstra et al., 2012 ; Figure 7-19). It is also a reasonably robust process driven by the wave direction (Figure 7-20), which can probably be modelled qualitatively in XBeach.

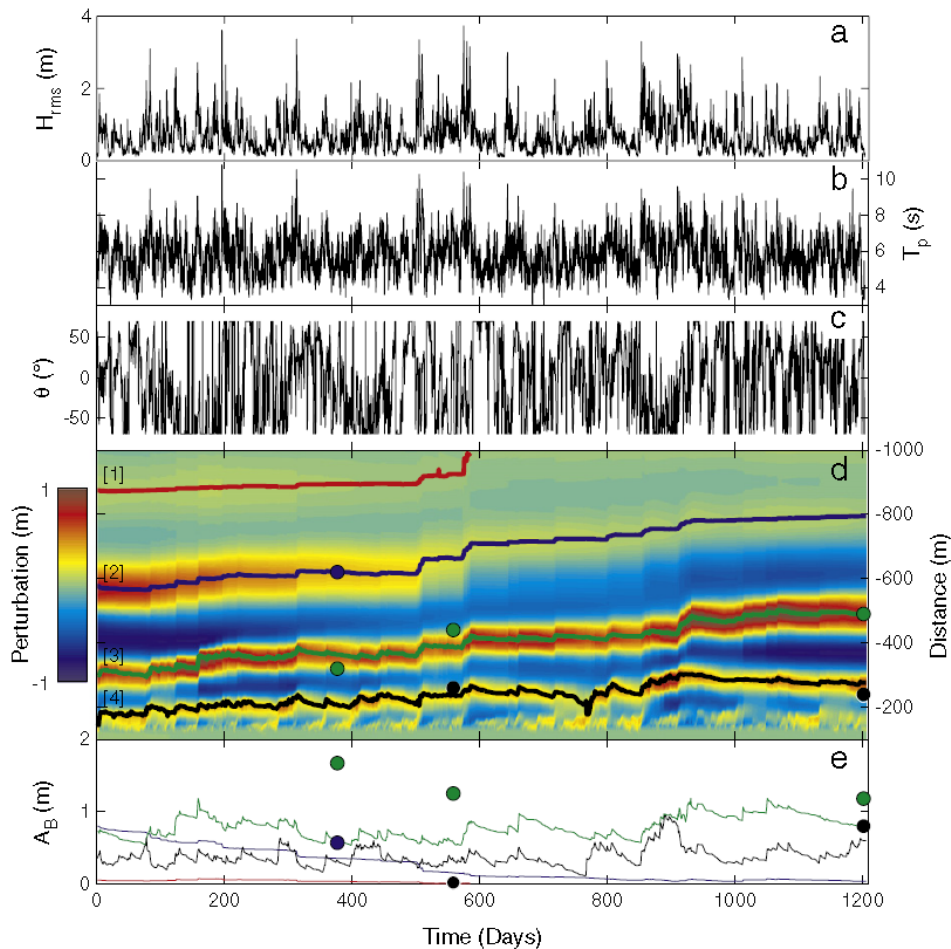


Figure 7-19 : Bar migration at Noordwijk modelled with Unibest TC (Walstra et al., 2012).

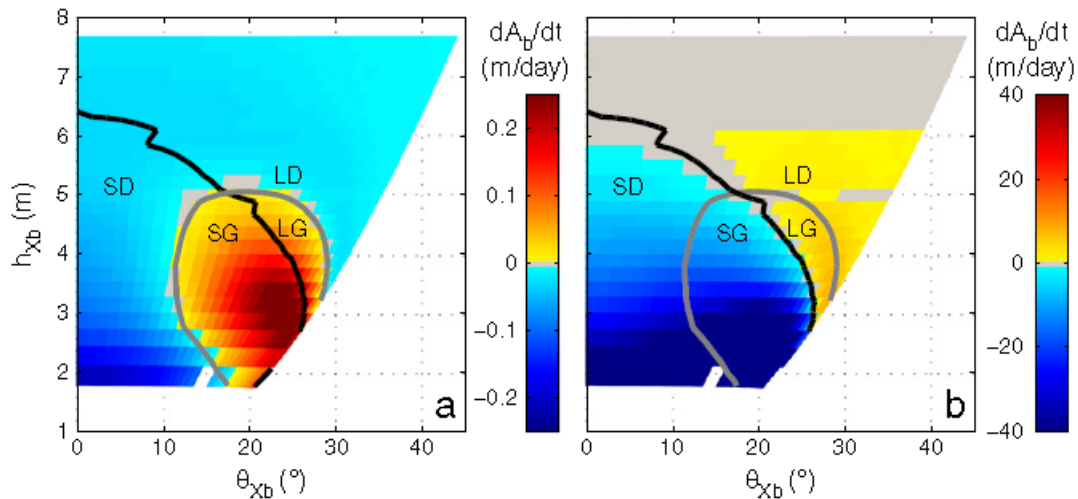


Figure 7-20 : Bar growth or decay (left) and bar migration (right) in Noordwijk as a function of water depth and wave direction (Walstra et al., 2012).

7.5 Very long term : geological profile development and stratigraphy

The longest time horizon which could be simulated with XBeach in the exercise above is 30 years, because the number of input files generated by the model became too large. In terms of computation time, at this stage a limit of 50-100 years is foreseen (computation time of 2 weeks to a month).

Longer time horizons generally fall outside the scope of coastal engineering, which focuses on the human time horizon. However geological models exist which can help in determining a profile shape or a stratigraphic record, giving extra information on the system behaviour. Barsim (Storms, 2002 ; Storms et al., 2013) is such a model (Figure 7-21, Figure 7-22). The CSDMS system (Community Surface Dynamics Modelling System ; http://csdms.colorado.edu/wiki/Main_Page) also contains several open source tools to deal with such issues.

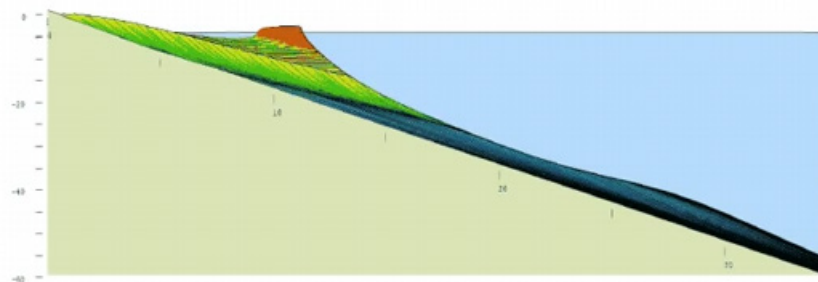


Figure 7-21 : Barrier island formation with the geological model Barsim (source : CSDMS website)

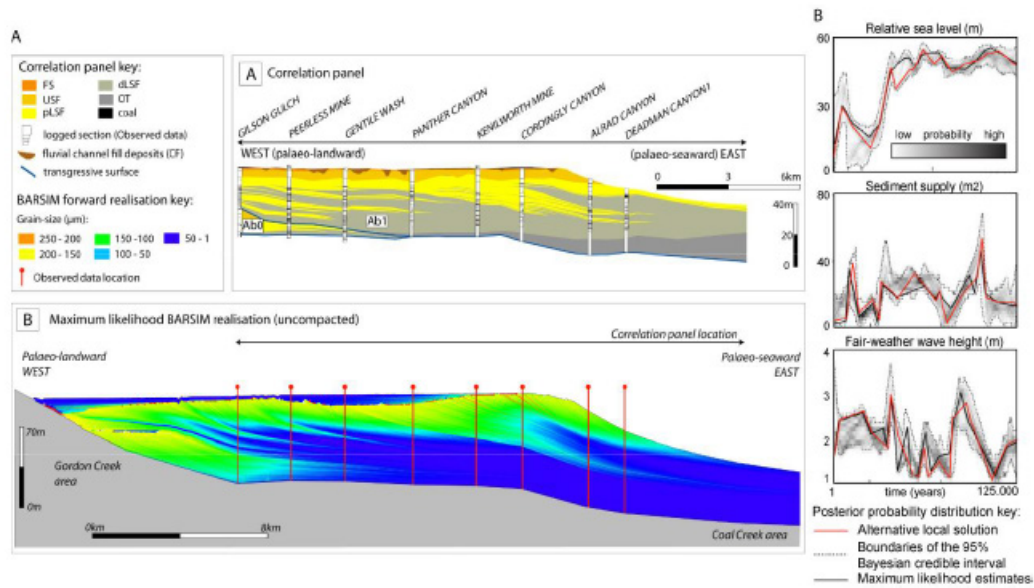


Figure 7-22 : Inverse simulation of coastal stratigraphy with the Barsim model (Storms et al., 2013)

7.6 Conclusion

We advise the following concerning modelling cross-shore profile development :

- For short term applications (1 day ; storm event), XBeach is well-suited. For the Belgian and the Dutch coast, the WTI 2017 settings combined to the Groundhog Day release and to a pseudo 2D approach yield outstanding results. A pseudo 2D model consists of a limited number of cells in the alongshore direction to resolve the edge waves (here 5 cells of 200m). The lack of directional spreading of the long waves in the superfast mode slightly overestimates the erosion. For other environments and/or a simpler approach, default settings and the superfast mode are a good starting point : it is easier to set up and shorter to compute.
- For medium term applications (1 year ; erosion and recovery cycles), XBeach is also well-suited, but it requires more attention to settings and calibration.
 - Concerning the settings, it is recommended to use the superfast mode, with measured time series in combination with the acceleration method morfacopt=1. The maximum morfac should be reasonably low to capture storms properly and to avoid mass balance issues (maximum of 10-30 suggested). In tidal environments such as on the Belgian coast, the morfac has to be lower to avoid excessive water and sediment fluxes at the boundary (maximum of 3-10 suggested).
 - Concerning the calibration, measured profiles during a year are probably ideal but will require an important effort. A more pragmatic approach in the absence of data is to focus on keeping the natural profile shape constant after a representative year, by calibrating with the onshore transport parameters. In the case of steep beaches and coarse material, including groundwater can significantly improve the results.
- For the Belgian coast, the simulations show that:
 - Using the WTI settings, Xbeach is able to regenerate the observed stable profile development. The measured shape of the cross shore profile is well represented.
 - For specific cases fine tuning of the parameters can be done to improve the quality
 - The default settings gives wrong profile development. The profiles become soon to flat due to an underestimation of the onshore transport
 - Not only the facSk and facAs parameters (that are changed in the WTI settings) are important, also to roughness (cb) and the wave parameters
 - Only small values of morfac can be used. With morfac 10, the spurious cross shore currents are too large.

- The grain size dependency on the results is smaller than expected. Further research is needed. Probably also facSk and facAs should become dependent on the grain size.
- After 1 year, the further profile development in Xbeach is limited. However, within a year, still some considerable fluctuations of the profile steepness is observed
- Xbeach is able to see the positive effect of foreshore nourishment (extra onshore transport). Further research is needed (e.g. for profiles that show offshore transport, optimisation of the berm size)
-
- For long term applications (>10 years), XBeach can be applied as for medium term applications. Depending on the application some shortcomings may exist.
 - Coastal retreat due to sea level rise cannot be modelled yet despite promising results, because the mass balance is not closed (problem exacerbated with a large morfac), a correction of the code is needed to prevent unrealistic results with multiple fractions, and some processes may be missing to model coastal retreat due to sea level rise (currently coastal advance due to profile reshaping predicted).
 - Beach and shoreface nourishments can be modelled over the medium to long term because they form a large departure from the equilibrium profile, its effect is hence more easily captured than the small changes due to sea level rise.
 - Long term bar migration has been modelled successfully in Unibest TC (Walstra et al., 2011). It is also a reasonably robust process driven by the wave direction, which can probably be modelled qualitatively in XBeach.
- For very long term applications (geological profile development and stratigraphy), geological models such as the model Barsim (Storms, 2002 ; Storms et al., 2013) and some tools of the CSDMS website are more suited.

8 Modelling structures

8.1 Overview

This chapter describes different structures commonly used in coastal models and how to model particular structures in Delft3D and XBeach.

8.2 Structure types

8.2.1 Overview

Structures in process-based models can be implemented in different ways. An earlier literature review made during the development of the morphodynamic model Coherens mentions the following types of structures (THV IMDC-Soresma, 2010) :

- Thin dams
- Dry points
- Levees
- Groynes
- Current deflecting walls (CDW)
- Discharges (not relevant for the present test case)

Additionally the following options may be considered:

- Variable bed roughness (vegetation option)
- Non-erodible layers

8.2.2 Thin dams

Thin dams represent small obstacles of subgrid dimension, but large enough to influence the flow pattern. They are defined as infinitely thin objects preventing 100% of the flow exchange between adjacent grid cells. They do not modify the total wet surface and volume of the model.

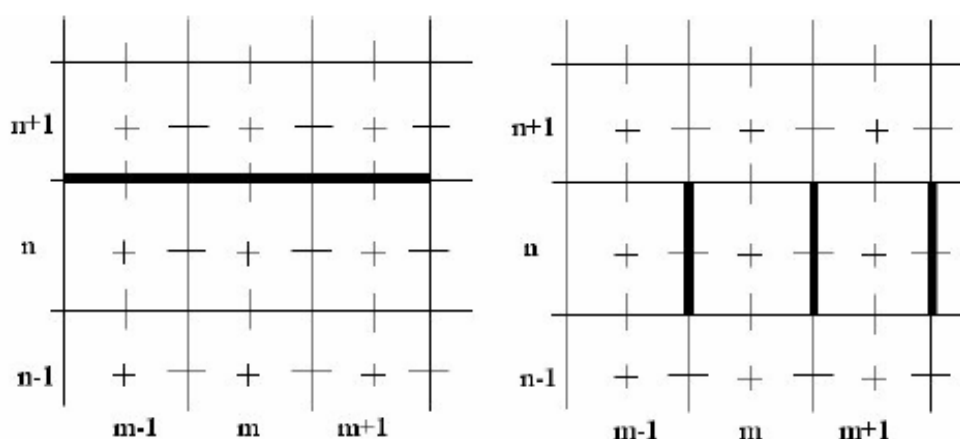


Figure 8-1 : Schematisation of thin dams blocking the flow in V (left) and U direction (right, thick lines) compared to the locations of water level points (crosses), depth points (intersections between full lines) and velocity points (dashes). Figure from THV IMDC-Soresma (2010).

Thin dams are present in Delft3D and Simona. They present some restrictions:

- They can only be parallel or perpendicular to staggered or structured grids (staircase effect);
- It is generally not a good idea to use them near grid and open boundaries;

- If the depth is defined in the cell corners, as in Delft3D, the bathymetry will be identical on both sides of the dam. If the depth is defined in the cell centres, as in Coherens, a different bathymetry on both sides is possible.

Further note that thin dams do not block waves : in Delft3D 'obstacles' have to be applied in the WAVE module.

8.2.3 Dry points

A dry point is a point which is removed from the hydrodynamic computation without changing its local water depth. A dry point is a grid cell centered on a water level point.

In Delft3D, the depth of the surrounding points is not influenced by the dry point. No special restrictions are mentioned in relation with its use near open boundaries.

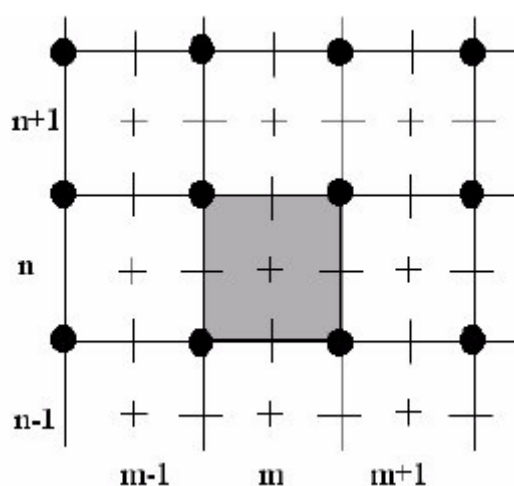


Figure 8-2 : Schematisation of a dry point (grey) compared to the locations of water level points (crosses), depth points (dots) and velocity points (dashes). Figure from THV IMDC-Soresma (2010).

Further note that a dry point does not block waves : in Delft3D 'dry values' should be applied to the bottom grid in order to model dry points in the WAVE module. Finally, a wall roughness can only be applied in combination with dry points in Delft3D (Dujardin et al., 2010b). This may be of importance to model the flow in a port entrance.

8.2.4 Levees

In commercial packages (Delft3D, Simona, Telemac), levees are schematized as 2D weirs, i.e. fixed constructions generating energy losses due to turbulence downstream of the flow constriction. The energy loss is modelled as an opposing quadratic or linear friction force in the momentum equation.

Weirs can be applied to model sudden changes in depth. They are defined at velocity nodes and are subgrid features, like thin dams. They are hence expected to have the same drawbacks.

In Delft3D several other structures are based on a similar principle (structures add-on): rigid sheets, floating structures, 3D gates, porous plates and bridge piers.

8.2.5 Groynes

A groyne is a structure perpendicular to the shoreline used to stabilize the coast. Groynes can be emerged, sloping or submerged. Most of the models do not present a specific functionality to model groynes, instead several methods can be used.

In research models, groynes are generally part of the bathymetry to reproduce their effects on the flow and the morphology. Yazdi et al. (2010) and Yossef and Klaassen (2002) present such kind of work. In the commercial packages Telemac and Mike, groynes are modelled by a combination of a modified bathymetry and the energy loss of a weir. The User Manual of Delft3D also suggests the use of a weir.

Visser (2002) investigates three ways to model a groyne in Delft3D: as a part of the bathymetry, as dry points or as thin dams. Conclusions are presented below and updated based on tests done within this project.

The modified bathymetry has a side effect for staggered grids, because the depth at the velocity nodes (used in the momentum equation) is interpolated between the two nearest depth nodes, one at the real depth and one above MSL. As a consequence the velocity on both sides of the groyne is reduced. This effect is expected to affect in turn the morphology, but may decrease with an increasing grid resolution. In newer Delft3D releases this interpolation effect can be avoided by specifying the depth in the cell centres instead of the cell corners. A modified bathymetry does further not allow to model a submerged groyne, which would erode. This can now also be prevented by adding a hard layer under the groyne into the model (paragraph 8.2.8). This solution has the large advantage of working also with waves.

The dry point option also has a side effect, because the morphology update occurs at the depth node, for which a mass balance is applied over the area of one grid cell, while one fourth of this area is actually located in the dry point cell. This results in an error in the calculation of the bed level. This effect is expected to affect in turn the velocity field, but may decrease with an increasing grid resolution. Like the modified bathymetry, this side effect can be avoided in newer Delft3D releases by specifying the depth in the cell centres. A dry point does further not allow to model a submerged groyne.

The thin dam option, as mentioned earlier, results in an equal depth on both sides. As a consequence two rows of thin dams have to be used to model a groyne. Again this can be avoided by defining the depth in the cell centres. This structure has been identified by the author as the most suitable to model the morphology around a groyne. Due to the workaround in grid definition, this conclusion is however outdated. A thin dam does not allow to model a submerged groyne, and is of limited use to model complex geometries. Coarse grids would further result in excessively wide groynes.

The weir option allows to model submerged groynes. To prevent the same issue as with thin dams, the depth has to be defined in the cell centres in Delft3D. To prevent staircase effects in the flow, the weir height should be specified in each grid cell individually. It further needs to be combined with obstacles in the WAVE module.

Weirs and a modified bathymetry can be expected to perform equally well when combined respectively with obstacles and a hard layer (Zimmermann et al, 2012a). The implementation of weirs and obstacles is however more difficult. We therefore advise the use of a modified bathymetry with a hard layer to model submerged groynes. For emerged groynes more options are possible, the choice should be driven by practicality and physics.

8.2.6 CDW

A current deflecting wall (CDW) alters the entrance flow into a harbour in such a way that the penetration of suspended sediments is substantially reduced (Van Leeuwen and Hofland, 1999). It consists of a plate stopping the flow at the surface, mounted on pylons generating a flow constriction and related friction losses, like for a weir.

This structure, present in Delft3D, is to be used in 3D simulations. Depending on the water level, the upper layers of the flow in the sigma grid will be stopped by the plate, while the lower layers will experience an energy loss downstream, modelled by an extra quadratic friction term in the momentum equation.

8.2.7 Variable bed roughness

To simulate the effect of vegetation on the flow, it is sometimes possible to define a variable bed roughness. Vegetation slows down the flow while reducing or even preventing erosion. Hence it has an effect similar to some structures. This option is essential to flooding simulations.

In Delft3D, this is implemented as “trachytopes”, which are basically classes of bed roughness predictors for various land uses. A predictor calculates the local bed roughness based on the flow and geometrical parameters. Trachytopes can be defined as a different kind of bed roughness on a point, a line or an area. Three main classes of trachytopes are included:

- simple trachytopes reduce to the use of the standard friction factors of White-Colebrook, Chézy or Manning;
- alluvial trachytopes include bed forms predictors for alluvial environments, based on zero to a large number of calibration factors;
- vegetation trachytopes predict the bed roughness of submerged and non-submerged vegetation areas, lines (hedges, bridges) or points (trees). A bridge further experiences a similar energy loss than a weir.

To be noted that the use of this option in another context should be considered with care since bed roughness, shear stress, flow and sediment transport are linked. This option is not expected to be able to model the flow on top of a submerged groyne while preventing sediment transport.

8.2.8 Non-erodible layers

Non-erodible layers are specified as depth points on top of which no sediment is present. It is combined to a change in bathymetry as used to model a groyne, except that these points can now also lie under water without being eroded. Depending on the grid definition, it is expected to have the same side effect on the velocity and morphology as a modified bathymetry. Non-erodible layers can be defined with the same tools as the model bathymetry.

8.3 Modelling structures in Delft3D and in XBeach

8.3.1 Modelling tests

Within this project several tests have been carried out concerning structure modelling :

- Comparison of a submerged groyne as a modified bathymetry and as a series of weirs, respectively combined with a hard layer and obstacles, in a simplified case of Blankenberge with waves, currents and morphology (Zimmermann et al, 2012a).
- Comparison of a submerged weir as a modified bathymetry and hard layer, and as a single weir, in a steady river flow in equilibrium, with currents and morphology (paragraph 8.3.2).
- Comparison of a submerged groyne as a modified bathymetry and a hard layer, in the stationary model Delft3D and in the instationary model XBeach (Zimmermann et al, 2012a).
- Implementation of the port of Zeebrugge in the coastal model (Zimmermann et al, 2012c).

The following paragraphs present the conclusions of the modelling tests.

8.3.2 Structure comparison

The steady river flow case is reproduced from the validation document of Delft3D (Deltares, 2008). It consists of a 1D horizontal model of a river with a constant slope, on which a constant discharge is imposed upstream and a constant water level downstream. Structures and morphology are then added.

In open channel flow theory, the flow over a slope establishes an equilibrium between the downward gravity force and the upward flow resistance. If a Chezy friction law is chosen for the flow resistance, the equilibrium velocity U is given by $U = C\sqrt{hi}$ where C is the Chezy coefficient, h the water depth and i the bed slope. In the model the solution is exactly reproduced by choosing carefully the upstream discharge and the downstream water level boundary (Figure 8-3).

When adding morphology, river morphology theory also makes it possible to determine the equilibrium slope and equilibrium depth of the channel as a function of the upstream discharge and sediment flux.

When adding a weir, transition conditions are needed at the weir location to solve the set of equations. However these transition conditions are not straight forward in the weir model of Delft3D, which prevents from actually getting an analytical solution which could be compared to the model results. Since this research task is not essential to the project, it has not been pursued. Model results yield however valuable insight into relative performance of the two structure types (modified bathymetry and weir).

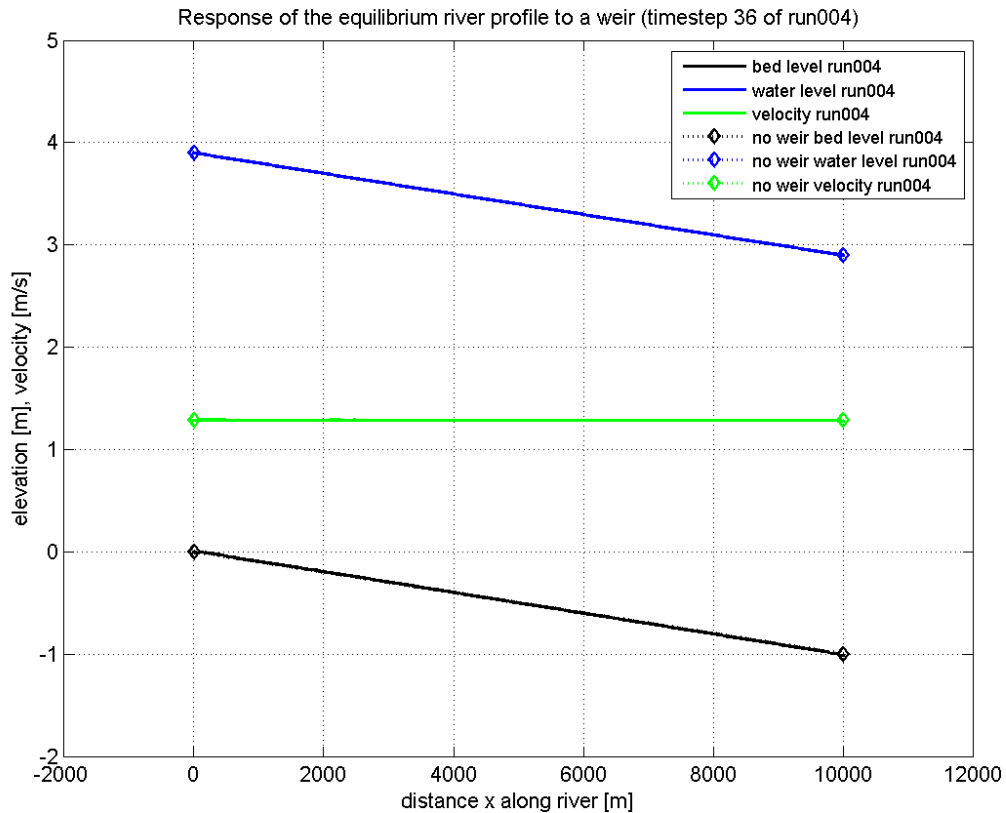


Figure 8-3 : Hydro- and morphodynamic equilibrium of the open channel case, showing the perfect agreement with the analytical solution (“no weir” legend). Model results in Delft3D.

Figure 8-4 shows that even for a large flow constriction (75% of water column at simulation start), the weir and the modified bathymetry predict almost the same water level and bed slope. The velocity is 20% higher with a hard layer, which is expected because the velocity is not imposed at all at the boundaries, and because the energy loss on top of the weir has not been calibrated in the simulation with the modified bathymetry. Local bed oscillations can be observed downstream of the weir with a modified bathymetry : this may be partly physical because contrary to the weir, this option resolves the flow constriction, although only with one grid point.

Note that the weir crest height is defined absolute to the bed level. Sedimentation values can never exceed the initial crest height imposed, so that even large morphological changes can remain realistic.

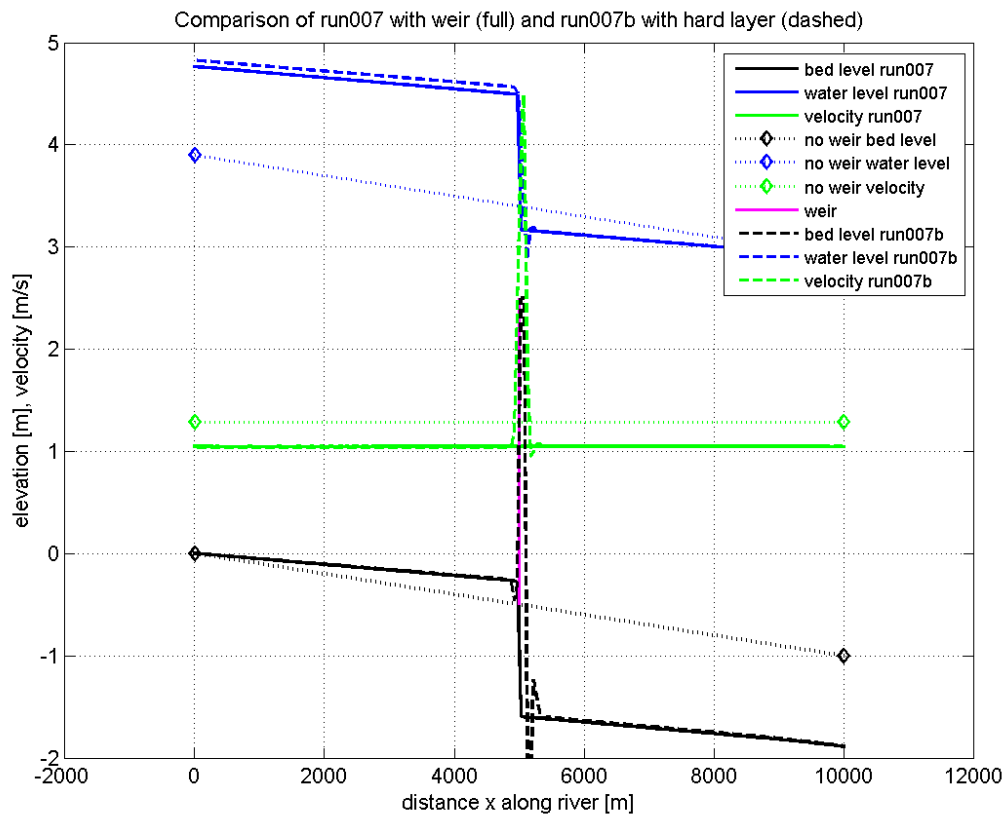


Figure 8-4 : Comparison of the morphodynamic equilibria of the open channel case with 3m weir as a structure and as a hard layer, showing the good agreement between methods and the effect of increasing the weir crest height. Model results in Delft3D.

8.3.3 Model comparison

The stationary model Delft3D and the instationary model XBeach have been compared in the simplified Blankenberge case (Zimmermann et al, 2012a). In this test several structures have been added step by step (two groynes and a port entrance channel) and both models compared. It led to the following conclusions regarding structures :

- Qualitatively, the same effects can be observed in both models at each step of the comparison : flow constriction, wave breaking, refraction, and related erosion-sedimentation. Spatial agreement is very good (Figure 8-5).
- Quantitatively, the effect of the structure was overshadowed by differences between models already visible without structure (wave dissipation by bottom friction, boundary conditions, implementation of the sediment transport formula). Some numerical oscillations were present near the groyne in XBeach, but this behaviour has been partly improved in subsequent releases.
- Threshold effects due to the instationarity of the model are therefore expected to be of secondary importance compared to other uncertainties.

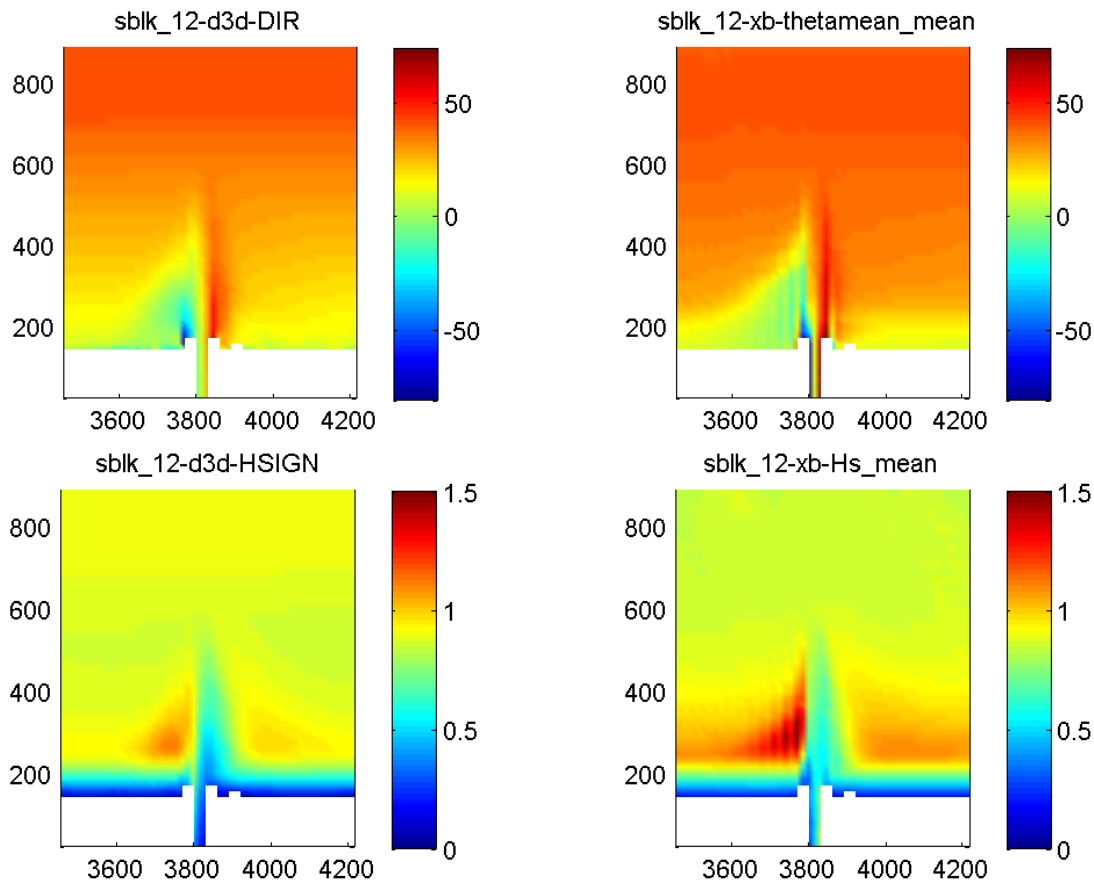


Figure 8-5: Delft3D (left) and XBeach results (right) of a simplified model of the port of Blankenberge, with its entrance channel and a submerged sloping groyne on each side. Mean wave direction (top, approach angle 45° offshore) and significant wave height (bottom), showing good spatial agreement between the models.

8.4 Conclusion

We advise the following to implement structures :

- Structures can be seen as internal, local boundaries. As with every boundary type, their modelling is not perfect and includes side effects. Different structure types with the same purpose or in different models perform similarly, structure types should hence be chosen according to physics and practicality of their implementation.
- The side effects of given structure types depend on the exact grid definition of each model. In Delft3D, with structures and morphology it is advised to always define the depth in the cell centres to reduce side effects. These side effects should be very local anyway. This is the only and default option in XBeach.
- Submerged groynes may be modelled in Delft3D with a modified bathymetry (flow, wave) and a hard layer (morphology), or with a series of 2D weirs (flow) and obstacles (waves). We think the former option is easier to implement. Side effects may include bed oscillations for the modified bathymetry (physical and numerical), and staircase effects for weirs if their implementation is too coarse. In XBeach only a modified bathymetry and hard layer are currently available.
- Emerged groynes may be modelled in Delft3D with a modified bathymetry and a hard layer, or with a series of thin dams and obstacles. Here thin dams are probably easier to implement. In XBeach a modified bathymetry and a hard layer have to be used.
- Dry points and thin dams are standard and easy options to model the complexity of a port. However in Delft3D a wall roughness can only be applied in combination with dry points. In XBeach a modified bathymetry and a hard layer have to be used.
- Generally speaking since flow and wave models are often separate modules, it is important to verify that the effect of the structure has been modelled in both modules.

9 Summary of proposed methodologies

This report has reviewed different modelling methodologies, from data collection to long-term morphological modelling. Individual conclusions have been summarized at the end of each chapter and in a more practical form below. For their real application, the reader is referred to the other project reports related to simplified or real cases modelling.

As in many modelling projects, much time has been spent on troubleshooting models which do not work as intended due to, amongst others, bad default settings and bugs. This experience is not part of the report and has been shared by other means (Wiki, knowledge exchange). The reader is also referred to the final “lessons learnt” presentation given at the end of the project in Flanders Hydraulics and illustrating some of these conclusions.

In general there is no standard recipe for modelling, however this chapter attempts to provide direct answers to specific questions as a starting point for morphological modelling. It is a limited compilation of the conclusions of individual chapters. It also contains links to data sources for the Belgian coast.

Data and models available	See Chapter 2
Which data sources are available for the Belgian coast ?	<ul style="list-style-type: none"> • De Winter et al.(2011) summarize data available for the Belgian coast. • Zimmermann et al.(2012c) discuss some issues with velocity data from the Meetnet Vlaamse Banken. • Trouw et al.(2010) summarize past coastal projects along the Belgian coast.
Which models are available at Flanders Hydraulics for the Belgian coast ?	<ul style="list-style-type: none"> • The Dutch Zuno model of the Southern North Sea in Simona software is extensively used. It is however still quite coarse and has possibly a too low roughness to compensate for a nesting error. • The Optos model of the Southern North Sea from MUMM and in Coherens software has a finer resolution and is extensively calibrated, but has to our knowledge not been used for boundary conditions yet. • Several smaller scale models are available for specific applications. The Kustzuid v4 model of the Belgian coast from Flanders Hydraulics is very fine but possibly of too limited extent. • Finally several morphological models have been developed within this project : the Delft3D models OKNO and N2V covering the Northern half of the Belgian surf zone, the XBeach models of Blankenberge and of Knokke. Their focus lies more on transport rates and bed changes than on hydrodynamics.
Which model should we choose for boundary conditions ?	<ul style="list-style-type: none"> • It depends on the purpose of the application and falls more under the model setup. Attention points are for instance the grid resolution, whether the model is 2D or 3D, includes wind, atmospheric pressure, salinity, river discharges and mud concentration.

Model setup	See Chapter 3
What should we know after the data analysis ?	<ul style="list-style-type: none"> • Dominant processes, spatial and temporal scales should already be more or less identified. The quality of model and input reduction will depend on it. Modelling is a refinement of the initial data analysis.
Which model should we choose if longshore transport is expected to be important ?	<ul style="list-style-type: none"> • Longshore transport is well-understood and can probably be modelled with any model including the effect of waves on currents (radiation stress). Both Delft3D and XBeach can model the longshore current.
Which model should we choose if cross-shore transport is expected to be important ?	<ul style="list-style-type: none"> • Cross-shore transport is more difficult but can for simplicity be reduced to a balance between onshore transport by wave non-linearity and offshore transport by the return flow. Additionally the model should be able to supply the profile with sediment from dune erosion (ideally by avalanching). • If bar growth and migration is important, results will greatly depend on the exact location of the convergence point of sediment transport. In addition to the processes above, the wave roller, the concentration profile via wave breaking turbulence, bed forms and 3D effects can all play a vital role. • Delft3D is not able to model the return flow in 2D nor avalanching in 2D and 3D. XBeach is a good start for cross-shore modelling and probably good enough for bar growth and migration.
Which resolution should our model have ?	<ul style="list-style-type: none"> • The resolution should be such that all features of interest are resolved sufficiently. We propose 5 cells across a navigation channel and ideally 10 cells across the surf zone in a 2D model. If a bar is present or in a profile model the resolution should be increased further.
How should we generate boundary conditions ?	<ul style="list-style-type: none"> • Boundary conditions can be generated by domain decomposition or nesting. • Domain decomposition offers an easy model setup but possibly a larger computation time. It can be used when a limited number of simulations are expected on a simple detailed model grid which is already included in the mother grid. • Nesting offers a flexible grid design but requires some scripts to automate the process. It can be used when the detailed model grid is complex and / or when many simulations are expected.
Which flow boundary conditions should we use ?	<ul style="list-style-type: none"> • All boundary conditions consist in imposing water levels, velocities or a combination of both. It is advised to apply both a water level and a velocity component along at least a boundary section, in order to keep some control over it. • For sediment transport and morphological modelling, it is more important to get the velocities right, so the priority may go towards velocity and Riemann boundaries. • If a wind- or wave-generated current is expected to pass the boundary of a nested model, Neumann boundaries should be used. • Astronomical boundary conditions are handy if individual tidal components need to be scaled.
Which wave boundary conditions	<ul style="list-style-type: none"> • Wave modelling has not been investigated in this project.

<p>should we use ?</p>	<p>However two small attention points regarding waves can be mentioned. Especially in shallow waters like on the Belgian coast, wave dissipation is important and has to be compensated by wind growth. If wind is excluded on purpose, it is advised to turn off or reduce strongly wave dissipation by bottom friction and by white-capping. Wind can also help compensate for outgoing wave energy lost at the boundaries. Finally instationary long waves are needed in combination with avalanching to model run-up, dune erosion, overwash and breaching.</p>
<p>Which sediment transport boundary conditions should we use ?</p>	<ul style="list-style-type: none"> • For sand the sediment concentration can most of the time be assumed to be in equilibrium with the flow. • For mud sediment under- and overloading is frequent and boundary conditions should be generated by nesting. • Van Rijn (1993) presents a criterion to estimate the importance of under- and overloading.
<p>Is it possible to set up a small model without nesting or domain decomposition, to save some computation time ?</p>	<ul style="list-style-type: none"> • In general it is difficult if realistic circulations are needed. However if the flow is known to propagate alongshore with little ellipticity, time series of the water level gradient can maybe be applied at the lateral boundaries (Neumann type) and of the water level at the offshore boundary. It is then very important to use measured time series instead of a harmonic tide to get realistic residual transport values. It has however not been tested here in detail yet.
<p>Is Xbeach able to model cross shore transport and profile development for the Belgian coast</p>	<ul style="list-style-type: none"> • Yes, if the morfac parameter is taken small enough (3 or less) and if the WTI settings are used. The small dependency on the grain size needs further research.

Model calibration	See Chapter 4
Does the calibration of a morphological model differ from that of a hydrodynamic model ?	<ul style="list-style-type: none"> • The calibration needs to take into account the flow, the waves, the sediment transport and the morphology. Since the flow affects sediment transport, it is not possible to decouple the calibration of the individual components. • The calibration should address both mathematical and physical errors at the same time. It is advised to always compare results of the mother model, the daughter model and measurement data at the same time. • Like any calibration, it is important to have spatially spread data and to not overcalibrate the model, in particular with sediment transport and morphology.
Which reasonable accuracy can be expected from a good calibration ?	<ul style="list-style-type: none"> • Commonly accepted accuracies can be derived from missing physical processes. • The natural variability or instationary model results also provide upper bounds for reasonable accuracies. • Some measurements often have an accuracy which is lower than that of the model, especially in the surf zone where measuring is difficult.
How do we calibrate the flow ?	<ul style="list-style-type: none"> • Roughness and viscosity are two parameters commonly used to calibrate respectively the flow and eddies. Both are artifices to model subgrid processes and are resolution dependent. However little data is usually available to justify detailed calibration of these parameters. • The roughness affects sediment transport via the bottom shear stress. A good calibration for the flow can easily be a bad one for sediment transport, especially in the surf zone. In addition, discontinuities in roughness fields create unrealistic erosion-sedimentation patterns at the transitions. • To sum it up, it is advised to keep it as simple as possible and to not change much the roughness if alternatives exist. Such an alternative may be to scale directly the boundary conditions. Default values may possibly already be good.
How do we calibrate sediment transport ?	<ul style="list-style-type: none"> • The residual sediment transport depends on the exact shape of the tide (impacted by the effect of waves on the sediment concentration). It can be estimated as the sum of interactions between tidal components with the help of a harmonic analysis. • A harmonic analysis can be done with the least square equation method (LSE) or a fast Fourier transformation (FFT). The LSE should be preferred, with for instance the T_TIDE toolbox which can determine the relevant tidal components and accuracies itself. • The residual sediment transport should not be computed with methods from literature, which are incomplete. A general method is described in this report, based on the combined approaches of Van de Kreeke and Robaczewska (1993) and of Hoitink et al.(2003).
How do we calibrate morphology ?	<ul style="list-style-type: none"> • Morphological models are not good enough yet at quantitative predictions. They should rather be calibrated on qualitative and visible long-term changes (bathymetry trends). The model can also be used to gain insight into the system behaviour, in which case calibration is not always necessary.

Input reduction	See Chapter 5
How can we reduce computation time of long-term morphology simulations ?	<ul style="list-style-type: none"> • A lower computation time can be achieved with morphological acceleration, model reduction, input reduction and computer power. • For some unidentified reason, the computation time of 2D XBeach models may be strongly reduced by decreasing the duration of instationary boundary time series (parameter rt).
What is input reduction ?	<ul style="list-style-type: none"> • Input reduction aims to reduce the full time series of input parameters to a manageable set of conditions. The reduced set can then be combined to morphological acceleration to shorten computation time. It should not be the limiting parameter of a study if executed correctly. However the reduction itself also takes time and errors can easily arise. • The quality of the reduction depends to a large extent on a good understanding of the system. Spatial scales, temporal scales and main driving processes should already be more or less identified before the reduction. • All input reduction techniques reduce complex input according to a target. This target should be chosen very carefully, because the error will arise in what it does not include. It is in particular very important to keep existing correlations between parameters in the reduction, and to verify the quality of the reduction at each step, in particular its spatial agreement.
How do we reduce the tide climate?	<ul style="list-style-type: none"> • The representative tide of Latteux (1995) is a common method to select a single tide with a sediment transport comparable to the long-term average value of the full tide climate. If needed several tides can be chosen instead of one. • A good spatial transport pattern may be preferable to good transport values, which can still be scaled later with various methods. • The scaling method also generates errors and should be selected according to the desired property. In a situation in which waves and currents are equally important, it is possibly better to scale the flow boundary conditions.
How do we reduce the wind climate ?	<ul style="list-style-type: none"> • The reduced wind climate should be such that it generates the good wave climate inside the model domain. Because wind and wave climate are generally correlated, it is advised to derive one wind class per wave class. If the wind and wave directions are close, multiple linear regressions for the wind speed should be appropriate.
How do we reduce the wave climate ?	<ul style="list-style-type: none"> • The wave climate can be reduced with many methods depending on the target desired. Because it is more complex than the tide, the automated statistical procedure OPTI can yield a more accurate reduced climate than a manual selection. However expert judgement is still necessary to include physics. • OPTI is however time-consuming and more simple approaches can be considered if time is short.
How do we run a long-term morphological simulation with the reduced input ?	<ul style="list-style-type: none"> • Generally speaking, continuity is very important for morphology. Space-varying input values such as a roughness field and probably a distribution of sediment fractions should not present discontinuities. The initial bathymetry should also be smoothed out before being used for morphology. • Morphological modelling can then be done with the reduced

	<p>set of conditions with a constant morfac, a time-varying morfac, or the MorMerge method. The last two methods are said to perform equally well. History effects are lost with MorMerge, and transition periods are needed with a time-varying morfac to prevent mass balance issues. Alternatively, the constant morfac approach is the most easy to implement and provides valuable information about individual storm events, but it comes with its own side effects. Mormerge, together with some specific settings to avoid stability issues, is the most suitable method to reach longer time horizons.</p> <ul style="list-style-type: none"> • The main difficulties of the constant morfac approach come from the choice of the wave update interval (computation time, stability, wind-generated currents), insufficient modulation of water levels when decoupling the hydro- and morphological time scales and the generation of suitable time series. Markov chains could be used to generate realistic records. • In Delft3D all methods are available. In XBeach only the constant morfac approach can be used, it has been shown to yield reasonable results.
<p>What can we do if the input reduction is good but morphological results still need to be improved ?</p>	<ul style="list-style-type: none"> • Current limitations of morphological modelling possibly lie in the roughness formulations, bed slope effects and transport formulae. Sediment fractions can have important effects on the results.
<p>How to increase the time horizon ?</p>	<ul style="list-style-type: none"> • In Delft3D, time horizons of 10 years and more can be achieved by increasing the wave update interval, combined with dry cell erosion for model stability, a reduced number of wave conditions and the application of the Mormerge or the variable morfac approach. • In XBeach, the instationary character and the lack of a Mormerge method restrict the time horizon to at most a few years with the constant morfac approach. The duration of the boundary time series (keyword rt) determines to a large extent the computation time of large models and should be kept low. Stationary wave computations and a variable morfac approach may yield an additional speed-up of a factor 2. The latter is not user-friendly, it is suggested to run one simulation per wave condition and sum up the results in the post-processing instead.

Modelling inlets and embayments	See Chapter 6
How to model tidal inlets ?	<ul style="list-style-type: none"> • Tidal inlets are subject to very complex behaviours because wind, waves, tide, surge and river discharge can all play an equally important role. For this reason, it is important to make important efforts in the (historical data) analysis of the system. • Tidal prism relationships and the stability criterion of Bruun et al. (1978) are the most simple tools, and can help in evaluating the cross-sectional area and the stability of an inlet. It is recommended to compute the minimum stable cross-sectional area $A = cP^d$ with coefficients c and d respectively equal to 10-4 and 1, and to apply an uncertainty of $\pm 30\%$, rather than to use empirical formulas such as those of Jarrett and O'Brien. If results differ by an order of magnitude with the measured stability, the physically based formulas of Stive and Rakhorst (2008) and of Kraus (1998) can be used, or one's own relation be calibrated on known systems. • If simple modelling is desired, without setting up a complex 2D model, the Escoffier diagram and the Inlet Reservoir Model can be used. The first allows to evaluate the sensitivity of the inlet stability to the temporal variations in forcing. The second allows to quantify the long term evolution of the different inlet elements interacting with each other, and in response to human impacts, and is to be preferred over the ASMITA model. • Complex morphological modelling is possible but should focus on qualitative behavior and relative impact (of processes or human impact), because input reduction is complex. Simulations on a time scale of decennia to centuries (inlet evolution) can be done in most cases by assuming that the tide is the dominant forcing, thus neglecting waves.
How to model embayments ?	<ul style="list-style-type: none"> • Bay beaches are interesting for design of artificial beaches because their shape generally corresponds to a kind of equilibrium shape. The state of this equilibrium can be assessed with the Mepbay software based on the empirical equation for a parabolic beach profile. Care and expert judgement is however necessary for the interpretation of results. • From a modelling perspective, bay beaches are related to longshore transport. A coastline model or a long term 2D model can therefore be used. However difficulties can be encountered with both methods. A coastline model is difficult to calibrate for strongly curved beaches. In a 2D model, the time horizon involved will often be a limiting factor. • Tidal flats in embayments such as the Baai van Heist are difficult to model. 2D morphological model are based on a relaxation time scale for suspended sediment, which formulation may present serious shortcomings for tidal flats. The Galappatti formulation used in Delft3D is better than the constant time scale used in XBeach, but may still be insufficient. Other major limitations include the lack of data on the spatial variability of the grain size, of the bed roughness, and the vertical stratigraphy. A 3D morphological model may perform better but can easily present instabilities.

<p>Modelling cross-shore profile development</p>	<p>See Chapter 7</p>
<p>How to model short term profile development (1 day) ?</p>	<ul style="list-style-type: none"> • For short term applications (1 day ; storm event), XBeach is well-suited. For the Belgian and the Dutch coast, the WTI 2017 settings combined to the Groundhog Day release and to a pseudo 2D approach yield outstanding results. • A pseudo 2D model consists of a limited number of cells in the alongshore direction to resolve the edge waves (here 5 cells of 200m). The lack of directional spreading of the long waves in the superfast mode slightly overestimates the erosion. • For other environments and/or a simpler approach, default settings and the superfast mode are a good starting point.
<p>How to model medium term profile development (1 year) ?</p>	<ul style="list-style-type: none"> • For medium term applications (1 year ; erosion and recovery cycles), XBeach is also well-suited, but it requires more attention to settings and calibration. • Concerning the settings, it is recommended to use the superfast mode, with measured time series in combination with the acceleration method $\text{morfacopt}=1$. The maximum morfac should be reasonably low to capture storms properly and to avoid mass balance issues (maximum of 10-30 suggested). In case of tide such as on the Belgian coast, the morfac has to be lower to avoid excessive water and sediment fluxes at the boundary (maximum of 3-10 suggested). • Concerning the calibration, measured profiles during a year are probably ideal but will require an important effort. A more pragmatic approach in the absence of data is to focus on keeping the profile shape constant after a representative year, by calibrating with the onshore transport parameters. In the case of steep beaches and coarse material, including groundwater can significantly improve the results.
<p>How to model long term profile development (>10 years) ?</p>	<ul style="list-style-type: none"> • For long term applications (>10 years) XBeach can be applied as for medium term applications. Depending on the application some shortcomings may exist. • Coastal retreat due to sea level rise cannot be modelled yet despite promising results, because the mass balance is not closed (problem exacerbated with a large morfac), a correction of the code is needed to prevent unrealistic results with multiple fractions, and some processes may be missing to model coastal retreat due to sea level rise (currently coastal advance due to profile reshaping predicted). • Beach and shoreface nourishments can be modelled over the medium to long term because they form a large departure from the equilibrium profile, its effect is hence more easily captured than the small changes due to sea level rise. • Long term bar migration has been modelled successfully in Unibest TC (Walstra et al., 2011). It is also a reasonably robust process driven by the wave direction, which can probably be modelled qualitatively in XBeach.
<p>How to model very long term profile development (geological time scale) ?</p>	<ul style="list-style-type: none"> • For very long term applications (geological profile development and stratigraphy), geological models such as the model Barsim (Storms, 2002 ; Storms et al., 2013) are more suited.

Modelling structures	See Chapter 8
How should we choose structure types in models ?	<ul style="list-style-type: none"> • Structures can be seen as internal, local boundaries. As with every boundary type, their modelling is not perfect and includes side effects. Different structure types with the same purpose or in different models perform similarly, structure types should hence be chosen according to physics and practicality of their implementation. • In Delft3D, with structures and morphology it is advised to always define the depth in the cell centres to reduce side effects. This is the only and default option in XBeach. • Generally speaking since flow and wave models are often separate modules, it is important to verify that the effect of the structure has been modelled in both modules.
How to model submerged groynes?	<ul style="list-style-type: none"> • The easiest option is to model them with a modified bathymetry (flow, wave) and a hard layer (morphology). In Delft3D, weirs and obstacles can also be used but are more difficult to implement. In XBeach only a modified bathymetry and hard layer are currently available. • Side effects may include bed oscillations for the modified bathymetry (physical and numerical), and staircase effects for weirs if their implementation is too coarse.
How to model emerged groynes ?	<ul style="list-style-type: none"> • Emerged groynes may be modelled in Delft3D with a modified bathymetry and a hard layer, or with a series of thin dams and obstacles. Both are relatively easy to implement in Delft3D, only the first option is available in XBeach.
How to model a port ?	<ul style="list-style-type: none"> • Dry points and thin dams are standard and easy options to model the complexity of a port in Delft3D. However in Delft3D a wall roughness can only be applied in combination with dry points. In XBeach a modified bathymetry and a hard layer have to be used.

References

- Ailliot, P. and Prevosto, M. (2001). Two methods for simulating the bivariate process of wave height and direction. *Proceedings of the 11th International Offshore and Polar Engineering Conference, June 17th-22nd 2001, Stavanger, Norway*.
- Baeye, M. (2012). *Hydro-meteorological Influences on the Behaviour and Nature of Sediment Suspensions in the Belgian-Dutch Coastal Zone*. PhD thesis, Ghent University, Belgium.
- Bailard, J. A. (1981). An Energetics Total Load Sediment Transport Model for Plane Sloping Beaches. *Journal of Geophysical Research*, vol. 86 (C11), pp. 10938-10954.
- Bijker, E. W. (1967). *Some considerations about scales for coastal models with moveable bed*. Tech. Rep. 50, WL Delft Hydraulics, Delft, The Netherlands.
- Brière, C. and Walstra, D.J. (2006). *Modelling of bar dynamics*. WL Delft Hydraulics report, project Z4099.00, prepared for Rijkswaterstaat – RIKZ, The Netherlands.
- Bruun, P. (1978). *Stability of tidal inlets*. Elsevier. ISBN 0444598243
- Cavaleri, L. and the WISE group (2007). Review: Wave Modelling - The state of the art. *Progress in Oceanography*, vol. 75, pp. 603-674.
- CFD-Online (2011). Computational Fluid Dynamics Online. Consulted on May 20th, 2011 at http://www.cfd-online.com/Wiki/Smagorinsky-Lilly_model .
- Cowell, P.J.; Stive, M.J.F.; Niedoroda, A.W.; de Vriend, H.J.; Swift, D.J.P.; Kaminsky, G.M.; Capobianco, M. (2003). The coastal-tract (Part 1): a conceptual approach to aggregated modeling of low-order coastal change. *J. Coast. Res.* 812–827
- Dastgheib, A. (2008). Oral presentation in 2009 at TU Delft, The Netherlands. See Dastgheib et al.(2008).
- Dastgheib, A., Roelvink, J.A., and Wang, Z.B. (2008). Long-term process-based morphological modeling of the Marsdiep Tidal Basin. *Marine Geology*, vol 256, pp.1-4.
- Dastgheib, A. (2012). Long term process-based morphological modelling of large tidal basins. PhD thesis, UNESCO-IHE, Delft, The Netherlands.
- Davies, A.G., and Thorne, P.D. (2008). Advances in the Study of Moving Sediments and Evolving Seabeds. *Surv Geophys.*, 29, pp.1-36.
- De Vet, L. (2014). Modelling sediment transport and morphology during overwash and breaching events. MSc thesis, TU Delft, the Netherlands.
- De Vriend, H.J., Zyserman, J., Nicholson, J, Roelvink, J.A., Pechon, P., and Southgate, H.N. (1993). Medium-term 2DH coastal area modelling. *Coastal Engineering*, 21, pp. 193-224.
- De Winter, J; Trouw, K.; Toro, F.; Delgado, R.; Verwaest, T.; Mostaert, F. (2010). *Scientific support regarding hydrodynamics and sand transport in the coastal zone: Literature review of data*. Version 2.0. WL Rapporten, 744_30. Flanders Hydraulics Research & IMDC: Antwerp, Belgium
- Deltares (2008). *Validation document Delft3D-FLOW: a software system for 3D flow simulations*. Report X0356, M3470, Deltares, The Netherlands.
- Deltares (2010a). *Delft3D-FLOW. Simulation of multi-dimensional hydrodynamic flow and transport phenomena, including sediments – User Manual*. Version 3.04, rev. 11114. Deltares, Delft, The Netherlands.
- Deltares (2015). *XBeach 1D – Probabilistic model: ADIS, Settings, Model uncertainty and Graphical User Interface*. 65p, Deltares, The Netherlands
- Doodson, A. T. (1921). The harmonic development of the tide generating potential. *Proceedings of the Royal Society of London, Ser. A*, 100, pp. 305– 329.

- Dujardin, A.; Van den Eynde, D.; Vanlede, J.; Ozer, J.; Delgado, R.; Mostaert, F. (2010a). *BOREAS - Belgian Ocean Energy Assessment: A comparison of numerical tidal models of the Belgian part of the North Sea. Version 2_0*. WL Rapporten, 814_03. Flanders Hydraulics Research, Soresma & MUMM: Antwerp, Belgium. BELSPO contract SD/NS/13A
- Dujardin A.; De Clercq B.; Vanlede J.; Delgado R.; van Holland G.; Mostaert F.(2010b). *Verbetering numeriek instrumentarium Zeebrugge: Bouw en afregeling detailmodel. Versie2_0* (in Dutch). WL Rapporten, 753_08, Waterbouwkundig Laboratorium, Soresma en IMDC, Antwerpen, België.
- Fettweis, M., Francken, F., Pison, V. and Van den Eynde, D. (2003). *Bepaling van de Sedimentbalans voor de Belgische Kustwateren (SEBAB-III). Activiteitsrapport 2 (oktober 2002 - maart 2003) : Naar een 3D model van het BCP en de sedimentologische analyse van bodemstalen* (in Dutch). Report SEBAB/3/MF/200304/NL/AR/2, BMM, Brussels, Belgium.
- Hassan, W.N., and Ribberink, J.S. (2005). Transport processes of uniform and mixed sands in oscillatory sheet flow. *Coastal Engineering*, 52 (9). pp. 745-770.
- Hassan, W.N. (2012). Oral presentation at Flanders Hydraulics, Belgium. See Hassan and Ribberink (2005).
- Hoitink, A.J.F., Hoekstra, P., and Van Maren, D.S. (2003). Flow asymmetry associated with astronomical tides: Implications for the residual transport of sediment. *Journal of Geophysical Research*, vol. 108 (C10), p. 3315.
- Holthuisen, L. (2010). *Waves in oceanic and coastal waters*. Cambridge University Press, UK.
- Houthuys, R. (2012). *Update of the sediment budget for the nearshore of Blankenberge Zeebrugge. Version 1.0*. WL Rapporten, 744_30. Flanders Hydraulics Research & IMDC: Antwerp, Belgium.
- Hsu, J.R.C., Evans, C. (1989). Parabolic bay shapes and applications. Proc. Instn Ciu. Engrs, Part 2, 1989,87, Maritime engineering group, paper 9411.
- Hsu, J.R.C., Yu, M.J., Lee, F.C., and Benedet, L. (2010). Static bay beach concept for scientists and engineers: A review. *Coastal Engineering*, vol. 57, pp. 76-91.
- Jarrett, J.T. (1976). *Tidal prism-inlet area relationships*. DTIC Document
- Kragtwijk, N.G., Zitman, T.J., Stive, M.J.F. and Wang, Z.B. (2004). Morphological response of tidal basins to human interventions. *Coastal Engineering*, vol. 57, pp. 221.
- Kraus, N.C. (1998). Inlet cross-sectional area calculated by process-based model. *Coast. Eng. Proc.* 1(26)
- Kraus, N. (2000). Reservoir model of ebb-tidal shoal evolution and sand bypassing. *Journal of Waterway, Port, Coastal, and Ocean Engineering*, vol. 126 (3), pp. 305-313.
- Lanckriet, T., Trouw, K., Zimmerman, N., Wang, L., De Maerschallck, B., Delgado, R., Verwaest, T., Mostaert, F. (2015). Scientific support regarding hydrodynamics and sand transport in the coastal zone: Hindcast of the morphological impact of the 5-6 December 2013 storm using XBeach. Version 1.0. Report, 12_107. Flanders Hydraulics Research & IMDC: Antwerp, Belgium.
- Lanckriet, T.; Zimmermann, N.; Trouw, K.; Wang, L.; De Maerschallck, B.; Delgado, R., Verwaest, T., Mostaert, F. (2015b). Wetenschappelijke bijstand voor de hydrodynamica en zanddynamica in de kustzone: Advies suppletie Knokke – Effect op de morfologie van het Zwin en van de Baai van Heist: XBeach - modellering. Versie 1.0. Rapport, 12_107. Waterbouwkundig Laboratorium & IMDC: Antwerpen, België.
- Latteux, B. (1995). Techniques for long-term morphological simulations under tidal action. *Marine Geology*, 126, pp. 129-141.
- Lesser, G.R. (2009). *An approach to medium-term coastal morphological modeling*. PhD dissertation, Unesco-IHE Institute for Water Education and Delft University of Technology, The Netherlands.
- Leyssen, G.; Vanlede, J.; Decrop, B.; Van Holland, G.; Mostaert, F. (2012). *Modellentrein CSM-ZUNO. Deelrapport 2: Validatie* (in Dutch). WL Rapporten, 753_12. Waterbouwkundig Laboratorium & IMDC: Antwerpen, België
- Liang, L. (2010). *A fundamental study of the morphological acceleration factor*. MSc thesis, Delft University of Technology, The Netherlands.

- Longuet-Higgins, M.S. (1970a). Longshore currents generated by obliquely incident sea waves, 1. *Journal of Geophysical Research*, 75 (33), pp. 6778-6789.
- Longuet-Higgins, M.S. (1970b). Longshore currents generated by obliquely incident sea waves, 2. *Journal of Geophysical Research*, 75 (33), pp. 6790-6801.
- Mol, A.C.S. (2007). *R&D Kustwaterbouw Reductie Golfstrandvoorwaarden. OPTI Manual*. Rapport H4959.10, WL|Delft Hydraulics, Nederland.
- Monbet, V., Ailliot, P., and Prevosto, M. (2007). Survey of stochastic models for wind and sea state time series. *Probabilistic Engineering Mechanics*, vol. 22, pp. 113-126.
- O'Brien, M.P. (1966). Equilibrium flow areas of tidal inlets on sandy coasts. *Coast. Eng. Proc.* 1(10)
- O'Donoghue, T., van der A, D. A. (2012). Laboratory Experiments for Wave-Driven Sand Transport Prediction. Jubilee Conference Proceedings, NCK-Days 2012, The Netherlands.
- Pawlowicz, R., Beardsley, B. and Lentz, S. (2002). Classical tidal harmonic analysis including error estimates in MATLAB using T-TIDE. *Computers & Geosciences*, vol. 28, pp. 929–937.
- Pugh, D. (1987). *Tides, Surges and Mean Sea-Level*. 472 pp., John Wiley, Hoboken, N. J., USA.
- Ranasinghe, R., Swinkels C., Luijendijk A., Roelvink J.A., Bosboom J., Stive M.J.F. and Walstra D.J.R (2011). Morphodynamic upscaling with the morfac approach: dependencies and sensitivities. *Coastal Engineering*, 58 (8), pp. 806-811.
- Ranasinghe et al.(in prep.). Unknown reference, see Liang (2010) and Walstra (2011).
- Roelvink J.A. (2006). Coastal morphodynamic evolution techniques. *Coastal Engineering*, vol. 53, pp 277-287.
- Roelvink, D., and Reniers, A. (2011, in press). *Guide to modelling coastal morphology. Advances in coastal and ocean engineering, Vol. 12*. World Scientific Book.
- Scheffner, N.W. and Borgman, L.E. (1992). Stochastic time series representation of wave data. *Journal of Waterways, Port, Coastal and Ocean Engineering*, vol. 118 (4), pp. 337-351.
- Shannon, C.E. (1948). A mathematical theory of communication. *Reprinted with corrections from The Bell System Technical Journal, Vol. 27*, pp. 379–423, 623–656.
- Song, D., Wang, X., Kiss, A. E., Bao, X. (2011). The contribution to tidal asymmetry by different combinations of tidal constituents. *Journal of geophysical research*, vol. 116, C12007.
- Soulsby, R.L. (1997). *Dynamics of marine sands : a manual for practical applications*. Thomas Telford Publications, 249 p.
- Stive, M.J.F.; Capobianco, M.; Wang, Z.B.; Ruol, P.; Buijsman, M.C. (1998). Morphodynamics of a tidal lagoon and the adjacent coast. *Phys. estuaries Coast. seas* 397–407
- Stive, M.J.F. (2003). Advances in morphodynamics of coasts and lagoons. *International Conference on Estuaries and Coasts*, November 9th-11th , 2003, Hangzhou, China.
- Stive, M.J.F.; Rakhorst, R.D. (2008). Review of empirical relationships between inlet cross-section and tidal prism. *J. Water Resour. Environ. Eng.* 2008
- Stive, M.J.F.; Tran, T.T.; Nghiem, T.L. (2012, October 10). Stable and unstable coastal inlet cross-sectional behaviour. *ICEC 2012 4th Int. Conf. Estuaries Coasts*, Hanoi, Vietnam, 8-11 Oct. 2012. Retrieved from <http://repository.tudelft.nl/view/ir/uuid:dffbde0b-ef26-4d2f-b998-0f0db8001965/>
- Storms, J. (2002). Controls on shallow marine stratigraphy : a process-response approach. PhD thesis, TU Delft, The Netherlands.
- Storms, J., Walstra, D.J., Geleynse, N., de Jager, G., Forzoni, A., Charvin, K., Gallagher, K., Li, L., Hampson, G., Jagers, B. (2013). Prediction of Multi-Scale Fluvio-Deltaic Stratigraphy by Forward and Inverse Modeling of Integrated Source-to-Sink Sediment Flux. Search and Discovery Article #120112.
- Sutherland, J., Peet, A.H. and Soulsby, R.L. (2004). Evaluating the performance of morphological models. *Coastal Engineering*, 51, pp. 917– 939.

Ter Brake, M., and Schuttelaars, H.M. (2011). Channel and shoal development in a short tidal embayment : an idealized model study. *Journal of Fluid Mechanics*, vol 677, pp. 503-529.

Trouw, K. (2013) Sediment transport due to irregular waves, Ph.D. thesis Katholieke Universiteit Leuven

Trouw, K.; Mathys, M.; Toro, F.; Delgado, R.; Verwaest, T.; Mostaert, F (2010). *Scientific support regarding hydrodynamics and sand transport in the coastal zone: Literature review of physical processes*. Version 2.0. WL Rapporten, 744_30. Flanders Hydraulics Research & IMDC: Antwerp, Belgium.

Trouw, K., Zimmermann, N., Wang, Li., De Maerschack, B., Delgado, R., Mostaert, F. (2014). Scientific support regarding hydrodynamics and sand transport in the coastal zone: Literature review coastal zone Zeebrugge - Zwin. Version 1_0. WL Rapporten, 12_107. Flanders Hydraulics Research. Antwerp, Belgium.

Trouw, K., Houthuys, R., Lanckriet, T., Zimmerman, N., Wang, L., De Maerschack, B., Verwaest, T., Mostaert, F. (2015). Wetenschappelijke bijstand zanddynamica: Inventarisatie randvoorwaarden en morfologische impact Sinterklaasstorm (6 december 2013). Version 1.0. Report, 00_072. Flanders Hydraulics Research & IMDC: Antwerp, Belgium.

THV IMDC-Soresma (2010). *Coherens II Technical report: Subtask 11 Structures Module, preliminary design*.

Van de Kreeke, J., and Robaczewska, K. (1993). Tide-induced transport of coarse sediment : Application to the Ems estuary. *Netherlands Journal of Sea Research*, vol. 31 (3), pp. 209-220.

Van de Kreeke, J. (1992). Stability of tidal inlets; Escoffier's analysis. *Shore and Beach* 60(1): 9–12

Van der Wegen, M., and Roelvink, J.A. (2008). Long-term morphodynamic evolution of a tidal embayment using a two-dimensional, process-based model, *J. Geophysical Research*, 113, C03016.

Van der Wegen, M., and Roelvink, J.A. (2010). Reproduction of the Western Scheldt bathymetry by means of a process-based model. Oral presentation at PECS 2010.

Van Dijk, T.A.G.P., Lindenbergh, R.C., and Egberts, P.J.P. (2008). Separating bathymetric data representing multiscale rhythmic bed forms: A geostatistical and spectral method compared. *Journal of Geophysical Research*, vol. 113, F04017.

Van Leeuwen C.W., Hofland B. (1999), The current deflecting wall in a tidal harbour with density influences, Final Reports in the Framework of the European Community's Large Scale Installations and Facilities Program II, Delft, The Netherlands.

Van Rijn, L.C. (1993). *Principles of Sediment Transport in Rivers, Estuaries and Coastal Seas*. Aqua Publications, Amsterdam, The Netherlands.

Villaret, C., Huybrechts, N. and Davies, A.G. (2012). A large scale morphodynamic process-based model of the Gironde estuary. *Jubilee Conference Proceedings*, NCK-Days 2012, Enschede, The Netherlands.

Visser R. (2002), *Morphological modeling in the vicinity of groynes – an extended application in Delft3D-RAM including tidal impact*. MSc. Thesis, Delft University of Technology, Delft.

Walstra, D.J. (2011). How to perform realistic morphodynamic simulations with acceptable run-times. Deltares webinar, December 14th 2011. Avail. at <http://oss.deltares.nl/web/morphology/inputreduction>

Walstra, D.J.R., Reniers, A.J.H.M., Ranasinghe, R., Roelvink, J.A., and Ruessink, B.G. (2012). On bar growth and decay during interannual net offshore migration. *Coastal Engineering*.

Walstra, D.J.R., Hoekstra, R., Tonnon, P.K., Ruessink, B.G. (2013). Input reduction for long-term morphodynamic simulations in wave-dominated coastal settings. *Coastal Engineering* 77: 57–70.

Walton, T.L. (2004). Escoffier Curves and Inlet Stability. *J. Waterw. Port, Coastal, Ocean Eng.* 130(1): 54–57. doi:10.1061/(ASCE)0733-950X(2004)130:1(54)

Wang, Z.B. and De Vriend, H.J. (2004). Comment on "Depth-integrated modeling of suspended sediment transport" by M. Bolla Pittaluga and G. Seminara. *Water resources research*, vol. 40, W10801.

Wang, L.; Zimmermann, N.; Trouw, K.; Delgado, R.; Toro, F.; Verwaest, T.; Mostaert, F. (2012). *Scientific support regarding hydrodynamics and sand transport in the coastal zone: Longshore modelling: Realistic Blankenberge case*. Version 1_0. WL Rapporten, 744_30. Flanders Hydraulics Research & IMDC: Antwerp, Belgium.

Wang, L.; Zimmermann, N.; Trouw, K.; De Maerschalck, B.; Mostaert, F. (2015). Long term morphological model of the Belgian shelf: Calibration. Version 3.0. WL Rapporten, 12_107. Flanders Hydraulics Research & IMDC: Antwerp, Belgium. I/RA/11355/14.175/LWA/NZI. IMDC, Antwerp, Belgium.

Winter, C., Chiou, M.D., Riethmüller, R., Ernstsen, V.B., Hebbeln, D. and Flemming, B.W. (2006). The concept of "representative tides" in morphodynamic numerical modelling. *Geo-Marine Letters*, 26 (3), pp. 125-132.

Yazdi J., Sarkardeh H., Azamathulla H., Ghani A. (2010), 3D simulation of flow around a single spur dike with free surface flow. *Intl. J. River Basin Management*, vol. 8 (1), pp. 55-62.

Yossef M., Klaassen G.J. (2002), Reproduction of groynes-induced river bed morphology using LES in a 2D morphological model. *River Flow 2002, Proceedings of the International Conference on Fluvial Hydraulics*, Louvain-la-Neuve, Belgium.

Zimmermann, N., Mathys, M., Trouw, K., Toro, F., Delgado, R., Verwaest, T., Mostaert, F. (2010). *Scientific support regarding hydrodynamics and sand transport in the coastal zone: Literature review of models*. Version 2_0. WL Rapporten, 744_30. Flanders Hydraulics Research & IMDC: Antwerp, Belgium.

Zimmermann, N.; Mathys, M.; Trouw, K.; Delgado, R.; Verwaest, T.; Mostaert, F. (2012a). *Scientific support regarding hydrodynamics and sand transport in the coastal zone: Simplified Blankenberge case: comparison of Delft3D and XBeach model results*. Version 2_0. WL Rapporten, 744_30. Flanders Hydraulics Research & IMDC: Antwerp, Belgium.

Zimmermann, N.; Wang, L.; Trouw, K.; Delgado, R.; Verwaest, T.; Mostaert, F. (2012b). *Effect of a beach nourishment on the sedimentation of the entrance channel of the port of Blankenberge: Application of a simplified model for the Blankenberge area*. Version 3_0. WL Rapporten, 744-30. Flanders Hydraulics Research & IMDC: Antwerp, Belgium.

Zimmermann, N.; Wang, L.; Mathys, M.; Trouw, K.; Delgado, R.; Toro, F.; Verwaest, T.; Mostaert, F. (2012c). *Scientific support regarding hydrodynamics and sand transport in the coastal zone: Calibration of the Oostende-Knokke hydrodynamic and sediment transport model (OKNO)*. Version 1_0. WL Rapporten, 744_30. Flanders Hydraulics Research & IMDC: Antwerp, Belgium.

Zimmermann, N.; Wang, L.; Mathys, M.; Trouw, K.; Delgado, R.; Toro, F.; Verwaest, T.; Mostaert, F. (2015b). *Scientific support regarding hydrodynamics and sand transport in the coastal zone: Modelling tools and methodologies*. Version 3_0. WL Rapporten, 744_30. Flanders Hydraulics Research & IMDC: Antwerp, Belgium.

Zimmermann, N.; Wang, L.; Trouw, K.; Vanlede, J.; De Maerschalck, B.; Verwaest, T.; Mostaert, F. (2013a). Toegankelijkheid haven Blankenberge: Optimalisatie van de haveningang. Versie 4.0. WL Rapporten, 00_063. Waterbouwkundig Laboratorium & IMDC: Antwerp, Belgium.

Zimmermann, N.; Wang, L.; Delecluyse, K.; Suzuki, T.; Trouw, K.; De Maerschalck, B.; Vanlede, J.; Verwaest, T.; Mostaert, F. (2013b). Energy atolls along the Belgian coast: Effects on currents, coastal morphology and coastal protection. Version 5.0. WL Rapporten, 13_105. Flanders Hydraulics Research & IMDC: Antwerp, Belgium. Ref. IMDC: I/RA/11355/13.222/LWA/NZI.

Zimmermann, N.; Trouw, K.; De Maerschalck, B.; Toro, F.; Verwaest, T.; Mostaert, F. (2015). Scientific support regarding hydrodynamics and sand transport in the coastal zone: Evaluation of XBeach for long term cross-shore modelling. Version 1_0. WL Rapporten, 744_30. Flanders Hydraulics Research & IMDC: Antwerp, Belgium.

Annex A – Residual sediment transport calculation

Below a more generic approach is proposed to estimate all possible residual transport contributions for any set of tidal components.

A very similar approach, published about at the same time as this method was being developed, is presented in Song et al. (2011).

Derivation

The time-varying velocity can be defined as the sum of N components with amplitudes A_k , frequencies ω_k and phases α_k obtained with a harmonic analysis :

$$u(t) = \sum_{k=1}^N A_k \cos(\omega_k t + \alpha_k)$$

The sediment transport is assumed to be a power function of the velocity and is integrated over time to get the residual transport :

$$\begin{aligned} \langle q \rangle &= f \langle u^3 \rangle \\ \langle u^3 \rangle &= \lim_{T \rightarrow \infty} \left(\frac{1}{T} \int_0^T u(t)^3 dt \right) \\ \langle u^3 \rangle &= \lim_{T \rightarrow \infty} \frac{1}{T} \int_0^T \left[\sum_{k=1}^N A_k \cos(\omega_k t + \alpha_k) \right]^3 dt \\ \langle u^3 \rangle &= \lim_{T \rightarrow \infty} \frac{1}{T} \int_0^T \left[\sum_{i,j,k=1}^N A_i A_j A_k \cos(\omega_i t + \alpha_i) \cos(\omega_j t + \alpha_j) \cos(\omega_k t + \alpha_k) \right] dt \end{aligned}$$

Since

$$\begin{aligned} \cos A \cos B \cos C &= \frac{1}{2} [\cos(A+B) + \cos(A-B)] \cos C \\ \cos A \cos B \cos C &= \frac{1}{4} [\cos(A+B+C) + \cos(A-B+C) + \cos(A+B-C) + \cos(A-B-C)] \end{aligned}$$

That for convenience will be written as

$$\cos A \cos B \cos C = \frac{1}{4} [\cos(A \pm B \pm C)]$$

The generic residual transport can be written as

$$\langle u^3 \rangle = \lim_{T \rightarrow \infty} \frac{1}{4T} \sum_{i,j,k=1}^N \sum_{\pm} \int_0^T A_i A_j A_k \cos[(\omega_i \pm \omega_j \pm \omega_k)t + (\alpha_k \pm \alpha_k \pm \alpha_k)] dt$$

A similar calculation can be done with any other exponent n in the transport formula (even and odd).

Discussion

What may look very complicated is actually very simple. The equation above states that the sediment transport is the sum of the interaction of any set of three tidal components (i, j, k), that this transport contribution has a frequency ω_{ijk} of $\omega_i \pm \omega_j \pm \omega_k$ and a phase α_{ijk} of $\alpha_i \pm \alpha_j \pm \alpha_k$. Note that the frequency ω_{ijk} is a function of the basic Doodson frequencies ω_1 to ω_6 with integer coefficients. The importance of this contribution to the residual transport then depends on the frequency compared to the (inverse of the) data or modelling period T. Three cases can occur based on the decomposition of ω_{ijk} on the basic Doodson frequencies (Figure A-1) :

- $\omega_{ijk} = 0$: in that case the interaction (i, j, k) results in a constant term, hence a residual transport component. This happens when all basic frequencies ω_1 to ω_6 cancel each other out in the interaction (i, j, k).
- $\omega_{ijk} \ll \frac{2\pi}{T}$: if the beat frequency ω_{ijk} is small enough, the interaction (i, j, k) results in a time-varying beat contribution which is too slow to be averaged to zero over the period of interest. This happens when the highest frequencies compared to the simulation time scale cancel each other out in the interaction (usually ω_1 and ω_2 are already enough, a beat frequency which is function of ω_3 and up has a period of the order of a year).
- $\omega_{ijk} \geq \frac{2\pi}{T}$: if the beat frequency ω_{ijk} is large enough, the interaction (i, j, k) results in a time-varying contribution which can be considered as noise (gross transport) and will average to zero over the period of interest. This happens in all other cases, when the highest basic frequencies ω_1 and ω_2 do not cancel each other out.

We will choose here as writing convention to denote the interactions with its components in ascending order in terms of diurnal band, in ascending amplitudes within a diurnal band and to omit their sign in the integral (positive or negative). This is possible by noting that the sum of their diurnal bands always need to be zero to generate a net transport or a significant beat contribution, and because interactions like (M2, M4, -M6), (M4, -M6, M2) and (-M2, -M4, M6) for instance all contribute to the same term.

Example : The net transport contribution between M2, M4 and M6 actually corresponds to the frequency $\omega_{M6} - \omega_{M4} - \omega_{M2} = 0$. Other interactions between the three components do exist, such as $\omega_{M6} - \omega_{M4} + \omega_{M2} = \omega_{M4}$ but do not generate a net transport or beat contribution because the sum of their diurnal bands is not zero, meaning that their period will always be at most one day. It will hence be noted (M2, M4, M6).

To account for all permutations of a set of three components interacting with the same frequency, a multiplying constant has to be added. It can easily be verified that this constant is 3/4 if the three components are distinct, 3/2 if it includes the residual current and 3/2 if it includes twice the same component.

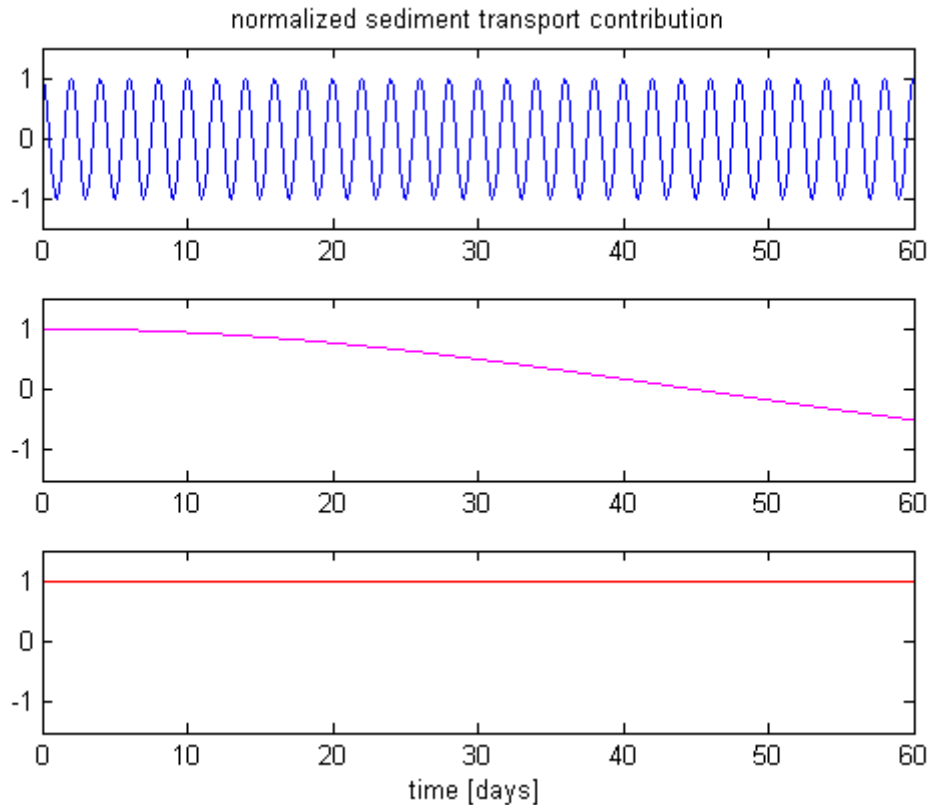


Figure A-1 : From top to bottom, example of noise (semi-diurnal contribution), beat contribution (beat frequency of six months) and residual transport component (constant), compared to a simulation period of two months.

We can see from this that the residual transport is generally not a simple function of the amplitude ratio $M4/M2$ (when normalized) and of the phase difference $2\alpha_{M2} - \alpha_{M4}$. In fact, the number of interactions to take into account for the residual transport, and in a similar way, for the beat contribution, increases with each new harmonic component added to the analysis. The Table 4-4 (in Chapter 4) can be considered as a matrix with tidal components in the rows and their decomposition on the Doodson frequencies in the columns. A matrix has a rank, or number of independent rows/columns, which is at most the lowest of its two dimensions, or 6 here. This implies that if, say, 15 components are taken into account in the analysis, 9 of them at least can be expressed as a function of other ones.

If we consider that often the time scale of interest is a couple of months, then the relevant rank is only 2 (ω_1 and ω_2 for beat contribution) and 13 components are functions of the other two. Not all of these interactions will directly lead to a net residual transport : for this only those which decomposition restricts to three components (and not 2 or 4 ; including the component being decomposed itself) will be included in the generic expression of the residual transport.

Two additional things are noteworthy. Firstly, this entire approach depends on the power assumed for the transport formula (also Van de Kreeke and Robaczewska ,1993; Hoitink et al, 2003). If 5 instead of 3 is chosen, a similar calculation would show a similar result with interactions between 5 components instead of 3. Secondly, the residual current $Z0$, although not properly a tidal constituent, plays a vital role in this approach since it interacts with every other component : $(Z0, M2, M2)$ is a residual transport component, as well as $(Z0, Z0, Z0)$, $(Z0, K1, K1)$, $(Z0, MS4, MS4)$, etc. The sum of all these may be significantly different than just the $(Z0, M2, M2)$ contribution (15% in the example below).

Finally we have seen that if frequencies are too close to each other, like $K1$ and $P1$, results of the harmonic analysis will differ if one or two components are included, because their beat frequency cannot be resolved. This should not affect the residual transport because the beat frequencies will then have an important contribution to the results.

Example

We consider a case of flow with little ellipticity. The velocity signal has been decomposed with a LSE harmonic analysis. Table A-1 presents all tidal components for which the measured velocity amplitude is larger than 2cm/s, plus K1 and O1 which are used by Hoitink et al.(2003). The modeled velocity still comprises a couple other components with a velocity amplitude larger than 2cm/s, but they do not affect the general outcome.

To be sure that no net contribution and low beat frequency is forgotten a brute force computation with for instance Matlab should ideally be used, here it will be done manually. The notation used for the tidal component already shows where the component comes from. The last number indicates the diurnal band the component belongs to, and the first number and the letters seems to indicate which main components it is composed of. For instance it can easily be verified that 2MN6 is the combination of 2*M2 and of N2, the total belonging to the 6th diurnal band.

Table A-1 : Measured and modeled velocity amplitude and phase of selected tidal components on major axis (amplitude >2cm/s). Model results in Delft3D.

Component	Measured velocity ampl. in Blankenberge [m/s]	Modelled velocity ampl. in Blankenberge [m/s] (OKNO)	Measured velocity phase in Blankenberge [deg]	Modelled velocity phase in Blankenberge [deg] (OKNO)
Z0	-0.018	-0.044	NA	NA
M2	0.530	0.609	31	25
S2	0.100	0.130	76	66
N2	0.087	0.108	31	18
M6	0.065	0.060	337	341
M4	0.057	0.093	43	48
2MS6	0.046	0.044	18	20
MN4	0.036	0.032	31	34
2MN6	0.036	0.039	338	329
M8	0.028	0.023	8	1
MS4	0.028	0.050	81	84
K1*	0.013	0.022	238	189
O1*	0.008	0.022	68	80

*K1 and O1 are not dominant components but are added because they are frequently referred to in literature and they are used for the residual sediment transport

From this observation it can be deduced that the table comprises the following net transport contributions due to three components interacting :

- (Z0, all, all), factor 3/2, as in Roelvink and Reniers (2011)
- (M2, M2, M4), factor 3/2, as in Van de Kreeke and Robaczewska (1993)
- (M2, M4, M6), factor 3/4, as in Van de Kreeke and Robaczewska (1993)
- (S2, M4, 2MS6), factor 3/4
- (M2, N2, MN4), factor 3/4
- (N2, M4, 2MN6), factor 3/4
- (M2, M6, M8), factor 3/4
- (M2, S2, MS4), factor 3/4
- (K1, O1, M2), factor 3/4, as in Hoitink et al.(2003)

In addition the table also comprises many beat frequencies due to three components interacting, but all have here a beat period lower than one month.

Table A-2 shows the residual transport contribution of each interaction of three components. Although the residual current and the interaction between M2 and its overtide M4 are the two main contributions, in this particular case two new contributions play an important role for the total residual transport because the two main contributions have opposing signs. The interactions between M2 and its overtimes M4 and M6, as well as the interaction between the diurnal components K1 and O1, only have a limited contribution due to their respective phases.

Table A-2 : Residual sediment transport due to three components interacting, for the measured velocity. Main contributions are marked in bold. Positive is in eastward direction.

Interaction	Permutation factor	Amplitude contribution	Phase contribution (cos)	Total net residual transport [$*10^{-3}$]
(Z0, all, all)	3/2	-5.50	1.00	-8.25
(M2, M2, M4)	3/2	16.06	0.95	11.42
(M2, M4, M6)	3/4	1.98	-0.12	-0.37
(S2, M4, 2MS6)	3/4	0.26	-0.19	-0.07
(M2, N2, MN4)	3/4	1.65	0.86	2.13
(N2, M4, 2MN6)	3/4	0.18	-0.09	-0.03
(M2, M6, M8)	3/4	0.09	0.19	0.01
(M2, S2, MS4)	3/4	0.98	1.00	1.47
(K1, O1, M2)	3/4	0.06	0.10	0.01
Total	NA	NA	NA	8.31

The same calculation can be done for the model results. Figure A-2 shows a comparison of the main contributions between measurements and model results. The contributions presented correspond to the following net transport :

$$\begin{aligned}
 \langle u^3 \rangle_{\infty} = & \frac{3}{2} A_{Z0} * \left(\sum_k A_k^2 \right) + \frac{3}{4} A_{M2}^2 A_{M4} \cos(2\alpha_{M2} - \alpha_{M4}) + \frac{3}{2} A_{M2} A_{M4} A_{M6} \cos(\alpha_{M6} - \alpha_{M4} - \alpha_{M2}) \\
 & + \frac{3}{2} A_{K1} A_{O1} A_{M2} \cos(\alpha_{K1} + \alpha_{O1} - \alpha_{M2}) + \frac{3}{2} A_{M2} A_{S2} A_{MS4} \cos(\alpha_{MS4} - \alpha_{M2} - \alpha_{S2}) \\
 & + \frac{3}{2} A_{M2} A_{N2} A_{MN4} \cos(\alpha_{MN4} - \alpha_{M2} - \alpha_{N2})
 \end{aligned}$$

In practice it is maybe not always worth the effort to go into such details for the residual sediment transport. However this example shows that if the residual transport approach is chosen, it is better to use a generic approach than to apply formulae from literature. In any case, residual sediment transport involves small differences of large values and conclusions about model calibration should not be made too hastily.

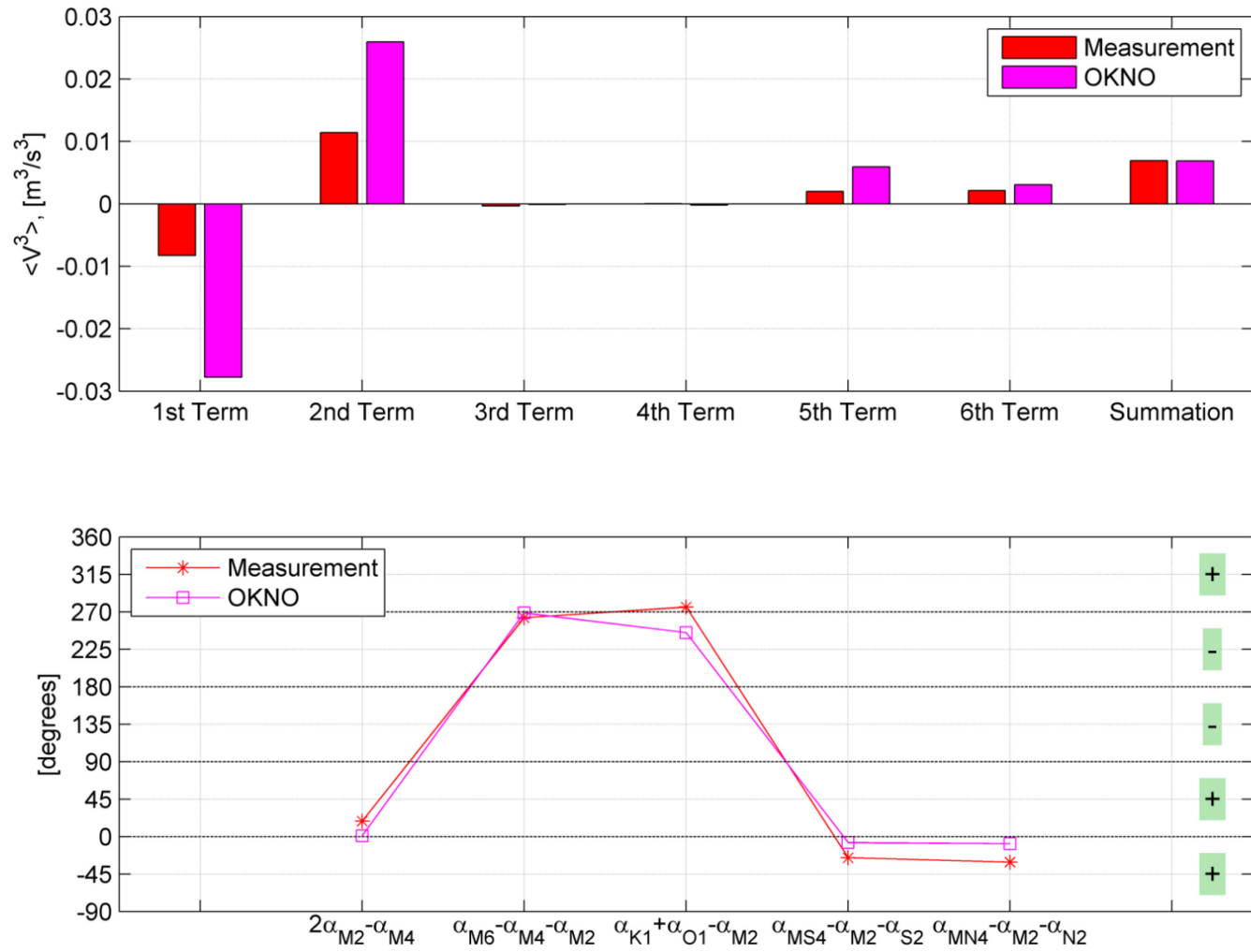


Figure A-2 : Main contributions to residual sediment transport due to interaction between three tidal components: first term (Z0, all, all), second term (M2, M2, M4), third term (M2, M4, M6), fourth term (K1, O1, M2), fifth term (M2, S2, MS4), sixth term (M2, N2, MN4). The third and fourth terms are not dominant but are included because mentioned in literature.

Annex B – Mormerge installation

Installation of Mormerge as executed at Flanders Hydraulics :

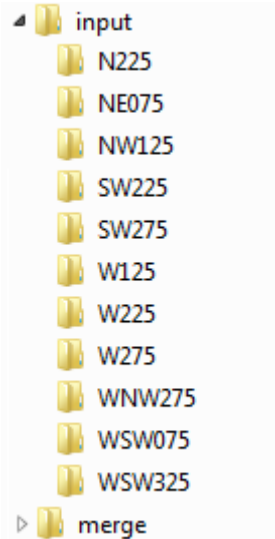
- Work under the `/home` folder with a strict folder structure, it does not seem to work elsewhere (figure below)
- Prepare the MorMerge input file `mormerge.mm` in the `/merge` folder :
 - Change the scheduler in the input file with `queuesystem=torque` instead of `sgc` (Sun Grid Engine)
 - Add the debug option `debug=1`
 - Set the number of nodes to one per wave condition, else one node has to do several computations and it results in a time out, i.e. `nodes=11` here
 - Add the paths to the executables and the weights of the wave conditions with `condition:weight = N225:0.143` for instance
- Prepare the content of the `/input` folder :
 - Add all input files of the base simulation
 - For each wave condition prepare a subfolder named after the condition and containing all simulation specific files for that condition (i.e. `wave.mdw` in subfolder `N225` for instance). These files will overwrite the respective input files of the base simulation when the given wave condition is run.
 - In the MOR file of the base simulation, add the keyword `multi=true` to activate the MorMerge functionality
- Prepare a generic script to kill the process if something goes wrong. This is needed because although the main job is submitted via the scheduler, it creates a lot of other scripts which continue to run if the main process is stopped in the scheduler. The entire MorMerge procedure consists of the following scripts :
 - The user starts `run_mormerge`
 - It calls `mormerge.tcl`
 - It creates and calls :
 - `d3d-mormerge_qsubwait.sh`
 - `d3d-mormerge_qsubgo.sh`
 - `d3d-flow_shell*.sh`, with `*` being the wave condition
 - `d3d-flow_run*.sh`, with `*` being the wave condition
 - `d3d-mormerge_shell*.sh`, with `*` being the base simulation
 - `d3d-mormerge_run*.sh`, with `*` being the base simulation
 - each condition calls the various Delft3D executables
- Run MorMerge with the script `run_mormerge` in the `/home` folder. During the run one folder per wave condition will be created such as `/home/N225` for instance, in which this condition is run. The resulting trim files of each condition should be identical, a difference plot of erosion-sedimentation will return zero.
- Debugging information can be found in the `/merge` folder in the output file `d3d-mormerge_qsubgo.sh.o*`, where `*` is the run ID. Several other output files are available there, such as `mormerge_*.log` for the user options, `mormerge_*.scr` for the merging process, or the log files of the individual simulations in their respective folder under `/home`.
- If it cannot find some libraries, adapt some lines in `mormerge.tcl` which is part of the Delft3D installation. At Flanders Hydraulics this meant to replace lines 1191 and 1393 (version 5.00.00.1234)

`puts $scriptfile "export LD_PRELOAD=[file join $libdir libgfortran.so.3]"`

by a call to `use_d3d_version` which loads the required libraries

```
puts $scriptfile "# Imposing D3D settings once more (GSI)"  
puts $scriptfile ". use_d3d_version 5.00.00.1234"
```

Note that MorMerge creates lots of files and folders, because in `mormerge.tcl` one line copies the entire content of the `/input` folder into each folder of the individual wave conditions, instead of just copying the input files (and ignoring the subfolders). This is probably unnecessary and could be easily fixed if the lines responsible for this are identified in the code.



Annex C – Script for time-varying morfac simulation in XBeach

Example of a bash script starting successively 4 simulations for the 4 wave conditions and reusing the final bathymetry of the previous run as the initial bathymetry of the next. The input file *params.txt* of each simulation is adapted from a profile in the */base* subfolder.

Note that the call to Matlab to convert this bathymetry works only standalone, and not within the PBS scheduler. This is probably a bug which has to be fixed.

```
#!/bin/sh -x
#
#PBS -q euler
#PBS -l nodes=1:ppn=1
#PBS -N test006

#-----
#prepare XBeach
#-----

if [ -n "$PBS_ENVIRONMENT" ]; then
    cd $PBS_O_WORKDIR
fi

module add openmpi/intel/64/1.4.3 intel/compiler/64/11.1/046

export XBDIR=/opt/xbeach/revEaster2012
export PATH=$XBDIR/bin:$PATH
export LD_LIBRARY_PATH=$XBDIR/lib:$LD_LIBRARY_PATH

#-----
#run varying morfac simulation
#-----

HOMEDIR=/projects/12_107_Knokke_Zwin/XB_realKnokke/test006/ #run folder
BASEDEPTH=dep002.dep #base depth file
SUBRUNS=('SW125' 'W275' 'N175' 'W175') #wave conditions in the order to be run
WEIGHTS=(425 22 193 68) #OPTI weights of the wave conditions x1000 (integers)
TIMEREAL=$(bc <<< "365 * 86400") #morphodynamic duration of full run
#hydrodynamic duration of single condition [s], excluding spinup :
TIMECOND=$(bc <<< "1 * ( 24 * 3600 + 50 * 60 )" )
TIMESPINUP=14400 #spinup
TSTOP=$(bc <<< "$TIMESPINUP + $TIMECOND")

#run counter
#j=0

#loop
DIR=dummydir
for (( j=0; j<${#SUBRUNS[@]}; j++ ));

#for i in $SUBRUNS
do
```

```

#create folder
PREVDIR=$DIR
DIR=run${j}_${SUBRUNS[$j]}
mkdir $DIR
cp $HOMEDIR/base/* $HOMEDIR/$DIR/
cd $DIR

#compute morfac
MORFAC=$(echo "scale=2; (${WEIGHTS[$j]} * $TIMEREAL) / $TIMECOND / 1000" | bc)
#MORFAC=$(bc <<< "(${WEIGHTS[$j]} * $TIMEREAL)")
#MORFAC=$(bc <<< "$MORFAC / $TIMECOND")
echo "run $j : waves ${SUBRUNS[$j]} morfac $MORFAC"

#prepare run
sed -e "s/{depth}/$BASEDEPTH/" params.txt > temp.txt
sed -e "s/{morfac}/$MORFAC/" temp.txt > params.txt
sed -e "s/{bcfile}/waves_${SUBRUNS[$j]}.sp2/" params.txt > temp.txt
sed -e "s/{morstart}/$TIMESPINUP/" temp.txt > params.txt
sed -e "s/{tstart}/$TIMESPINUP/" params.txt > temp.txt
sed -e "s/{tstop}/$TSTOP/" temp.txt > params.txt
rm temp.txt

#change initial depth
if [[ $j != 0 ]]
then
#echo bla
cp ../$PREVDIR/newdepth.dep depth.dep
sed -e "s/$BASEDEPTH/depth.dep/" params.txt > temp.txt
mv temp.txt params.txt
rm temp.txt
fi

#run XBeach
#mpiexec -n 1 $XBDIR/bin/xbeach

#exit folder
cd $HOMEDIR

#plot results and prepare next bathy in Matlab
printf {"addpath pwd;cd $DIR;MyJob_xb_subrun;exit;"} | matlab -nodisplay

#increment
cd $HOMEDIR
#j=j+1

done

```

Associated Matlab script for conversion of the output depth :

```
%% user options output
OPT.strOpenEarthDir='P:\openearthtools\trunk\matlab'; % Open Earth Tools



---


%% code
% install Open Earth Tools
if exist('xb_read_input')~=2;
    addpath(OPT.strOpenEarthDir);
    oetsettings;
end;

% read final depth
xbi=xb_read_input; % read input
xbo=xb_read_output('zb_mean.dat'); % read mean depth

% peel variables
xs_peel(xbo); % XBeach results
xs_peel(DIMS); % XBeach dimensions

% write new initial depth
zb_new=squeeze(zb_mean(end,:,:)); % depth at last time steps
zb_new=permute(zb_new,[2 1]); % change x y order for Delft3D script
zb_new(:,end+1)=-999; % dummy row
zb_new(end+1,:)=-999; % dummy column
zb_new=-zb_new; % depth positive downwards
%dlmwrite('newdepth.dep',zb_new,'delimiter',' ','precision','%7.2f');
wldep('write','newdepth.dep','',zb_new); % Delft3D format used
```



Waterbouwkundig Laboratorium

Flanders Hydraulics Research

B-2140 Antwerp

Tel. +32 (0)3 224 60 35

Fax +32 (0)3 224 60 36

E-mail: waterbouwkundiglabo@vlaanderen.be

www.watlab.be